Design and Structure-Performance Relationship Studies on Strained Hexaazaisowurtzitanes, Bicyclo[1.1.1]pentanes and Nitrogen-rich Azoles & Azines as Energetic Materials

A Thesis

Submitted for the Degree of

DOCTOR OF PHILOSOPHY

in

CHEMISTRY

by

Ghule Vikas Dasharath

Advanced Centre of Research in High Energy Materials

University of Hyderabad

Hyderabad - 500 046

India

July-2011

STATEMENT

I hereby declare that the matter embodied in this thesis is the result of investigations carried out by me in the Advanced Centre of Research in High Energy Materials (ACRHEM), University of Hyderabad, Hyderabad and High Energy Materials Research Laboratory, Pune, under the supervision of Prof. M. Durga Prasad and Dr. S. Radhakrishnan.

In keeping with the general practice of reporting scientific observations, due acknowledgements has been made wherever the work described is based on the findings of other investigators.

Place: Hyderabad (**Ghule Vikas Dasharath**)

Date: July-2011

Advanced Centre of Research in High Energy Materials
University of Hyderabad

CERTIFICATE

Certified that the work embodied in this thesis entitled "**Design and Structure-Performance Relationship Studies on Strained Hexaazaisowurtzitanes, Bicyclo[1.1.1]pentanes and Nitrogen-rich Azoles & Azines as Energetic Materials**" has been carried out by Mr. Ghule Vikas Dasharath under our supervision and the same has not been submitted elsewhere for a Degree.

(Dr. S. RADHAKRISHNAN)
Co-supervisor

(Prof. M. DURGA PRASAD)
Supervisor

(Prof. SURYA P. TEWARI)
Director
Advanced Centre of Research in High Energy Materials
University of Hyderabad.

Place: Hyderabad
Date: July-2011

ACKNOWLEDGEMENT

It’s my pleasure to write this part of my thesis and express my gratitude to one and all for helping me in a long run. I thank all of them who are involved directly or indirectly for the successful completion of this thesis.

I wish to express my sincere gratitude towards my research guide, Prof. M. Durga Prasad, ACRHEM and School of Chemistry, University of Hyderabad and Dr. S. Radhakrishnan, High Energy Materials Research Laboratory, Pune. I will be always obliged to them for their suggestions, criticism and constant encouragement. I sincerely thank them for their splendid guidance, constant support, inspiration and personal freedom rendered to me during my research period. Their endless enthusiasm and receptive attitude will always remain a source of inspiration for me.

It’s my privilege to thank Prof. Surya P. Tewari, Director, Advanced Centre of Research in High Energy Materials (ACRHEM), University of Hyderabad, for his valuable discussions, support and encouragement through out my research work.

I also thank Dr. A. Subhananda Rao, Director, High Energy Materials Research Laboratory, Pune for providing all necessary research facilities at HEMRL. I wish to thank Mr. T. Soman and Mr. V. L. Narasimhan, High Energy Materials Research Laboratory, Pune for their support. I am grateful to Dr. S. N. Asthana, Dr. A. K. Sikder, Mr. G. M. Gore and Dr. R. B. Pawar, for their useful discussions during RAB meetings.

I also want to thank Prof. S. Mahapatra, Dr. K. Muralidharan, Dr. G. Vaitheeswaran, Dr. Tushar Jana, Dr. P. K. Panda, Dr. A. K. Sahoo, Dr. A. K. Chaudhary, Dr. S. V. Rao, Dr. P. Prem Kiran, Dr. G. Manoj Kumar, Dr. B. Ashok for their help and support.

My special thanks go to Mr. P. M. Jadhav, Mr. R. S. Patil and Dr. Nilesh Naik, Scientists, High Energy Materials Research Laboratory, Pune for their constant encouragement, superb guidance, honorable support and best wishes which made me what I am today.

I acknowledge all my college teachers for their support and help. I am immensely thankful to all my B. Sc. and M. Sc. friends-cum-family, Prashant Wayker, Dinesh Dixit, Dada Gadakh, Sandip Kadam, Sanjay Ambre, Vivek Chaudhary, Latif Sheikh, Satish Malwal, Sandip Ugale, Sudhir Chaskar, Yogesh Shinde, Deepak Kudekar, Kiran Fatangare, Sachin Darade, Vaibhav Sonawane, Rahul Mote, Rajendra Wakchaure, Devachand Kalewar, Atul Somavanshi, Jyoti Gunjal, Asma Sheikh for their best wishes. I am also thankful to Sekhar, Hanumantha, Ganesh, Ravi, Narsimhappa, Rajesh, Balaji, Srinivas, Debasis, Paramsivam and all the research scholars in ACRHEM for helping me directly or indirectly.

I wish to thank all non-teaching staff of ACRHEM for providing necessary help. Financial assistance from ACRHEM, University of Hyderabad, Hyderabad is greatly acknowledged.

Without understanding what I am doing, my beloved parents have supported me through out my career with lots of patience. I am indeed very grateful to them whose constant love, care, support and encouragement have been the main force and motivation so far and will continue so in the days to come. The best wishes of my brother Sanjay and the rest of family members have helped me to arrive at this point of my journey. Thank you, all.

Ghule Vikas Dasharath

Contents

Chapter I

Overview and Computational Approaches for the Performance Prediction of High Energy Materials

1.1 Introduction

Energetic materials are the molecules or formulations whose enthalpy of formation is as high as possible, and which are capable of releasing on demand, in a controlled fashion and without oxygen, the chemical energy stored in the molecular building blocks forming the substance. Energetic materials encompass various chemical compositions of fuel and oxidant that react rapidly upon initiation and release large quantities of force or energy.[1,2] Energetic materials come in various physical forms like solid, powder, gel and liquid. The release of energy stored in the energetic materials occurs on demand, based on mechanisms such as,

- Rapid decomposition with generation of a large volume of gas.
- Intra-molecular oxidoreduction mechanisms.
- Oxidoreduction mechanisms between the neighboring molecules (in black powder or composite propellants).
- Combustion (conductive propagation), occurs when the non-porous surface of the energetic material starts to react under the dual impact of radiation and thermal conduction from the heat generated by the material which has already reacted. Combustion takes place in parallel layers, with a propagation rate in the non-decomposed material of several millimeters per second. The speed vector of the materials decomposition byproducts is opposed to the combustion front. Operating modes of energetic materials are listed in Table 1.1.
- Deflagaration (convective propagation), happens when the porous, pulverulent or damaged energetic material starts to react under the effect of heat from radiation, conduction and convection of the material that has already reacted. In this case, combustion is no longer in parallel layers, and the propagation

rate in the non-decomposed material ranges from several millimeters to several thousands of meters per second.

- Detonation (propagation by shock wave) takes place, when the propagation rate of the energetic material decomposition front is several thousands of meters per second. The detonation starts and propogates in the material via a supersonic shock wave. As the wave front passes there is complete decomposition of the initial solid into a gas. In a detonation, the speed vector of the energetic materials decomposition byproducts is in the direction of the propagation of the reaction front (unlike combustion or deflagaration).

1.2 Brief history of explosives

It is generally acknowledged that black powder was invented by the Chinese in the first century B.C. and was primarily used for fireworks.[3] The fast-paced development of chemistry in the 19th to the mid-20th century led to the creation of new substances. In the energetic material field, these new substances were often based on the nitration process. The first high explosive discovered was probably nitrocellulose (also known as guncotton) but its development was long delayed by difficulties in obtaining a stable product. In 1847 Soberot discovered glycerin nitration, leading to the development of nitroglycerin. In about 1884, Alfred Nobel invented the flegmatization of nitroglycerin by having it absorbed by siliceous earth (kieselguhr). This made nitroglycerin much less sensitive to mechanical threats, and turned it into dynamite, widely used as explosive in mining. The period leading upto the First World War also saw the birth of modern explosives. TNT (trinitrotoluene), produced by nitration of toluene, was manufactured at Germany starting in 1891, and was chosen by the Kaiser’s army in 1902 as the standard charge shells. TNT is still the standard explosive today. At the same time, Turpin in France introduced trinitrocresol as the equivalent of TNT. Picric acid would become the most commonly used French explosive during the First World War. A few years later (in 1920-40) the family of nitramines was introduced, in particular RDX (also known as cyclonite or hexogen) and HMX (also known as octogen). The over all aim of the high energy materials researchers is to develop the more powerful energetic material formulations in comparison to currently known benchmark materials/compositions.

Table 1.1: Energetic materials operating modes

Parameter	Gunpowder	Solid propellant for rocket motors	Explosives for warheads
Duration	Several tens of milliseconds	Several seconds to several minutes	Several nano-seconds to several micro-seconds
Pressure	100 to 500 MPa	5 to 20 MPa	1,000 to 10,000 MPa
Characteristic speed of reaction front in the material	20 to 200 mm/sec	1 to 50 mm/sec	3,500 to 10,000 m/sec

Factors which must be considered for design and synthesis of the novel energetic materials are,

- Raw material availability and cost
- Nontoxic, non-corrosive and non-hygroscopic nature of material
- High enthalpy of formation and high density for better performance
- Thermal and chemical stability for safe handling and storage
- Sensitivity
- Compatibility

- Combustion products (nontoxic and of low molecular weight)
- Material with better oxygen balance for complete combustion
- Burn rate and pressure exponent

1.3 Classification of explosives

Explosives are used for military as well as civil applications. A numerous progress in this field reveals that higher performance has always been a prime requirement. In addition to higher performance, safety, reliability, stability and sensitivity plays a vital role in their selection for the practical purpose. Energetic materials can be classified in a broad group like high explosives, propellants and pyrotechnics. The distinctions among the classes are usually in terms of the types of products generated and rates of reactions. High explosives and propellants that have been properly initiated evolve large volume of hot gases in short time. The difference between high explosives and propellants is the rate at which reaction proceeds. Pyrotechnics evolve large amount of heat but much less gas than propellants and high explosives.[4-6] High explosives need no confinement for the explosion, for their chemical reactions are far more rapid and undergo the physical phenomenon of detonation.[7-9] In these materials, the chemical reaction follows a high-pressure shock wave which propagates the reaction as it moves through the explosive substance. The classification of explosives[3,10,11] from a stability viewpoint is more relevant and organizes the reported energetic materials so far in the literature as,

- Thermally stable explosives
- High performance explosives
- Melt-castable explosives
- Insensitive high explosives

1.3.1 Thermally stable explosives

Explosives with improved high-temperature properties are usually termed as thermally stable explosives. Thermal stability is an important characteristic of the energetic materials (safe working limit 225^{o}C).[12] Improved thermal stability ensures safer production, increased shelf-life of munitions and low vulnerability to accidental initiations. Moreover, specific missions demand special class of high energy materials having decomposition temperatures superior to that of high performance explosives such as cyclotrimethylene trinitramine (RDX) and cyclotetramethylene tetranitramine (HMX) (>220^{0}C). Table 1.2 summarizes some of the thermally stable explosives. From an analysis of the structures of thermally stable explosives, it appears that there are general approaches to impart thermal stability to explosive molecules[13,14] such as,

- Introduction of amino groups
- Condensation with a triazole ring
- Salt formation
- Introduction of conjugation

The introduction of an amino group into the aromatic ring is one of the simplest approaches to enhance the thermal stability of explosives due to its electron donating nature. Amino group enhance the electron density toward ring which is deactivated by explosophores such as nitro, azido, etc. This is evident from the study on mono-amino-2,4,6-trinitro benzene (MATB), 1,3-diamino-2,4,6-trinitrobenzene and 1,3,5-triamino-2,4,6-trinitrobenzene (TATB), where the order of thermal stability is MATB < DATB < TATB. TATB is an explosive with unusual insensitivity and heat resistance, and respectable performance, which places it first on the list of thermally stable and safe explosives. In addition, there is an evidence of strong inter and intra-molecular hydrogen bonding in TATB. The introduction of amino group between two phenyl rings also improves the thermal stability.

Table 1.2: Some of the thermally stable explosives.

Name	Structure	M. P. (^{0}C)	Density (g/cm^3)	Velocity of detonation (m/s)
DATB	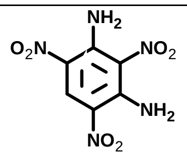	286	1.84	7500
TATB	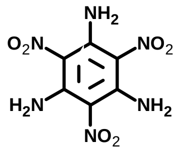	350	1.94	8000
TPM	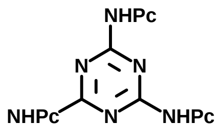	316	1.74	7420
TPAP	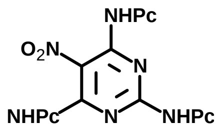	334	1.88	7880
HNS	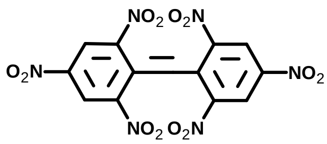	316	1.74	7000
PATO	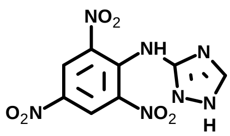	310	1.94	7850
SDATO	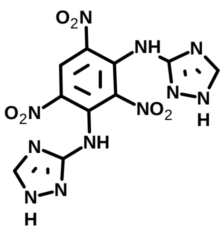	320	1.96	7600
PYX	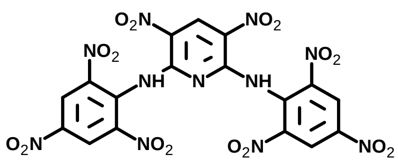	460	1.75	7450

Table 1.2 contd.

Name	Structure	M. P. (^{0}C)	Density (g/cm^3)	Velocity of detonation (m/s)
TACOT	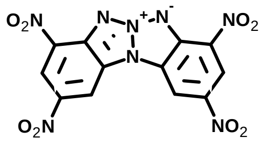	494	1.85	7250
NONA	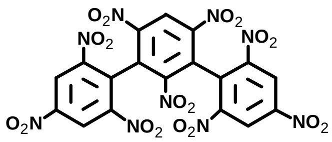	442	1.78	-

DATB: 1,3-Diarnino-2,4,6-trinitrobenzene; TATB: 1,3,5-Triamino-2,4,6-trinitrobenzene; TPAP: Tris(picrylamino)pyrimidine; TPM: *N*,*N*-nitropicrylmelamine; HNS: 2,2',4,4',6,6'-Hexanitrostilbene; PATO: 3-Picrylamino-1,2,4-triazole; SDATO: 2,4-Bis-(3-amino-1,2,4-triazole)-1,3,5-trinitrobenzene; HNAB: 2,2'4,4',6,6'-Hexanitroazobenzene; PYX: 2,6-Bis-(picrylamino)-3,5-dinitropyridine; TACOT: Tetranitrodibenzo-3,3a,4,4a-tetrazapentalene; NONA: 2,2',2",4,4',4",6,6',6"-Nonanitroterphenyl.

Heterocyclic compounds have received a great amount of interest over the decades than their carboxylic analogues for the best combination of thermal stability, oxygen balance, heat of formation (ΔH^0_f) and performance.[15-19] 3-Picrylamino-1,2,4-triazole (PATO), 1,3-bis(1,2,4-triazol-3-amino)-2,4,6-trinitrobenzene (SDATO), 2,6-bis(picrylamino)-3,5-dinitropyridine (PYX) etc., are some of the energetic formulations having heterocyclic ring in their molecular structure shows melting point higher than 300^{0}C. The best example of imparting higher thermal stability through the introduction of conjugation in an explosive molecules is 2,2',4,4',6,6'-hexanitrostilbene (HNS) (mp 316 ^{0}C). The decrease in thermal stability appears to be the result of increased steric crowding on the ring due to the repulsive effect of the explosophores. HMX with a melting point of 291°C is also considered as a heat resistant explosive in some countries,[20,21] and a safe working limit has been reported as 225°C.

1.3.2 High performance explosives

It has always been an aim of explosive researchers to achieve higher performance for warhead applications. Density has been referred as the primary physical parameter in detonation performance because detonation velocity and pressure of the explosives increase proportionally with the packing density and square of it, respectively. On the other hand, an increase in oxygen balance (O.B.) and heat of formation generally increases the sensitivity of an explosive as well as its performance.[22] The general approaches to enhance density and thus performance of explosives are:

- Insertion of pentafluorosulfonyl (SF_5) group
- Introduction of nitrogen-rich heterocyclic rings[23-27]
    - Five membered *N*-heterocycles derivatives
    - Six membered *N*-heterocycles derivatives
    - Fused heterocycles
- Presence of cage or strained structures in the molecular skeleton
- Polynitrogen complexes, guanidine derivatives[28-31]

1.3.2.1 *Insertion of pentafluorosulfonyl (SF_5) group*

The energetic materials having the pentafluorosulfonyl (SF_5) group in their molecular skeleton combines high performance with low vulnerability towards accidental detonation.[32,33] The more energy is released due to the formation of HF in the detonation of SF_5 explosives (S-F bond energy ~ 79 kcal/mol, that of H-F ~ 136 kcal/mol). Further, it is well established that the substitution of H by F in hydrocarbons leads to a significant increase in density, implies that the SF_5 group would provide nitro explosives with higher density or improved performances.

However, SF_5 containing energetic materials also couples higher energy with better thermal stability and insensitivity.

1.3.2.2 *Introduction of nitrogen-rich heterocyclic rings*

Heterocycles that contain large amount of nitrogen are relatively dense, they possess higher heat of formation due to higher percentage decomposition products usually dinitrogen. Such compounds are classically energetic and release large amounts of energy on combustion and often exhibit high performance. The high nitrogen content of these compounds often leads to a high crystal density which is itself associated with increased performance.

a. *Energetic five membered N-heterocyclic derivatives*

Five membered heterocycles such as pyrrole, imidazole, pyrazole, triazoles, triazolones and furazans have been used in the synthesis and computational study of energetic materials. Such compounds are classically energetic and release large amounts of energy on combustion and exhibit high performance. The high nitrogen content of these compounds often leads to a high crystal density which is itself associated with increased performance. Nitro derivatives of pyrrole[18,34,35] are not considered practical explosives due to (a) the heat of formation of the pyrrole ring offers no benefits and, (b) during nitration, pyrroles are much more prone to oxidation and shows acid-catalyzed ring opening. As more nitro groups are introduced, the pyrrole ring becomes more electrons deficient and less prone to nitration.

Polynitro imidazoles[36-41] and pyrazoles[42-44] are promising candidates of high energy materials due to their favorable insensitivity, thermal stability and energetic performance. Imidazole and pyrazole derivatives with more than two nitro groups are expected to be potential energetic ingredients for insensitive high energy formulations. These derivatives exhibit moderate performance and is regarded as a shock insensitive explosive. The relatively low cost and facile synthesis of these compounds makes a realistic alternative to TNT and RDX for mass use in ordnance.

The furoxan ring is a highly energetic heterocycle whose introduction into organic compounds is a known strategy for increasing crystal density and improving explosive performance. Nitro and amino derivatives of the furazan (1,2,5-oxadiazole) are nitrogen-rich energetic materials with potential use in both propellant and explosive formulations. Some nitro-substituted furazans have excellent oxygen balance and exhibit detonation velocities close to very powerful military explosives. 3,4-Diaminofurazan (DAF) has been an important precursor to a series of furazan-based energetic materials that are necessary as propellant ingredients and explosives.[45-51] The picryl,[45,52,53] nitramine,[54-56] tetranitramine[57] and azoxyfurazan[58-60] derivatives of furazan show positive heat of formation and better performance. Simple nitro derivatives of furoxan have not attracted much interest for use as practical energetic materials due to their poor thermal stability and the reactivity of nitro groups toward nucleophilic displacement.[61-63]

Incorporation of a triazole ring into a compound is a known approach for increasing thermal stability. Analyses of the structures and properties of a large number of energetic materials reveal that a combination of amino and nitro groups in a molecule often leads to better thermal stability, lower sensitivity to shock and impact, and increased explosive performance because of an increase in crystal density. Such observations are attributed to both intermolecular and intramolecular hydrogen bonding interactions between adjacent amino and nitro groups. Modern triazole-based explosives have been designed and synthesized with this strategy.[64-72] The high nitrogen content and the endothermic nature of the tetrazole ring makes it useful in the synthesis of energetic materials.[73,74] Various salts and substituted tetrazole derivatives shows high energetic performance over other azoles due to its high nitrogen content.[75-81]

b. *Energetic six membered N-heterocycles derivatives*

The synthesis of polynitro derivatives of pyridine by electrophilic aromatic substitution is often not feasible due to electron deficiency in these rings and needs to incorporate electron-releasing groups into the pyridine ring. Such approach was used for the synthesis of thermally stable explosives.[82-85] Pyrazine and pyrimidine heterocycles, like pyridine, are electron deficient and need the presence of an activating/electron-releasing group to allow efficient electrophilic nitration to occur.[86,87] The energetic compounds synthesized from pyrazine and pyrimidine shows high thermal and chemical stability.[88,89] The conversion of tertiary nitrogen in the pyrazine and pyrimidine to their corresponding *N*-oxides improves density and oxygen balance in heterocyclic systems.[90] The formation of a heterocyclic *N*-oxide changes the charge distribution of the heterocyclic ring and thus stabilizing the ring system.

There has been considerable interest in the study of the energetic and stability properties of various triazine and tetrazine derivatives. The 1,3,5-triazine and 1,2,4,5-tetrazine ring system is electroactive and has a high electron affinity. Both these rings possess high positive heats of formation and large crystal densities, which are essential properties in energetic materials applications. Additionally, they seem to be insensitive to destructive stimuli such as friction, impact, and electrostatic discharge. Tetrazine-based explosives are often highly energetic. Triazine[91-99] and tetrazine[100-110] are most essential class of six membered heterocycles used in the synthesis of energetic materials due to high nitrogen content (> 52%) and their thermal stability.

Due to the high nitrogen content, triazine and tetrazine based energetic compounds are used as energetic additive in high performance propellants and smoke-free pyrotechnic ingredients.

c. *Fused heterocycles*

There have been many attempts to synthesize compounds with a large content of nitrogen and low (or zero) content of hydrogen in recent years due to formation of very stable N_2 as an ultimate decomposition product. These studies reveals that high detonation velocity, reduced vulnerability, low shock and impact sensitivities over those in current use are highly desirable for synthesizing more powerful energetic compounds and can be obtained from the fused heterocycles. As a result, nitrogen-rich fused rings have been synthesized and theoretically studied for their energetic performance. Fused rings such as pyrazolo-pyrazole,[111-113] tetraazacyclooctatetraene (TACOT),[114-120] benzofuroxans,[121-124] benzotriazoles,[125-127] polynitrazines,[128] and s-heptazine[129,130] have been synthesized. Different explosophore were incorporated in their molecular backbone to improve their energetic performance.

Among the different pyrazolopyrazole, the performance of dinitro pyrazolopyrazole (DNPP) and 3,6-dinitropyrazolo[4,3-*c*]pyrazole-1,4-diamine (LLM-119) is predicted to be 85 % and 104 % of HMX, respectively.[131,132] The good thermal stability and performance of DNPP make this compound an attractive explosive ingredient. When compared to common explosives, TACOT is more sensitive than RDX, HMX and TNT. Advancement of the performance of TACOT by further substitution was also tried; addition of four amino groups increases the density and performance to some extent, while the alternating amino and nitro groups should ensure stability and insensitivity.[133] Benzofuroxans are far more stable than simple furoxans and are more favorable for practical applications.[134] The benzofuroxans have been an extremely plentiful area of energetic compounds in which nitro group is replaced by furoxan rings to improve density, detonation performance, stability and insensitivity of energetic materials. The highly electrophilic nature of some benzofuroxans readily yields stable salts, a number of which promise as primary (initiators) explosives.[135,136] Polynitrazines are thermally insensitive explosives with zero- to low-hydrogen content, high melting points, good insensitivity, and significantly better thermal stabilities. The s-heptazine structure was first postulated as a component of polymer melon, studies on the geometry of heptaazaphenalenes derivatives reveal that they have highly symmetric structure with a planar and rigid hetero ring. Further, considerable conjugation in the heptazine ring is an advantage to stabilities of these compounds.[129,137]

1.3.2.3 *Energetic materials having cage and strained rings*

Energetic materials of the strained-ring and cage families may constitute a promising new class of explosives as this family of compounds has high strain energies locked in the molecules (steric strain is expressed as increased positive heat of formation as compared with a corresponding unstrained system and is released as additional energy on detonation). They also possess rigid and highly compact structures, which decreases the molecular motion, results in increased density. Thus greater mass of polynitro polycyclic strained and cage compounds may be accommodated in a given volume which, along with their high molecular strain energies, results in a better performance on detonation. Preliminary evaluations of polynitropolycyclic compounds reveal that this class of energetic materials is relatively powerful and shock insensitive, and so, well suited for use in future explosive and propellant formulations. Table 1.3 lists the selective high performance energetic strained and cage compounds.

The search for energetic compounds with high crystal densities and heat of formation has focused attention on the polynitro derivatives of cage and strained compounds. The heat of formation of cyclopropane is approximately 276 kJ/mol with corresponding bond strain energy of 230 kJ/mol. Consequently, polynitro derivatives of cyclopropane and spirocyclopropane constitute a class of low molecular weight energetic materials.[138,139] Various cyclobutane and azitidine energetic derivatives have been synthesized and theoretically studied for their performance.[140,141] 1,3,3-Trinitroazetidine (TNAZ)[142,143] is one of the most energetic cage nitramine compound and more powerful than RDX, which may be less vulnerable than most other nitramines, and suitable for plasticizer applications.

The cubane ($\Delta H^0_f \sim$ 620 kJ/mol) and homocubane skeleton is highly energetic and shows a high degree of molecular strain. Additionally, the higher decomposition temperatures of some nitro derivatives, as compared to cubane itself, could infer that the electron-withdrawing nitro groups stabilize the cubane system and enhance thermal stability.[144] Polynitrocubanes show high crystal densities coupled with better explosive performances significantly greater than *C*-nitro explosives like TNT.[145-148]

Octanitrocubane (ONC) has a very high density (1.97 g/cm^3), and calculated heat of formation is of ~594 kJ/mol.[149] The explosive performance of octanitrocubane from theoretical calculations is predicted to be extremely high (VOD is ~9900 m/s), making this compound one of the most powerful explosives synthesized to date. The polynitro derivatives of homocubanes are found to be thermally stable and may find potential use as an energetic plastisizer in futuristic explosive and propellant formulations.[150-152] Prismane, bicyclo[3.3.0]octane and bicyclo[3.3.1]nonane are similar to cubane and their polynitro derivatives show higher densities and better energetic performance.[153-156] Theoretical investigation on 1,3-bishomopentaprismanes and polyazidoprismanes also proves that these compounds have high heats of formation, densities, detonation characteristics, and thermal stability.[157,158]

Table 1.3: Energetic properties of high performance energetic strained and cage compounds.

Compd.	Structure	O.B. (%)	ΔH^0_f (kJ/mol)	Density (g/cm^3)	VOD (m/s)	DP (GPa)
TNAZ	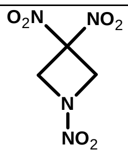	-17	2	1.84	8600	35.6
CL-20	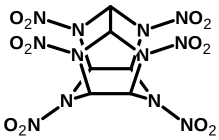	-11	454	2.04	9580	46.6
TEX	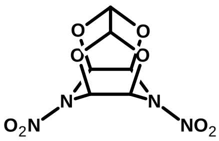	-42	-25	1.99	8560	31.4
ONC[a]	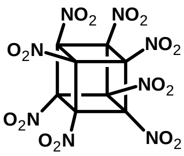	0	594	1.98	10100	50.0
2,4,6,8-TNHAA[a]	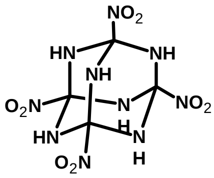	-15	459	1.97	9550	42.6
OAC[a]	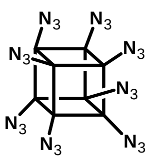	-59	3352	2.06	9360	42.1
TNBPP[a]	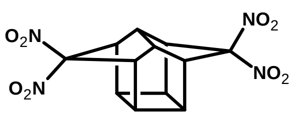	-99	383	1.76	7340	23.66

TNAZ: 1,3,3-Trinitroazetidine; CL-20: 2,4,6,8,10,12-Hexanitro-2,4,6,8,10,12-hexaazaisowurtzitane; TEX: 4,10-Dinitro-4,10-diaza-2,6,8,12-tetraoxaisowurtzitane; ONC: Octanitrocubane; 2,4,6,8-TNHAA: 2,4,6,8-Tetranitrohexaazaadamantane; OAC: Octaazidocubane; TNBPP: 11,11,12,12-Tetranitro-1,3-bishomopentaprismane, [a] shows predicted properties in gas phase.

The highly rigid skeleton of adamantane results in much higher crystal densities compared to its open chain counterparts, and hence, higher performance for its nitro derivatives.[159-162] The adamantane core shows little to almost no strain and so some of its polynitro derivatives show exceptionally high thermal stability. Xiao et al.[163,164] designed polynitrohexaazaadamantanes (PNHAAs) and studied their structural and energetic properties. Their results reveals that 2,4,6,8,9,10-hexanitrohexaazaadamantane possess better properties than the well-known CL-20 (hexanitrohexaazaisowurtzitane).

Polynitro derivatives of norbornane have been explored as a class of energetic materials. Of particular interest in this area are derivatives like 2,2,5,5,7,7-hexanitronorbornane, which has an excellent carbon to nitro group ratio. At present, only the 2,2,5,5-tetranitro and 2,2,7,7-tetranitro isomers of norbornane have been synthesized.[156,165] Cage poly aza-polycyclic nitramines such as 4,10-dinitro-4,10-diaza-2,6,8,12-tetraoxaisowurtzitane (TEX),[166,167] 2,4,6,8,10,12-hexanitro-2,4,6,8,10,12-hexaazaisowurtzitane (CL-20), 3,5,12-trinitro-3,5,12-triazawurtzitane and 2,4,10-trinitro-2,4,10-triazaadamantane[168] have very high crystal densities and heat of formation due to their energetic backbone. These derivatives are most essential energetic materials and find their application in secondary explosives.

1.3.2.4 *Polynitrogen complexes, guanidine derivatives*

Molecules consisting entirely or predominantly of nitrogen are the focus of much research for their potential as high energy density materials (HEDM). An all-nitrogen molecule N*x* can undergo the reaction $Nx \rightarrow (x/2)\ N_2$, a reaction that can be exothermic by 50 kcal/mol or more per nitrogen atom. Experimental progress in the synthesis of nitrogen molecules has been very encouraging, with the $N5^+$ and $N5^-$ ions having been produced in the laboratory.[169-171] Haiges et al.[172] reported the synthesis of high energy density materials (HEDMs) composed of polynitrogen containing compounds including $N_5^+[P(N_3)_6]^-$, $N_5^+[B(N_3)_4]^-$, $N_5^+[HF_2]^-$.nHF, $N_5^+[BF_4]^-$, $N_5^+[PF_6]^-$, and $N_5^+[SO_3F]^-$. Recent theoretical predictions on cage stability for N12, N14, N16, N18, N24, N30 and N36 indicate that the most thermodynamically stable isomer has 3-fold symmetry.[173-179] Such molecules have a triangle-pentagon bonding group on each end with a band of hexagons around the midsection. The existence of this symmetric isomer depends on the number of nitrogen atoms being a multiple of six. For a practical energy source, a molecule N*x* would have to resist dissociation well enough to be a stable fuel. The nitrogen-rich clusters found to be of higher energy than the all nitrogen structures, especially if one takes into account the energy balance of bonds involving hydrogen. Guanidine chemistry has extended over a period of more than 100 years, and many useful compounds have been identified. Guanidine and its derivatives has been the subject for many important, interesting, and fruitful investigations.[180-182] Disodium, mercury, silver, potassium and ammonium salts of guanidine derivatives show moderate and primary explosive properties.[23-25]

1.3.3 Melt-castable explosives

Melt-cast explosive are explosives loaded in the munition in a melt state. In general, to avoid compression by inertia, the charge density must be at least equal to the inertial pressure (impact). Explosives such as RDX and HMX are important military explosives and generally a binder is used along with these explosives for two reasons:

- Improves safety in processing, handling, transportation and storage.
- Imparts mechanical integrity to the explosive charge.

However, these binders brings down the overall energy of the systems; this can be improved by the use of an energetic binder such as 2,4,6-trinitrotoluene (TNT), which is a low melting explosive and also has the capability of binding explosive particles. TNT is the most commonly used high explosive. TNT derives its virtues from its relative insensitivity to shock, high chemical stability and low melting point (80.4 ^{0}C). As it can be melted with steam, it may be safely cast into shells. TNT is usually used in conjunction with other high explosives such as RDX and HMX where it acts as an energetic binder in addition to explosive. The commonly used melt-cast explosives are given in Table 1.4.

The low melting point of Tris-X indicates its suitability as a melt-castable explosive using steam processing. However, its thermal stability is only marginally acceptable. The low m.p. and predicted high performance make DNBF a very attractive melt-castable explosive. However, it is very sensitive to impact demanding more safety measures during synthesis, handling, transportation and storage. Based on energetic properties, it may safely be concluded that TNAZ is a steam-castable explosive which is attractive as an explosive or as a near-term candidate component for explosives or propellants with low sensitivity, good stability and enhanced performance (high energy and density) over existing military formulations. MTNI contains heterocyclic ring in the molecular skeleton, have low m. p., insensitive high explosive and its performance comparable to that of RDX.

It is well-known that the introduction of SF_5 groups has a strong tendency to lower melting points of nitro explosives.[32] Therefore, introduction of SF_5 groups into nitro explosives may also prove to be advantageous for the synthesis of melt-castable explosives or low melting energetic plasticizers. Russians have proposed an approach to bring down the melting points of explosives by the replacement of picryl group by nitrofurazanyl moiety. At the same time, nitrofurazanyl explosives possess high positive heat of formation, high detonation performance.[183]

Table 1.4: Commonly used melt-cast explosives and their energetic properties.

Name	Structures	M.P. (^{0}C)	Density (g/cm^3)	VOD (m/s)	DP (GPa)
TNT	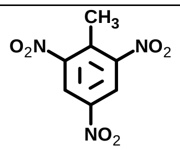	80	1.65	6900	19.0
Tris-X	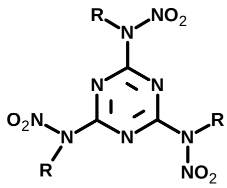 R = $CH_2CH_2ONO_2$	68	1.73	8700	30.0
TNAZ	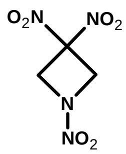	101	1.84	8600	35.7
DNBF	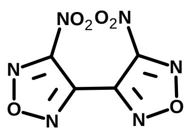	85	1.92	8800	35.6
MTNI	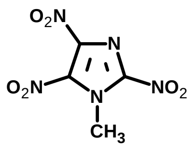	82	1.78	8800	34.6
DNAN	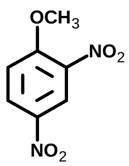	94	1.34	5344	9.51

TNT: 2,4,6-Trinitrotoluene; Tris-X: 2,4,6-Tris(2-nitroxyethylnitramino)-1,3,5-triazine; TNAZ: 1,3,3-Trinitroazetidine; DNBF: 4,4'-Dinitro-3,3'-bifurazan; MTNI: 1-Methyl-2,4,5-trinitroimidazole; DNAN: 2,4-Dinitroanisole.

1.3.4 Insensitive high explosives

An ideal explosive is one, having high performance, but insensitive enough to handle during its use, storage and transport. Most common explosives such as 2,4,6-trinitrotoluene (TNT), hexahydro-1,3,5-trinitro-1,3,5-triazine (RDX) and octahydro-1,3,5,7-tetranitro-1,3,5,7-tetrazocine (HMX) are used as key energetic ingredients for different weapons applications, but these explosives have now become less attractive due to a number of accidents involving initiation of munitions by impact or shock aboard ships, aircraft carriers and ammunition trains. So the trend of current research worldwide to design and synthesize explosives which have high performance coupled with low sensitivity. Physico-chemical properties of the promising insensitive energetic materials are presented in Table 1.5.

The insensitivity in the material can be achieved by the introduction of a) nitrogen-rich heterocycles or their *N*-oxides, b) nitro and amino groups in the ring *ortho* to each other and c) picryl moiety.[184-188] The formation of hydrogen bond between nitro and amino groups increases the stability of the molecule. The development of these classes of explosives have led to the reduction of quantity distances between storage sites, decrease the battle field vulnerability of armoured vehicles, personnel and increased capacity to carry a large quantity of ordnance. 2,4,6-Triamino-1,3,5-trinitrobenzene (TATB) is the most important insensitive high explosive of this series which may be used in modern warheads. It shows greater thermal, chemical, physical and shock stability, which are greater than that of any other known material of comparable energy. TATB based insensitive high explosive formulations significantly improve the safety and survivability of munitions, weapons, and personnel in the vicinity.

Table 1.5: Physico-chemical properties of the potential insensitive energetic materials.

Name	Structures	Density (g/cm^3)	ΔH^0_f (kcal/mol)	M.P. (^{0}C)	D (m/s)	P (GPa)	Impact sensitivity ($h_{50\%}$, cm)
TATB	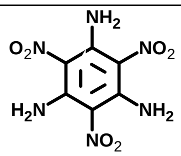	1.94	-33	330	8108	31.1	>177
FOX-7	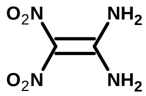	1.88	-32	254	9090	36.6	126
TEX	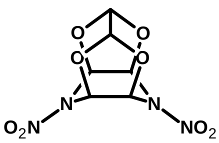	1.99	-25	299	8560	31.4	>177
NTO	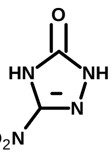	1.93	-28	270	8564	31.2	93
LLM-105	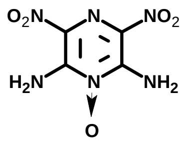	1.91	-3	354	8560	35.0	117

RDX: hexahydro-1,3,5-trinitro-1,3,5-triazine; HMX: octahydro-1,3,5,7-tetranitro-1,3,5,7-tetrazocine; TATB: 2,4,6-Triamino-1,3,5-trinitrobenzene; FOX-7: 1,1-diamino-2,2-dinitroethylene; NTO: 3-Nitro-1,2,4-triazol-5-one; LLM-105: 2,6-diamino-3,5-dinitropyrazine-1-oxide; D is the detonation velocity; P is the detonation pressure.

In last 65 years, various types of thermally stable, high performance and insensitive energetic formulations were developed. Common explosives such as hexahydro-1,3,5-trinitro-1,3,5-triazine (RDX), octahydro-1,3,5,7-tetranitro-1,3,5,7-tetrazocine (HMX) and 2,4,6-trinitrotoluene (TNT) were considered adequate for all weapon applications. Because of many catastrophic explosions resulting from unintentional initiation of munition by either impact or shock, aboard ships, aircraft carriers, and munition trains, these explosives have become less attractive. There are continuous research programmes worldwide to develop new materials with higher performance and enhanced insensitivity than the existing ones in order to meet the requirements of future military and space applications. Thus, in modern ordnance there are strong requirements for explosives having good thermal stability, impact & shock insensitivity and better performance. However, these requirements are somewhat mutually exclusive. The explosives having good thermal stability and impact insensitivity usually exhibit poorer performance and vice versa. Therefore, the foremost objective at this stage is the screening of hypothetical energetic materials through computational modeling, which allow experimental researchers to expend resources only on those molecules that show promise of enhanced performance, reduced sensitivity, or reduced environmental hazards.

1.4 Computational studies on high energy materials

Computational chemistry is an emerging field, where computer is used as an 'experimental' tool to generate data, by which one may gain insight and rationalize the behavior of a large class of chemical systems. The increase in the threshold of this subfield of theoretical chemistry is due to the advancements in computer technology, availability of practical algorithms for theoretical methods and success in explaining the problems.[189,190] It is developed into an important tool in almost all areas of chemistry. It is an eminent tool for both theoreticians and experimentalists in analyzing the chemistry related problems. The ability to design new materials from quantum mechanical principles with computers is currently one of the fastest growing and most exciting areas of theoretical research. These efforts focus on simulations that explore problems at the fundamental, microscopic level.

The ultimate objective of a modeling and simulating materials at the microscopic level is:

- How the matter really like at the atomic level?
- How can we modify the bonding between atoms to create novel materials with optimized properties?
- How can bulk materials be combined to exhibit new, desirable properties absent in the starting constituents?
- How to understand the role of different chemical groups in the molecule?

1.5 Overview of computational methods

There are various levels of theoretical methods and can be broadly classified as quantum mechanical (QM) and molecular mechanical (MM).[191-194] The choice of these methods depends on the size of the system, accuracy and property that need to be calculated. These differ in parameterization and approximation. The quantum mechanical methods are sub divided into:

- Semi-empirical methods which consider only the valence shell electrons, with some big simplifications and use empirically pre-set parameters for each element to produce results comparable with experiment.
- *Ab initio* methods those consider all the electrons without using parameters from experimental data.

Molecular mechanics is completely parameterized and algebraic expressions are used, which describe how changes in bond length, bond angles, torsion angles, etc. affect the energy of a particular structure. Hence, it may reproduce the stable conformations of common organic molecules and their relative energies. Therefore molecular mechanics methods will yield very reliable results for compounds closely related to the parameter set, which were used for fitting. Molecular mechanics is fast but it is to be noted that molecular mechanics methods do not involve a description of the electrons and their behavior. They are not meant to calculate properties that are determined by electronic effects.

The quantum mechanical methods attempt to calculate structures and energies, at different levels of approximation of the Schrödinger equation. Semi-empirical methods are partly parameterized. All electronic contributions are not computed; instead some of them are replaced by parameters, chosen so as to reproduce preferred conformations, and to a lesser extent, the corresponding heat of formation. The most widely used semi-empirical 'Hamiltonians' are AM1 (Austin Model 1) and PM3 (Parameterization Method 3). *Ab initio* methods do not contain parameters, but can be used with increasing accuracy of the description of all electronic contributions.

The choice between any of the above methods is a matter of balance between required accuracy and computational time.

Computing time required: Force fields < semi-empirical << *ab initio*

For stable conformations of simple organic molecules, MM methods give good results whereas quantum chemical methods are used for compounds where electronic effects play a role (e.g. conjugation), (for structures outside the parameter set, and for non-stable configurations, like transition states). Usually, quality of results: *ab initio* > semi-empirical > force fields

Generally geometry optimizations (which require repeated calculations of energy) are carried out initially using a faster method. Then 'single point calculations' are performed using a slower, better method on the geometry which obtained in optimization. Single point calculations can be used to model properties such as total energy, electron distribution, orbital energies etc. But at least one of the electronic methods should be used to get electronic properties, e.g. UV/vis spectrum or NMR shielding.

1.5.1 Semi-empirical quantum chemistry

The semi-empirical methods are based on the Hartree-Fock approach.[195-197] A Fock-matrix is constructed and the Hartree-Fock equations are iteratively solved. The common feature of semi-empirical methods is that it only considers the valence electrons. The core electrons are accounted for in a core-core repulsion function, together with the nuclear repulsion energy. All semi-empirical methods make use of the 'zero-differential overlap approximation' to some extent. This approximation simply says that the overlap between many atomic orbital will be small and thus the electron repulsion integrals will have negligible values. This is called the NDDO approximation (Neglect of Diatomic Differential Overlap). The next step is to replace many of the remaining integrals by parameters, which can either have fixed values, or depend on the distance between the atoms on which the basis functions are located. At this stage empirical parameters can be introduced, which can be derived from measured properties of atoms or diatomic molecules. In the modern semi-empirical methods, the parameters are however mostly devoid of this physical significance. They are just optimized to give the best fit of the computed molecular properties to experimental data. Different semi-empirical methods differ in the details of approximations (e.g. the core-core repulsion functions) and in particular in the values of the parameters. In contrast to molecular mechanics, only parameters for single atoms and for atom pairs are needed. The semi-empirical methods can be optimized for different purposes. The MNDO, AM1 and PM3 methods were designed to reproduce heats of formation and structures of a large number of organic molecules. Other semi-empirical methods are specifically optimized for spectroscopy, e.g. INDO/S or CNDO/S, which involve CI calculations and are quite good at prediction of electronic transitions in the UV/VIS spectral region.

Semi-empirical methods are parameterized on the basis of specific properties of a selected set of molecules. The bad side of semi-empirical calculations is that the results can be erratic. If the molecule being computed is similar to molecules in the database used to parameterize the method, then the results may be very good. If the molecule being computed is significantly different from anything in the parameterization set, the answers may be very poor. Semi empirical calculations have been very successful in the description of organic chemistry, where there are only a few elements used extensively and the molecules are of moderate size. For molecular structure and heats of formation of closed-shell molecules, MNDO, AM1 and PM3 are quite good. Practical experience has shown that for some particular problems, one of the above three performs markedly better than the others; but in general, the most recent methods like AM1 and PM3 are preferred. PM3 is parameterized for a greater number of elements, but sometimes the parameters are based upon a very small set of data.

Limitations

- Partly based on experimental data - parameters are no better than the information used to obtain them
- Neglect or parameterization of overlap integrals can lead to errors
- Restricted to smaller systems than empirical methods
- Takes More CPU time than empirical methods

- Core orbital are omitted which can lead to errors
- Electron correlation is included implicitly through parameterization
- There is no systematic way to improve a semi-empirical MO calculation

Quantum chemistry is based on the postulates of Quantum Mechanics where, the system is described by a wave function, which can be found by solving the Schrödinger equation.[198,199] This equation relates the stationary states of the system and their energies to the Hamiltonian operator for obtaining the energy associated with a wave function describing the positions of the nuclei and electrons in the system. But in practice, the Schrödinger equation cannot be solved exactly and approximations have to be made. One such approach is called "*ab initio*" when it makes no use of empirical information, except for the fundamental constants of nature such as the mass of the electron, Planck's constant etc., which are required to arrive at numerical predictions. The major disadvantage of *ab initio* quantum chemistry is the heavy demands on computer power.

The most common type of *ab initio* calculation is called a Hartree-Fock calculation (HF), in which the primary approximation is called the central field approximation. This means that the Columbic electron-electron repulsion is not specifically taken into account. However, its net effect is included in the calculation. This is a variational calculation, meaning that the approximate energies calculated are all equal to or greater than the exact energy. Because of the central field approximation, the energies from HF calculations are always greater than the exact energy and tend to a limiting value called the Hartree-Fock limit.

The second approximation in HF calculations is that some functional form, which is only known exactly for a few one-electron systems, must describe the wave function. The functions used most often are linear combinations of Slater type orbitals exp(-ax) or gaussian type orbitals exp(-ax^2), abbreviated STO and GTO.

1.5.2 Molecular orbitals and basis sets

Molecular Orbitals can be written as linear combinations of basis orbitals, which resemble the orbitals of atoms ("Atomic Orbitals"). The expansion of the wave function in terms of basis functions leads to a limitation of the accuracy of the *ab initio* Hartree-Fock approach only because there is a limited number of basis functions available. The greater the number of basis functions the better the wave function, the lower the energy.

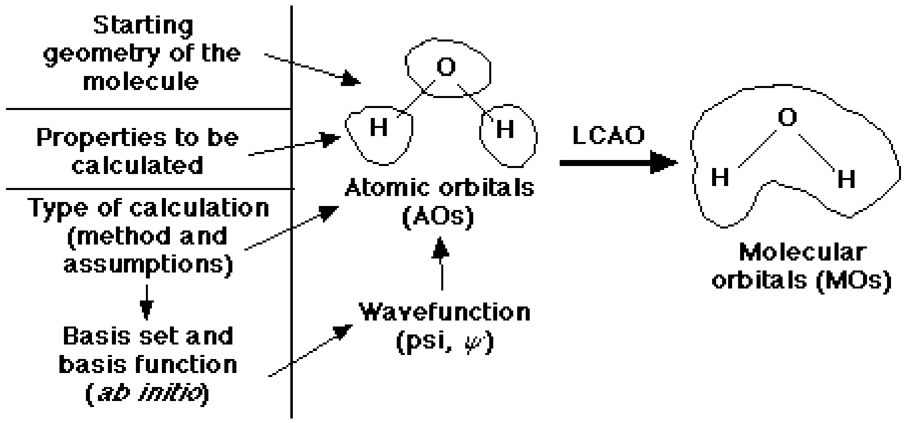

There are two general categories of basis sets:

Minimal basis sets describes only the most basic aspects of the orbitals. Extended basis sets, a basis set with a much more detailed description J. C. Slater first developed basis sets. Slater fit linear least squares to data that could be easily calculated. The general expression for a basis function is given as:

$$\textbf{Basis Function} = \mathbf{N} * \mathbf{e}^{(-\alpha * r)}$$

Where N= Normalization constant

α= orbital exponent

r = radius in angstroms

This expression given for a Slater Type Orbital (STO) is:

$$\mathbf{STO} = \frac{\zeta^3}{\pi^{0.5}} e^{(-\zeta r)}$$

It is important to remember that STO is a tedious calculation. Later Gaussian Type Orbital (GTO) has been developed.

$$\mathbf{GTO} = \frac{2x}{\pi^{0.75}} e^{(-xr^2)}$$

The difference between the STO and GTO is in the "r." The GTO squares the "r" so that the product of the gaussian "primitives" is another gaussian. Because of this, the equation is much easier; however, it leads to loss of accuracy. Combining of more gaussian equations will lead to the more accuracy. All basis set equations in the form STO-NG (where N represents the number of GTOs combined to approximate the STO) are considered to be "minimal" basis sets. The "extended" basis sets, then, are the ones that consider the higher orbitals of the molecule and account for size and shape of molecular charge distributions.

There are several types of extended basis sets:

- Double-Zeta, Triple-Zeta, Quadruple-Zeta
- Split-Valence
- Polarized Sets
- Diffuse Sets

1.5.2.1 *Double-Zeta, Triple-Zeta, Quadruple-Zeta*

In the case of minimal basis sets, it is approximated that all orbitals to be of the same shape. However, it is not true. Hence the double-zeta basis set is important because it allows treating each orbital separately while performing the Hartree-Fock calculation. This gives us a more accurate representation of each orbital. In order to do this, each atomic orbital is expressed as the sum of two Slater-type orbitals (STOs). The two equations are the same except for the value of zeta. The zeta value accounts for how diffuse (large) the orbital is. The two STOs are then added in some proportion. The constant 'd' determines how much each STO will count towards the final orbital. Thus, the size of the atomic orbital can range anywhere between the value of either of the two STOs. For example, a 2s orbital:

$$\Phi_{2s}(r) = \underbrace{\Phi_{2s}^{STO}(r,\zeta_1)}_{\text{Slater Orbital 1}} + \underset{\text{Constant}}{d}\,\underbrace{\Phi_{2s}^{STO}(r,\zeta_2)}_{\text{Slater Orbital 2}}$$

In this case, each STO represents a different sized orbital because the zetas are different. The 'd' accounts for the percentage of the second STO to add in. The linear combination then gives the atomic orbital. Since each of the two equations is the same, the symmetry remains constant. The triple and quadruple-zeta basis sets work the same way, except use three and four Slater equations instead of two. The typical trade-off applies here as well, better accuracy, more time/work.

1.5.2.2 *Split-Valence*

Often it takes too much effort to calculate a double-zeta for every orbital. Instead, it can be simplified by calculating a double-zeta only for the valence orbital. Since the inner-shell electrons aren't as vital to the calculation, they are described with a single Slater Orbital. This method is called a split-valence basis set. A few examples of common split-valence basis sets are 3-21G, 4-31G, and 6-31G.

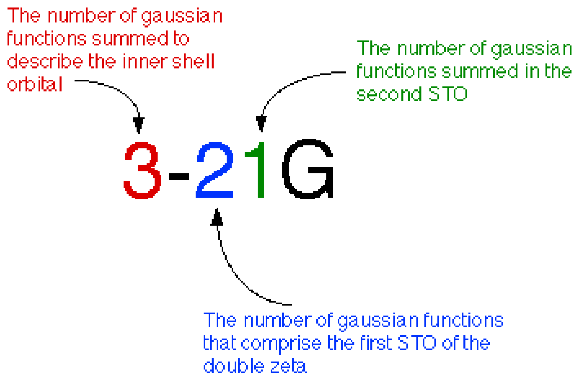

Here a 3-21G basis set is used to calculate a carbon atom and it means that summing 3 gaussians for the inner shell orbital, two gaussians for the first STO of the valence orbital and 1 gaussian for the second STO.

1.5.2.3 *Polarized Sets*

In the previous basis sets, atomic orbitals are assumed to exist only as 's', 'p', 'd', 'f' etc. Although those basis sets are good approximations, a better approximation is to acknowledge and account for the fact that sometimes orbitals share qualities of 's' and 'p' orbitals or 'p' and 'd', etc. and not necessarily have characteristics of only one or the other. As atoms are brought close together, their charge distribution causes a polarization effect (the positive charge is drawn to one side while the negative charge is drawn to the other), which distorts the shape of the atomic orbitals. In this case, 's' orbitals begin to have a little of the 'p' flavor and 'p' orbitals begin to have a little of the 'd' flavor. One asterisk (*) at the end of a basis set denotes that polarization has been taken into account in the 'p' orbitals. The polarized basis set represents the orbital as more than just 'p', by adding a little 'd'. Two asterisks (**) means that polarization has taken into account the 's' orbitals in addition to the 'p' orbitals. Below is another illustration of the difference of the two methods.

1.5.2.4 *Diffuse Sets*

In chemistry, the valence electrons are concerned much, which interact with other molecules. However, many of the basis sets discussed previously concentrate on the main energy located in the inner shell electrons. However, when an atom is in an anion or in an excited state, the loosely bound electrons, which are responsible for the energy in the tail of the wave function, become much more important. To compensate for this area, diffuse functions are used. Diffuse functions are functions that reach outside the usual valence region. Such functions are necessary for electron rich systems and especially anions. Diffuse functions usually do not exceed the angular characteristic of the highest occupied orbital of the respective atom. Diffuse basis sets are represented by the '+' signs. '+' accounts for the 'p' orbitals, while '++' signals accounts both 'p' and 's' orbitals.

The more complex basis sets are more accurate but it uses a great deal of computing time. Thus, it is important that it act responsibly when choosing which basis set to use. This means that one should consider how much time it will take to run the molecule and use the basis set that will run the fastest without compromising your desired level of accuracy.

Strengths:

- No experimental bias
- Can improve a calculation in a logical manner (basis sets, level of theory)
- Provides information on intermediate species, including spectroscopic data
- Can calculate novel structures (no experimental data is required)
- Can calculate any electronic state

Limitations: The wave function in HF calculations is formed from linear combinations of atomic orbitals or more often from linear combinations of basis functions. Because of this approximation, most HF calculations give a computed energy greater than the Hartree-Fock limit. In general, *ab initio* calculations give very good qualitative results and can give increasingly accurate quantitative results as the molecules in question become smaller.

1.5.3 Density functional methods

Quantum mechanical equations governing the behavior of electrons can be written in a relatively compact form. However, practical calculations become exceedingly difficult because of the large number of degrees of freedom and interactions between particles. Hence instead of attempting an exact and ultimately impossible calculation, approximations were made on physical laws to yield a feasible, inexact calculation. One among them is density functional theory, which postulates that the ground state energy (i.e., the lowest energy state) of a system of electrons moving in a given external potential can be obtained from knowledge of the electron charge density.[200-205]

This concept offers tremendous computational advantages because the electron density becomes the basic variable rather than the complicated many-body wave function of all the electrons. Moreover, this powerful theory reduces the problem of describing the tangled, mutually dependent motion of electrons to one of describing the motion of a single, independent electron in an effective potential. The framework of the density functional theory (DFT) gives us an extremely powerful and accurate technique to calculate the properties of materials on a first-principles, or *ab* *initio*, basis that is, from the identities of the atoms making up a material and the laws of quantum theory.

In the first stage of DFT, the energy is expressed as a functional of the density of a uniform electron gas. This is then modified to express the electron density around molecules. Despite its simple origins, DFT works very well in most cases. For about the same cost of doing a Hartree-Fock calculation, DFT includes a significant fraction of the electron correlation. Note that DFT is *not* a Hartree-Fock method, nor is it (strictly speaking) a post-Hartree-Fock method. The wave function is constructed in a different way (the spin and spatial parts are different to those developed in Hartree-Fock theory) and the resulting orbitals are often referred to as "Kohn-Sham" orbitals. Nevertheless, the same SCF procedure is used as in Hartree-Fock theory.

The choice of the functional is the only limitation of the DFT method. At the present time, there is no systematic way of choosing the functional and the most popular ones in the literature have been derived by careful comparison with experiment. Some of the most common methods are

BP86 - developed by Becke and Perdew in 1986

BLYP - developed by Becke, Lee, Yang and Parr

B3LYP - a modification of BLYP in which a three-parameter functional developed by Axel Becke is used.

1.6 Computational design of high energy materials

The development of accurate models and simulations of explosives has been aggressively pursued within the energetic material research since the arrival of computational capabilities. The high time and costs associated with the synthesis or formulation, testing and fielding of a new energetic material has called for the inclusion of modeling and simulation into the energetic materials design process. This has resulted in growing demands for accurate models to predict properties and behavior of notional energetic materials before committing resources for their development. Predictive models that will allow for the screening and elimination of poor candidates before the expenditure of time and resources on synthesis and testing of advanced materials promise significant economic benefit in the development of a new material. Therefore, great attention has been given towards developing computational tools for use in explosives research and has resulted in a dramatic evolution of methods and applications of these to explosives. Of particular importance in designing new explosives, is the ability to predict performance of compounds before the laborious and expensive task of synthesizing them. The significant key properties of energetic materials are,

- Oxygen balance
- Heat of formation
- Density
- Detonation performance
- Thermal stability
- Sensitivity.

1.6.1 Oxygen balance

Oxygen balance is the percentage of oxygen chemically bound in a molecule to oxidize it completely. Oxygen is needed for the conversion of explosive into their gaseous reaction products, such as CO_2, CO, H_2O, and NO_X, is available within the molecule. Explosophoric nitro groups are responsible for appropriate oxygen balance in explosive. The oxygen balance (O.B.) is calculated from an explosive containing the general formula $C_aH_bN_cO_d$ with molecular mass M.

$$\mathbf{O.B.(\%)} = \frac{\mathbf{[d\text{-}(2a)\text{-}(b/2)] \times 1600}}{\mathbf{M}}$$

Where, O.B. is oxygen balance (%), M is molecular mass of the compound and a, b, c are the number of C, H and O in the compound, respectively.

1.6.2 Computational approaches for heat of formation

Heat of formation is a measure of energy content of an energetic material that can decompose, ignite and explode by heat or impact. It enters into the calculation of explosive and propellant properties such as detonation velocity, detonation pressure, heat of detonation and specific impulse.[206-208] However, it is impractical to determine the heat of formation of novel energetic materials because of their unstable intermediates and unknown combustion mechanism. There are various methods known for the calculation of heat of formation such as:

- Group additivity method
- Atomization reactions
- Linear regression correction approach
- Bond correction terms
- Homodesmic reactions
- Isodesmic reaction approach

1.6.2.1 *Group additivity method*

In the group additivity methods, the properties of the molecules can be derived from atoms or functional groups from which they are made. Benson and Joback methods are two group additivity methods which commonly used to estimate thermochemical quantities of various organic molecules.[209] Jobak's method assigns incremental heat of formation values to the ideal gas phase of common functional groups. Benson's method incorporate the effects of second-nearest neighbors that produce values of gas phase heats of formation at the greater complexity. Keshavarz presented group additivity method for calculating heats of formation of nitramines, nitrate esters, nitroaliphatics and related energetic compounds which contain at least one of the functional groups including N-NO_2, C-ONO_2 or nonaromatic C-NO_2.[210,211] This approach assumes elemental composition, various structural and functional group parameters of CHNO energetic compounds.

Limitations:

- Cannot handle positional isomers. Group additivity approach predicts -16.74 kJ/mol heat of formation for ortho, meta and para isomers of dinitrobenzene, while their experimental values are -1.67, -27.19 and -38.49 kJ/mol, respectively.
- The effect of steric crowding and repulsive interaction between bulky groups on the heat of formation is not accounted.
- Applicable to CHNO explosives.
- Deviation of the predicted values from the experimental is high.[211]

1.6.2.2 *Atomization reactions*

The most direct route to calculating the heat of formation of a compound is to simply apply the definition of heat of formation; it is ΔH for the reaction whereby the compound is formed from its elements. Curtiss, Rauk et al. and Petersson et al. used known heat of formation of isolated atoms and calculated atomization energies to predict gas-phase heats of formation of molecules.[212-216] The use of formation or atomization reactions for determining heat of formation is rigorous and there is no arbitrariness, as there is only one possible formation reaction. The G2-type atomization energies in combination with experimental gas phase heat of formation for the constituent atoms were used for obtaining heat of formation. The corrections required to give heat of formation at finite temperatures obtained using scaled theoretically derived vibrational frequencies for the species under consideration together with temperature correction terms for the constituent elements based on experimental data. While the degree of accuracy of the predictions using this level of theory has been reliable, the calculations require computationally expensive electron correlation treatments which might be prohibitive for systems containing a large number of atoms or where computational resources are limited.

Limitations:

- Computationally expensive and time consuming.
- Applicable to small size molecules (including 5 to 6 atoms).
- Use of theoretical energies of the atomization reaction in conjuction with experimental data for the atoms gives somewhat better values of heats of formation; hence experimental data is needed for the calculations.
- Need approximations for most of vibrational modes, internal rotations with relatively low frequencies.

1.6.2.3 *Linear regression correction approach*

Fan et al.[217] developed linear regression correction approach, which accounts the electron correlation energy missing in Hartree-Fock calculation and to reduce the calculation errors of density functional theory. The numbers of lone-pair electrons, bonding electrons and inner layer electrons in molecules, and the number of unpaired electrons in the composing atoms in their ground states were chosen to be the most important physical descriptors to determine the correlation energy unaccounted by Hartree-Fock method or to improve the results calculated by B3LYP density functional theory method.

Limitations

- There are many descriptors considered to account 1) the number of lone-pair electrons in molecules, 2) the number of bonding electrons in molecules, 3) the number of inner layer (core) electrons in molecules, and 4) the number of unpaired electrons for ground state atoms. The inner layer electrons are further divided into several subsets according to the shell they belong to in the corresponding atoms. Hence, calculations are more complicated.
- This approach is used for closed shell molecules (the number of the unpaired electrons of the molecules is not included).

1.6.2.4 *Bond correction terms*

Bond correction approaches take the advantage of the approximate conservation of electron correlation energy in certain types of chemical transformations; usually invoke isodesmic[218] or homodesmotic reactions.[219] Cioslowski et al.[220] presented bond correction term approach to convert HF and DFT energies of molecules, ions, and radicals to standard enthalpies of formation. A combination of atomic equivalents, bond density functions, and corrections for molecular charge and spin multiplicity was employed to estimate the enthalpy for most organic and inorganic compounds of the first- and second-row elements. The formulation of the bond density function schemes accounts for the electron correlation effects associated with bond formation. The bond density function formalism has the advantage of low computational cost that makes it applicable to large molecules over G2 methods.

Limitations

- More complicated formalism and correction needed to explicit function of the electron and spin densities, and their positions.
- Large errors are encountered in the calculations due to self consistent field convergence (SCF) problem.

1.6.2.5 *Homodesmic reaction*

In the homodesmic reaction, numbers of bonds of various types are conserved along with preservation of valence environment around each atom. The improvement arises from further balancing carbon atoms in their various states of hybridization and matching the carbon-hydrogen bonds in terms of the number of hydrogen atoms joined to individual carbon atoms. When larger model compounds are introduced, it could carry extra properties, such as the conformational effects, which are not present in the molecule of interest in reactant side.[221-223] Chen et al.[224] used the homodesmic reactions to obtain $\Delta H^0{}_f$ for tetrazole derivatives. They had the advantage of having available reliable $\Delta H^0{}_f$ for two parent molecules, so that they needed to model only the bonds to the substituents.

Limitations:

- For various reference compounds experimental data is not available.
- In large size molecule, difficult to predict homodesmic reaction.
- Cannot handle large heterocyclic compounds.

1.6.2.6 *Isodesmic reaction approach*

The isodesmic reaction approach, in which the number of each kind of formal bond is conserved, is used with application of the bond separation reaction (BSR) rules (Fig. 1.1). In principle, if the heat of formation of a species is not known, then it can be obtained from the Hess cycle for a reaction if the heats of formation of all the other species are known and the heat of reaction is known.[225] Thus, all that is required is to construct an appropriate reaction and the simplest possible reaction is to fragment the molecule of interest. Hehre et al.[218] showed in the early development of *ab initio* molecular orbital theory the importance of bond separation (BS) isodesmic reactions, which refer to reactions in which the number and type of bonds are retained. Raghavachari et al.[226, 227] have suggested the use of BS isodesmic reactions to estimate ΔH^0_f, since the cancellation of errors in electron correlation energy is more complete and well characterized with experimental ΔH^0_f (uncertainty 0.1 kcal/mol) and using higher level (G2 and G2MP2) methods (uncertainty 0.1-0.2 kcal/mol).

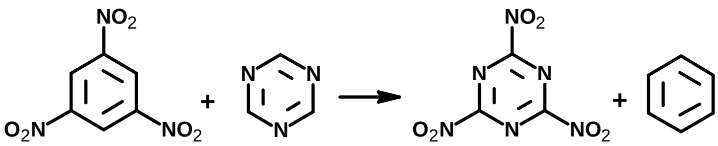

Fig. 1.1 Isodesmic reaction for 2,4,6-trinitrotriazine.

In general, the use of an isodesmic reaction scheme leads to more effective cancellation of errors in computing enthalpies of reaction than atomization reactions or group additivity methods. However, as demonstrated by Petersson et al.[228] the application of bond separation isodesmic reactions to the estimation of heats of formation for large molecules such as polynuclear aromatic hydrocarbons can lead to errors in the estimated value simply due to the large number of molecules involved in the isodesmic reaction. For a single molecule, many types of isodesmic reactions can be predicted. The question would then arise as to which isodesmic reaction should be used to estimate ΔH^0_f. On the basis of the least number of molecules involved as per the argument of Petersson et al.[228] would be the appropriate choice. However, for aromatic systems a different scheme is required as compared to that used for simple hydrocarbons. However, the BS isodesmic reactions technique does not take into account the resonance energy in the molecule which is significant in aromatic molecules, and thus, an isodesmic reaction scheme that preserves the aromatic nature of the molecules should be preferred.

Errors in the absolute quantities from quantum chemical calculations are often systematic and these errors can be compensated by employing isodesmic reactions. A previous study also proves that this approach is reliable.[229-231] For the isodesmic reaction, heat of reaction $\Delta H_{298\mathrm{K}}$ at 298 K can be calculated from the following equation:

$$\boldsymbol{\Delta H_{298\mathrm{K}} = \Delta H_{\mathrm{f,\,p}} - \Delta H_{\mathrm{f,\,R}}}$$

Where, $\Delta H_{\mathrm{f,\,R}}$ and $\Delta H_{\mathrm{f,\,p}}$ are the heats of formation of reactants and products at 298 K, respectively. The ΔH^0_f of the designed molecules can be evaluated when the heat of reaction $\Delta H_{298\mathrm{K}}$ is known. Therefore, the principle thing is to compute the $\Delta H_{298\mathrm{K}}$. $\Delta H_{298\mathrm{K}}$ can be calculated using following expression:

$$\boldsymbol{\Delta H_{298\mathrm{K}} = \Delta E_{298\mathrm{K}} + \Delta(PV) = \Delta E_0 + \Delta ZPE + \Delta H_{\mathrm{T}} + \Delta \mathrm{n}RT}$$

Where, ΔE_0 is the change in total energy between the products and the reactants at 0 K, ΔZPE is the difference between the zero point energies (ZPE) of the products and the reactants, and ΔH_{T} is the thermal correction from 0 to 298 K. $\Delta(PV)$ the equals to $\Delta \mathrm{n}RT$ for the reactions of ideal gas.

Among the various approaches for the prediction of ΔH^0_f, researchers in the energetic molecules field are widely using the isodesmic reaction approach due to the reliability and ease of use. Xiao et al.[232-237] has used the isodesmic reaction approach for the estimation of ΔH^0_f of the different energetic compounds such as, neopentyl difluoroamino derivatives, piperidine and diazocine compounds, polynitrohexaazaadamantanes, difurazans, polydifluoroamino adamantanes, nitro-arenes, adamantly-nitrates, tetrazine substituted derivatives, etc. The study of Xiao research group reveals that predicted ΔH^0_f was comparable with the experimental results. The deviation of predicted values from experimental is 4-10 kJ/mol. Xiao et al. also performed studies on energetic materials composed of nitrogen-rich heterocycles, cage and strained compounds, polycyclic rings, compounds with different substituents like $-NO_2$, $-NH_2$, $-N_3$, $-NHNH_2$, $-NF_2$, $-NHNO_2$, $-ONO_2$, -CN, -COOH, -OH, etc.

ΔH^0_f of the different nitroimidazole, polynitroimidazoles, and their methyl derivatives have been predicted by Cheng et al. using isodesmic reactions.[30] Their results show that the calculated ΔH^0_f for the MTNI is close to the experimental value. Ju et al.[229,238] predicted the ΔH^0_f for polyazidocubanes, imidazole derivatives and pyrazole with $-NH_2$, $-NF_2$, $-N_3$ & $-NO_2$ substituents. Similarly, Zhou et al.,[239] Turker et al.,[240] Li et al.,[241] Chen et al.,[242] Lai et al.,[243] Catoire et al.,[244] etc. have used the isodesmic reactions for the ΔH^0_f prediction of different unsynthesized nitrogen-rich and aromatic compounds. Their results estimate the reliability of isodesmic reactions in the prediction of ΔH^0_f. Table 1.6 compares the predicted and experimental gas phase heat of formation and shows the reliability of isodesmic approach. Quantum mechanical calculations for the prediction of liquid, and solid phase heats of formation of energetic molecules were used by Politzer et al.,[245-247] Rice et al.,[248,249] and Abou-Rachid et al.[230,231] They have established the functional relationships between heats of vaporization, heats of sublimation, gas phase ΔH^0_f obtained from the isodesmic reactions and properties associated with quantum mechanically determined electrostatic potentials of isolated molecules.

Table 1.6: Predicted gas phase heats of formation from isodesmic reactions and their experimental values.

Compd.	Predicted ΔH^0_f(g) (kJ/mol)	Expt. ΔH^0_f(g) (kJ/mol)	Deviation (kJ/mol)
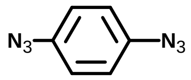	1112.1[a]	1101.0[b]	-11.1
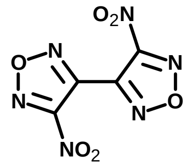	421.3[d]	422.2[e]	0.9
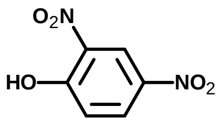	-122.1[f]	-128.3[f]	6.2
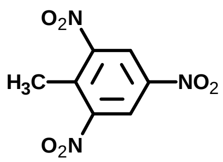	43.1[f]	51.4[f]	8.3
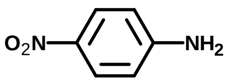	66.0[f]	67.7[f]	1.7
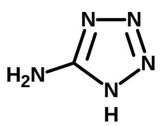	318.8[g]	323.9[h]	5.1

[a- Ref. 232; b- Ref. 106; c- Ref. 251; d- Ref. 235; e- Ref. 252; f- Ref. 242; g- Ref. 229; h- Ref. 253]

Advantages

- At low level of theory, reliable ΔH^0_f can be obtained.[244,250]
- In isodesmic reaction, experimental ΔH^0_f of the reference molecules are used and hence the accuracy of the calculation is high.
- Large size molecules can be treated easily.[232,240]
- Experimental heats of formation are available for small reference molecules.

Limitations

- Experimental values must be available for all reaction components.
- Different isodesmic reactions will predict different values for the same heat of formation.

The isodesmic reaction approach is proven to be simple and reliable method for the prediction of heats of formation for various types of compounds and hence, the gas phase heats of formation in the present study have been calculated using isodesmic approach.

1.6.3 Prediction of density

One of the most important physical properties of energetic materials that are used to initially assess potential performance in a weapon is its density.[254] Important performance parameters such as the detonation velocity and pressure are proportional to density; the velocity increases linearly with density while the Chapman-Jouguet pressure is proportional to the square of the initial density.[255,256] Density is a condensed phase property and its prediction involves challenges as it is associated with different intermolecular interactions, which affect the crystal pattern and cell volume. An increase in density is also desirable in terms of the amount of material that can be packed into volume-limited warhead or propulsion configurations. Therefore, substantial efforts have been directed toward developing a procedure that will accurately predict this property without a prior knowledge of the crystal structure. Some of the methods for a prediction of density are as following:

- Group/volume additivity
- Quantum mechanical methods
- Crystal packing calculations

Group/volume additivity has the advantage of speed, low cost and ease of use; it is truly a fast procedure requiring only a list of appropriate atom and group volumes and a hand-held calculator. Group additivity approach utilizes atom and group volumes to estimate a molecular volume (volume additivity) for a substance which when combined with the molecular mass provides an estimate of the crystal density. Shreeve et al. discussed the quantitative impact of strong hydrogen bonding on the densities of energetic materials using atom/group additivity method.[257] They have suggested different corrections for molecular volume containing $NHNO_2$, NH_2 or NH group and N-oxide (N-O) energetic materials. Keshavarz introduced a group additivity method to predict the crystal densities of the nitroaromatic explosives.[258] He has classified the compounds according to functionalities present in their molecular skeleton such as azido, nitro, amino, hydroxyl or aromatic and correlations were given for the prediction of crystal density. Researchers in high energy materials field have widely used the group/volume additivity methods due to the speed and low cost associated with this method.[163,240,259,260]

Limitations

- Group additivity methods do not account for molecular conformation and isomerization. That is, it yields the same density values for different isomers or conformations of the same compound or even for different compounds with the same functional group composition, and ignores the density differences due to crystal polymorphism. For example, group additivity approach predicts density 1.58 g/cm^3 for ortho, meta and para isomers of dinitrobenzene, while their experimental values are 1.56, 1.57 and 1.63 g/cm^3, respectively.
- Inter and intra-molecular interactions and hydrogen bonding in the compounds are not accounted.

- Effect of steric hindrance, conjugation, and ring systems is not considered.

Quantum mechanical methods are widely used for the prediction of densities. Studies have indicated that, when the average molar volume (V) estimated by the Monte Carlo method based on 0.001 electrons/bohr^3 density space, the theoretical molecular density (ρ = M/V, where M is the molecular weight) is comparable to the experimental crystal density. It is worth noting that the average volume used here should be the statistical average of at least 100 volume calculations.[261-263] Most of the research groups used this approach to predict density using different correlations and approximations. Rice et al. predicted a quantum mechanically based procedure for estimation of crystal densities of neutral and ionic crystals.[264,265] Klapotke et al. used the semiempirical PM3/VSTO-3G computations to estimate the highest possible density in the crystalline state of nitramine based high energy materials.[266] Molecular volume of each molecule was calculated but it was found that calculated molecular volumes were sensitive towards distortion of the molecular structure and lowest energy isomer should be selected. Xiao et al.[267] reported the crystalline densities of energetic nitramines based on the quantum chemical calculations. Density functional theory (DFT) with different basis sets and various semiempirical molecular orbital (MO) methods have been employed to predict the molecular volumes of acyclic, monocyclic, and polycyclic molecules. Reliability of this method was demonstrated by experimental verification of the calculated data, which seems to be of essential interest and significance. Comparisons between the calculated and experimental densities suggest that quantum mechanical method is economical for predicting the solid-state densities of the organic nitramines, (especially for the monocyclic) but the densities of the compounds containing the fluorine element are all overestimated.

Limitations

- The densities predicted by the semiempirical MO methods are all systematically larger than the experimental ones.[267]
- The calculation shows that if the selected basis set is larger, it will expend more CPU (central processing unit) time, larger molecular volume and smaller density will be obtained.[268]

Molecules tend to exhibit polymorphism, that is, they crystallize in many modifications, as a result of the physical conditions and the manner in which the crystals are obtained. The structure of a molecular crystal is efficiently mathematically defined by specifying the content of the unit cell and the values of the unit cell parameters; that is, the lengths of the unit cell vectors (a, b, and c) and the angles between them (α, β, and γ). The content of the unit cell is specified by the coordinates of the asymmetric unit and by the space group. Therefore, to find the most probable crystal structures, it may at first appear that all possible space groups (230 in total) must be searched with different numbers of molecules in the asymmetric unit, a very time-consuming process. It is well known that among the 230 space groups quite a small fraction is typical of organic crystals. It has been found that over 80% organic compounds crystalline in 10 typical space groups ($P2_1/c$, $P\text{-}1$, $P2_12_12_1$, $P2_1$, $C2/c$, $Pbca$, $Pna2_1$, $Pbcn$, Cc, and $C2$).[269,270] Hence, the approach was based on the generation of possible packing arrangements in these space groups to search for the low-lying minima in lattice energy surface. The different force fields such as dreiding, pcff, compass, cvff, and universal can be used to predict the density. These aspects are not found in volume additivity approaches.[271] Table 1.7 compares the predicted and experimental densities of different energetic materials and shows the reliability of crystal packing calculations.

Table 1.7: The experimental and predicted densities of the different compounds using crystal packing calculations.[275]

Name	Compd.	Experimental density (g/cm^3)	Predicted density (g/cm^3)	% Deviation
TNAZ	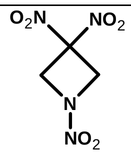	1.84	1.79	2.70
RDX	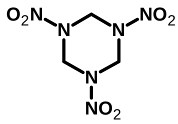	1.80	1.78	1.11
1,2-Dinitrocyclopropane	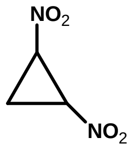	1.58	1.60	1.27
2,4-Dinitrobenzoic acid	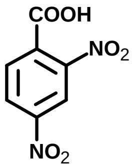	1.68	1.67	0.59
1,3,5-Trinitrobenzene	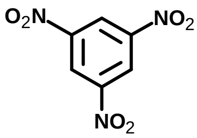	1.73	1.72	0.57
Keto-RDX or K-6	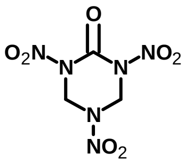	1.90	1.93	1.58

The possible crystal polymorph has been predicted using crystal packing calculations as implemented in polymorph module of the Material Studio by the different steps:

- *Packing*: During the Packing step the contents of the asymmetric unit are packed into a crystal of a given space group symmetry. The packing algorithm (performs a search for the lowest minima of the energy function of molecular crystals) modifies cell parameters and the orientation and position of the fragments in the asymmetric unit cell to generate thousands of trial packings. A Monte Carlo Simulated annealing procedure is applied to select potential low energy packings efficiently. The first step of a polymorph prediction sequence is a Monte Carlo simulation of the thermodynamic movement of the system for each selected space group. The simulation consists of two phases, heating and cooling, and is thus termed simulated annealing. The result of the packing step is a sequence of unoptimized or pre-optimized crystal structures which sample the phase space of crystal packing arrangements for the specified asymmetric unit cell contents and space group. The Packing step generates a large number of raw, high-energy, low-density crystal structures. At this stage the energy provides unreliable measure of the stability of the optimized structure. In addition, there may be no obvious relationship between the similarity of these structures and those of the optimized structures.

- *Clustering*: The Polymorph prediction sequence potentially outputs large numbers of structures for each space group, which include unfavorable high-energy structures and clusters of many very similar structures. The Clustering allows to find clusters of duplicate crystal structures and to retain the lowest energy representative of a cluster only, discarding the rest.
- *The geometry optimization*: The packing step of a Polymorph prediction generates a large number of unoptimized crystal structures. Polymorph geometry optimization is based on reducing the magnitude of calculated forces and stresses until they become smaller than defined convergence tolerances. Geometry optimization is done using the atomic coordinates and possibly the cell parameters, are adjusted until the total energy of the structure is minimized. In

general, therefore, the optimized structure corresponds to a minimum in the potential energy surface.

- *Clustering*: Clustering at this point is similar to the second step and it is to find similar clusters of crystal structures and to retain the lowest energy representative of the cluster.
- The final structures are ranked according to lattice energy. By analyzing the final trajectory of prediction of molecular packing, the packing will be arranged in their ascending energies, and the packing with the lowest energy was selected as the most possible packing in this space group.

Xiao et al.[164,233,272] predicted crystal density of adamantly nitrates, polynitrohexaazaadamantanes, using polymorph packing calculations with compass and dreiding force field. The crystal packing calculations show better densities over quantum chemical calculations. Ravi et al.[273,274] used the crystal packing calculations for amino-, methyl-, and nitro- substituted 3,4,5-trinitro-1*H*-pyrazoles, polynitroazoles and fused nitroazoles. Their packing calculations reveal that predicted densities are comparable with experimental values. Densities for well-known explosives such as RDX, HMX, TNAZ, etc. using crystal packing approach were calculated by Durga Prasad et al.[275] The predicted densities were closest to the experimental densities with a standard deviation of 0.082-0.096 g/cm^3. Further, they have extended this approach to the large number of strained and nitrogen-rich novel energetic molecules. Zhang et al.[276] reported the crystal packing of TATB and hydrogen-bonding exist in the crystal. They have extended this study to mono-layers of TATB with graphene to find their effect on energetic properties. Fujimoto et al.[277] used the packing calculations to estimate polymorphic transition frequently occurs during crystallization from the supersaturated solutions of organic compounds. Valencia et al.[278] used the crystal packing calculation to understand nitrate encapsulation within the cavity of polyazapyridinophane. Cabeza et al.[279] performed the calculations on carbamazepine in an attempt to examine the predictability and relative stability of the various polymorphs. Moreno-Calvo et al.[280] studied the relationship between crystal structure and morphology. The predicted results were comparable to the experimental morphologies.

Advantages of crystal packing method

- Due to the larger size of the molecules and too many packing structures in different space groups, an empirical force field is more suitable to perform molecular packing searching than quantum mechanics.
- Crystal packing calculations accounts the molecular conformation and isomerization.
- Inter- and intra-molecular interactions and their effect on packing efficiency of compounds are considered.
- This method calculates structures for different polymorphs and bonding patterns such as hydrogen bonding or conjugation can be considered.

The present study estimates the crystal densities using the crystal packing calculations as are superior to group additivity approaches and quantum mechanical methods.

1.6.4 Empirical methods for detonation performance

The driving force behind the development of any new materials for the defence use is, and almost certainly will be, performance. Among the criteria used in evaluating potential energetic systems is detonation velocity and pressure for explosives, refer to the pressure and the rate of propagation of the shock wave front through the material.[281] Detonation performance depends on the energy release that accompanies the decomposition and combustion processes occurring.[282] Simple reliable prediction of the performance of notional energetic materials from a given molecular structure and the known or estimated crystal density is highly desirable to chemist for the expenditure connected with the development and synthesis of new and formulation of energetic materials. Prediction of the performance of new energetic materials should be evaluated prior to their actual synthesis because it reduces the costs associated with synthesis and test as well as evaluation of the materials.

Cowan and Fickett[283] calculated detonation properties of solid explosives with the Kistiakowsky and Wilson equation of state.[284,285] These equations use the decomposition products of the explosive (N_2, H_2O, CO_2, CO, H_2, NO, C) without including the oxygen balance and density of the explosive. Keshavarz et al. introduced a method for estimating the detonation velocity and pressure of large class of CHNO explosives based elemental composition and specific structural groups.[286] The calculation of detonation parameters involves only elemental composition and the number of special structural groups without using heat of formation of explosive. This correlation requires no prior knowledge of any measured, estimated or calculated physical, chemical or thermochemical properties of explosive and assumed detonation products. Correlation derived by Keshavarz for the calculation of detonation velocity and pressure was given as follows,

$$\boldsymbol{D}\ \mathbf{(km/s) = 1.6439 + 3.5933\rho - 0.1326a - 0.0034b + 0.1206c + 0.0442d - 0.2768n - NRR'}$$

$$\boldsymbol{P}\ \mathbf{(kbar) = 221.53 - 20.437b_1 - 2.2538b_2 + 17.216b_3 + 16.140b_4 - 79.067C_{SSP} - 66.335n_N}$$

Where, a, b, c, d are the number of moles of carbon, hydrogen, oxygen, nitrogen, ρ is the loading density, n is adjustable parameter and -NRR' is specific group in explosives, C_{SSP} is equal to one which contain at least -N=N-, $-ONO_2$, or $-N_3$ in the molecular structure and zero in their absence, n_N is depend on number of nitro groups in the molecular structure, and b_1, b_2, b_3, b_4 are the number of moles of carbon, hydrogen, oxygen, nitrogen. This correlation has few restrictions for predicting detonation velocities of various CHNO explosives:

- Deviation from experimental data increases with non-energetic additives in the case of mixture of explosives.
- Correlation cannot be used for very high over-oxidized explosives.
- Chemical energy of detonation is not accounted.

Based on a semiempirical procedure, Keshavarz et al.[206] estimated the detonation velocities of CHNO explosives at various loading densities. It was assumed that the product composition consists almost of CO, CO_2, H_2O and N_2 for oxygen-rich explosives. In addition solid carbon and H_2 were also counted for an oxygen-lean explosive. The approximate detonation temperature, as a second needed parameter, can be calculated from the total heat capacity of the detonation products and the heat of formation of the explosive by PM3 procedure.

$$\mathbf{V_{C\text{-}J} = 0.314\ (nT_{app})^{0.5}\ \rho + 1.95}$$

Where, $V_{C\text{-}J}$ is the Chapman-Jouguet detonation velocity, ρ is the loading density, n is the number of moles of gaseous products per unit weight of explosive, and T_{app} is approximation for the detonation temperature. This method uses the theoretical treatment to the detonation products and detonation temperature.

Xiong reported the Simole method for calculating detonation parameters of explosives.[287] This method was valid for CHNO explosives and their mixtures. In order to calculate the detonation velocity and detonation pressure, chemical energy of detonation (Q), potential energy (w) and adiabatic exponent (calculated from detonation products and initial loading density) of both the commonly used explosives and components of explosive mixtures should be known. The detonation velocity and pressure were calculated by an empirical equation,

$$\boldsymbol{D} = \mathbf{aQ^{1/2} + bw\rho}$$

$$\boldsymbol{P} = \frac{\rho\ \mathbf{D^2\ x\ 10^{-5}}}{\mathbf{t + 1}}$$

Where, D is the detonation velocity (m/s), ρ is the initial density (g/cm^3), Q is the heat of detonation (cal/g), w is the potential energy and the constants a = 67.6, b = 243.2, P is the detonation pressure (kbar) and t is the adiabatic exponent depend on initial density and detonation products.

Limitations

- Need the experimental data for the detonation products, specific heat at constant volume and pressure for the calculation of adiabatic exponent.
- Compounds with positive or negative oxygen balance require separate calculation for adiabatic exponent and more complicated.
- Valid only for CHNO explosives.

The Stine method is simple method for the calculation of detonation performance based on the molecular composition of the pure or mixture of explosive.[290-292] The Stine method used for the estimation of detonation velocity D (m/s) and detonation pressure P (GPa) by following expressions:

$$\boldsymbol{D} = \mathbf{D_0} + \frac{\boldsymbol{d}\ [\mathbf{c_1 n_C + c_2 n_N + c_3 n_O + c_4 n_H + c_5\ (\Delta \boldsymbol{H}^0_{\boldsymbol{f}\mathbf{solid}})}]}{\boldsymbol{M}}$$

$$\boldsymbol{P} = \mathbf{0.26}\boldsymbol{d}\mathbf{D^2}$$

Where, D is the detonation velocity in m/s, P is detonation pressure in GPa, d is the density (g/cm^3) of the molecular system, M is the molecular mass, D_0 and c_i (i = 1, 2, 3, 4, 5) are the characteristic velocity of the void assumed equal to 3.69 km/s and coefficients respectively. The coefficients c_i (c_1 = -13.85, c_2 = 37.74, c_3 = 68.11, c_4 = 3.95 and c_5 = 0.1653) are provided using the least-square sense technique, $\Delta H^0_{f\,\mathrm{solid}}$ is the solid phase heat of formation in kJ/mol and n_C, n_N, n_O, and n_H are numbers of C, N, O, and H atoms present in the molecule, respectively. Stine method is depend on number of C, H, N, and O, density, heat of formation and coefficient defined from least-square method and hence did not account the detonation products and their chemical energy of detonation. According to Stine,[293] the detonation velocity and pressure of a pure compound and that of mixture are identical if the densities, ΔH^0_f and atomic compositions are same.

Limitations

- Stine method overestimates the detonation velocities and pressures in few of the cases viz. energetic furazans.[232]
- Stine method is depend on number of C, H, N, and O, density, heat of formation and coefficient defined from least-square method, hence did not account the detonation products and their chemical energy of detonation.

Kamlet and Jacobs[255,256] estimated the detonation properties CHNO explosives by means of relatively simple empirical equations. These equations imply that the mechanical properties of the detonation depend only on the number of moles of detonation gases per unit weight of explosive, the average molecular weight of these gases, the chemical energy of the detonation reaction, and the loading density. Explosive compound of composition, $C_aH_bN_cO_d$, in which there is at least enough oxygen to convert hydrogen to H_2O but no more than is also required to convert carbon to CO_2, the H_2O-CO_2 arbitrary calls for the formation of detonation products according to the following expression:

$$C_aH_bN_cO_d \longrightarrow 0.5c\ N_2 + 0.5b\ H_2O + (0.5d + 0.25b)\ CO_2 + (a - 0.5d + 0.25b)\ C$$

It follows then that,

$$N_{arb} = \frac{2c + 2d + b}{48a + 4b + 56c + 64d}$$

$$M_{arb} = \frac{56c + 88d - 8b}{2c + 2d + b}$$

$$Q_{arb} = \frac{28.9b + 47.0(d - b/2) + \Delta H^0_{f\ \mathrm{Explosive}}}{12a + b + 14c + 16d}$$

Where in above equations, N_{arb} is the moles of gaseous detonation products per gram of explosives, M_{arb} is average molecular weights of gaseous products, Q_{arb} is chemical energy of detonation, a, b, c and d are the number of C, H, N and O in the compound and ΔH^0_f is the heat of formation of explosive. The empirical equations predicted to estimate the values of detonation velocity and pressure for the high energy materials containing CHNO as following equations:

$$\mathbf{D = 1.01(NM^{1/2}Q^{1/2})^{1/2}(1 + 1.30\rho_o)}$$

$$\mathbf{P = 1.55\rho_o^{\ 2}\ (NM^{1/2}Q^{1/2})}$$

Where in above equations D is detonation velocity (km/s), P is detonation pressure (GPa), N is moles of gaseous detonation products per gram of explosives, M is average molecular weights of gaseous products, Q is chemical energy of detonation (kJ/mol) defined as the difference of the ΔH^0_f between products and reactants, and ρ_o

is the density of explosive (g/cm^3). Values of N, M, and Q estimated from the H_2O-CO_2 arbitrary decomposition assumption, so that the calculations require no other input information than the explosive elemental composition, heat of formation and loading density. Further, it is proved that detonation velocities and pressures calculated with Kamlet-Jacobs method are closer to experiment than the Stine method.[232] Table 1.8 compares the calculated detonation velocity (*D*) and pressure (*P*) for the energetic materials with different methods.

Advantages

- Accuracy of the results is high, as it accounts the decomposition products of explosives.
- Simple method for application to CHNO explosives.

Table 1.8: The calculated detonation velocity (D) and pressure (P) for the energetic materials with different methods.

Compd.	Keshavarz approach[a]		Simole method[b]		Stine method		Kamlet-Jacobs method[c]		Expt.[a]	
	D	*P*	*D*	*P*	*D*	*P*	*D*	*P*	*D*	*P*
RDX	8.75	34.1	8.74	35.2	8.79	36.2	8.74	34.2	8.75	34.7
HMX	9.09	39.0	9.09	39.4	9.02	40.0	9.10	38.9	9.10	39.3
TNT	6.93	21.0	6.96	20.2	6.90	20.4	6.95	20.0	6.95	19.0
TATB	7.76	26.0	7.88	29.0	7.74	32.1	7.80	30.2	7.86	31.5
PETN	8.27	33.7	8.54	34.0	8.44	30.3	8.35	33.2	8.30	33.5

a- Ref. 288, 289; b- Ref. 287; c- Ref. 256; *D* in km/s and *P* in GPa.

In the present study, the detonation parameters (*D* and *P*) are calculated using the Kamlet-Jacobs equations. These equations account the gaseous detonation products per gram of explosives, molecular weights of gaseous products, and chemical energy of detonation; hence improve the accuracy of the calculation.

1.6.5 Assessment of thermal stability

Stability of the energetic compounds is the prime importance for the practical interest and safe handling of the explosive material. Explosives with improved high-temperature properties are usually termed as "heat-resistant" or "thermally stable" explosive. The thermal stability of energetic material determines its applicability for practical purpose. Nitro compounds have received remarkable attention because of their ability to withstand the high temperatures and low pressures encountered in space environments. From the analysis of the structures of thermally stable explosives, it appears that introduction of amino groups and conjugation, condensation with azole rings, salt formation etc., are general approaches to improve thermal stability to explosive molecules.[294-296] The well known methods used for the prediction of thermal stability[297-299] are:

- Bond dissociation energy (BDE)
- Nucleus independent chemical shift (NICS)

Generally, in nitro explosives, X-NO_2 (X= C, N, O) is the weakest bond and cleaves initially upon initiation. The bond dissociation energy (BDE) is the difference between the zero point energy corrected total energies at 0K of the parent molecules and those of the corresponding radicals in the unimolecular bond dissociation.[300,301] The strength of the weakest bond of explosive molecule plays an important role in the initiation event. The smaller the BDE, weaker the bond is. In the present study, BDE has been calculated using this equation:

$$\mathbf{BDE_{298}(R_1\text{-}R_2) = [\Delta_f H_{298}(R_1) + \Delta_f H_{298}(R_2)] - \Delta_f H_{298}(R_1\text{-}R_2)}$$

Where, R_1-R_2 is the neutral molecule, R_1 and R_2 are the corresponding radicals, $\Delta_f H_{298}(R_1)$, $\Delta_f H_{298}(R_2)$, and $\Delta_f H_{298}(R_1\text{-}R_2)$ are the heats of formation at 298 K of R_1, R_2, and R_1-R_2, respectively. According to the criteria of HEDMs, BDE should be higher than 80-120kJ/mol.[157,302] The designed compounds possessing X-NH_2 or X-N_3 substituents, where BDEs cannot be calculated for these bonds, thermal stability has been estimated using nucleus independent chemical shift.

Nucleus independent chemical shift (NICS) was defined by Schleyer et al.[303,304] as the negative value of the absolute magnetic shielding computed in centers of ring or 1 Å above the molecular plane. Schleyer advocated the use of the absolute magnetic shielding computed at the geometric center of the ring. NICS may be useful indicator of aromaticity that usually correlates well with the energetic, structural and magnetic criteria. Negative NICS values denote aromaticity (e.g. -11.5ppm for benzene and -11.4ppm for naphthalene) and positive NICS values denote anti-aromaticity (e.g. 28.8ppm for cyclobutadiene) while small NICS values indicate non-aromaticity (e.g. -2.1ppm for cyclohexane, -1.1ppm for adamantane). Nucleus independent chemical shifts (NICS) at the ring centre of the different rings in the gas phase were predicted using the gauge invariant atomic orbitals (GIAO) method. It must first be remarked that there is no way to compare these computed NICS values with an experimental measurement, because there is no nucleus (typically) at the center of aromatic rings. Schleyer recommended the use of diffuse functions for the evaluation of NICS. NICS is a local measure, a magnetic property at a single point. There are concerns over using such a local property to evaluate the global nature of a molecule, such as whether it is aromatic or not. This is particularly troubling when the molecule has multiple rings. Negative values of NICS indicate shielding presence of induced diatropic ring currents understood as aromaticity at specific point. Recently, Turker et al. reported the NICS study for the nitro derivatives of pyridine[305] and nitrotriazines[240] to judge the aromatic stabilities. The results are proven to be very useful toward the stabilities of these energetic compounds via π-electron delocalization and conjugation.

1.6.6 Sensitivity correlations

The impact sensitivity of an energetic material is a measure of the tendency of the material to undergo an explosive detonation when experiencing an impact.[306] Experimentally, impact tests involve subjecting a sample to the impact of the standard weight falling from different heights. Thus, a height of 50% probably in causing an explosion (h_{50}) was measured during hitting of sample by a hammer (typically, with a 2.5 kg weight).[307] The drop height impact sensitivity test is relatively easy to implement, but often provides experimental results with a low degree of reproducibility. Materials having smaller h_{50} values are considered more sensitive to impact because less kinetic energy results in reaction in the drop weight impact test. For the scientist developing notional energetic materials it would therefore be useful to have a tool with which to screen the impact sensitivity of a candidate energetic material. Some of the attempts made for the development of sensitivity correlation with,

- Molecular structure and vibrations in the molecule
- Electrostatic surface potentials
- Band gap between the HOMO and LUMO
- Charge on nitro group

Cho et al. used a neural network approach to identify descriptors of molecular structure that were a prior correlated to impact sensitivity (log10 h_{50} %) for a series of

234 energetic materials.[308] They have used 39 descriptors based on constitutional and quantum mechanical in nature. The quantum mechanical descriptors were computed using the AM1 semiempirical method. Subsets of the descriptors (treated as regression variables) were correlated into regression equations using neural network architectures with either one or two hidden layers in the architecture. Cho et al. made several comparisons to a similar study that was conducted by Legendre et al. Legendre also used a neural network approach to find correlations between subsets of 39 constitutional and AM1 quantum mechanical descriptors and impact sensitivities (log10 h50%)[309] for 204 energetic materials, coming from the same molecular database. The work of Cho and Legendre assumes that from relatively few descriptors of molecular structure one can develop predictive tools for impact sensitivity. Their work also assumes that those descriptors are among relatively small groups of constitutional or quantum mechanical descriptors. Their assumptions are not entirely unreasonable given the good fits to impact sensitivity observed. Their success is likely due, in a gross sense, to the nature of what is known about the relationship between molecular structure and impact sensitivity (i.e. increasing the number of nitro groups in a molecule generally tends to increase its sensitivity to impact). The use of various assumptions and constitutional or quantum mechanical descriptors restricts its use for application in sensitivity correlation.

Hong et al.[310] correlated the normal mode vibrations and impact sensitivities of some secondary explosives. They have evaluated frequencies of normal mode vibrations of various nitroaromatic compounds by means of density functional theory (DFT). Their results reveals that the number of low frequency vibrational modes shows a linearly correlation to the impact sensitivities derived from drop hammer tests. It can be predicted that the energy transfer rates are directly proportional to the number of vibration states in the doorway region and that the energy transfer rates linearly correlated to the impact sensitivities in these secondary explosives that have similar molecular structure and similar molecular weight. Ramaswamy[311] has applied mesoscopic approach to energetic materials sensitivity. Mesoscopic physics refers to the physics of condensed structures of sizes ranging from a few atomic radii or single molecules to several microns. Mesoscopic phenomena and observations include the formation of initiation sites at the atomic and molecular levels, and their propagation to form submicron reaction sites, which expand and combine to produce micron-scale hot spots.

Politzer et al.[312-314] established correlations between the quantum chemically determined electrostatic potential surrounding an isolated molecule and sensitivity. The molecular and surface electrostatic potential reveals a remarkable distinction between energetic polynitro organic compounds and the great majority of other organic molecules. Table 1.9 represents the computed molecular surface potential quantities for some nitro derivatives. In contrast to organic compounds, in energetic molecules the positive surface potentials still cover the larger areas and stronger than the negative one. Politzer and Murray have proposed that the metastabilities of energetic compounds are associated with an anomalous imbalance between positive and negative surface potentials and that it can serve as a basis for correlating and predicting sensitivity. Imbalance between positive and negative surface potentials depends on mutual effects of electron-withdrawing and electron-donating functional groups present in the energetic molecule. In the aromatic systems, resonance effects will stabilize the molecule (i.e. will act in opposition to this imbalance), while in aza-aromatic systems this stabilization could be weaker, and in aliphatic compounds such stabilization is missing. Therefore, the correlations found by Politzer and Murray is restricted to specific classes (i.e. nitroaromatics, nitroheterocycles and nitramines).

Table 1.9: Computed molecular surface potential quantities for some nitro derivatives.[316]

Compd.	Π (kcal/mol)	V^{+}_{s} (kcal/mol)	V^{-}_{s} (kcal/mol)	σ^{2}_{+} (kcal/mol)^2	σ^{2}_{-} (kcal/mol)^2
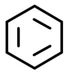	4.9	4.8	-5.0	7.1	9.2
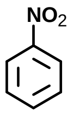	12.3	10.4	-22.1	16.9	105.2
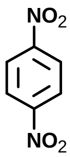	16.5	17.9	-17.2	29.3	61.9
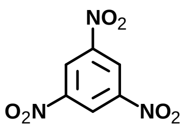	19.5	23.9	-15.3	109.0	55.3
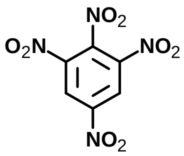	21.4	27.9	-13.6	214.0	46.0

Π, V^{+}_{s}, V^{-}_{s}, σ^{2}_{+} and σ^{2}_{-} are the average deviation in the electrostatic potential on a molecular surface, positive and negative values of electrostatic potential, positive and negative variance on electrostatic potential, respectively.

Rice and Hare[315] developed a hybrid model of prediction of impact sensitivity of CHNO explosives and continued to findings of Politzer. They adopted the approximation to the electrostatic potentials and bond midpoints, statistical parameters of these surface potentials, and generalized interaction properties function or calculated heats of detonation. They showed that patterns of charge on the electrostatic potentials for isosurfaces of electron densities surrounding energetic molecules are useful guides in assessing the degree of sensitivity of explosive to impact. The most sensitive molecules have regions of very positive electrostatic potential localized over covalent bonds. This localized region of electron deficiency is not apparent in the insensitive explosives. They pointed out that the build-up of positive charge over covalent bonds within the molecular framework of energetic materials was related to the degree of impact sensitivity.

Edwards et al.[317] compared the correlation of impact sensitivities to various quantum mechanically derived quantities, such as the energies of the highest energy occupied molecular orbital (HOMO), lowest energy unoccupied molecular orbital (LUMO) and heats of detonation corresponding to various detonation reaction mechanisms. Although, coefficients of multiple determinations were not reported for all correlations examined, Edwards et al. found moderate degrees of correlation for the orbital and reaction energies investigated. They found higher degrees of correlation with quantities that describe the constitutional makeup of energetic materials (number of NO_2 groups) than with orbital energies. Xu et al. analyzed relationship between impact sensitivities and electronic structures of some nitro compound.[318] Analysis of the band gap between highest occupied molecular orbital (HOMO) and lowest unoccupied molecular orbital (LUMO) has been suggested relative to the sensitivity of the material.[229,319] In general, the band gap (ΔE) between HOMO and LUMO is used as criterion to predict sensitivity of the material, and the smaller the ΔE, easier the electron transits and larger the sensitivity.

Zhang et al.[320] computed the total charge on nitro groups ($-Q_{NO_2}$) as the sum of individual atomic charges of each of the atoms in the group. In most of the explosives, nitro groups are their common parts and the root for their detonation properties. As a matter of fact, the sign and quantity of $-Q_{NO_2}$ reflect the chemical environment of interested nitro group. The more negative nitro charges correspond to the more stable nitro compounds.[321] Secondly, for all nitro explosives in which the X-NO_2 (X= C, N, O) bond is the weakest, charge on nitro group can be regarded as a structural parameter to assess and predict the impact sensitivity.[322,323] The chemical environment of nitro group can be characterized by its charge.

Generally, covalent compounds are composed of atoms or groups that have the potential to offer or attract electrons, and they will be more stable if the atoms or groups offer or attract adequate electrons. As for nitro groups in nitro compounds, they are very strong for attracting electrons, that is, they have large potentials for attracting electrons. Hence, primary conclusion can be drawn as, the more negative charges the nitro groups have, and the more their potentials decrease, the more stable the nitro compounds become. Usually the more substituted the nitro group, the less stable the compound. Methane and its nitrated derivatives are taken as an example in Table 1.10. The introduction of nitro groups on the methane decreases the charge on nitro group, increases the C-NO_2 bond length and oxygen balance of corresponding compounds. When the number of the nitro group increases, offering electrons become more and more difficult because H atoms, which offer electrons, become fewer and fewer. Meanwhile, the nitro group's potentials to attract electrons decrease to less and less, and the compound becomes more and more unstable accordingly.

Table 1.10: Relevant calculation results of nitro substitutes of methane.[324]

Parameters	CH_3NO_2	$CH_2(NO_2)_2$	$CH(NO_2)_3$	$C(NO_2)_4$
$-Q_{NO_2}$ (e)	0.285	0.192	0.152	0.050
C-NO_2 (Å)	1.517	1.542	1.548	1.582
O.B. (%)	-39.3	15.1	37.1	48.9

Zhang found that when the most negatively charged nitro group of a compound has a net negative charge, Q_{NO2} < 0.23e that impact sensitivity was less than 40 cm. Table 1.11 summarizes the calculated charge on nitro group and h_{50} of the well-known energetic materials. The charge on the nitro group ($-Q_{NO2}$) has been considered for its correlation to impact sensitivity. The charge on nitro group can be computed as:

$$Q_{NO2} = Q_N + Q_{O1} + Q_{O2}$$

Where, Q_{NO2} is charge on the nitro group calculated by the sum of net charges on the nitrogen (Q_N) and oxygen atoms (Q_{O1} and Q_{O2}) in the nitro group.

Table 1.11: Charge on nitro group and h_{50} of the nitrobenzenes and other nitro compounds.[324]

Compd.	$-Q_{NO2}$ (e)	$h_{50\%}$ (cm)	C-NO_2 (Å)
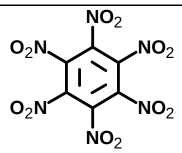	0.134	12	1.473
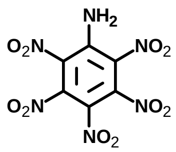	0.137	15	1.466
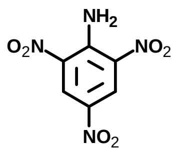	0.289	177	1.483

Previous studies prove the reliability of this method by correlating charge on nitro group and sensitivity of different well-known nitroarenes, nitroheterocycles, nitro in cage and polycyclic compounds. The present study estimates the sensitivity correlation using charge on nitro group.

1.7 Origin and objective of the present investigation

High energy materials, which have abundant chemical energy that can be released instantly to produce high pressure and high temperature effects on ambient gases, have been widely used as the main constituents of explosives. The amount of research into the development of a new type of HEM has recently increased, the aim being to synthesize a substance with enhanced properties over the benchmark explosives such as RDX, HMX, TATB, TNT, etc. The available literature classifies the known energetic materials on the basis of stability point of view as: thermally stable, high performance, melt-castable and insensitive high explosives. The high performance has always been a prime requirement in the development of explosives and the quest for the most powerful high explosives still continues and this search seems to be never ending. Along with the high performance, other important properties which decide the fate of newly developed energetic material for its practical application include sensitivity, chemical and thermal stability. The high performance and better insensitivity during its use, storage and transport are the key properties of an ideal explosive. However, these requirements are somewhat mutually exclusive. The explosives having good thermal stability and impact insensitivity usually exhibit poorer performance and vice versa.

In view of the above, present study aimed to design strained systems and nitrogen-rich energetic azoles & azines in search of high performance and insensitive energetic materials. Molecular structure containing fused and strained ring systems occupies a prominent role in high performance explosives as they possess high density and energy. The isowurtzitane and bicyclo[1.1.1]pentane cage has been tailored with different explosophores to improve energetic performance with reduced sensitivity. On the other hand, heterocycles that contain large amount of nitrogen are relatively dense, they possess higher heat of formation due to higher percentage decomposition products usually dinitrogen. The azoles including imidazole, pyrazole, triazole, and tetrazole are the natural framework for energetic materials as possesses high nitrogen content. Their performance has been optimized and improved through substituting hydrogen atoms with explosophore like nitro, amino, azido, etc. Similarly, nitrogen-rich heptazine, triazine and tetrazine have been designed with the substitution of azole rings and different explosophores to improve the energy content of these molecules. The high nitrogen content of these molecules favors their use in the energetic materials and may finds promising applications in gas generators, smoke-free pyrotechnic fuels, etc.

Significant attention has been given to prediction of energetic properties that are used to provide an initial assessment of the potential performance and stability of a material: heat of formation, density, detonation performance, thermal stability and sensitivity of the material. Computational modeling performs the screening of hypothetical energetic materials, which allow experimental researchers to expend resources only on those molecules that show promising performance and reduced sensitivity. The present study approaches the problems in following levels:

- Design of strained and nitrogen-rich molecules
- Optimization of structures with density functional methods and calculation of enthalpy of formation via isodesmic reaction approach
- Force field based crystal packing calculation for density prediction
- Prediction of key properties of an energetic material such as detonation performance, thermal stability and sensitivity using various computational approaches

- Understanding the role of explosophores such as $-NO_2$, $-NH_2$ and $-N_3$ on the energetic properties and estabilishment of structure-performance relationships
- Screening of the promising candidates for deemed applications

Performance metrics (detonation velocities and pressures) are dependent on the energy content of the charge, reflected by the heat of formation of the energetic material, and the density, which is an indicator of how much material, can be packed into the charge. Among the popular approaches such as group additivity, atomization reactions, homodesmic reaction, etc., the isodesmic reaction approach is proven to be simple and reliable method for the prediction of heats of formation. Hence, the gas phase heats of formation in the present study have been calculated using isodesmic approach. An increase in density is desirable in terms of the amount of material that can be packed into volume-limited warhead configurations and assess the potential performance. Density is predicted by the crystal structure packing calculations as it is superior to the group additive approaches. The explosive performance characteristics (detonation velocity and pressure) are evaluated by Kamlet-Jacobs empirical relations from their theoretical densities (ρ_o) and calculated heat of formation as it account the gaseous detonation products per gram of explosives, molecular weights of gaseous products, and chemical energy of detonation. Stability of the energetic compounds is of prime importance for the practical interest and safe handling of the explosive material. Approaches such as bond dissociation energy of the trigger bond and nucleus independent chemical shift are used to predict the thermal stability. The charge analysis on the nitro group and the energy difference between highest occupied molecular orbital (HOMO) and lowest unoccupied molecular orbital (LUMO) have been correlated with impact sensitivity.

The present thesis is a systematic investigation on design and structure-performance relationship studies by quantum/molecular mechanical calculations, centered on the following objectives:

- To design a high performance hexaazaisowurtzitanes & bicyclo[1.1.1]pentanes
- To study the chemistry of azoles in the design of energetic materials
- To study azines as energetic nitrogen-rich molecular framework.

1.8 References

1. Fordham, S. *High explosives and propellants*, Pergamon, Press, Oxford, 1980.
2. Bailey, A.; Murrey, S. G. *Explosives propellants and pyrotechnics*, Brassey's, London, 2000.
3. Akhavan, J. *The chemistry of explosives*, RSC Paperbacks, Cambridge, 1998.
4. Kalb, C. D. *Manual of explosives*, Biblio Bazaar, LLC, 2009.
5. Quinan, W. R. *High explosives*, Biblio Bazaar, LLC, 2009.
6. Kubota, N. *Propellants and explosives: Thermochemical aspects of combustion*, Wiley-VCH, 2007.
7. Barlow, E.; Barth, R. H.; Snow, J. E. *The pentaerythritols*, Reinhold, New York, 1958.
8. Miles, F. D. *Cellulose nitrate*, Oliver& Boyd, London, 1955.
9. Nauckhoff, S.; Bergstrom, O. *Nitroglycerine and dynamite*, *Nitroglycerin*, Sweden, 1959.
10. Agrawal, J. P.; Hodgson, R. D. *Organic chemistry of explosives*, John Willey and Sons Ltd, The Atrium, Chichester, England, 2007.

11. George, G. S.; Barsode, U. M.; Kanavade, S. A.; Mhaske, B. R. *Applied science II*, Technical publications, 2007.

12. Agrawal, J. P. *Prog. Energy Combust. Sci.* **1998**, *24*, 1.

13. Sikder, A. K.*;* Sikder, N. *J. Hazard. Mater.* **2004**, *112*, 1.

14. Badgujar, D. M.; Talawar, M. B.; Asthana, S. N.; Mahulikar, P. P. *J. Hazard. Mater.* **2008**, *151*, 289.

15. Chavez, D. E.; Tappan, B. C.*;* Mason, B. A. *Propell. Explos. Pyrotech.* **2009**, *34*, 475.

16. Chavez, D. E.; Parrish, D. A. *J. Heterocyclic Chem.* **2009**, *46*, 88.

17. Licht, H. H.; Ritter, H. *Propell. Explos. Pyrotech.* **1997**, *22*, 333.

18. Pagoria, P. F.; Lee, G. S.; Mitchell, A. R.; Schmidt, R. D. *Thermochimica Acta* **2002**, *384*, 187.

19. Xue, H.; Gao, Y.; Twamley, B.; Shreeve, J. M. *Chem. Mater.* **2005**, *17*, 191.

20. Gilbert, E. E.; Sollott, G. P. *Chem. Eng. News* **1980**, *58*, 32.

21. Gilbert, E. E. *Propell. Explos. Pyrotech.* **1980**, *5*, 15.

22. Bliss, D. E.; Christian, S. L.; Wilson, W. S. *J. Energ. Mater*. **1991**, *9*, 319.

23. Ingle, H.; Thiele. *J. Liebigs Ann. Chem*. **1895**, *287*, 233.

24. Thiele. *J. Liebigs Ann. Chem*. **1898**, *303*, 66.

25. von Herz, E. *Chem. Abstr*. **1933**, *27*, 1013.

26. Henry, R. A.; Makosky, R. C.; Smith, G. B. L. *J. Am. Chem. Soc*. **1951**, *73*, 474.

27. Hammerl, A.; Hiskey, M. A.; Holl, G.; Klapotke, T. M.; Polborn, K.; Stierstorfer, J.; Weigand, J. *J. Chem. Mater*. **2005**, *17*, 3784.

28. Miller, D. R.; Swenson, D. C.; Gillan, E. G. *J. Am. Chem. Soc*. **2004**, *126*, 5372.

29. Ye, C.; Gard, G. L.; Winter, R. W.; Syvret, R. G.; Twamley, B.; Shreeve, J. M. *Org. Lett.* **2007**, *9*, 3841.

30. Su, X.; Cheng, X.; Meng, C.; Yuan, X. *J. Hazard. Mater*. **2009**, *161*, 551.

31. Gutowski, K. E.; Rogers, R. D.; Dixon, D. A. *J. Phys. Chem. A*. **2006**, *110*, 11890.

32. Sitzmann, M. E.; Gilligan, W. H.; Omellas, D. L.; Trasher, J. S. *J. Energ. Mater*. **1990**, *8*, 352.

33. Hudlicky, M. *Chemistry of organic fluorine compounds*, 2nd ed., Halstead Press, New York, 1976.

34. Doddi, G.; Mencarelli, P.; Razzini, A.; Stegel, F. *J. Org. Chem.* **1979**, *44*, 2321.

35. Edwards, W. W.; George, C.; Gilardi, R.; Hinshaw, J. C. *J. Heterocycl. Chem*. **1992,** *29*, 1721.

36. Coburn, M. D. US Pat. 4028154, 1977.

37. Atkins, R. L.; Nielsen, A. T.; Norris, W. P. US Pat. 4248798, 1981.

38. Cho, S. G.; Cho, J. R.; Goh, E. M.; Kim, J. K.; Damavarapu, R.; Surapaneni, R. *Propell. Explos. Pyrotech*. **2005**, *30*, 445.

39. Cho, S. G.; Goh, E. M.; Cho, J. R.; Kim, J. K. *Propell. Explos. Pyrotech*. **2006**, *31*, 33.

40. Gao, H.; Ye, C. F.; Gupta, O. D.; Xiao, J. C.; Hiskey, M. A.; Twamley, B.; Shreeve, J. M. *Chem. Eur. J.* **2007**, *13*, 3853.

41. Duddu, R.; Dave, P. R.; Damavarapu, R.; Gelber, N.; Parrish, D. *Tetrahedron Lett*. **2010**, *51*, 399.

42. Dalinger, I. L.; Gulevskaya, V. I.; Kanishchev, M. I.; Shevelev, S. A.; Shkineva, T. K.; Ugrak, B. I. *Russ. Chem. Bull*. **1993**, *42*, 1063.

43. Badol, P.; Goujon, F.; Guillard, J.; Poullain, D. *Tetrahedron Lett.* **2003**, *44*, 5943.

44. Ivanov, P. A.; Latypov, N. V.; Pevzner, M. S.; Silevich, V. A. *Chem. Heterocyclic Compd*. **1976**, *12*, 1355.

45. Coburn, M. D. *J. Heterocyclic Chem*. **1968**, 5, 83.

46. Trudell, M. L.; Zelinin, A. K. *J. Heterocyclic Chem*. **1997**, *34*, 1057.

47. Boyer, J. H.; Gunasekaren, A.; Jayachandran, T.; Trudell, M. L. *J. Heterocyclic Chem*. **1995**, *32*, 1405.

48. Sinditskii, V. P.; Vu, M. C.; Sheremetev, A. B.; Alexandrova, N. S. *Thermochimica Acta*. **2008**, *473*, 25.

49. Chavez, D.; Hill, L.; Hiskey, M.; Kinkead, S. *J. Energ. Mater*. **2000**, *18*, 219.

50. Aleksandrova, N. S.; Kharitonova, O. V.; Khmelnitskii, L. I.; Kulagina, V. O.; Melnikova, T. M.; Novikov, S. S.; Novikova, T. S.; Pivina, T. S.; Sheremetev, A.; B. *Mendeleev Commun.* **1994**, 230.

51. Talawar, M. B.; Sivabalan, R.; Senthilkumar, N.; Prabhu, G.; Asthana, S. N. *J. Hazard. Mater*. **2004**, *113*, 11.

52. Coburn, M. D. US Pat. 3414570, 1968.

53. Coburn, M. D. *Chem Abstr.* 70:47505d, 1969.

54. Gunasekaran, A.; Boyer, J. H. *Heteroatom. Chem*. **1993**, *4*, 521.

55. Willer, R. L. US Pat. 4503229, 1985.

56. Moore, D. W.; Willer, R. L. *J. Org. Chem*. **1985**, *50*, 5123.

57. Du, Y.; Jiang, M.; Sun, Q.; Fu, X. Detonation properties and thermal stabilities of furazano fused cyclic nitramines, in Proc International Symposium on Pyrotechnics and Explosives, China Academic Publishers, Beijing, China. 1987, 412.

58. Sheremetev, A. B.; Aleksandrova, N. S.; Mantseva, E. V.; Dmitriev, D. E. *Mendeleev Commun*. **2000**, *10*, 67.

59. Sheremetev, A. B.; Aleksandrova, N. S.; Dmitriev, D. E. *Mendeleev Commun*. **2006**, *16*, 163.

60. Sheremetev, A. B.; Andrianov, V. G.; Mantseva, E. V.; Shatunova. E. V.; Aleksandrova, N. S.; Yudin, I. L.; Dmitriev, D. E.; Averkiev, B. B.; Antipin, M. Y. *Russ. Chem. Bull*. **2004**, *53*, 596.

61. Godovikova, T. I.; Golova, S. P.; Khmelnitskii, L. I.; Rakitin, O. A.; Vozchikova, S. A. *Mendeleev Commun*. **1993**, 209.

62. Antipin, M. Y.; Godovikova, T. I.; Golova, S. P.; Khmelnitskii, L. I.; Strelenko, Y. A.; Struchkov, Y. T. *Mendeleev Commun*. .**1994**, 7.

63. Fridman, A. L.; Ismagilova, G. S.; Nikolaeva, A. D. *Chem. Heterocyclic Compd*. **1971**, *7*, 804.

64. Berlin, J. K.; Coburn, M. D. *J. Heterocyclic Chem*. **1975**, *12*, 235.

65. Agrawal, J. P.; Mehilal; Prasad, U. S.; Surve, R. N. *New J. Chem*. **2000**, *24*, 583.

66. Agrawal, J. P.; Mehilal; Sikder, A. K.; Sikder, NIndian. *J. Eng. Mater. Sci*. **2004**, *11*, 516.

67. Kendall, R. V.; Olofson, R. A. *J. Org Chem*. **1970**, *35*, 2246.

68. Lee, G. S.; Mitchell, A. R.; Pagoria, P. F.; Schmidt, R. D. *Thermochimica Acta* **2002**, *384*, 187.

69. Drake, G. W.; Hawkins, T. W.; Hall, L. A.; Boatz, J. A.; Brand, A. J. *Propell. Explos. Pyrotech*. **2005**, *30*, 329.

70. Baryshnikov, A. T.; Erashko, V. I.; Zubanova, N. I.; Ugrak, B. I.; Shevelev, S. A.; Fainzilberg, A. A.; Laikhter, A. L.; Melnikova, L. G.; Semenov, V. V. *Bull. Russ. Acad. Sci. Chem. Ser*. **1992**, *41*, 751.

71. Bedford, C. D.; Bottaro, J. C.; George, C.; Gilardi, R.; Schmitt, R. J. *J. Org. Chem*. **1990***, 55,* 1916.

72. Dixon, D. A.; Feller, D.; Christe, K. O.; Wilson, W. W.; Vij, A.; Vij, V.; Brooke, H. D. B.; Olson, M. R.; Gordon, M. S. R. *J. Am. Chem. Soc*. **2004**, *126*, 834.

73. Adolph, H. G.; Chaykovsky, M. *J. Energ. Mater*. **1990**, *8*, 392.

74. Henry, R. A.; Willer, R. L. *J. Org. Chem*. **1988**, *53*, 5371.

75. Klapotke, T. M.; Steemann, F. X. *Propell. Explos. Pyrotech*. **2010**, *35*, 114.

76. Klapotke, T. M.; Laub, H. A.; Stierstorfer, J. *Propell. Explos. Pyrotech*. **2008**, *33*, 421.

77. Karaghiosoff, K.; Klapotke, T. M.; Mayer, P.; Piotrowski, H.; Polborn, K.; Willer, R. L.; Weigand, J. J. *J. Org. Chem*. **2006**, *71*, 1295.

78. Karaghiosoff, K.; Klapotke, T. M.; Mayer, P.; Sabate, C. M.; Penger, A.; Welch, J. M. *Inorg. Chem*. **2008**, *47*, 1007.

79. Klapotke, T. M.; Mayer, P.; Sabate, C. M.; Welch, J. M.; Weigand, J. *J. Inorg. Chem*. **2008**, *47*, 6014.

80. Xue, H.; Gao, H.; Twamley, B.; Shreeve, J. M. *Chem. Mater*. **2007**, *19*, 1731.

81. Joo, Y. H.; Shreeve, J. M. *J. Am. Chem. Soc*. **2010**, *132*, 15081.

82. Coburn, M. D. *J. Heterocycl*. Chem. **1974**, *11*, 1099.

83. Licht, H. H.; Ritter, H. *J. Heterocycl. Chem*. **1995**, *32*, 585.

84. Licht, H. H.; Ritter, H. *Propell. Explos. Pyrotech*. **1988**, *13,* 25.

85. Li, J.; Huang, Y. G.; Dong, H. S. *J. Energ. Mater*. **2005**, *23*, 133.

86. Pagoria, P. F.; Mitchell, A. R.; Schmidt, R. D.; Simpson, R. L.; Garcia, F.; Forbes, J.; Cutting, J.; Lee, R.; Swansiger, R.; Hoffman, D. M. P. resented at the Insensitive Munitions and Energetic Materials Technology Symposium, San Diego, CA. 1998.

87. Gilardi, R. X-ray crystallographic determination, Naval Research Laboratory, Washington, DC, Donald DS, US Pat. 3808209, 1974.

88. Coombes, R. G.; Millar, R. W.; Philbin, S. P. *Propell. Explos. Pyrotech*. **2000**, *25*, 302.

89. Claridge, R. P.; Hamid, J.; Millar, R. W.; Philbin, S. P. *Propell. Explos. Pyrotech*. **2004**, *29,* 81.

90. Albini, A.; Pietra, S. *Heterocyclic-N-oxides,* CRC Press, Boca Raton, FL, 1991.

91. Agrawal, J. P.; Bapat, V. K.; Mehilal; Polke, B. G.; Sikder, A. K. *J. Energ. Mater.* **2000**, *18*, 299.

92. Li, X. T.; Li, S. H.; Pang, S. P.; Yu, Y. Z.; Luo, Y. *J. Chinese Chemical Letters* **2007**, *18*, 1037.

93. Huynh, M. H. V.; Hiskey, M. A.; Hartline, E. L. *Angew. Chem. Int. Ed*. **2004**, *43,* 4924.

94. Huynh, M. H. V.; Hiskey, M. A.; Hartline, E. L.; Montoya, D. P.; Gilardi, R. *Angew. Chem. Int. Ed*. **2004**, *43*, 4924.

95. Huynh, M. H. V.; Hiskey, M. A.; Chavez, D. E.; Naud, D. L.; Gilardi, R. *J. Am. Chem. Soc*. **2005**, *127*, 12537.

96. Kessenich, E.; Polborn, K.; Schulz, A. *Inorg. Chem*. **2001**, *40*, 1102.

97. Chapyshev, S. V. *Mendeleev Commun*. **2003**, *13*, 53.

98. Gillan, E. G. *Chem. Mater*. **2000**, *12*, 3906.

99. Ye, C. F.; Gard, G. L.; Winter, R. W.; Syvret, R. G.; Twamley, B.; Shreeve, J. M. *Org. Lett*. **2007**, *9*, 3841.

100. Coburn, M. D.; Hiskey, M. A.; Lee, K. Y.; Ott, D. G.; Stinecipher, M. M. *J. Heterocyclic Chem*. **1993**, *30*, 1593.

101. Chavez, D. E.; Gilardi, R. D.; Hiskey, M. A. *Angew. Chem. Int. Ed*. **2000**, *39*, 1791.

102. Chavez, D. E.; Hiskey, M. A. *J. Heterocyclic Chem*. **1998**, *35*, 1329.

103. Frumkin, A. E.; Churakov, A. M.; Strelenko, Y. A.; Tartakovsky, V. A. *Russ. Chem. Bull*. **2006**, *55*, 1654.

104. Huynh, M. H. V.; Hiskey, M. A.; Archuleta, J. G.; Roemer, E. L.; Gilardi, R. *Angew. Chem. Int. Ed*. **2004**, *43*, 5658.

105. Gao, H. X.; Wang, R.; Twamley, B.; Hiskey, M. A.; Shreeve, J. M. *Chem. Commun*. **2006**, 4007.

106. Chavez, D. E.; Hiskey, M. A.; Gilardi, R. D. *Org. Lett*. **2004**, *6*, 2889.

107. Adam, W.; Berneveld, C.; Golsch, D. *Tetrahedron* **1996**, *52*, 2377.

108. Sagot, E.; Roux, A. L.; Soulivet, C.; Pasquinet, E.; Poullain, D.; Girard, E.; Palmas, P. *Tetrahedron* **2007**, *63*, 11189.

109. Chavez, D. E.; Gilardi, R. D. *J. Energ. Mater*. **2009**, *27*, 110.

110. Clavier, G.; Audebert, P. *Chem. Rev*. **2010**, *110*, 3299.

111. Shevelev, S. A.; Dalinger, I. L.; Shkineva, T. K.; Ugrak, B. I.; Gulevskaya, V. I.; Kanishchev, M. I. *Russ. Chem. Bull*. **1993**, *42*, 1063.

112. Vinogradov, V. M.; Dalinger, I. L.; Shevelev, S. A. *Mendeleev Commun*. **1993**, 111.

113. Tamura, Y; Minamikawa, J.; Sumoto, K.; Fujii, S.; Ikeda, M. *J. Org. Chem*. **1973**, *38*, 1239.

114. Chia, Y. T.; Simmons, H. E. *J. Am. Chem. Soc*. **1976**, *89*, 2638.

115. Carboni, R. A.; Castle, J. E.; Kauer, J. C.; Simmons, H. E. *J. Am. Chem. Soc*. **1967**, *89*, 2618.

116. Carboni, R. A.; Kauer, J. C. *J. Am. Chem. Soc*. **1967**, *89*, 2633.

117. Huynh, M. H. V.; Hiskey, M. A.; Chavez, D. E.; Gilardi, R. D. *Angew. Chem. Int. Ed.* **2005**, *44*, 7089.

118. Muthurajan, H.; Sivabalan, R.; Talawar, M. B.; Venugopalan, S.; Gandhe, B. R. *J. Hazard. Mater*. **2006**, *136*, 475.

119. Boyer, J. H.; Eck, G.; Stevens, E. D.; Subramanian, G.; Trudell, M. L. *J. Org. Chem*. **1996**, *61*, 5801.

120. Subramanian, G.; Boyer, J. H.; Trudell, M. L. *J. Org. Chem*. **1996**, *61*, 1898.

121. Mehilal; Sikder, A. K.; Sinha, R. K.; Gandhe, B. R. *J. Hazard. Mater*. **2003**, *102*, 137.

122. Atkins, R. L.; Nielsen, A. T.; Norris, W. P. US Pat. 4248798, 1981.

123. Christian, S. L.; Chafin, A. P.; Nielsen, A. T.; Atkins, R. L.; Norris, W. P.; Hollins, R. A. US Pat. 5149818, 1990.

124. Chen, B.; Ou, Y.; Wang, N. M. *Propell. Explos. Pyrotech*. **1994**, *19*, 145.

125. Coburn, M. D. *J. Heterocyclic Chem*. **1973**, *10*, 743.

126. Flippen-Anderson, J. L.; Gilardi, R. D.; Pitt, A. M.; Wilson, W. S. *Aust. J. Chem*. **1992**, *45*, 513.

127. Buncel, E.; Cohen, S.; Renfrow, R. A.; Strauss, M. J. *Aust. J. Chem*. **1983**, *36*. 1843.

128. Chapman, R. D.; Wilson, W. S.; Fronabarger, J. W.; Merwin, L. H.; Ostrom, G. S. *Thermochimica Acta* **2002**, *384*, 229.

129. Kroke, E.; Schwarz, M.; Bordon, E. H.; Kroll, P.; Noll, B.; Norman, A. D. *New J. Chem*. **2002**, *26*, 508.

130. Zheng, W.; Wong, N.; Wang, W.; Zhou, G.; Tian, A. *J. Phys. Chem. A*. **2004**, *108*, 97.

131. Pagoria, P. F.; Lee, G. S.; Mitchell, A. R.; Schmidt, R. D. *Thermochimica Acta* **2002**, *384*, 187.

132. Fried, L. E.; Manaa, M. R.; Pagoria, P. F.; Simpson, R. L. *Annu. Rev. Mater. Res*. **2001**, *31*, 291.

133. Nissan, R. A.; Wilsorn, W. S.; Gilardi, R. D. *High nitrogen eyplosives*, Part 1, AD-A285388, Naval Air Warfare Center Weapons Division China Lake, 1994.

134. Turker, L.; Varis, S. *Polycyclic Aromatic Compounds,* **2009**, *29*, 228.

135. Spear, R. J.; Norris, W. P. *Propell. Explos. Pyrotech*. **1983**, *8*, 85.

136. Norris, W. P. *7-Amino-4,6-dinitrobenzofuroxan, an insensitive high explosive*, NWC TP 6522, Naval Weapons Center, China Lake*, CA,* **1984**.

137. Pauling, L.; Sturdivant, J. H. *Proc. Natl. Acad. Sci. USA*. **1937**, *23*, 615.

138. Carroll, P. J.; Kondracki, P. A.; Wade, P. A. *J. Am. Chem. Soc*. **1991**, *113*, 8807.

139. Waddell, S. T.; Wiberg, K. B. *J. Am. Chem. Soc*. **1990**, *112*, 2194.

140. Archibald, T. G.; Baum, K.; Cohen, M. C.; Garver, L. C. *J. Org. Chem*. **1989**, *54*, 2869.

141. Chapman, R. D.; Fischer, J. W.; Hollins, R. A.; Lowe-Ma, C. K.; Nissan, R. A. *J. Org. Chem*. **1996**, *61*, 9340.

142. Borman, S. *Chem. Eng. News*. **1994**, *72*, 18.

143. Jalovy, Z.; Zeman, S.; Suceska, M.; Vavra, P.; Dudek, K.; Rajic, M. *J. Energ. Mater*. **2001**, *19*, 219.

144. Alster, J.; Eaton, P. E.; Gilbert, E. E.; Pluth, J. J.; Price, G. D.; Ravi Shankar, B. K.; Sandus, O. *J. Org. Chem*. **1984**, *49*, 185.

145. Eaton, P. E.; Wicks, G. E. *J. Org. Chem*. **1988**, *53*, 5353.

146. Marchand, A. P. *Tetrahedron* **1988**, *44*, 2377.

147. Eaton, P. E.; Gilardi, R.; Hain, J.; Kanomata, N.; Li, J.; Lukin, K. A.; Punzalan, E. *J. Am. Chem. Soc*. **1997**, *119*, 9591.

148. Eaton, P. E.; Gilardi, R.; Xiong, Y. *J. Am. Chem. Soc*. **1993**, *115*, 10195.

149. Gilardi, R. D.; Karle, J. *Chemistry of energetic Materials*, Ed. Squire, D. R.; Olah, G. A. Academic Press, San Diego, 1991.

150. Annapurna, G. S.; Madhava Sharma, G. V.; Marchand, A. P.; Pednekar, P. R. *J. Org. Chem*. **1987**, *52*, 4784.

151. Fessner, W. D.; Prinzbach, H. *Tetrahedron* **1986**, *42*, 1797.

152. Arney, Jr. B. E.; Dave, P. R.; Marchand, A. P. *J. Org. Chem*. **1988**, *53*, 443.

153. Browne, A. R.; Doecke, C. W.; Paquette, L. A.; Williams, R. V. *J. Am. Chem. Soc*. **1983**, *105*, 4113.

154. Browne, A. R.; Doecke, C. W.; Fischer, J. W.; Paquette, L. A. *J. Am. Chem. Soc*. **1985**, *107*, 686.

155. Engel, P.; Nakamura, K.; Paquette, L. A. *Chem. Ber*. **1986**, *119*, 3782.

156. Gilardi, R.; Olah G. A.; Ramaiah, P.; Surya Prakash, G. K. *J. Org. Chem*. **1993**, *58*, 763.

157. Qiu, L. M.; Gong, X. D.; Zheng, J.; Xiao, H. M. *J. Hazard. Mater*. **2009**, *166*, 931.

158. Xu, W. G.; Liu, X. F.; Lu, S. X. *J. Mol. Struct. (THEOCHEM)* **2008**, *864*, 80.

159. Gilbert, E. E.; Sollott, G. P. *J. Org. Chem*. **1980**, *45*, 5405.

160. Mohan, L.; Murray, R. W.; Rajadhyaksha, S. N. *J. Org. Chem*. **1989**, *54*, 5783.

161. Archibald, T. G.; Baum, K. *J. Org. Chem*. **1988**, *53*, 4645.

162. Ammon, H. L.; Choi, C. S.; Dave, P. R.; Ferraro, M. *J. Org. Chem*. **1990**, *55*, 4459.

163. Xu, X. J.; Xiao, H. M.; Ju, X. H.; Gong, X. D.; Zhu, W. H. *J. Phys. Chem. A*. **2006**, *110*, 5929.

164. Xu, X. J.; Zhu, W. H.; Xiao, H. M. *J. Mol. Struct. (THEOCHEM)* **2008**, *853*, 1.

165. Kashyap, R. P.; Marchand, A. P.; Sharma, R.; Watson, W. H.; Zope, U. R. *J. Org. Chem*. **1993**, *58*, 759.

166. Highsmith, T. K.; Edwards, W. W.; Wardle, R. B. US Pat. 5498711, 1996.

167. Highsmith, T. K.; Edwards, W. W.; Wardle, R. B. *Chem. Abstr*. **1996**, *125*, 14677.

168. Nielsen, A. T.; ChaWn, A. P.; Christian, S. L.; Moore, D. W.; Nadler, M. P.; Nissan. R. A.; Vanderah, D. J.; Gilardi, R. D.; George, C. F.; Flippen-Anderson, J. L. *Tetrahedron* **1998**, *54*, 11793.

169. Christe, K. O.; Wilson, W. W.; Sheehy, J. A.; Boatz, J. A. *Angew. Chem. Int. Ed*. **1999**, *38*, 2004.

170. Vij, A.; Pavlovich, J. G.; Wilson, W. W.; Vij, V.; Christe, K. O. *Angew. Chem. Int. Ed*. **2002**, *41*, 3051.

171. Butler, R. N.; Stephens, J. C.; Burke, L. A. *Chem. Commun*. **2003**, *8*, 1016.

172. Haiges, R.; Schneider, S.; Schroer, T.; Christe, K. O. *Angew. Chem. Int. Ed*. **2004**, *43*, 4919.

173. Chung, G.; Schmidt, M. W.; Gordon, M. S. *J. Phys. Chem. A* **2000**, *104*, 5647.

174. Strout, D. L. *J. Phys. Chem. A*. **2002**, *106*, 816.

175. Thompson, M. D.; Bledson, T. M.; Strout, D. L. *J. Phys. Chem. A*. **2002**, *106*, 6880.

176. Li, Q. S.; Liu, Y. D. *Chem. Phys. Lett*. **2002**, *353*, 204.

177. Li, Q. S.; Zhao, J. F. *J. Phys. Chem. A*. **2002**, *106*, 5367.

178. Bruney, L. Y.; Bledson, T. M.; Strout, D. L. *Inorg. Chem*. **2003**, *42*, 8117.

179. Zhou, H. W.; Wong, N. B.; Zhou, G.; Tian, A. *J. Phys. Chem. A* **2006**, *110*, 3845.

180. Davis, T. L.; Rosenquist, E. N. *J. Am. Chem. Soc*. **1937**, *59*, 2112.

181. Hock, H.; Hoffmann, K. A. *Chem. Ber*. **1910**, *43*, 1866.

182. Hock, H.; Hoffmann, K. A. *Chem. Ber*. **1911**, *44*, 2946.

183. Sheremetev, A. B.; Pivina, T. S.; Nitrofurazanyl moiety as an alternative to picryl one for high energy materials construction. Proc 27th Intl Ann Conf ICT, Karlsruhe, Germany, 30/1, 1996.

184. Anniyappan, M.; Talawar, M. B.; Gore, G. M.; Venugopalan, S.; Gandhe, B. R. *J. Hazard. Mater*. **2006**, *137*, 812.

185. Latypove, N. V.; Bergman, J.; Langlet, A.; Wellmar, U.; Bemm, U. *Tetrahedron* **1998**, *54*, 11525.

186. Singh, G.; Kapoor, I. P.; Tiwari, S. K.; Felix, P. S. *J. Hazard. Mater*. **2001**, *81*, 67.

187. Sorescu, D. C.; Boatz, J. A.; Thompson, D. L. *J. Phys. Chem. A* **2001**, *105*, 5010.

188. Aminov, Y. A.; Gorshkov, M. M.; Zaikin, V. T.; Kovalenko, G. V.; Nikitenko, Y. R.; Rykovanov, G. N. *Combust. Explos. Shock Waves* **2004**, *38*, 235.

189. Jensen, F. *Introduction to computational chemistry*, John Wiley & Sons, Inc, New York, 1999.

190. Schaeffer, III H. F. *Electronic structure of atoms and molecules*, Addison-Wesley, Massachusetts, USA, 1972.

191. Young, D. *Computational chemistry: A practical guide for applying techniques to real world problems*, John Wiley & Sons, Inc, New York, 2001.

192. Clark, T. A. *Handbook of computational chemistry*, John Wiley & Sons, Inc, New York, 1985.

193. Leach, A. R. *Molecular modeling principles and applications*, Pearson Education Limited, 1996.

194. Hinchliffe, A. *Molecular modeling for beginners*, John Wiley & Sons, Inc, New York, 2003.

195. Sadlej, J. *Semi-empirical methods of quantum chemistry*, Ellis Harwood, Chichester, 1985.

196. Kohanoff, J. *Electronic structure calculations for solids and molecule*, Cambridge University Press, New York, 2006.

197. Pople, J. A.; Beveridge, D. L. *Approximate molecular orbital theory*, Mc-Graw Hill Publishing Co, New York, 1970.

198. Levine, I. N. *Quantum chemistry*, Fourth Ed, Prentice Hall of India New Delhi, 2001.

199. Foresman, J. B.; *Frisch, Exploring chemistry with electronic structure methods*, II Ed, Gaussian Inc Pittsburgh, PA, 1996.

200. Hohenberg, P.; Kohn, W. *Phys. Rev*. **1964**, *136*, B864.

201. Hohenberg, P.; Kohn, W.; Sham, L. J. *Advances in quantum chemistry*, Vol. 21, Academic Press, 1990.

202. Kohn, W.; Sham, L. J. *Phys. Rev*. **1965**, *140*, A1133.

203. Perdew, J. P. *Phys. Rev. B*. **1986**, *33*, 8822.

204. Lee, C.; Yang, W.; Parr, R. G. *Phys. Rev. B*. **1988**, *37*, 785.

205. Pople, J. A.; Head-Gorden, H.; Fox, D. J.; Raghavachari, K.; Curtiss, L. A. *J. Chem. Phys*. **1989**, *90*, 5622.

206. Keshavarz, M. H.; Pouretedal, H. R. *Propell. Explos. Pyrotech*. **2005**, *30*, 105.

207. Keshavarz, M. H. *Thermochemica Acta* **2005**, *428*, 95.

208. Keshavarz, M. H. *Indian J. Eng. Mater. Sci*. **2005**, *12*, 158.

209. Reid, R. C.; Prausnitz, J. M.; Poling, B. E. *The properties of gases and liquids*, 4thed, McGraw-Hill, New York, 1987, 154.

210. Keshavarz, M. H. *J. Hazard. Mater*. **2006**, *136*, 145.

211. Keshavarz, M. H. *J. Hazard. Mater*. **2006**, *136*, 425.

212. Curtiss, L. A.; Raghavachari, K.; Redfern, P. C.; Pople, J. A. *Chem. Phys. Lett*. **1997**, *270*, 419.

213. Redfern, P. C.; Zapol. P.; Curtiss. L. A.; Raghavachari, K. *J. Phys. Chem. A* **2000**, *104*, 5850.

214. Curtiss, L. A.; Raghavachari, K.; Trucks, G. W.; Pople, J. A. *J. Chem. Phys*. **1991**, *94*, 7221.

215. Curtiss, L. A.; Raghavachari, K. *Quantum mechanical electronic structure calculations with chemical accuracy*, Langhoff, S. R.; Ed, Kluwer: Dordrecht, The Netherlands, 1995.

216. Raghavachari, K.; Curtiss, L. A. *Modern electronic structure theory*, Yarkony, D. R. Ed. World Scientific: Singapore, 1995.

217. Duan, X. M.; Song, G. L.; Li, Z. H.; Wang, X. J.; Chen. G. H.; Fan, K. N. *J. Chem*. *Phys*. **2004**, *121*, 7086.

218. Hehre, W. J.; Ditchfield, R.; Radom, L.; Pople, J. A. *J. Am. Chem. Soc*. **1970**, *92*, 4796.

219. George, P.; Trachtman, M.; Bock, C. W.; Brett, A. M. *Tetrahedron* **1976**, *32*, 317.

220. Cioslowski, J.; Liu, G.; Piskorz. P. *J. Phys. Chem. A* **1998**,*102*, 9890.

221. George, P.; Trachtman, M.; Bock, C. W.; Brett, A. M. *Theor. Chim. Acta* **1975**, *38*, 121.

222. Hess, B. A.; Schaad, L. J. *J. Am. Chem. Soc*. **1983**, *105*, 7500.

223. Chesnut, D. B.; Davis, K. M. *J. Comput. Chem*. *18*, 584.

224. Chen, Z. X. ; Xiao, J. M. ; Xiao, H. M. ; Chiu, Y. N. *J. Phys. Chem. A* **1999**, *103*, 8062.

225. Sivaramakrishnan, R.; Tranter, R. S.; Brezinsky, K. *J. Phys. Chem. A* **2005**, *109*, 1621.

226. Raghavachari, K.; Stefanov, B. B.; Curtiss, L. A. *Mol. Phys*. **1997***,* 91, 555.

227. Raghavachari, K.; Stefanov, B. B.; Curtiss, L. A. *J. Chem. Phys*. **1997**, *106*, 6764.

228. Petersson, G. A.; Malick, D. K.; Wilson, W. G.; Ochterski, J. W.; Montgomery, Jr. J. A.; Frisch, M. J. *J. Chem. Phys.* **1998**, *109*, 10570.

229. Li, Y. F.; Fan, X. W.; Wang, Z. Y.; Ju, X. H. *J. Mol. Struct. (THEOCHEM)* **2009**, *896*, 96.

230. Rachid, H. A.; Song, Y.; Hu, A.; Dudiy, S.; Zybin, S. V.; Goddard III, W. A. *J. Phys. Chem. A* **2008**, *112*, 11914.

231. Jaidann, M.; Roy, S.; Rachid, H. A.; Lussier, L. S. *J. Hazard. Mater*. **2010**, *176*, 165.

232. Wei, T.; Zhu, W.; Zhang, X. W.; Li, Y. F.; Xiao, H. M. *J. Phys. Chem. A* **2009**, *113*, 9404.

233. Xu, X. J.; Zhu, W. H.; Gong, X. D.; Xiao, H. M. *Sci. China Ser. B Chem*. **2008**, *51*, 427.

234. Wang, G.; Xiao, H. M.; Ju, X. H.; Gong, X. D. *Propell. Explos. Pyrotech.* **2006**, *31*, 361.

235. Ju, X. H.; Ji, G. F.; Xiao, H. M. *J. Phys. Chem. A* **2010**, *114*, 603.

236. Xu, X. J.; Xiao, H. M.; Ju, X, H.; Gong, X. D.; Zhu, W. H. *J. Phys. Chem. A* **2006**, *110*, 5929.

237. Zhu, W. H.; Zhang, X. W.; Wei, T.; Xiao, H. M. *J. Mol. Struct*. (*THEOCHEM)* **2009**, *900*, 84.

238. Ju, X. H.; Wang, X.; Bei, F. L. *J. Comput. Chem*. **2005**, *26*, 1263.

239. Zhou, Y.; Long, X. P.; Shu, Y. J. *J. Mol. Model.* DOI: 10.1007/s00894-009-0605-z, **2010**.

240. Turker, L.; Atalar, T.; Gumus, S.; Camur, Y. *J. Hazard. Mater*. **2009**, *167*, 440.

241. Li, X. H.; Zhang, R. Z.; Yang, X. D.; Zhang, H. *J. Mol. Struct. (THEOCHEM)* **2007**, *815*, 151.

242. Chen, P. C.; Chieh, Y. C.; Tzeng, S. C. *J. Mol. Struct. (THEOCHEM)* **2003**, *634*, 215.

243. Lai, W. P.; Lian, P.; Yu, T.; Chang, H. B.; Xue, Y. Q. *Comput. Theor. Chem*. **2011**, *963*, 221.

244. Osmont, A.; Catoire, L.; Gokalp, I.; Yang, V. *Combust. Flame* **2007**, *151*, 262.

245. Murray, J. S.; Politzer, P. *Quantitative treatment of solute/solvent interactions*, (Politzer, P.; Murray, J. S. Eds) Theoretical and computational Chemistry, Vol 1, Elsevier Scientific, Amsterdam, 1994.

246. Politzer, P.; Murray, J. S.; Grice, M. E.; DeSalvo, M.; Miller, E. *Mol. Phys*. **1997**, *91*, 923.

247. Politzer, P.; Murray, J. S. *J. Phys. Chem. A* **1998**, *102*, 1018.

248. Rice, B. M.; Pai, S. V.; Hare, J. *Combust. Flame*. **1999**, *118*, 445.

249. Rice, B. M.; Byrd, E. F. C. *J. Mater. Res*. **2006**, *21*, 2444.

250. Su, X. F.; Cheng, X. L.; Ge, S. H. *J. Mol. Struct. (THEOCHEM)* **2009**, *895*, 44.

251. Singh, R. P.; Gao, H. X.; Meshri, D. T.; Shreeve, J. M. *Struct. Bonding (Berlin)* **2007**, *125*, 35.

252. Sheremetev, A. B.; Kulagina, V. O.; Aleksandroval, N. S.; Dmitrive, D. E.; Strelenko, Y. A.; Lebedev, V. P.; Matyushin, Y. N.*; Propell. Explos. Pyrotech.* **1998***, 23*, 142.

253. Pedley, J. B.; Rylance, T. *Computer analyzed thrmochemical data: Organic and organometallic compounds,* University of Sussex, Brighton, 1977.

254. Mader, C. L. *Organic energetic compounds*, Markinas PL (ed), Nova Science Publishers, Commack, NY, 1966.

255. Kamlet, M. J.; Jacobs, S. J. *J. Chem. Phys*. **1968**, *48*, 23.

256. Kamlet, M. J.; Dickinson, C. *J. Chem. Phys*. **1968**, *48*, 43.

257. Ye, C. F.; Shreeve, J. M. *J. Chem. Eng. Data* **2008**, *53*, 520.

258. Keshavarz, M. H. *J. Hazard. Mater*. **2007**, *145*, 263.

259. Wang, G. X.; Xiao, H. M.; Ju, X. H.; Gong, X. D. *Propell. Explos. Pyrotech*. **2006**, *31*, 361.

260. Ju, X. H.; Wang, X.; Bei, F. L. *J. Comput. Chem*. **2005**, *26*, 1263.

261. Qiu, L.; Xiao, H. M.; Gong, X. D.; Ju, X, H.; Zhu, W. H. *J. Phys. Chem. A* **2006**, *110*, 3797.

262. Wang, G. X.; Shi, C. H.; Gong, X. D.; Xiao, H. M. *J. Phys. Chem. A* **2009**, *113*, 1318.

263. Jalbout, A. L. *J. Mol. Struct. (THEOCHEM)* **2003**, *624*, 81.

264. Rice, B. M.; Hare, J. J.; Byrd, E. F. C. *J. Phys. Chem. A* **2007**, *111*, 10874.

265. Rice, B. M.; Sorescu, D. C. *J. Phys. Chem. B* **2004**, *108*, 17730.

266. Klapotke, T. M.; Ang, H. G. *Propell. Explos. Pyrotech*. **2001**, *26*, 221.

267. Qiu. L.; Xiao, H. M.; Gong, X. D.; Ju, X. H.; Zhu, W. H. *J. Hazard. Mater*. **2007**, *141*, 280.

268. Qiu, L.; Xiao, H. M.; Gong, X. D.; Ju, X. H.; Zhu, W. H. *J. Hazard. Mater*. **2007**, *141*, 280.

269. Belsky, V. K.; Zorkii, P. M. *Acta. Crystallogr. Sect. A* **1977**, *33*, 1004.

270. Kitaigorodsky, A. I. *Organic chemical crystallography*, Consultants Bureau, New York, 1961.

271. Peralta-Inga, Z.; Degirmenbasi, N.; Olgun, U.; Gocmez, H.; Kalyon, D. M. *J. Energ. Mater*. **2006**, *24*, 69.

272. Zhu, W.; Xiao, J.; Zhu, W. H.; Xiao, H. M. *J. Hazard. Mater*. **2009**, *164*, 1082.

273. Ravi, P.; Gore, G. M.; Tewari, S. P.; Sikder, A. K. *J. Mol. Struct. (THEOCHEM)* **2010**, *958*, 52.

274. Ravi, P.; Gore, G. M.; Venkatesan, V.; Tewari, S. P.; Sikder, A. K. *J. Hazard. Mater*. **2010**, *183*, 859.

275. Mondal, T.; Saritha, B.; Ghanta, S.; Roy, T. K.; Mahapatra, S.; Durga Prasad, M. *J. Mol. Struct. (THEOCHEM)* **2009**, *897*, 42.

276. Zhang, C. Y.; Cao, X.; Xiang, B. *J. Phys. Chem. C* **2010**, *114*, 22684.

277. Fujimoto, D.; Tamura, R.; Lepp, Z.; Takahashi, H.; Ushio, T. *Crystal Growth & Design* **2003**, *3*, 973.

278. Valencia, L.; Bastida, R.; Espana, E. G.; De Juli an Ortiz, J. V.; Llinares, J. M.; Macias, A.; Lourido, P. P. *Crystal Growth & Design* **2010**, *10*, 3418.

279. Cabeza, A. J. C.; Day, G. M.; Motherwell, W. D. S.; Jones, W. *Crystal Growth & Design* **2006**, *6*, 1858.

280. Moreno-Calvo, E.; Calvet, T.; Angel, M.; Aquilano, D. *Crystal Growth & Design* **2010,** *10*, 4262.

281. Iyer, S.; Slagg, N.; in Liebman, J. F.; Greenberg, A. *Structure and reactivity*, VCH publishers, New York, 1988.

282. Politzer, P.; Murray. J. S.; Grice, M. E.; Sjoberg, P. In Olah, G. A.; Squire, D. R.; *Chemistry of energetic materials,* Academic press, New York, 1991.

283. Cowan, R. D.; Fickett, W. *J. Chem. Phys*. **1956**, *24*, 932.

284. Kistiakowsky, G. B.; Wilson, Jr. E. B.; OSRD-114, 1941.

285. Brinkley, S. R.; Wilson Jr, E. B. OSRD-1707, 1943.

286. Keshavarz, M. H.; Mofrad, R. T.; Alamdari, R. F.; Moghadas, M. H.; Mostofizadeh, A. R.; Sadeghi, H. *J. Hazard. Mater*. **2006**, *137*, 1328.

287. Xiong, W. *J. Energ. Mater*. **1985**, *3*, 263.

288. Keshvarz, M. H.; Motamedoshariati, H.; Moghayadnia, R.; Nazari, H. R.; Azarniamehraban, J. *J. Hazard. Mater*. **2009**, *172*, 1218.

289. Keshvarz, M. H.; Mofrad, R. T.; Alamdari, R. F.; Moghadas, M. H.; Mostofizadeh, A, R,; Sadeghi, H. *J. Hazard. Mater*. **2006**, *137*, 1328.

290. Zukas, J. A.; Walters, W.; Walters, W. P. *Explosive effects and applications*, Springer, 2002.

291. Li, J. S.; Huang, H.; Huang, Y.; Dong, H. S. *J. Energ. Mater*. **2008**, *26*, 230.

292. Li, J. S.; Huang ,Y.; Dong, H. S. *J. Energ. Mater*. **2005**, *23*, 133.

293. Stine, J. R. *Mater Res. Soc. Symp*. **1993**, *296*, 3.

294. Iyer, S. *Propell. Explos. Pyrotech*. **1982**, *7*, 37.

295. Hutchinson, C. D.; Mohan, V. K.; Millar, R. W. *Propell. Explos. Pyrotech.* **1984**, *9*, 161.

296. Hasman, E.; Gvishi, M.; Carmel, Y. *Propell. Explos. Pyrotech.* **1986**, *11*,144.

297. Zhang, F. P.; Cheng, X. L.; Liu, Z. J.; Lou, Q. H.; Zhou, J.; Wang, Z. J. *J. Hazard*. Mater. **2007**, *147*, 658.

298. Zeman, S. *J. Hazard.Mater*. **2006**, *132*, 155.

299. Chen, H.; Cheng, X.; Ma, Z.; Su, X. *J. Mol. Struct. (THEOCHEM)* **2007**, *807*, 43.

300. Shao, J.; Cheng, X.; Yang, X. *J. Mol. Struct. (THEOCHEM)* **2005**, *755*, 127.

301. Yao, X. Q.; Hou, X. J.; Wu, G. S.; Xu, Y. Y.; Xiang, H. W.; Jiao, H.; Li, Y. W. *J. Phys. Chem. A* **2002**, *106*, 7184.

302. Chung, G. S.; Schimidt, M. W.; Gordon, M. S. *J. Phys. Chem. A* **2000**, *104*, 5647.

303. Cyranski, M. K.; Krygowski, T. M.; Katritzky, A. R.; Schleyer, P. v. R. *J. Org. Chem*. **2002**, *67*, 1333.

304. Schleyer, P. v. R. *Chem. Rev*. **2001**, *101*, 1115.

305. Turker, L.; Gumus, S.; Atalar, T. *J. Energ. Mater*. **2010**, 28, 139.

306. Macek, A. *Chem. Rev*. **1962**, *62*, 41.

307. Zhang, G.; Weeks, B. L. *Propell. Explos. Pyrotech*. **2010**, *35*, 440

308. Cho, S. G.; No, K.T.; Goh, E. M.; Kim, J. K.; Shin, J. H.; Joo, Y. D.; Seong, S. *Bull. Korean Chem. Soc*. **2005**, *26*, 399.

309. Nefati, H.; Cense, J. M.; Legendre, J. J. *J. Chem. Inf. Comput. Sci*. **1996**, *36*, 804.

310. Ge, S. H.; Cheng, X. L.; Wu, L. S.; Yang, X. D. *J. Mol. Struct. (THEOCHEM)* **2007**, *809*, 55.

311. Ramaswamy, A. L. *J. Energ. Mater*. **2006**, *24*, 35.

312. Politzer, P.; Murray, J. S.; Seminario, J. M.; Lane, P.; Grice, M. E.; Concha, M. C. *J. Mol. Struct. (THEOCHEM)* **2001**, *573*, 1.

313. Politzer, P.; Boyd, S. *Struct. Chem*. **2002**, *13*, 105.

314. Murray, J. S.; Lane, P.; Politzer, P. *Mol. Phys*. **1998**, *93*,187.

315. Rice, B. M.; Hare, J. J. *J. Phys. Chem. A*. **2002**, *106*, 1770.

316. Murray, J. S.; Lane, P.; Politzer, P. *Mol. Phys*. **1998**, *93*, 187.

317. Edwards, J.; Eybl, C.; Johnson, B. *Int. J. Quant. Chem*. **2004**, *100*, 713.

318. Xu, X. J.; Zhu, W. H.; Xiao, H. M. *J. Phys. Chem. B*. **2007**, *111*, 2090.

319. Badders, N. R.; Wei, C.; Aldeeb, A. A.; Rogers, W. J.; Mannan, M. S. *J. Energ. Mater*. **2006**, *24*, 17.

320. Zhang. H.; Cheung, F.; Zhao, F.; Cheng, X. L. *Int. J. Quant. Chem*. **2009**, *109*, 1547.

321. Zhang, C. *J. Hazard. Mater*. **2009**, *161*, 21.

322. Delpuech, A.; Cherville, J. *J. Propell. Explos*. **1979**, *4*, 121.

323. Xiao, H. M. *Molecular orbital theory of nitro-compounds*, Peking, Publishing House of Defense Industry, 1994.

324. Zhang, C.; Shu, Y.; Huang, Y.; Wang, X. F. *J. Energ. Mater*. **2005**, *23*, 107.

Chapter II

Design of High Performance Hexaazaisowurtzitanes & Bicyclo[1.1.1]pentanes

Energetic materials of the strained-ring and cage families constitute a promising new class of high explosives. This was based on the fact that the compounds of this family have high strain energies locked in the molecules (steric strain is expressed as increased positive heat of formation (ΔH^0_f) as compared with a corresponding unstrained system and is released as extra energy on detonation). The increased strain in the ring shows substantial weakening of the bonds of ring. However, the large bond angle deformations in the ring makes it power house of stored energy and each bond can be thought as storage site for potential energy. They also possess rigid and highly compact structures, which decrease the molecular motion, results in increased density.[1-5] Thus greater mass of polynitro-polycyclic strained and cage compounds may be accommodated in a given volume which, along with their high molecular strain energies, results in a better performance on detonation.

Polynitro strained cage compounds of cyclopropane,[6-8] cyclobutane and azetidine,[9-14] cubane and homocubane,[15-28] adamantane,[29-35] prismane,[36-41] tricyclo[3.3.0]octane,[42] bicyclo[3.3.1]nonane,[33] norborane,[42,43] etc., were studied experimentally and theoretically. These compounds show promising performance as compared to RDX, HMX and TNT. The search for energetic compounds with high crystal densities and heat of formation has focused attention on the polynitro derivatives of cage compounds. Molecular structures of the selective promising cage and strained compounds are shown in Fig. 2.1. Preliminary evaluations of polynitropolycyclic compounds reveal that this class of energetic materials is relatively powerful and shock insensitive, and so, well suited for use in future explosive and propellant formulations. Among the various cage and strained compounds, this study evaluates the substituted hexaazaisowurtzitane and bicyclo[1.1.1]pentane as promising energetic materials.

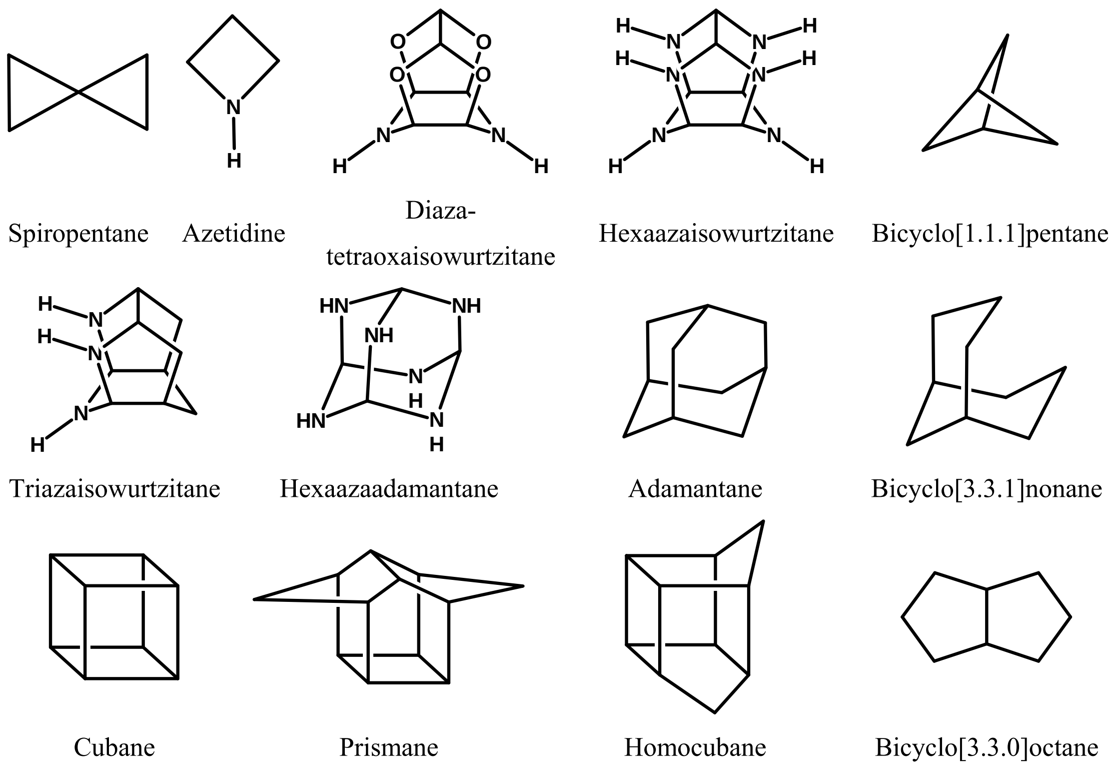

Fig. 2.1 Strained and polycyclic rings used in caged energetic compounds

2.1 Hexaazaisowurtzitanes

Polycyclic amines with a cage structure known as isowurtzitanes have been raising interest since the last 20 years. One of the most interesting representatives of this class of compounds is 2,4,6,8,10,12-hexanitro-2,4,6,8,10,12-hexaazaisowurtzitane (CL-20) due to its highest density and energy.[46-48] CL-20 was first synthesized by Arnold Nielsen.[47-49] The basic structure of CL-20 consists of a rigid isowurtzitane cage, which includes two five-membered rings and a six-membered ring. CL-20 has six nitro groups attached to each of the six bridging nitrogen atoms in the cage (Fig. 2.2).[49] Both spatial orientations of these nitro groups with respect to the five-member and six-member rings in the cage, and the differences in crystal lattice packing define four experimentally isolated polymorphs: α-, β-, γ-, and ε-CL-20.[50,51] Relative to HMX and RDX, CL-20 has a higher molecular weight, density, ΔH^0_f, and number of $N\text{-}NO_2$ bonds.

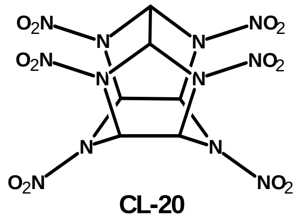

Fig. 2.2 Molecular structure of CL-20.

Though the molecule is superior in performance, this molecule is highly sensitive to impact and friction. Hence, it would be desirable to tailor the molecular structure of CL-20 with improved sensitivity characteristics. Imidazole, triazole, and tetrazole are natural frameworks for energetic materials, as they have inherently high nitrogen contents. The introduction of an amino and triazole group is the simplest means to enhance thermal stability of an energetic material.[52,53] Adding these functionalities to the ring typically alters the ΔH^0_f, making them more positive, which is a desired characteristic for most energetic materials.[54]

Results and discussion

Polynitrogen compounds are environmentally acceptable high energy materials.[55-59] Recently, polynitrofullerenes, polynitro-1,2-bishomopentaprismanes, and polynitroimidazoles have also been studied by quantum-chemical calculations.[40,60,61] The predicted performance characteristics of the hexaazaisowurtzitane family of compounds have been discussed. A systematic structure-property relationship has been established by varying different substituents on the hexaazaisowurtzitane cage. Fig. 2.3 represents the molecular structures of the designed hexaazaisowurtzitane derivatives.

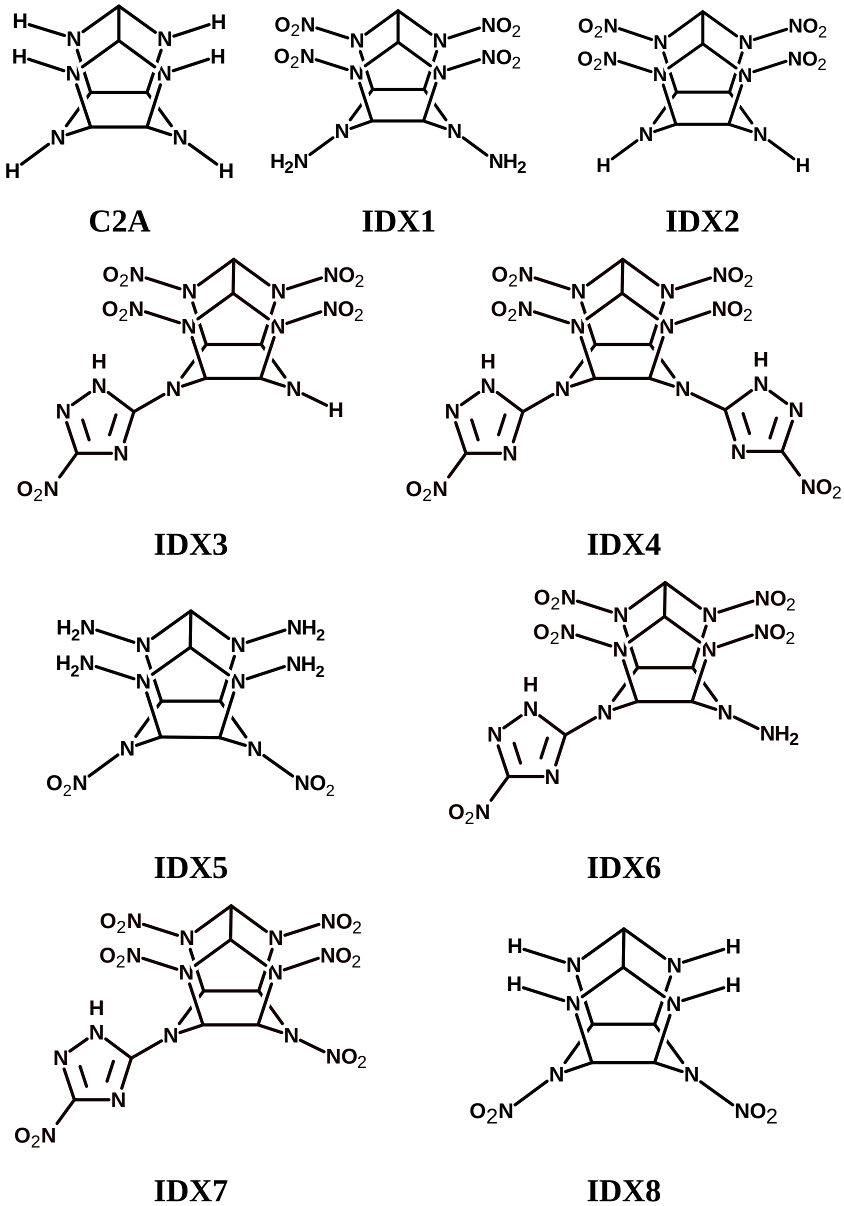

Fig. 2.3 Molecular structure of the designed hexaazaisowurtzitane derivatives.

2.1.1 Molecular geometries

The structure of 2,4,6,8,10,12-hexaazaisowurtzitane present interesting features of strained, fused five and six member azo ring systems. The cyclic and cage structures significantly improve the oxygen balance.[62] The structural parameters of the **CL-20** cage obtained from X-ray diffraction studies show C-C and C-N bond lengths as 1.580 and 1.455 Å, respectively.[49] The optimized structure of **CL-20** cage at the B3LYP/6-31G* level reveals that C-C and C-N bond lengths close to 1.582 and

1.457 Å, respectively, comparable to the experimental values. Introduction of amino group on aza nitrogen shows that the increase in bond lengths of the cage, while reduction in the dihedral angle. This may be due to the negative inductive effect of N-NH_2 functionality. Fig. 2.4 represents the molecular backbone of the hexaazaisowurtzitane derivatives. The replacement of nitro groups in **CL-20** with amino group (**IDX1** and **IDX5**) shows the increase in bond lengths of cage. However, replacement of nitro group of **CL-20** with hydrogen (**IDX2** and **IDX8**) reduces the C-C and C-N bond lengths in the cage. The selected structural parameters of the designed molecules are summarized in Table 2.1.

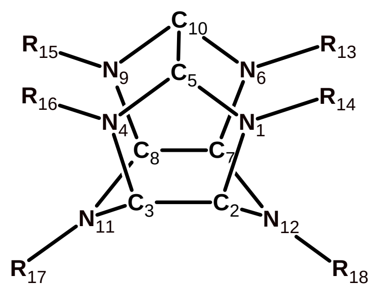

Fig. 2.4 Molecular backbone of the hexaazaisowurtzitane derivatives (R represents the substituted groups like nitro, amino, or nitrotriazole).

Generally, detonation starts with the breakage of weakest bonds in the energetic materials. In order to design insensitive hexaazaisowurtzitane derivatives, it is aimed to strengthen the weakest bonds (N-NO_2) in the designed compounds. Replacement of nitro group of **CL-20** with nitrotriazole at N11 (**IDX3**, **IDX6** and **IDX7**) and N11 & N12 position (**IDX4**), show the decrease in bond lengths of C-C, C-N and N-NO_2 bonds. Among the different N-NO_2 bonds, the N-NO_2 with maximum bond length in **CL-20**, **IDX3**, **IDX4**, **IDX6** and **IDX7** are found to be 1.45, 1.435, 1.413, 1.429, and 1.443 Å, respectively. The replacement of nitro group of the **CL-20** with the amino and nitrotriazole groups slightly reduces the C-N-C angle in the cage.

Table 2.1: Selected structural parameters of the hexaazaisowurtzitane derivatives.

	Parameter	C2A	CL-20	IDX1	IDX2	IDX3	IDX4	IDX5	IDX6	IDX7	IDX8
Bond Length (Å)	C5-C10	1.572	1.586	1.587	1.579	1.584	1.603	1.590	1.585	1.583	1.581
	C7-C8, C2-C3	1.568	1.582	1.584	1.573	1.574	1.616	1.587	1.578	1.575	1.574
	N1-C5, N6-C10	1.455	1.458	1.462	1.453	1.455	1.460	1.468	1.457	1.456	1.456
	N4-C5, N9-C10	1.455	1.458	1.462	1.453	1.455	1.460	1.468	1.457	1.456	1.456
	N1-C2, N6-C7	1.452	1.457	1.465	1.463	1.465	1.484	1.476	1.490	1.484	1.458
	C3-N4, C8-N9	1.452	1.457	1.465	1.463	1.465	1.484	1.476	1.492	1.482	1.458
	C2-N12, C7-N12	1.459	1.462	1.469	1.451	1.491	1.456	1.454	1.449	1.441	1.477
	C3-N11, C8-N11	1.459	1.462	1.469	1.451	1.489	1.456	1.454	1.451	1.441	1.477
	N1-N14, N6-N13	1.021	1.445	1.423	1.442	1.435	1.413	1.412	1.429	1.443	1.042
	N4-N16, N9-N15	1.021	1.445	1.421	1.442	1.435	1.407	1.434	1.427	1.441	1.042
	N11-N17	1.046	1.418	1.419	1.051	1.382	1.413	1.400	1.389	1.386	1.403
	N12-N18	1.046	1.418	1.419	1.051	1.047	1.413	1.400	1.408	1.421	1.403
Angle (°)	C5-N1-C2, C10-N6-C7	110.2	107.6	103.8	106.1	107.5	105.7	106.2	107.7	107.5	105.7
	C5-N4-C3, C10-N9-C8	110.2	109.8	104.2	108.6	107.8	105.2	106.2	108.5	107.8	105.7
	C2-N12-C7, C3-N11-C8	110.8	117.6	113.5	112.3	114.6	113.8	116.8	113.2	116.0	115.8

2.1.2 Gas phase heat of formation

Heat of formation of model compounds has been predicted using the B3LYP method in combination with the 6-31G* basis set through the appropriate design of isodesmic reactions.[63,64] The designed isodesmic reactions for the prediction of gas phase ΔH^0_f are shown in Fig. 2.5. The experimental ΔH^0_f of the reference molecules[65-72] used in the isodesmic approach are summarized in Table 2.2, while for NH_2NO_2, it has been obtained from the atomization approach using the G3 theory. It is evident from the data listed in Table 2.3 that the ΔH^0_f values of all compounds are quite large and positive. They are significantly higher than that of the basic hexaazaisowurtzitane cage (**C2A**), which shows that introduction of a nitro group is the main origin of energy. The positive value of ΔH^0_f for **C2A** shows that energy can be brought into the system by strained ring systems and introduction of a heteroatom in the ring (replacement of the ring carbons).

Table 2.2: Total energy (E_0) at the B3LYP/6-31G* level and experimental gas phase ΔH^0_f for the reference compounds.

Compd.	E_0 (au)	ΔH^0_f (kJ/mol)
CH_4	-40.46935	-74.6
CH_3CH_3	-79.75076	-84.0
NH_3	-56.50961	-45.9
CH_3NH_2	-95.78444	-22.5
CH_3NO_2	-244.95385	-74.7
$NH(CH_3)_2$	-135.06455	-18.6
NH_2NH_2	-111.79616	95.2
$C_2H_2N_3$	-242.18480	199.3
NH_2NO_2	-260.98726	8.0[a]
Azetidine	-173.14430	98.2
Bicyclo[1.1.1]pentane	-195.13799	202.89[a]

[a]Value obtained from G3 atomization calculations.

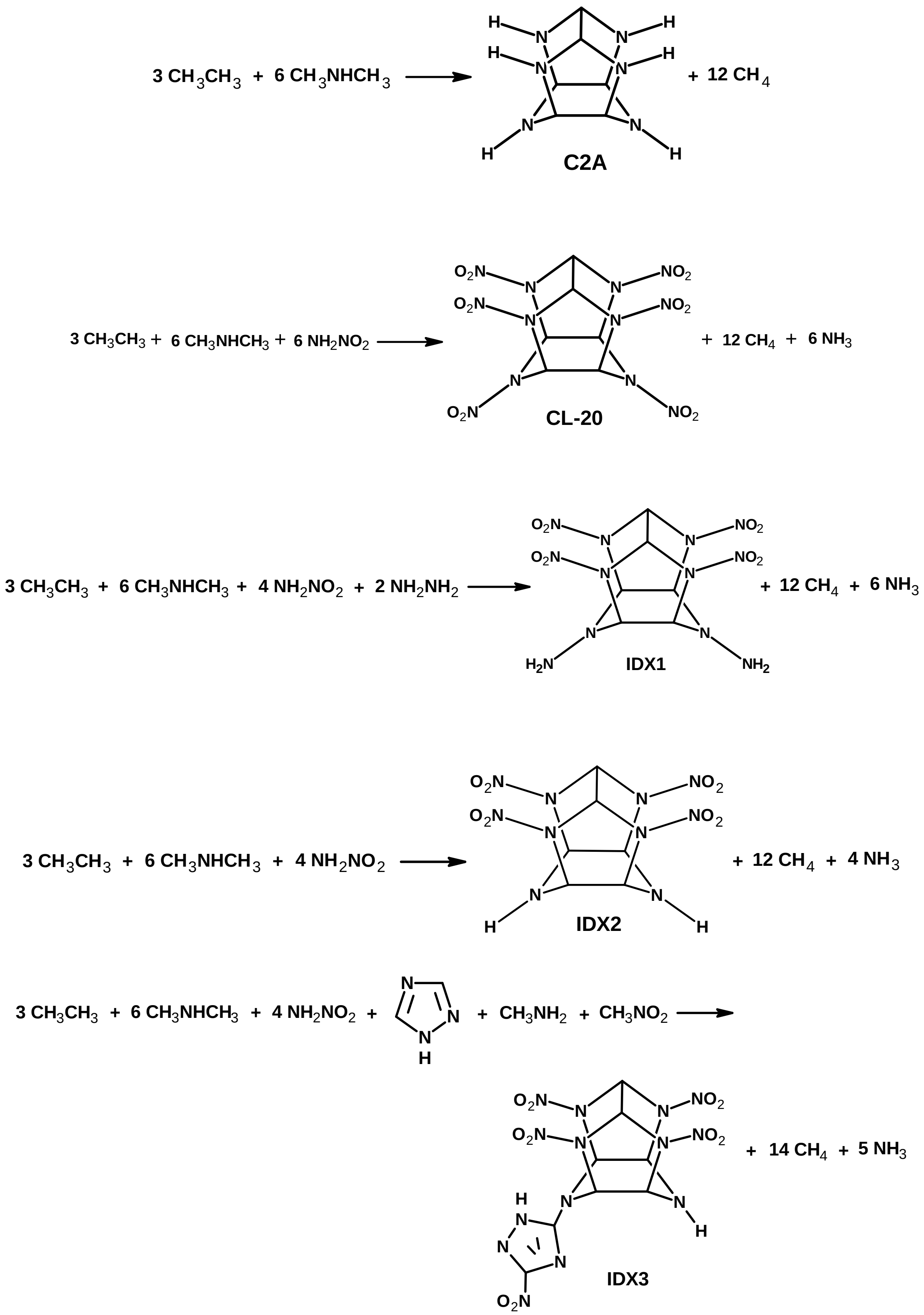

Fig. 2.5 Isodesmic reaction schemes for the prediction of gas phase ΔH^0_f.

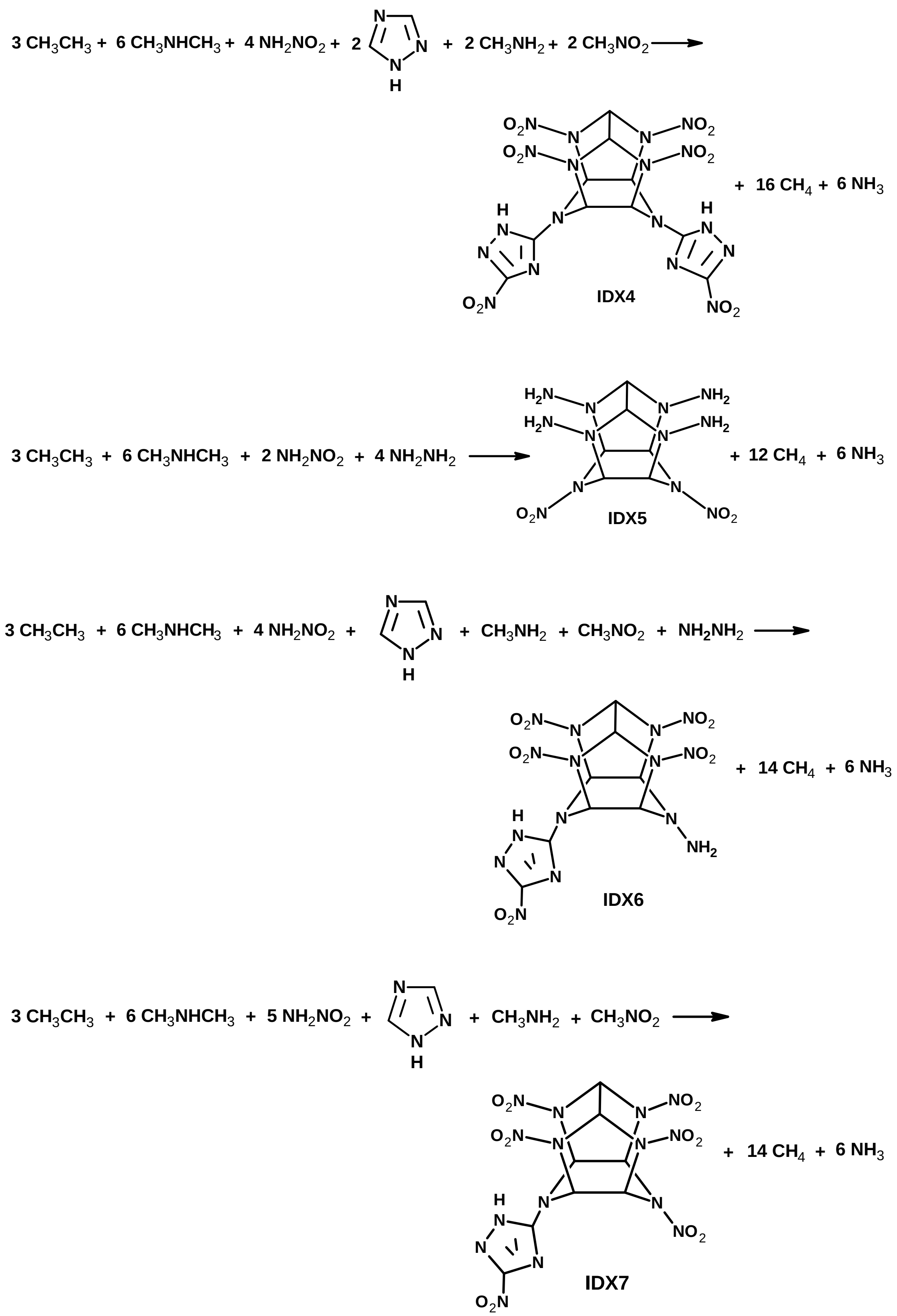
3 CH3CH3 + 6 CH3NHCH3 + 4 NH2NO2 + 2 + 2 CH3NH2 + 2 CH3NO2
+ 16 CH4 + 6 NH3
IDX4
3 CH3CH3 + 6 CH3NHCH3 + 2 NH2NO2 + 4 NH2NH2
+ 12 CH4 + 6 NH3
IDX5
3 CH3CH3 + 6 CH3NHCH3 + 4 NH2NO2 + + CH3NH2 + CH3NO2 + NH2NH2
+ 14 CH4 + 6 NH3
IDX6
3 CH3CH3 + 6 CH3NHCH3 + 5 NH2NO2 + + CH3NH2 + CH3NO2
+ 14 CH4 + 6 NH3
IDX7

(**Fig. 2.5** Contd.)

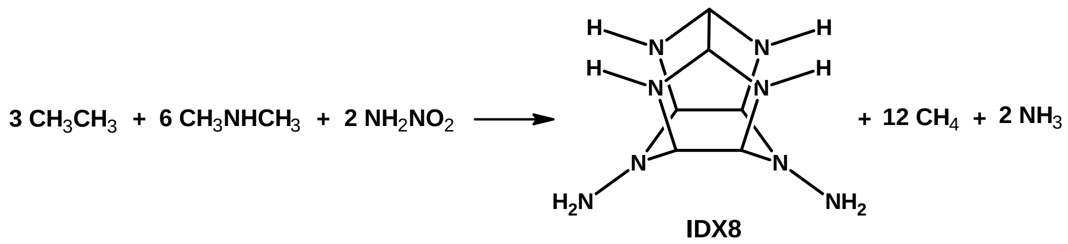

(**Fig. 2.5** Contd.)

Table 2.3: Calculated energetic properties of the hexaazaisowurtzitane derivatives.

Compd.	E_0 (au)	O.B. (%)	ΔH^0_f (kJ/mol)	ρ_0 (g/cm^3)	Q (kJ/mol)	D (km/s)	P (GPa)
C2A	-564.08800	-171.2	319.9	1.57	839.7	5.56	12.56
CL-20	-1790.93586	-11.0	691.3	1.97	1738.2	9.73	44.64
IDX1	-1492.59063	-38.1	768.0	1.96	1623.2	9.34	40.64
IDX2	-1382.00320	-36.8	537.6	1.87	1572.9	8.87	35.66
IDX3	-1827.50079	-34.8	760.6	1.87	1510.1	8.81	35.51
IDX4	-2272.89415	-33.6	1044.5	1.84	1497.2	9.21	40.41
IDX5	-1194.25507	-75.4	819.9	1.72	1444.1	8.09	28.23
IDX6	-1882.79267	-35.4	867.3	1.84	1527.4	8.68	33.88
IDX7	-2031.96156	-23.8	859.0	1.90	1597.5	9.02	37.29
IDX8	-973.05904	-80.6	386.4	1.79	1291.1	8.30	30.45

O.B.: Oxygen balance

The gas-phase ΔH^0_f of **CL-20** is calculated to be 691 kJ/mol; however, the condensed phase value will be lower due to the contribution of the enthalpy of sublimation.[45] It is also clear from Table 2.3 that, with an increase in the number of nitro groups, ΔH^0_f of the corresponding compound increases, which may be attributed to repulsion of the nitro groups. Compound **C2A** represents the basic skeleton (hexaazaisowurtzitane cage), while **IDX8**, **IDX2**, and **CL-20** contain two, four, and six nitro groups, respectively. Fig. 2.6 shows the graph of the number of nitro groups versus ΔH^0_f and reveals that ΔH^0_f increases linearly with an increase in the number of nitro groups. This indicates that the explosive performance of **CL-20** is superior among the model compounds. Comparison of **IDX2**, **IDX3**, and **IDX4** clearly indicates the introduction of a nitrotriazole group increases the energy content significantly and **IDX4** is calculated to have the highest ΔH^0_f (1044.5 kJ/mol) compared to the others.

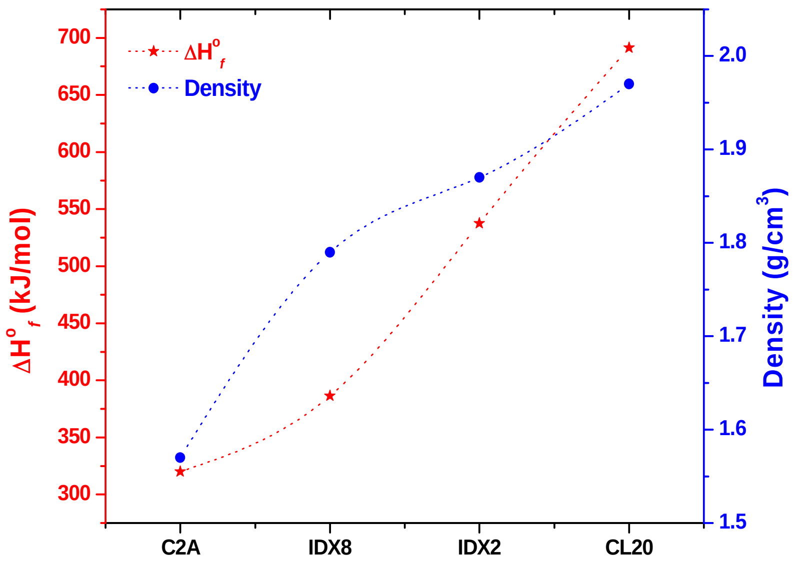

Fig. 2.6 Effect of nitro groups on ΔH^0_f (kJ/mol) and density (g/cm^3) of the hexaazaisowurtzitane derivatives.

2.1.3 Density

The high densities in the compounds can be achieved if the molecular structure contains fused ring systems.[2] Crystal structure density is predicted by the molecular packing calculations. The high-density polymorph is sorted out from the large number of potential crystal structures, and the lattice parameters of the same are presented in Table 2.4. The results reveal that all the molecules fall under four space groups, viz., *Pbca*, *P2$_1$/c*, *Pna2$_1$* and *P1*. The density of **CL-20** is calculated to be 1.97 g/cm^3 and is comparable to the experimental density.[44] **C2A** offers a density of 1.57 g/cm^3, and further the packing efficiency in the condensed phase increased by the introduction of substituents to the basic cage skeleton. It is also clear from Fig. 2.6 that an increase in the density is observed with an increase in the number of nitro groups (from two to six in **IDX8**, **IDX2**, and **CL-20**, respectively), while the density decreases with the introduction of an amino group.

Table 2.4: Crystal structure details of the minimum energy polymorph obtained from dreiding force field.

Compd.	Density (g/cm^3)	Space group	Length (Å)			Angle (°)		
			a	b	c	α	β	γ
C2A	1.57	*P-1*	6.8	10.8	6.5	98.6	54.9	100.9
CL-20	1.97	*Pbca*	15.1	12.8	15.4	90.0	90.0	90.0
IDX1	1.96	$Pna2_1$	12.3	8.0	13.4	90.0	90.0	90.0
IDX2	1.87	*P-1*	6.1	18.2	8.2	101.5	68.1	59.7
IDX3	1.87	*P-1*	12.9	10.7	6.9	94.1	110.7	107.9
IDX4	1.84	*Pbca*	8.4	36.2	13.8	90.0	90.0	90.0
IDX5	1.72	$P2_1/c$	23.1	13.2	13.9	90.0	162.4	90.0
IDX6	1.84	$P2_1/c$	9.9	19.8	12.2	90.0	47.1	90.0
IDX7	1.90	*P-1*	7.1	16.9	9.0	115.1	110.2	90.5
IDX8	1.79	*P-1*	7.1	7.0	11.2	104.7	107.0	72.2

However, the role of the amino group cannot be clearly defined since the packing pattern is highly dependent on the electronic structure of the molecule.[73] Comparison of **IDX2**, **IDX3**, and **IDX4** reveals that there is no significant change in density by the introduction of nitrotriazole. Overall, except the molecules **IDX5** and **IDX8**, all molecular structures have a density of about 1.9 g/cm^3. Crystal structures of the hexaazaisowurtzitane derivatives are shown in Fig. 2.7.

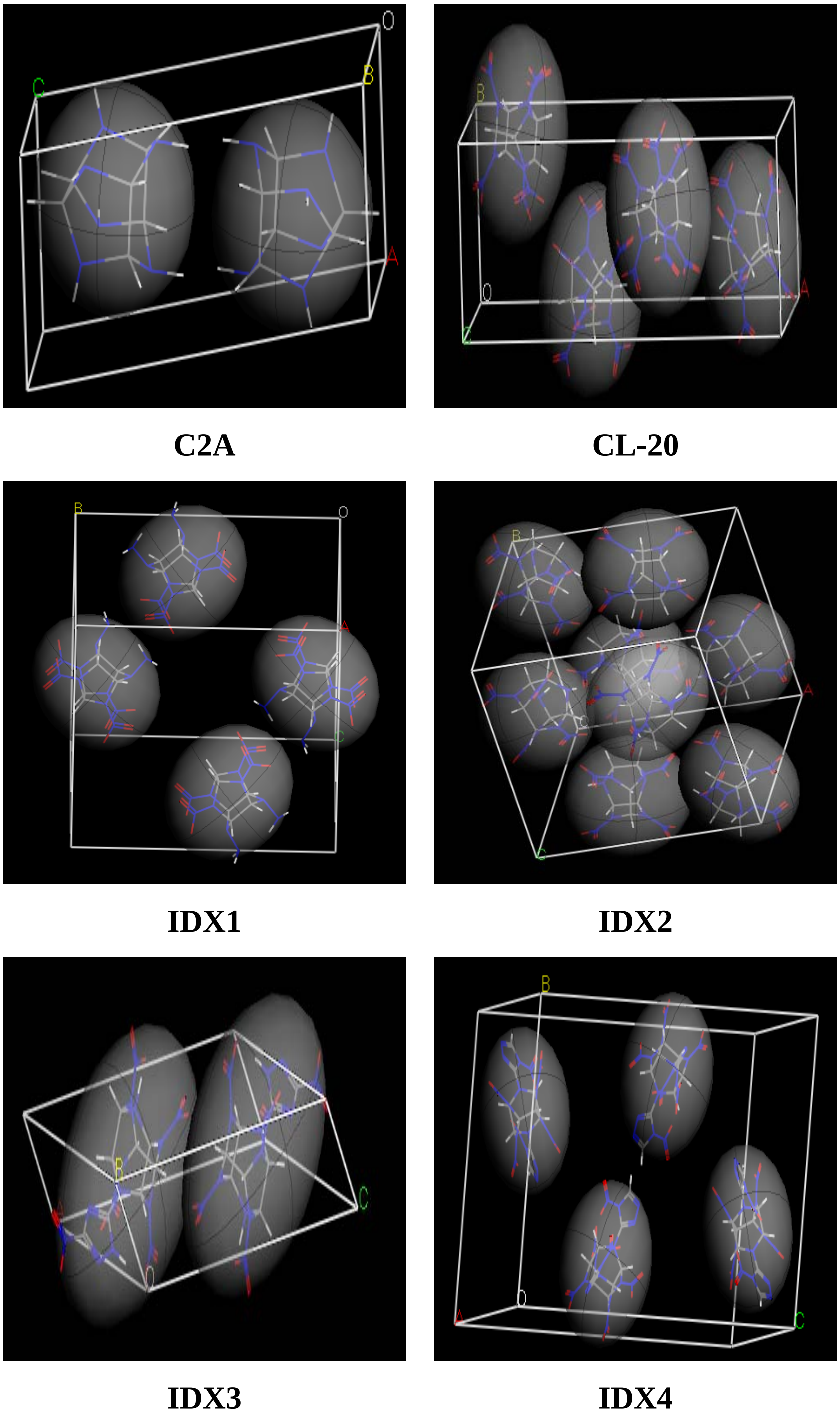

Fig. 2.7 Crystal structures of the hexaazaisowurtzitane derivatives.

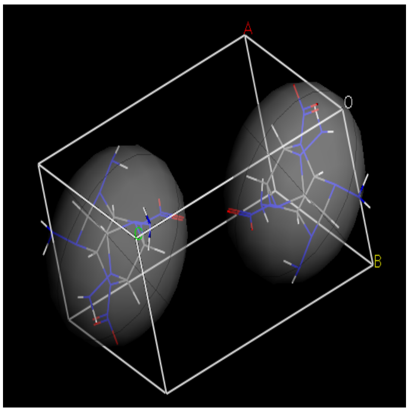

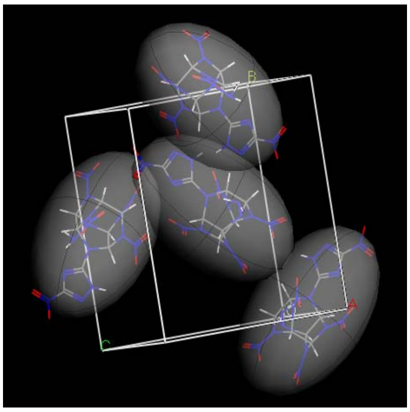

IDX5 **IDX6**

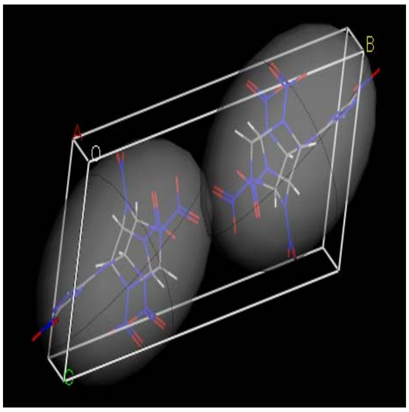

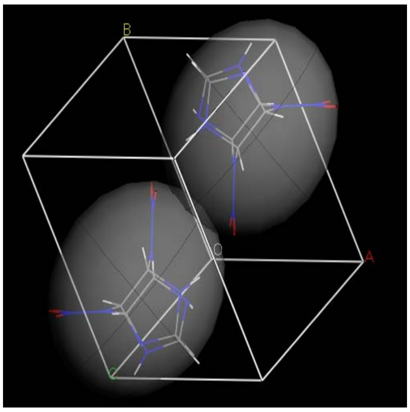

IDX7 **IDX8**

Fig. 2.7 (Contd.)

2.1.4 Detonation characteristics

The velocity of detonation (*D*) and pressure (*P*) of the molecules are computed by Kamlet-Jacobs empirical equations[74,75] on the basis of their theoretical densities (ρ_o) and calculated gas-phase $\Delta H^0{}_f$. The detonation velocity is proportional to the density, while the Chapman-Jouguet detonation pressure is proportional to the square of the initial density.[76,77] Table 2.3 summarizes the calculated velocity of detonation (*D*), and detonation pressure (*P*) for the designed molecules. The model compounds (**IDX1** to **IDX8**) have a *D* higher than 8 km/s and a pressure above 30 GPa. Though their $\Delta H^0{}_f$ values are higher than that of **CL-20**, due to the lower densities, all the compounds have *D* and *P* values that are less than those of **CL-20**. This is because the performance characteristics *D* and *P* are mainly dependent on the crystal density of the molecule rather than its $\Delta H^0{}_f$. **IDX1** is calculated to have the highest *D* among the designed molecules, and the replacements of nitro groups in **CL-20** by amino groups bring the *D* down in **IDX1**. It is also observed that an increase in the number of nitro groups (from two to six in **IDX8**, **IDX2**, and **CL-20**, respectively) increases the ρ_o, *Q*, *D*, and *P* values of the corresponding compounds.

Fig. 2.8 compares the *D* of model compounds. Introduction of a nitro group in the hexaazaisowurtzitane cage increases the density of the molecules and therefore has a significant contribution to the *D* and *P* performance characteristics. Though the introduction of one nitrotriazole in **IDX2** does not alter the *D* significantly in **IDX3**, further addition of nitrotriazole increases the *D* to 9.2 km/s in **IDX4**. Introduction of nitrotriazole ring on the hexaazaisowurtzitane (**IDX3**, **IDX4**, **IDX6**, and **IDX7**) also reveals an improvement in the performance characteristics. Comparison of **IDX2**, **IDX3**, and **IDX4** indicates that, in these cases, the *D* is also dependent on *N* and *M* in addition to *Q* and ρ_o. Overall, **IDX1**, **IDX4**, and **IDX7** have moderately comparable performance characteristics.

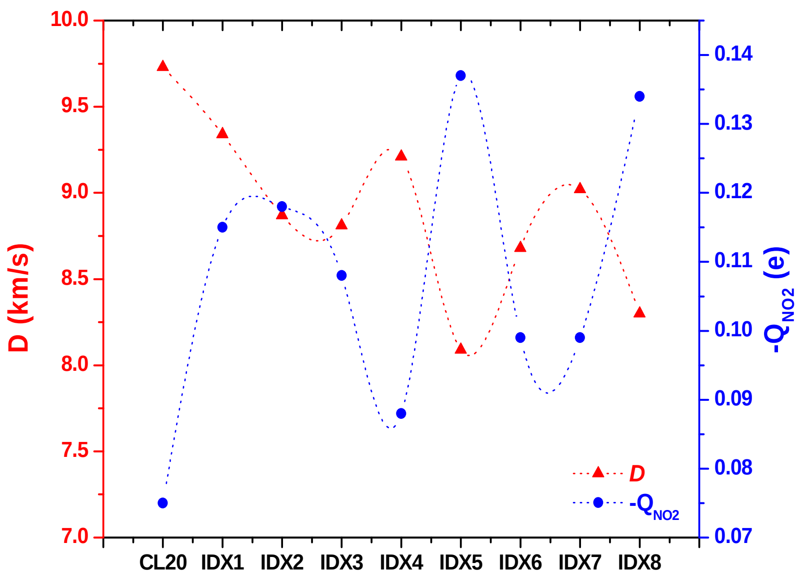

Fig. 2.8 Velocity of detonation (km/s) and $-Q_{NO2}$ (e) profile of the hexaazaisowurtzitane derivatives.

2.1.5 Thermal stability

Thermal stability of the designed compounds was predicted by analyzing the bond dissociation energies (BDEs) of the weak N-NO_2 bonds. Generally, higher the bond length is, the weaker and more sensitive is the bond. The increase in the number of nitro groups increases the strain in the skeleton, affecting the space orientation of nitro groups due to the steric strain. Predicted values of BDE for the designed compounds (**IDX1**-**IDX8**) were found to be higher than **CL-20** (146.8 kJ/mol) and listed in Table 2.5. The increase in the number of nitro groups in the molecule decreases the BDE being responsible for the subsequent weakening of the N-NO_2 bonds. It is clearly observed in **IDX8**, **IDX2**, and **CL-20** having two, four and six nitro groups, respectively in the molecular structure. There predicted BDEs are 175.6, 155.8 and 146.8 kJ/mol, respectively. The replacement of nitro groups with amino in the **CL-20** increases the BDEs. The replacement of two and four nitro groups with amino in **IDX1** and **IDX5** increases the BDE of **CL-20** by 12.5 and 30.4 kJ/mol, respectively. The substitution of nitro group with nitrotriazoles (**IDX3**, **IDX4**, **IDX6**, and **IDX7**) in the **CL-20** slightly increases the BDEs of the respective compounds. **CL-20** shows lowest BDE (146.8 kJ/mol) in the series may be due to the six nitro groups in the molecular structure, which increases the strain due to the steric hindrance and repulsion.

Table 2.5: Computed -Q_{NO2} from Mulliken charges by MP2/6-31G* method.

Compd.	CL-20	IDX1	IDX2	IDX3	IDX4	IDX5	IDX6	IDX7	IDX8
-Q_{NO2} (e)	0.075	0.115	0.118	0.108	0.088	0.137	0.099	0.099	0.134
R_{N-NO2} (Å)	1.445	1.425	1.419	1.435	1.407	1.401	1.408	1.447	1.403
BDE (kJ/mol)	146.8	159.3	155.8	152.0	148.3	177.2	148.7	162.4	175.6

2.1.6 Sensitivity correlations

The relationship between the impact sensitivity and electronic structures of some nitro compounds can be established by the charge analysis of the nitro group.[78] Nitro compounds are very strong electron acceptors and have a strong ability to attract electrons. Such ability can be represented by the net charges of the nitro group. The higher the negative charge on the nitro group, the lower the electron attraction ability and therefore the more stable the nitro compound. In nitro-containing covalent compounds, C-NO_2, N-NO_2, and O-NO_2 bonds denoted as R-NO_2 bonds are usually the weakest in the molecule, and their breaking is the initial step in the decomposition or detonation. Computed -Q_{NO2} values of the molecules are presented in Table 2.5. The higher the -Q_{NO2}, the larger the impact insensitivity, and hence, -Q_{NO2} can be regarded as the criterion for estimating the impact sensitivities. -Q_{NO2} is calculated to be 0.075 e for **CL-20**, and for the other compounds it ranges from 0.088 to 0.137 e. This shows that the designed model compounds are more insensitive than **CL-20** (Fig. 2.8). An increase in the number of nitro groups (from two to six in **IDX8**, **IDX2**, and **CL-20**) increases the impact sensitivity. Similarly, replacement of a nitro group with an amino group decreases the sensitivity. This can be attributed to an increase in the strength of the adjacent N-NO_2 bond by the introduction of the amino group. Comparison of **IDX2**, **IDX3**, and **IDX4** reveals that introduction of a single nitrotriazole ring does not play any role in altering the sensitivity behavior, but this role increases with introduction of two nitrotriazoles. Overall, the designed model compounds were found to have less impact sensitivity than **CL-20**.

2.1.7 Conclusions

Structure-property studies have been performed on hexaazaisowurtzitanes to achieve energetic performance comparable to that of **CL-20** with better insensitivity characteristics. The $\Delta H^0{}_f$ values of the model compounds have been computed by constructing reasonable isodesmic reactions using the DFT-B3LYP/6-31G* method. It has been found that the nitrotriazole bearing hexaazaisowurtzitane cage possesses a very high positive $\Delta H^0{}_f$. The crystal density has been predicted using molecular packing calculations. The density of the designed molecules is predicted to be about 1.9 g/cm^3 in general, and the introduction of nitrotriazoles does not affect the density significantly. The model compounds (**IDX1** to **IDX8**) have velocity of detonation higher than 8 km/s and pressures above 30 GPa. The charge on the nitro group has been analyzed to correlate the impact sensitivity. The NBO study reveals that the designed molecules have better impact insensitivity than the **CL-20** molecule. The computational study identified **IDX1**, **IDX4**, and **IDX7** as potential replacements for **CL-20** in various energetic formulations.

2.2 Bicyclo[1.1.1]pentanes

Bicyclo[1.1.1]pentane is a highly strained hydrocarbon system due to close proximity of non-bonded bridge head carbons (Fig. 2.9). The increased strain in the ring shows substantial weakening of the bonds of the ring, and the large bond angle deformations in the ring make it more energetic. Chiang and Bauer[79] reported molecular structure investigations of bicyclo[1.1.1]pentane by electron diffraction in the vapor phase. Wiberg et al.[80] reported the synthesis of bicyclo[1.1.1]pentane for the first time and found it to be a remarkably stable strained system.

Bicyclo[1.1.1]pentane has been widely used in synthetic chemistry,[81-87] and its mono and dinitro derivatives have been reported.[88-91] The interaction between two exocyclic bridge head bonds is expected to destabilize the bicyclo[1.1.1]pentane cage in the ground state. Such repulsion between the back lobes of the exocyclic bridge head hybrids has been proposed to be one of the main contributors to the strain energy of the bicyclo[1.1.1]pentane cage.[92,93] Nitro groups introduced into these structures can effectively improve the oxygen balance and ΔH^0_f. The more nitro groups were introduced, the better performance of the high energy materials (HEMs) was achieved.

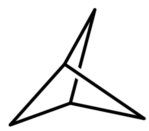

Fig. 2.9 Molecular structure of bicyclo[1.1.1]pentane.

Theoretical studies have been performed to investigate the performance and structure of polynitrobicyclo[1.1.1]pentane. The tertiary bridgehead position reported to be more reactive than the secondary methylene position and hence first nitrated derivatives are selected at tertiary position. The study investigates 1-nitrobicyclo[1.1.1]pentane (**S1**), 1,3-dinitrobicyclo[1.1.1]pentane (**S2**), 1,2,3-trinitrobicyclo[1.1.1]pentane (**S3**), 1,2,3,4-tetranitrobicyclo[1.1.1]pentane (**S4**), and 1,2,3,4,5-pentanitrobicyclo[1.1.1]pentane (**S5**) using *ab initio* calculations based on the hybrid density functional theory. Among the possible isomers, the study was limited only to the above molecules due to their synthetic feasibility and stability. The study is focused on a detailed structure-property relationships description recognizing polynitro bicyclo[1.1.1]pentanes as a promising high energy density materials.

Results and discussion

Levin et al.[84] explored the synthesis and stability of mono and dinitrobicyclo[1.1.1]pentanes; however, energetic properties are unknown. The present study discusses the energetic characteristics of polynitrobicyclo[1.1.1]pentanes. 1,3,3-Trinitroazetidine (TNAZ) is a high performance, melt cast cyclic nitramine explosive well known due to its highly strained cage of azetidine skeleton. Its performance is by approximately 30 % higher than that of TNT.[12,94]

2.2.1 Molecular geometries

The bicyclo[1.1.1]pentane present significant features of strained, fused four member ring systems (Fig. 2.10). It appears that nonbonded carbon-carbon interactions are strong in this molecule, viz. a) both the bridgehead and methylene positions incorporate considerable strain, which should result in a marked decrease in stability and b) the secondary hydrogens are sterically not so accessible so in cyclohexane. The different structural parameters of the nitrated bicyclo[1.1.1]pentane are listed in Table 2.6.

It has an extremely short C1-C3 nonbonded distance which leads to the steric hindrance in the molecular structure. The distance between the methylene carbons (C2, C4 and C5) varies from 1.9 to 2.4 Å depending on substitution of nitro groups on these carbons. The increased distance between methylene carbons is due to the repulsive effect of nitro groups on these carbons. The dihedral angle at the bridge head position is slightly higher than the angle at methylene carbons. The introduction of nitro groups from one to five (**S1**-**S5**) in the designed molecules slightly reduces the angle at bridgehead position (C1 & C3) from 89 to 82^0. The nitro groups on methylene carbons shows higher C-N bond lengths than the nitro groups at bridgehead position. The C1-NO_2 and C3-NO_2 bond lengths are close to 1.48 Å, while C2-NO_2, C4-NO_2 and C5-NO_2 bond lengths are found above 1.50 Å. The increase of nitro groups from one to five on the bicyclo[1.1.1]pentane boost the bond lengths of

$C-NO_2$ bonds. The increase of nitro groups from one to five reduces the dihedral angle at bridgehead position from 89 to 82^0.

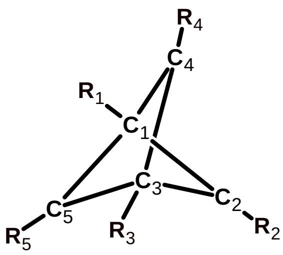

Fig. 2.10 Molecular backbone of the polynitrobicyclo[1.1.1]pentanes (R represents the nitro groups).

Table 2.6: Selected structural parameters of the polynitrobicyclo[1.1.1]pentanes.

	Parameter	**S1**	**S2**	**S3**	**S4**	**S5**
Bond length (Å)	C1-C2	1.546	1.542	1.549	1.537	1.549
	C1-C4	1.546	1.542	1.548	1.540	1.549
	C1-C5	1.546	1.542	1.559	1.563	1.549
	C3-C2	1.562	1.543	1.549	1.537	1.551
	C3-C4	1.562	1.543	1.548	1.540	1.551
	C3-C5	1.562	1.543	1.559	1.563	1.551
	C1-N1	1.485	1.478	1.479	1.477	1.479
	C2-N2		1.478	1.498	1.502	1.505
	C3-N3	-		1.479	1.478	1.479
	C4-N4		-	-	1.502	1.505
	C5-N5			-	-	1.505
Angle (°)	C1-C2-C3	72.6	71.5	72.8	73.2	73.8
	C1-C4-C3	72.6	71.5	72.4	73.2	73.8
	C1-C5-C3	72.6	71.5	72.4	72.5	73.8
	C2-C1-C5	89.2	89.1	85.6	83.5	82.8
	C2-C3-C5	87.8	89.1	85.6	83.5	82.8

2.2.2 Gas phase heat of formation

Heat of formation (ΔH^0_f) is one of the most important thermochemical properties of energetic materials because it is directly related to the detonation performance. DFT-B3LYP methods were used to calculate the $\Delta H^0{}_f$ of the designed compounds via isodesmic reactions using the 6-31G* basis set. The designed isodesmic reactions for the prediction of gas phase $\Delta H^0{}_f$ are shown in Fig. 2.11. The experimental $\Delta H^0{}_f$ of the reference molecules used in the isodesmic approach is presented in Table 2.2. Generally, common saturated hydrocarbons have negative $\Delta H^0{}_f$ but designed compounds show positive due to high ring strain and large number of nitro groups. Calculated $\Delta H^0{}_f$ of the designed compounds were compared with those of TNAZ to evaluate the performance. Gas phase $\Delta H^0{}_f$ of TNAZ reported by Politzer et al.[95] at the B3LYP/6-31G(d,p) level is 128.45 kJ/mol, by Wilcox et al.[96] at the B3LYP/6-31G(d,p) level is 125.02 kJ/mol, and by Fan and Ju[61] at the B3LYP/6-311G** level is 127.31 kJ/mol. $\Delta H^0{}_f$ calculated for TNAZ using the isodesmic reaction approach at the B3LYP/6-31G* is 126.39 kJ/mol. Predicted $\Delta H^0{}_f$ of the designed compounds using hybrid DFT-B3LYP methods with 6-31G* basis set are listed in Table 2.7.

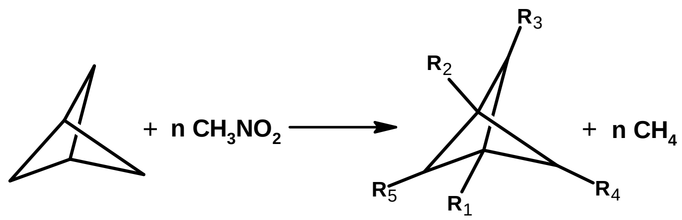

S1 R_1=NO_2, R_2=R_3=R_4=R_5=H n=1
S2 R_1=R_2=NO_2, R_3=R_4=R_5=H n=2
S3 R_1=R_2=R_3=NO_2, R_4=R_5=H n=3
S4 R_1=R_2=R_3=R_4=NO_2, R_5=H n=4
S5 R_1=R_2=R_3=R_4=R_5=NO_2 n=5

Fig. 2.11 Molecular frameworks of the designed compounds and predicted isodesmic reactions for the calculation of $\Delta H^0{}_f$.

A plot of the $\Delta H^0{}_f$ versus the number of nitro groups of the designed bicyclo[1.1.1]pentane molecules is shown in Fig. 2.12. Initially, $\Delta H^0{}_f$ decreases when the number of nitro groups increases from zero to two (**S1** and **S2**). Similar phenomena were found in polynitrocubanes[97] and polynitroprismanes.[40] Introduction of a nitro group into free methylene carbon of **S2** increases the ΔH^0_f of **S3**, **S4**, and **S5** by 13 kJ/mol, 39 kJ/mol, and 87 kJ/mol, respectively. The presence of more than two nitro groups in the skeleton (**S3-S5**) causes an increase in the total energy of molecule due to the strong repulsion energy between nitro groups. Relative position of the nitro group and its space orientation creates a strain in the compound. Among the designed compounds, **S5** has shown the highest ΔH^0_f (245.43 kJ/mol) possibly due to its large number of nitro groups. Positive ΔH^0_f is directly attributable to a large number of inherently energetic C-NO_2 and C-C bonds of the strained bicyclo[1.1.1]pentane skeleton. The order of the increase of ΔH^0_f in the designed compounds is as follows: **S2**, **S1**, **S3**, **S4**, **S5**. All compounds show ΔH^0_f higher than TNAZ due to higher energy contribution from the strained molecular skeleton.

Table 2.7: Calculated explosive properties of the designed compounds.

Compd.	O.B. (%)	E_0 (au)	ΔH^0_f (kJ/mol)	Q (cal/g)	D (km/s)	P (GPa)
S1	-162.8	-399.634782	170.52	1383.53	6.24	14.64
S2	-91.1	-604.123957	158.13	1503.71	7.59	24.12
S3	-51.2	-808.603392	171.32	1368.90	8.72	33.51
S4	-25.8	-1013.077893	197.46	1461.68	9.53	41.83
S5	-8.2	-1217.544079	245.44	1754.79	10.10	49.01
TNAZ	-16.6	-786.588627	126.39	1524.36	9.35	39.32

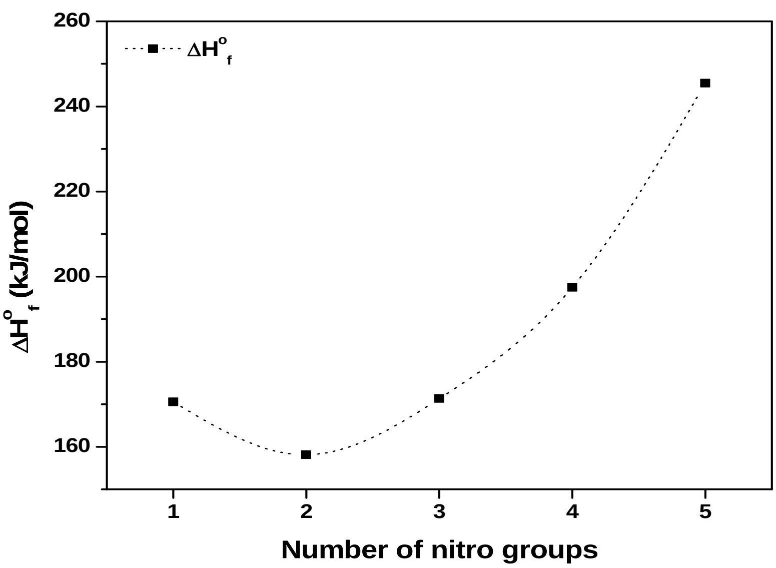

Fig. 2.12 Number of nitro groups (n) versus heats of formation (kJ/mol) of the designed compounds using B3LYP/6-31G* method.

2.2.3 Density

Density (ρ_0), detonation velocity (*D*), and pressure (*P*) are the most important parameters when evaluating the explosive performance of energetic materials. Density is the crucial factor for the prediction of the performance of energetic materials; hence, it has to be predicted correctly. Introduction of strained rings and nitro groups into the molecular framework is a possible way to improve the density prediction.[4] Presently, determination of crystal density rather than a detail study of crystal structure have been given prime importance. Values of density, space group, and lattice parameters of the lowest energy crystal structure obtained from the dreiding force field are listed in Table 2.8. The dreiding force field is optimized for molecular crystals; it can model C, H, N, and O most accurately and allows reasonable predictions for a large number of structures including those with novel combinations of elements and those for which there is little or no experimental data.[98] Predicted density of the TNAZ molecule using the dreiding force field (1.84 g/cm^3) was found to be very close to the experimental value of 1.86 g/cm^3.[99] Fig. 2.13 shows an increase in the density with the increasing number of nitro groups in the bicyclo[1.1.1]pentane skeleton. Molecule **S5** shows the highest density in the series (2.07 g/cm^3) probably caused by the presence of more nitro groups. Crystal densities predicted for **S3** and **S4** are 1.78 and 1.92 g/cm^3, respectively. Representative crystal structures of designed compounds are shown in Fig. 2.14.

Table 2.8: Crystal structure details of the minimum energy polymorph obtained from dreiding force field.

Compd.	Density (g/cm^3)	Space group	Lattice parameters					
			Length (Å)			Angle (°)		
			a	b	c	α	β	γ
S1	1.40	$P2_1/c$	7.535	16.175	6.768	90.0	136.3	90.0
S2	1.64	$P2_1/c$	12.421	10.279	6.465	90.0	126.3	90.0
S3	1.78	$P2_1/c$	11.943	11.884	10.322	90.0	148.0	90.0
S4	1.92	$Pna2_1$	12.846	9.734	6.978	90.0	90.0	90.0
S5	2.07	$P2_12_12_1$	6.444	11.221	13.087	90.0	90.0	90.0
TNAZ	1.84	$Pbca$	9.975	7.053	20.209	90.0	90.0	90.0

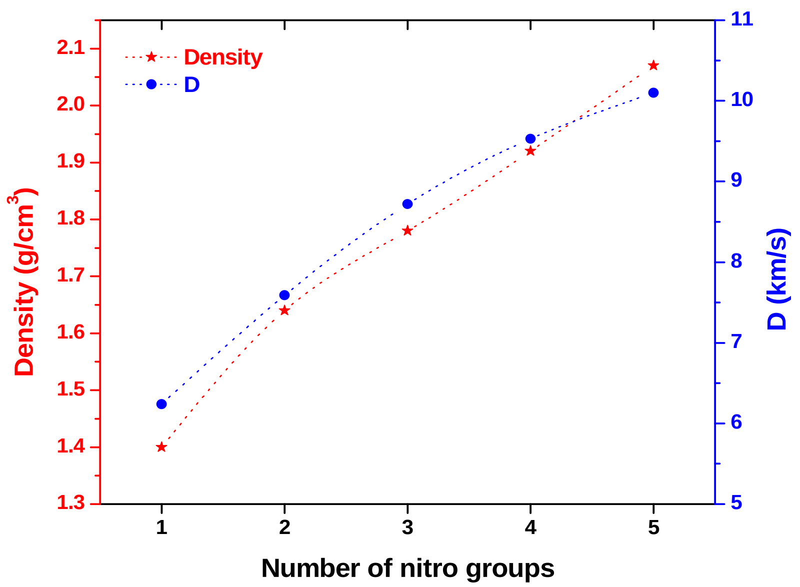

Fig. 2.13 Plot of density (g/cm^3) and velocity of detonation (D) (km/s) against the number of nitro groups (n).

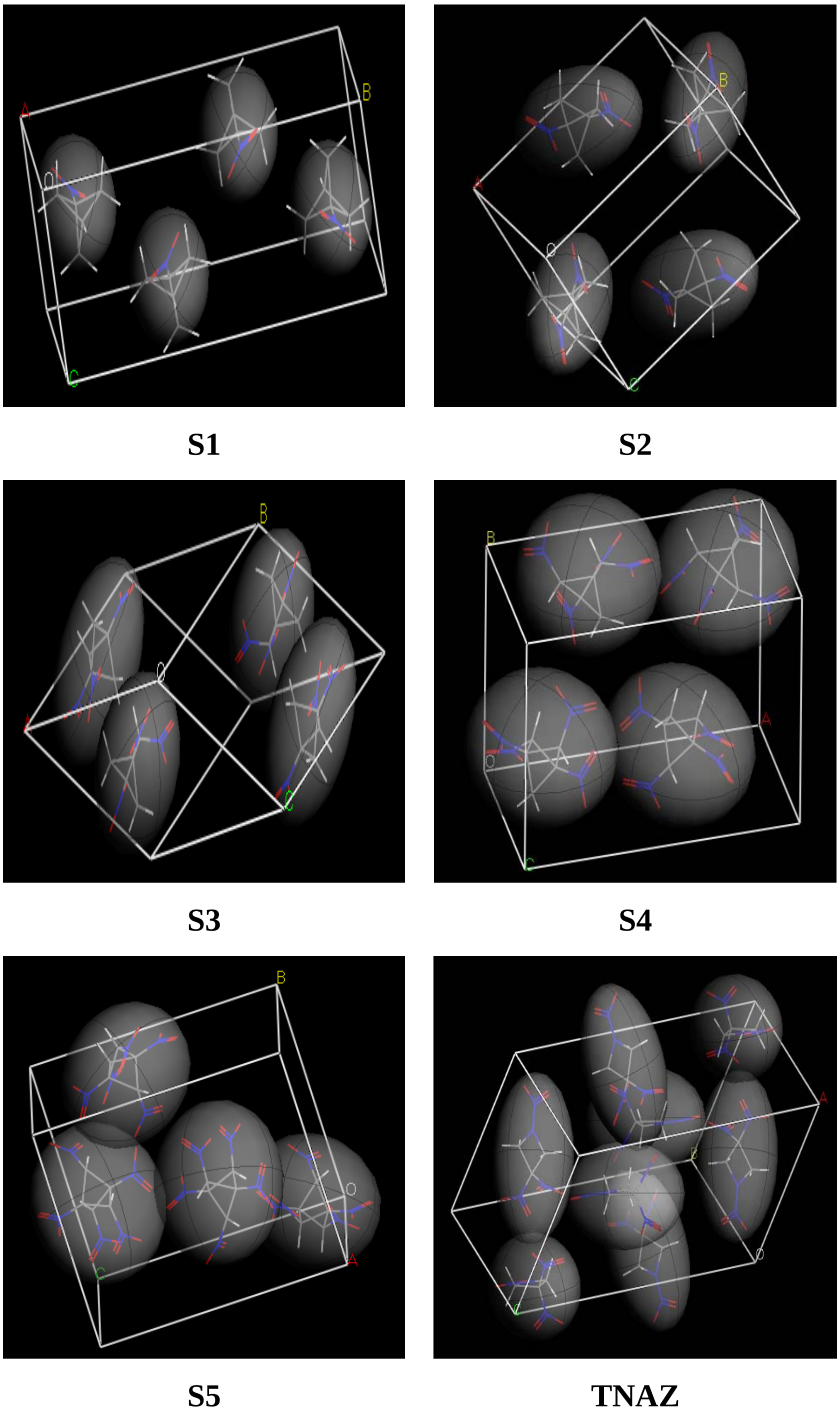

Fig. 2.14 Crystal structures of the minimum energy polymorph obtained from dreiding force field for the designed compounds.

2.2.4 Detonation characteristics

Detonation velocity (*D*) and pressure (*P*) are proportional to density according to Kamlet-Jacobs equations. Fig. 2.13 shows the relation between density and velocity of detonation, and summarizes that an increase in the density increases the detonation velocity of the corresponding compounds. Table 2.7 presents calculated *D* and *P* values of the designed compounds. Compounds **S3**, **S4**, and **S5** show detonation velocity higher than 8.7 km/s and pressure over 33 GPa. Detonation performance increases with the increase in the amount of nitro groups responsible for the increase in the oxygen balance. The increase in the *D* and *P* values can be given in order: **S1**, **S2**, **S3**, **S4**, **S5**. Nitro groups at the bridge head position introduce a strain into the compounds due to a strong repulsion between them.

2.2.5 Thermal stability

Thermal stability of the designed compounds was predicted by analyzing the bond dissociation energies (BDEs) of the weak C-NO_2 bonds. Generally, higher the bond length is, weaker and more sensitivity is the bond. The increase in the number of nitro groups increases the strain in the skeleton affecting the space orientation of nitro groups due to the steric strain. According to previous studies, energetic materials should have BDE higher than 80-120 kJ/mol.[40] The calculated BDEs of designed compounds are listed in Table 2.9. Predicted values of BDE for the designed compounds (**S1-S5**) were found to be higher than 190 kJ/mol.

Table 2.9: Computed -Q_{NO2}, C-NO_2 bond length of weakest bond and BDE of the designed compounds at B3LYP/6-31G* level.

Compd.	**S1**	**S2**	**S3**	**S4**	**S5**	**TNAZ**
$-Q_{NO_2}$ (e)	0.230	0.207	0.197	0.182	0.162	0.161
$R_{C\text{-}NO2}$ (Å)	1.485	1.478	1.499	1.502	1.501	1.523
BDE (kJ/mol)	263.57	251.48	233.11	221.99	193.71	169.03

Fig. 2.15 show that the increase in number of nitro groups in the molecule decreases the BDE value being responsible for the subsequent weakening of the C-NO_2 bonds. **S5** shows the lowest value of BDE in the series due to the presence of five nitro groups, which creates a strain in the compound and the C-NO_2 bond becomes weaker. All designed compounds possess higher BDE than TNAZ because the azetidine ring is more strained due to the nitramino and geminal nitro groups.

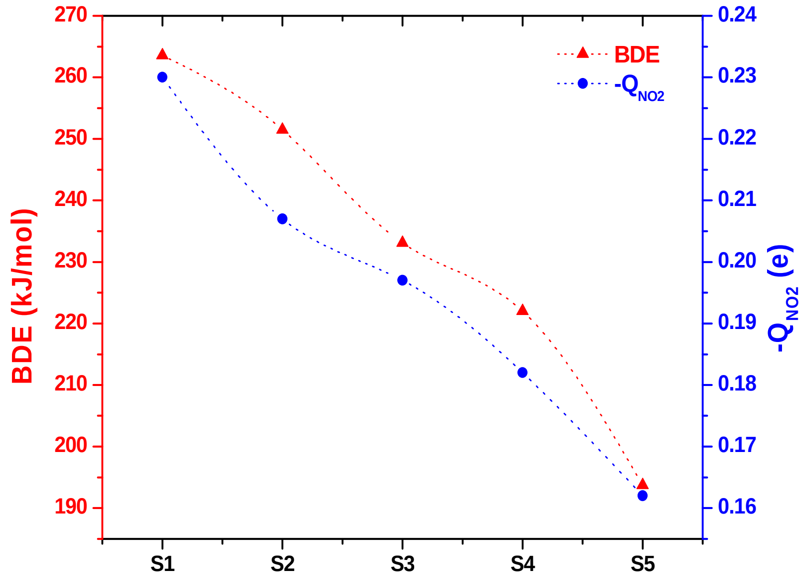

Fig. 2.15 Relationship between bond dissociation energy (kJ/mol) and charge on nitro groups (e).

2.2.6 *Sensitivity correlations*

The present study explores the sensitivity correlations based on the charge on nitro groups ($-Q_{NO_2}$). In nitro compounds, nitro groups have a strong ability to attract electrons, which can be represented by their net charges. The higher negative charge the nitro group possesses the lower is its electron attraction ability and, therefore, the more stable the nitro compound is.[100,101] Calculated C-NO_2 bond lengths of the weakest bond are listed in Table 2.9. All designed compounds (**S1-S2**) exhibit $-Q_{NO_2}$ values higher than that of TNAZ. Results reveal that the designed compounds are found to be more insensitive than TNAZ in which high sensitivity is caused by a strained azetidine ring and geminal nitro groups. Fig. 2.15 shows that the increase in the number of nitro groups in the bicyclo[1.1.1]pentane skeleton causes an increase in the molecules sensitivity. Simultaneous introduction of nitro groups reduces the electron density at ring carbons via negative inductive effects diminishing their charge.[102]

2.2.7 Conclusions

The density functional theory was employed to calculate ΔH^0_f of polynitrobicyclo[1.1.1]pentanes through a successful design of isodesmic reactions. An increase in number of nitro groups increased the ΔH^0_f and the density. The study reveals that the bicyclo[1.1.1]pentane skeleton contributes to the total energy content and thereby improves the ΔH^0_f of the designed compounds. Bond dissociation energy of the weakest C-NO_2 bond of the designed molecules was calculated to predict relative stability. An increase in the number of nitro groups decreases the bond dissociation energy. Sensitivity correlation was established by analyzing the negative charge on the nitro groups. This analysis revealed that the designed compounds are more insensitive than TNAZ. Molecules **S3**, **S4**, and **S5** show better energetic characteristics and can find their application as HEMs.

2.3 References

1. Pagoria, P. F.; Lee, G. S.; Mitchell, A. R.; Schmidt, R. D. *Thermochim. Acta* **2002**, *384*, 187.
2. Bircher, H. *Chimia* **2004**, *58*, 355.
3. Qui, L.; Xiao, H. M.; Gong, X. D.; Ju, X. H.; Zhu, W. H. *J. Phys. Chem. B* **2006**, *110*, 3797.

4. Xu, X. J.; Xiao, H. M.; Ju, X. H.; Gong, X. D.; Zhu, W. H. *J. Phys. Chem. A* **2006**, *110*, 5929.
5. Richard, R. M.; Ball, D. W. *J. Mol. Struct.* **2008**, *858*, 85.
6. Carroll, P. J.; Dailey, W. P.; Wade, P. A. *J. Am. Chem. Soc.* **1987**, *109*, 5452.
7. Carroll, P. J.; Kondracki, P. A.; Wade, P. A. *J. Am. Chem. Soc.* **1991**, *113*, 8807.
8. Iushin, V. P.; Komelin, M. S.; Tartakovsky, V. A. *Zh. Org. Khim.* **1999**, *35*, 489.
9. Archibald, T. G.; Baum, K.; Cohen, M. C.; Garver, L. C. *J. Org. Chem.* **1989**, *54*, 2869.
10. Borman, S. *Chem. Eng. News* **1994**, *72*, 18.
11. Ofah, G. A.; Squire, D. R. *Chemistty of energetic materials*, Acad. Press, Inc., San Diego, 1991.
12. Jalovy, Z.; Zeman, S.; Suceska, M.; Vavra, P.; Dudek, K.; Rajic, M. *J. Energ. Mater.* **2001**, *19*, 219.
13. Chapman, R. D.; Fischer, J. W.; Hollins, R. A.; Lowe-Ma, C. K.; Nissan, R. A. *J. Org. Chem.* **1996**, *61*, 9340.
14. Fan, X. W.; Ju, X. H. *J. Comput. Chem.* **2008**, *29*, 505.
15. Alster, J.; Eaton, P. E.; Gilbert, E. E.; Pluth, J. J.; Price, G. D.; Ravi Shankar, B. K.; Sandus, O. *J. Org. Chem.* **1984**, *49*, 185.
16. Cady, H. H. *Estimation of the density of organic explosives from their structural formulas*, Report LA-7760-MS, Los Alamos National Laboratory, New Mexico, 1979.
17. Grice, M. E.; Murray, J. S.; Politzer, P. *Decomposition, combustion and detonation chemistry of energetic materials*, Eds Brill, T. B.; Russell, T. P.; Tao, W. C.; Wardle, R. B. Materials Research Society, Pittsburgh, PA, **1996**, *418*, 55.
18. Eaton, P. E.; Wicks, G. E. *J. Org. Chem.* **1988**, *53*, 5353.

19. Marchand, A. P. *Tetrahedron*, **1988**, *44*, 2377.

20. Eaton, P. E.; Gilardi, R.; Hain, J.; Kanomata, N.; Li, J.; Lukin, K. A.; Punzalan, E. *J. Am. Chem. Soc.* **1997**, *119*, 9591.

21. Eaton, P. E.; Gilardi, R.; Xiong, Y. *J. Am. Chem. Soc.* **1993**, *115*, 10195.

22. Eaton, P. E.; Gilardi, R.; Zhang, M. X. *Angew. Chem. Int. Ed.* **2000**, *39*, 401.

23. Eaton, P. E.; Zhang, M. X.; Gilardi, R.; Gelber, N.; Iyer, S.; Surapaneni, R. *Propell. Explos. Pyrotech.* **2002**, *27*, 1.

24. Gilardi, R. D.; Karle, J. *Chemistry of energetic materials*, Ed., Squire, D. R.; Olah, G. A. Academic Press, San Diego, 1991, 2.

25. Chander Suri, S.; Marchand, A. P. *J. Org. Chem.* **1984**, *49*, 2041.

26. Annapurna, G. S.; Madhava Sharma, G. V.; Marchand, A. P.; Pednekar, P. R. *J. Org. Chem.* **1987**, *52*, 4784.

27. Fessner, W. D.; Prinzbach, H. *Tetrahedron*, **1986**, *42*, 1797.

28. Arney Jr., B. E.; Dave, P. R.; Marchand, A. P. *J. Org. Chem.* **1988**, *53*, 443.

29. Gilbert, E. E.; Sollott, G. P. *J. Org. Chem.* **1980**, *45*, 5405.

30. Gilbert, E. E.; Sollott, G. P. US Pat. 4535193, 1985.

31. Alster, J.; Gilbert, E. E.; Sandus, O.; Slagg, N.; Sollott, G. P. *J. Energ. Mater.* **1986**, *4*, 5.

32. Mohan, L.; Murray, R. W.; Rajadhyaksha, S. N. *J. Org. Chem.* **1989**, *54*, 5783.

33. Archibald, T. G.; Baum, K. *J. Org. Chem.* **1988**, *53*, 4645.

34. Ammon, H. L.; Cho, C. S.; Dave, P. R.; Ferraro, M. *J. Org. Chem.* **1990**, *55*, 4459.

35. Xu, X. J.; Zhu, W. H.; Xiao, H. M. *J. Mol. Struct. (THEOCHEM)* **2008**, *853*, 1.

36. Browne, A. R.; Doecke, C. W.; Paquette, L. A.; Williams, R. V. *J. Am. Chem. Soc.* **1983**, *105*, 4113.

37. Browne, A. R.; Doecke, C. W.; Fischer, J. W.; Paquette, L. A. *J. Am. Chem. Soc.* **1985**, *107*, 686.

38. Engel, P.; Fischer, J. W.; Paquette, L. A. *J. Org. Chem.* **1985**, *50*, 2524.

39. Engel, P.; Nakamura, K.; Paquette, L. A. *Chem. Ber.* **1986**, *119*, 3782.

40. Qiu, L. M.; Gong, X. D.; Zheng, J.; Xiao, H. M. *J. Hazard. Mater.* **2009**, *166*, 931.

41. Xu, W. G.; Liu, X. F.; Lu, S. X. *J. Mol. Struct. (THEOCHEM)* **2008**, *864*, 80.

42. Gilardi, R.; Olah, G. A.; Ramaiah, P.; Surya Prakash, G. K. *J. Org. Chem.* **1993**, *58*, 763.

43. Kashyap, R. P.; Marchand, A. P.; Sharma, R.; Watson, W. H.; Zope, U. R. *J. Org. Chem.* **1993**, *58*, 759.

44. Simpson, R. L.; Urtiew, P. A.; Ornellas, D. L.; Moody, G. L.; Scribner, K. J.; Hoffman, D. M. *Propell. Explos. Pyrotech.* **1997**, *22*, 249.

45. Geetha, M.; Nair, U. R.; Sarwade, D. B.; Gore, G. M.; Asthana, S. N.; Singh, H. *J. Therm. Anal. Calorim.* **2003**, *73*, 913.

46. Isayev, O.; Gorb, L.; Qasim, M.; Leszczynski, J. *J. Phys. Chem. B* **2008**, *112*, 11005.

47. Nielsen, A. T.; Nissan, R. A.; Vanderah, D. J.; Coon, C. L.; Gilardi, R. D.; George, C. F.; Flippen-Anderson, J. *J. Org. Chem.* **1990**, *55*, 1459.

48. Nielsen, A. T. Caged Nitramine Compound. US Pat. 5693794, 1997.

49. Nielsen, A. T.; Chawn, A. P.; Christian, S. L.; Moore, D. W.; Nadler, M. P.; Nissan, R. A.; Vanderah, D. J.; Gilardi, R. D.; George, C. F.; Flippen-Anderson, J. L. *Tetrahedron* **1998**, *54*, 11793.

50. Foltz, M. F.; Coon, C. L.; Garcia, F.; Nichols, A. L. *Propell. Explos. Pyrtech.* **1994**, *19*, 133.

51. Holtz, E. V.; Ornellas, D. O.; Foltz, M. F. *Propell. Explos. Pyrotech.* **1994**, *19*, 206.

52. Agrawal, J. P. *Prog. Energy Combust. Sci.* **1998**, *24*, 1.

53. Xue, H.; Gao, Y.; Twamley, B.; Shreeve, J. M. *Chem. Mater.* **2005**, *17*, 191.

54. Gutowski, K. E.; Rogers, R. D.; Dixon, D. A. *J. Phys. Chem. A* **2006**, *110*, 11890.

55. Chavez, D. E.; Hiskey, M. A.; Gilardi, R. D. *Angew. Chem. Int. Ed.* **2000**, *39*, 1791.

56. Fraenk, W.; Habereder, T.; Hammerl, A.; Klapotke, T. M.; Krumm, B.; Mayer, P.; Noth, H.; Warchhold, M. *Inorg. Chem.* **2001**, *40*, 1334.

57. Hammerl, A.; Holl, G.; Klapotke, T. M.; Kaiser, M.; Ticmanis, U.; Noth, H.; Warchhold, M. *Inorg. Chem.* **2001**, *40*, 3570.

58. Hammerl, A.; Holl, G.; Klapotke, T. M.; Kaiser, M.; Piotrowski, H. *Propell. Explos. Pyrotech.* **2001**, *26*, 161.

59. Guo, Y. Q.; Greenfield, M.; Bhattacharya, A.; Bernstein, E. R. *J. Chem. Phys.* **2007**, *127*, 154301.

60. Slanina, Z.; Zhao, X.; Chiang, L. Y.; Osawa, E. *Int. J. Quantum Chem.* **1999**, *74*, 343.

61. Fan, X. W.; Ju, X. H.; Xiao, H. M. *J. Hazard. Mater.* **2008**, *156*, 342.

62. Chapman, R. D. *Struct. Bond.* **2007**, *125*, 123.

63. Hehre, W. J.; Ditchfield, R.; Radom, L.; Pople, J. A. *J. Am. Chem. Soc.* **1970**, *92*, 4796.

64. Hehre, W. J.; Radom, L.; Schleyer, P. v. R.; Pople, J. A. *Ab initio molecular orbital theory*, John Wiley and Sons, New York, 1986.

65. Aston, J. G.; Siller, C. W.; Messerly, G. H. *J. Am. Chem. Soc.* **1937**, *59*, 1743.

66. Knobel, Y. K.; Miroshnichenko, E. A.; Lebedev, Y. A. *Bull. Acad. Sci.* USSR, Div. Chem. Sci. **1971**, 425.

67. Chase, M. W. Jr. *J. Phys. Chem. Ref. Data* **1998**, *9*, 1.

68. Manion, J. A. *J. Phys. Chem. Ref. Data* **2002**, 123.

69. Cox, J. D.; Wagman, D. D.; Medvedev, V. A. *CODATA Key values for thermodynamics*, Hemisphere Publishing Corp, New York, 1984.

70. Zaheeruddin, M.; Lodhi, Z. H. *Phys. Chem.* (Peshawar Pak) **1991**, *10*, 111.

71. Jimenez, P.; Roux, M. V.; Turrion, C. *J. Chem. Thermodyn.* **1989**, *21*, 759.

72. Balepin, A. A.; Lebedev, V. P.; Miroshnichenko, E. A.; Koldobskii, G. I.; Ostovskii, V. A.; Larionov, B. P.; Gidaspov, B. V.; Lebedev, Yu. A. *Svoistva Veshchestv Str. Mol.* **1977**, 93.

73. Li, J.; Huang, Y.; Dong, H. *Propellants, Explos., Pyrotech.* **2004**, *29*, 231.

74. Kamlet, M. J.; Jacobs, S. J. *J. Chem. Phys.* **1968**, *48*, 23.

75. Kamlet, M. J.; Huewitz, H. *J. Chem. Phys.* **1968**, *48*, 3685.

76. Mader, C. L. In *Organic Energetic Compounds*; Markinas, P. L., Ed.; Nova Science Publishers: Commack, NY, 1996, 193.

77. Strehlow, R. A. *Combustion Fundamentals*; McGraw-Hill: New York, 1985, 302.

78. Zhang, C.; Shu, Y.; Huang, Y.; Zhao, X.; Dong, H. *J. Phys. Chem. B* **2005**, *109*, 8978.

79. Chiang, J. F.; Bauer, S. H. *J. Am. Chem. Soc.* **1970**, *92*, 1614.

80. Wiberg, K. B.; Connor, D. S.; Lampman, G. M. *Tetrahedron Lett.* **1964**, *5*, 531.

81. Stulgies, B.; Pigg, D. P. Jr.; Kaszynski, P.; Kudzin, Z. H. *Tetrahedron* **2005**, *61*, 89.

82. Shtarev, A. B.; Pinkhassik, E.; Levin, M. D.; Stibor, I.; Michl, J. *J. Am. Chem. Soc.* **2001**, *123*, 3484.

83. Semmler, K.; Szeimies, G.; Belzner, J. *J. Am. Chem. Soc.* **1985**, *107*, 6410.

84. Levin, M. D.; Kaszynski, P.; Michl, *J. Chem. Rev.* **2000**, *100*, 169.

85. Della, E. W.; Elsey, G. M. *Tetrahedron Lett.* **1988**, *29*, 1299.

86. Costantino, G.; Maltoni, K.; Marinozzi, M.; Camaioni, E.; Prezeau, L.; Pin, J. P.; Pellicciari, R. *Bioorg. Med. Chem.* **2001**, *9*, 221.

87. Alkorta, I.; Elguero, J. *Tetrahedron*, **1997**, *53*, 9741.

88. Surya Prakash, G. K.; Bae, C.; Kroll, M.; Olah, G. A. *J. Fluorine Chem.* **2002**, *117*, 103.

89. Wiberg, K. B.; Ross, B. S.; Isbell, J. J.; McMurdie, N. *J. Org. Chem.* **1993**, *58*, 1372.

90. Wiberg, K. B.; Waddell, S. T. *J. Am. Chem. Soc.* **1990**, *112*, 2194.

91. Friedli, A. C.; Kaszynski, P.; Michl, J. *Tetrahedron Lett.* **1989**, *30*, 455.

92. Wiberg, K. B. *Tetrahedron Lett.* **1985**, *26*, 599.

93. Wiberg, K. B.; Hadad, C. M.; Sieber, S.; Schleyer, P. v. R. *J. Am. Chem. Soc.* **1992**, *114*, 5820.

94. Sikder, N.; Sikder, A. K.; Bulakh, N. R.; Gandhe, B. R. *J. Hazard. Mater.* **2004**, *113*, 35.

95. Politzer, P.; Lane, P.; Grice, M. E.; Concha, M. C.; Redfern, P. C. *J. Mol. Struct. (THEOCHEM)* **1995**, *338*, 249.

96. Wilcox, C. F.; Zhang, Y. X.; Bauer, S. H. *J. Mol. Struct. (THEOCHEM)* **2000**, *528*, 95.

97. Zhang, J.; Xiao, H.; Gong, X. *J. Phys. Org. Chem.* **2001**, *14*, 583.

98. Mayo, S. L.; Olafson, B. D.; Goddard, W. A. III *J. Phys. Chem.* **1990**, *94*, 8897.

99. Huynh, M. H. V.; Hiskey, M. A.; Hartline, E. L.; Montoya, D. P.; Gilardi, R. *Angew. Chem. Int. Ed.* **2004**, *43*, 4924.

100. Zhang, C.; Shu, Y.; Huang, Y.; Wang, X. *J. Energ. Mater.* **2005**, *23*, 107.

101. Zhang, C. *J. Phys. Chem.* A **2006**, *110*, 14029.

102. Zhang, C. *J. Hazard. Mater.* **2009**, *161*, 21.

Chapter III

Chemistry of Azoles in the Design of Energetic Materials

Heterocycles that contain a large amount of nitrogen are relatively dense, they possess higher heat of formation (ΔH^0_f) due to a higher percentage of decomposition products usually dinitrogen. Additionally, smaller amounts of hydrogen and carbon contribute to a better oxygen balance; with enhanced thermal stability more than normally found with their carbocyclic analogues.[1-5] Five member nitrogen containing rings such as imidazole, pyrazole, and triazole are the natural framework for energetic materials as possesses high nitrogen content.[6-8] Their performance can be optimized and improved through substituting hydrogen atoms with explosophore like nitro, amino, azido etc. Among various explosophores, nitro group is a vital constituent of energetic materials. The performance of the polynitro compounds is enhanced by excellent oxygen balance; results in a higher exothermicity of the combustion and detonation process, while ring strain improves ΔH^0_f and density. Hence in the search of novel high energy materials (HEMs), nitro azoles expected to be promising candidates. The enthalpies of energetic chemical systems are governed by their molecular structure. High-nitrogen compounds derive their high ΔH^0_f directly from the large number of inherently energetic N-N and C-N bonds rather than from the overall heats of combustion of hydrocarbon backbone.[9,10] The energy contribution of imidazole, pyrazole, 1,2,4-triazole, 1,2,3-triazole and tetrazole are 129.5, 179.4, 192.7, 271.7 and 326.0 kJ/mol, respectively. Fig. 3.1 lists the five member heterocycles used in the synthesis of energetic materials.

This chapter focuses on the theoretical prediction of energetic characteristics like ΔH^0_f, density, detonation performance, stability and sensitivity correlation of novel energetic azoles. The structure-property relationship has been attempted to understand the role of substituents and contribution of different heterocyclic azole rings towards the energetic behavior.

Imidazole Pyrazole 1,2,4-Triazole 1,2,3-Triazole

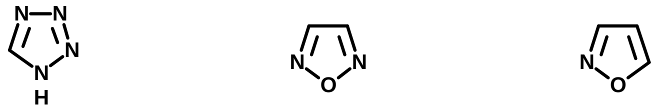

Tetrazole Furazan Isoxazole

Fig. 3.1 Nitrogen-rich five member heterocycles used in energetic materials.

3.1 Energetic Nitro-azoles

Polynitro-imidazoles and pyrazoles are promising candidates of HEMs due to their favorable insensitivity and energetic performance. Substitution of the hydrogen atoms of azoles by various nitrogen-containing energetic functional groups occurs in a straightforward manner. Increase in nitro group improves the density as well increases the chances of hydrogen bonding between oxygen and acidic hydrogen on ring nitrogen.[8,11] Different nitro azole isomers based on five membered heterocycles were designed and investigated using computational techniques. Molecules with bi and tri nitrogen heterocycles with varying nitro groups are designed and their structures are shown in Fig. 3.2.

Results and Discussion

Energetic azoles are nitrogen-rich and the designed molecules having nitrogen content of about 40% and oxygen balance is -12.7%. The present study brings out the structure-property relationships of energetic azole isomers possessing molecular formula $C_5HN_9O_8$ by comparing their characteristics like gas phase ΔH^0_f, density (ρ_o), detonation performance (D and P), stability and the insensitivity. The predicted energetic properties of the designed molecules have been compared with 1-methyl-

2,4,5-trinitroimidazole (MTNI) to evaluate the performance. MTNI is an insensitive melt-cast high explosive, whose explosive performance is comparable to RDX and its sensitivity is intermediate between RDX and TNT.[12,13]

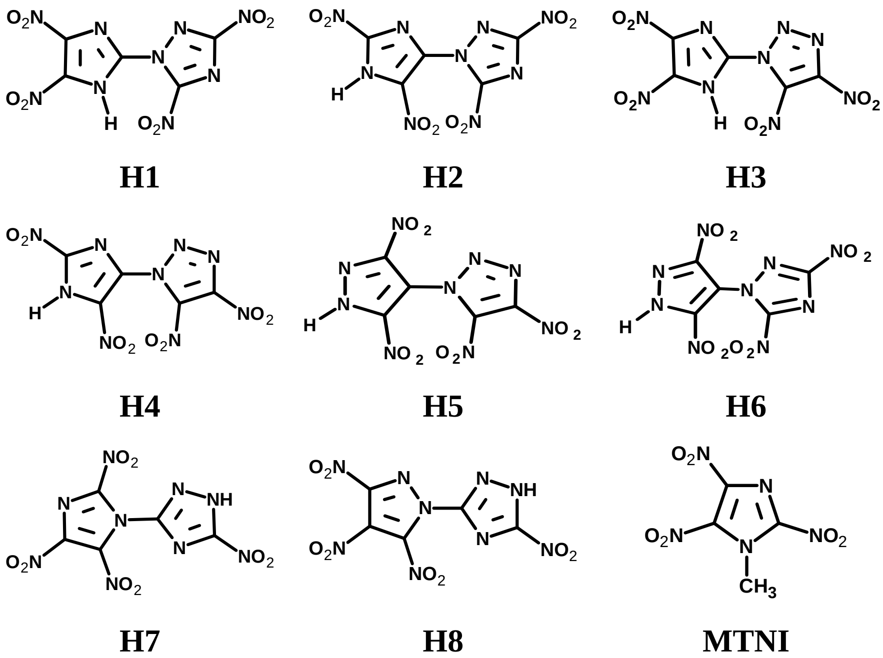

Fig. 3.2 Molecular structures of the designed azole isomers.

3.1.1 Molecular geometries

All designed compounds contain four nitro groups in their molecular skeleton. When two nitro groups on the azole rings are adjacent, oxygen atoms of other nitro group slightly modifies the molecular plane to reduce the steric hindrance and repulsive effect. The selected structural parameters of the designed molecules are listed in Table 3.1 to 3.4. The bond lengths of C-NO_2 bond found to be higher than other C-C and C-N bonds in the molecular structure.

Overall, the lengths of C-NO_2 linkages differ from isomer to isomer with the position of nitro groups and their surrounding. In the designed compounds, C-NO_2 bonds are found higher than 1.45 Å. The non-planarity in the molecular structure is due to the repulsion between the adjacent nitro groups. The torsional angle between the azole rings varies from 105 to 154^{o}. The close proximity of the nitro groups increases the distortion angle between azole rings linked via C-N bond to reduce the steric and repulsive effect of nitro groups. In the **H5**, **H6**, **H7** and **H8** molecules, plane of the azole rings deviates more to reduce the repulsion between nitro groups. In **H1** and **H2**, the change in the position of 1,2,4-triazole on the imidazole ring slightly increases the C-C and C-N bond lengths of **H2**, may be due to the torsion in the ring and repulsion between nitro groups on the imidazole and triazole rings. Replacement of imidazole with pyrazole (**H1** and **H6**) slightly reduces the bond lengths of C-NO_2 bonds in the structure. Similarly, replacement of 1,2,4-triazole with 1,2,3-triazole (in **H1** and **H3**) slightly increases the C-C and C-N bond lengths of molecular structure. Similar trend is observed in **H2-H4** and **H5-H6**. The introduction of three nitro groups on the imidazole (**H7**) and pyrazole (**H8**) significantly increases the C-C and C-N bond lengths in these molecules due to high repulsive effect between the adjacent nitro groups.

Table 3.1: Selected structural parameters of **H1** and **H2** computed at the B3LYP/6-31G*.

	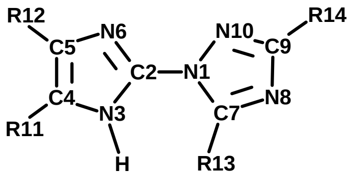		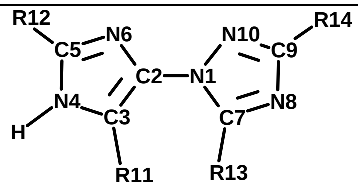	
	H1		**H2**	
Bond length (Å)	N1-C2	1.4015	N1-C2	1.4068
	C2-N3	1.3136	C2-C3	1.3878
	N3-C4	1.3538	C3-N4	1.3621
	C4-C5	1.3841	N4-C5	1.3526
	C5-N6	1.3726	C5-N6	1.3152
	N6-C2	1.3528	N6-C2	1.3515
	N1-C7	1.3687	N1-C7	1.3697
	C7-N8	1.3069	C7-N8	1.3061
	N8-C9	1.3514	N8-C9	1.3492
	C9-N10	1.3204	C9-N10	1.3222
	N10-N1	1.3574	N10-N1	1.3529
	C4-R11	1.4613	C3-R11	1.4307
	C5-R12	1.4375	C5-R12	1.4543
	C7-R13	1.4673	C7-R13	1.4605
	C9-R14	1.4682	C10-R14	1.4682
T.A. (°)	N6-N2-N1-C7	161.5	N6-C2-N1-C7	114.2
	N3-N2-N1-N10	154.2	C3-V2-N1-N10	118.1

R11, R12, R13, R14=NO_2; T.A. is the torsional angle.

Table 3.2: Selected structural parameters of **H3** and **H4** computed at the B3LYP/6-31G*.

	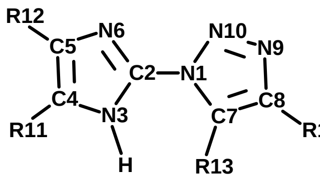		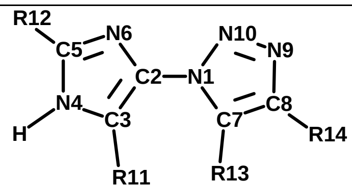	
	H3		**H4**	
Bond length (Å)	N1-C2	1.4088	N1-C2	1.4093
	C2-N3	1.3566	C2-C3	1.3895
	N3-C4	1.3677	C3-N4	1.3627
	C4-C5	1.3851	N4-C5	1.3519
	C5-N6	1.3506	C5-N6	1.3148
	N6-C2	1.3174	N6-C2	1.3521
	N1-C7	1.3661	N1-C7	1.3626
	C7-C8	1.3775	C7-C8	1.3773
	C8-N9	1.3514	C8-N9	1.3526
	N9-N10	1.2918	N9-N10	1.2957
	N10-N1	1.3769	N10-N1	1.3675
	C4-R11	1.4394	C3-R11	1.4304
	C4-R12	1.4618	C5-R12	1.4547
	C7-R13	1.4491	C7-R13	1.4471
	C8-R14	1.4547	C8-R14	1.4566
T.A. (^{o})	N6-C2-N1-C7	137.3	N6-C2-N1-C7	119.8
	N3-C2-N1-N10	136.6	C3-C2-N1-N10	123.4

R11, R12, R13, R14=NO_2; T.A. is the torsional angle.

Table 3.3: Selected structural parameters of **H5** and **H6** computed at the B3LYP/6-31G*.

	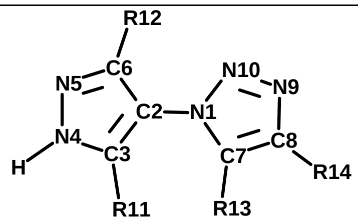		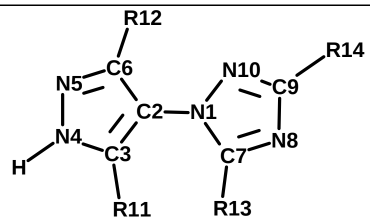	
	H5		**H6**	
Bond length (Å)	N1-C2	1.4064	N1-C2	1.4084
	C2-C3	1.4122	C2-C3	1.3842
	C3-N4	1.3284	C3-N4	1.3525
	N4-N5	1.3310	N4-N5	1.3298
	N5-C6	1.3511	N5-C6	1.3291
	C6-C2	1.3845	C6-C2	1.4114
	N1-C7	1.3597	N1-C7	1.3677
	C7-C8	1.3786	C7-N8	1.3065
	C8-N9	1.3508	N8-C9	1.3480
	N9-N10	1.2967	C9-N10	1.3230
	N10-N1	1.3655	N10-N1	1.3512
	C3-R11	1.4574	C3-R11	1.4375
	C6-R12	1.4401	C6-R12	1.4572
	C7-R13	1.4462	C7-R13	1.4587
	C8-R14	1.4559	C9-R14	1.4578
T.A. (°)	C6-C2-N1-C7	97.6	C6-C2-N1-C7	105.4
	C3-C2-N1-N10	97.9	C3-C2-N1-N10	106.9

R11, R12, R13, R14=NO_2; T.A. is the torsional angle.

Table 3.4: Selected structural parameters of **H7** and **H8** computed at the B3LYP/6-31G*.

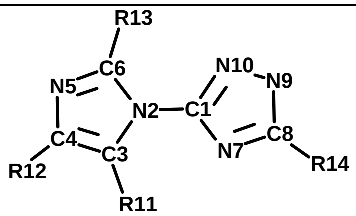

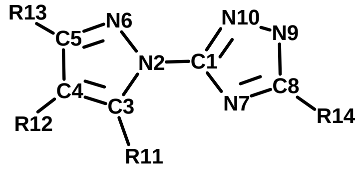

	H7		H8	
Bond length (Å)	C1-N2	1.4214	C1-N2	1.4167
	N2-C3	1.3748	N2-C3	1.3732
	C3-C4	1.3061	C3-C4	1.3773
	C4-N5	1.3492	C4-C5	1.4074
	N5-C6	1.3815	C5-N6	1.3242
	C6-N2	1.3805	N6-N2	1.3403
	C1-N7	1.3484	C1-N7	1.3508
	N7-C8	1.3126	N7-C8	1.3125
	C8-N9	1.3487	C8-N9	1.3494
	N9-N10	1.3415	N9-N10	1.3408
	N10-C1	1.3265	N10-C1	1.3275
	C3-R11	1.4609	C3-R11	1.4437
	C4-R12	1.4616	C4-R12	1.4651
	C6-R13	1.4490	C5-R13	1.4569
	C8-R14	1.4542	C8-R14	1.4542
T.A. (^{o})	C6-N2-C1-N7	74.8	N6-N2-C1-N7	111.5
	C3-N2-C1-N10	75.1	C3-N2-C1-N10	104.7

R11, R12, R13, R14=NO_2; T.A. is the torsional angle.

3.1.2 Gas phase heat of formation

The ΔH^0_f is the indicative of the energy content of the high energy materials and hence, important to predict accurately. The calculated total energies at 298K upon inclusion of zero point energy and thermal corrections and the experimental gas phase ΔH^0_f [14-24] of the reference compounds imidazole, pyrazole, triazoles, CH_4, NH_3,

CH_3NO_2, and CH_3NH_2 are listed in Table 3.5. $\Delta H^0{}_f$ has been predicted by designing appropriate isodesmic reactions. Previous studies[3] show that the theoretically predicted values are in good agreement with experiments by choosing the appropriate reference compounds in the isodesmic reaction. Fig. 3.3 represents the constructed isodesmic reaction scheme for the designed molecules. The calculated gas phase $\Delta H^0{}_f$ of designed compounds at 298.15K using isodesmic approach have been listed in Table 3.6.

The calculated $\Delta H^0{}_f$ of the designed molecules have been compared with MTNI to evaluate the performance. The predicted gas phase $\Delta H^0{}_f$ of MTNI using isodesmic reaction approach is 170.41 kJ/mol, which is comparable with earlier reported values by Su et al. (173.4 and 176.15 kJ/mol).[3,8] The high positive $\Delta H^0{}_f$ for the reference azole skeletons confirm that these will contribute for the positive $\Delta H^0{}_f$ of the designed isomers. The $\Delta H^0{}_f$ for predicted compounds show high positive values in the range of 420 to 660 kJ/mol. The high $\Delta H^0{}_f$ can be attributed to the presence of a large number of N-N and C-N bonds and energetic nitro groups. The molecules **H1** and **H2** differ only by the position of 1,2,4-triazole ring on the imidazole. **H1** shows higher $\Delta H^0{}_f$ than **H2**, this may be due to the repulsion associated with the adjacent nitro groups in the imidazole ring. Similar is observed in the case of **H3** and **H4** too. In general, it is observed that energy contribution by pyrazole and 1,2,3-triazole rings are higher than the imidazole and 1,2,4-triazole rings, respectively. Among the designed molecules, the molecules **H5** and **H6** show higher $\Delta H^0{}_f$ viz., 586.5 and 663.8 kJ/mol, respectively. This may be attributed to the presence of adjacent bulky nitro groups and energetic pyrazole, triazole rings. Comparison of **H7** and **H8** reveals that, **H8** has higher $\Delta H^0{}_f$ due to the higher repulsive energy between three adjacent nitro groups on the pyrazole ring. The adjacent nitro groups can affect the free orientation and arrangement on the ring and causes the repulsion. Overall study shows that all designed compounds possess higher positive ΔH^0_f than the MTNI due to the presence of four nitro groups and nitrogen-rich heterocyclic framework.

Table 3.5: Total energy (E_0) at 298.15K and gas phase ΔH^0_f for the reference compounds at the B3LYP/6-31G* level.

Compd.	E_0 (au)	ΔH^0_f (kJ/mol)
CH_4	-40.46935	-74.6
NH_3	-56.50961	-45.9
CH_3NH_2	-95.78444	-22.5
CH_3NO_2	-244.95385	-74.7
CH_3N_3	-204.03725	238.4
CH_3NNCH_3	-189.18439	159.4
Imidazole	-226.13859	129.5
Pyrazole	-226.12249	179.4
1,2,4-triazole	-242.18479	192.7
1,2,3-triazole	-242.15867	271.7
Tetrazole	-258.24639	326.0
Isoxazole	-245.97206	78.6
Furazan	-261.99676	196.2

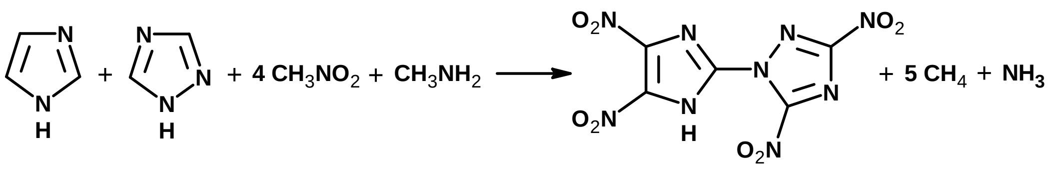

H1

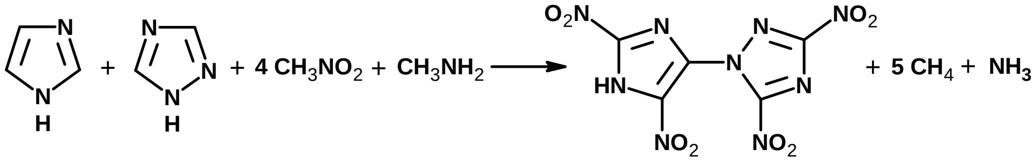

H2

Fig. 3.3 Isodesmic reaction schemes for designed molecules.

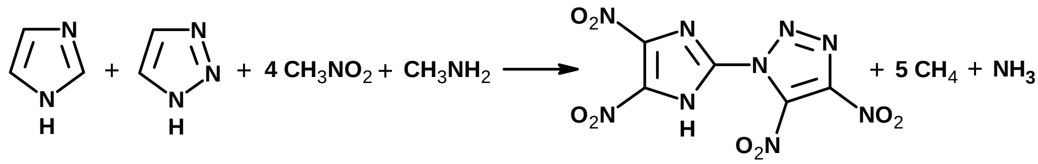

H3

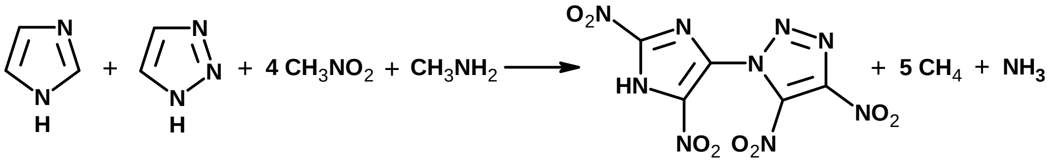

H4

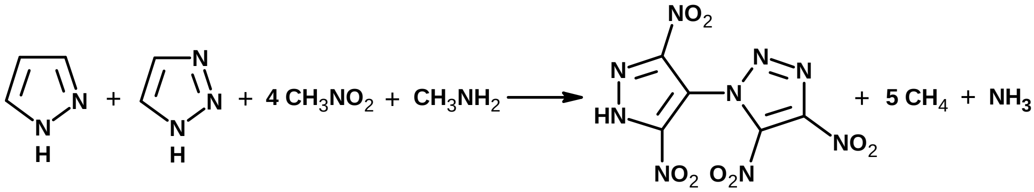

H5

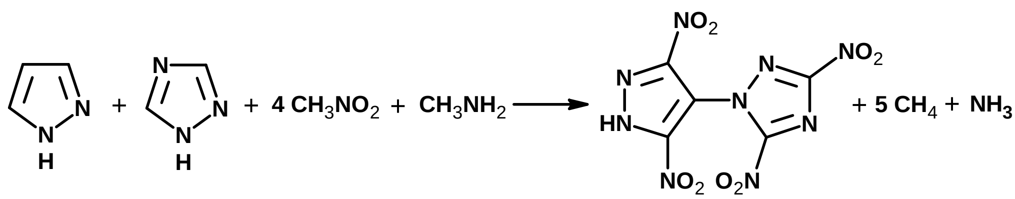

H6

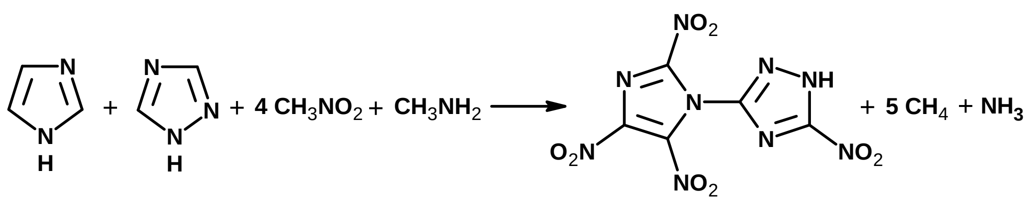

H7

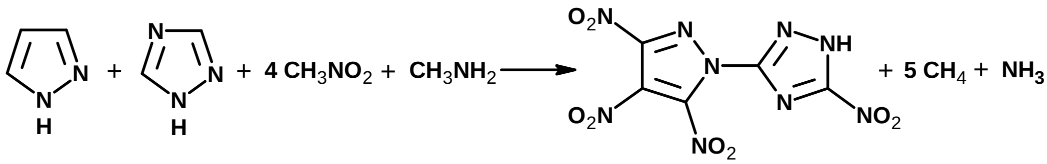

H8

Fig. 3.3 (Contd.)

Table 3.6: Predicted explosive characteristics for designed compounds.

Compd.	E_0 (a.u.)	ΔH^0_f (kJ/mol)	Q (cal/g)	*D* (km/s)	*P* (GPa)	BDE (kJ/mol)	$-Q_{NO2}$ (e)
H1	-1285.05725	445.01	1385.4	8.92	36.13	262.16	0.137
H2	-1285.06677	420.02	1366.5	9.03	37.44	261.33	0.179
H3	-1285.02644	535.15	1453.9	9.41	41.50	251.92	0.158
H4	-1285.03612	510.24	1434.9	9.11	37.96	253.58	0.162
H5	-1285.01027	586.47	1492.8	9.26	39.54	267.27	0.167
H6	-1285.04120	663.87	1551.5	9.39	40.73	260.29	0.186
H7	-1285.05729	444.92	1385.4	8.95	36.52	249.55	0.165
H8	-1285.03685	506.21	1431.9	9.07	37.51	250.98	0.103
MTNI	-876.86367	170.41	1229.9	8.82	34.75	250.34	0.170

3.1.3 Density

The most significant property of a high performance energetic material is crystal density as it is directly involved in detonation performance. Density and lattice parameters of the designed compounds are calculated by crystal packing calculations using cvff force field are presented in Table 3.7. Density predicted from cvff force field is used for the calculation of detonation characteristics as it provides marginally better results for nitro compounds.[25] Predicted density of MTNI molecule (1.82 g/cm^3) using cvff force field is found close to experimental value (1.79 g/cm^3).[26]

The density for designed molecules has been found to be remarkably high and varies from 1.86 to 1.98 g/cm^3. The molecule **H3** shows the highest density (1.98 g/cm^3) while, **H1**, **H7**, and **H8** shows lowest density of about 1.88 g/cm^3. Analysis of molecular framework of **H3** reveals that the two azole rings attached via C-N linkage are perpendicular to each other, minimizes the torsional strain and avoids the steric hindrance between nitro groups. This molecular arrangement minimizes the total molar volume and further, improves the density via intra and intermolecular hydrogen bonding. The repulsion associated with the adjacent nitro groups affects the molecular orientation in space and hence, molecules **H1**, **H7**, and **H8** exhibits lower densities. The predicted minimum energy crystal structures are shown in Fig. 3.4. **H2** shows density higher than **H1**. This may be due to adjacent nitro groups on the imidazole of **H1** which causes the repulsion while; **H2** shows less repulsion due to the better arrangement of nitro groups on the rings. Similar trend is found in the case of **H5** and **H6** and their predicted densities are 1.92 and 1.93 g/cm^3, respectively. Replacement of 1,2,4-triazole in **H1** with 1,2,3-triazole in **H3** increases the density. In general, pyrazole derivatives show higher densities than imidazole and this is clearly seen in pyrazole ring based molecules viz, **H5**, **H6** and **H8** in comparison to imidazole based molecules **H4**, **H2**, and **H7**. Fig. 3.5 shows the relation between density and detonation velocity.

Table 3.7: Density and lattice parameters of the designed compounds.

Compd.	Density (g/cm^3)	Space group	Lattice parameters					
			Length (Å)			Angle (^{o})		
			a	b	c	α	β	γ
H1	1.87	*PBCN*	20.30	8.36	13.29	90.0	90.0	90.0
H2	1.91	*P-1*	6.03	8.96	10.87	97.5	89.6	71.1
H3	1.98	*P21*	5.99	9.92	9.43	90.0	109.7	90.0
H4	1.90	*P21/C*	6.61	8.35	20.01	90.0	85.1	90.0
H5	1.92	*P21/C*	6.05	21.61	10.40	90.0	126.2	90.0
H6	1.93	*P-1*	10.14	6.82	12.49	124.3	85.8	124.6
H7	1.88	*C2/C*	23.69	8.34	28.31	90.0	156.5	90.0
H8	1.89	*P212121*	17.85	10.06	6.15	90.0	90.0	90.0
MTNI	1.82	*P212121*	12.95	9.52	6.41	90.0	90.0	90.0

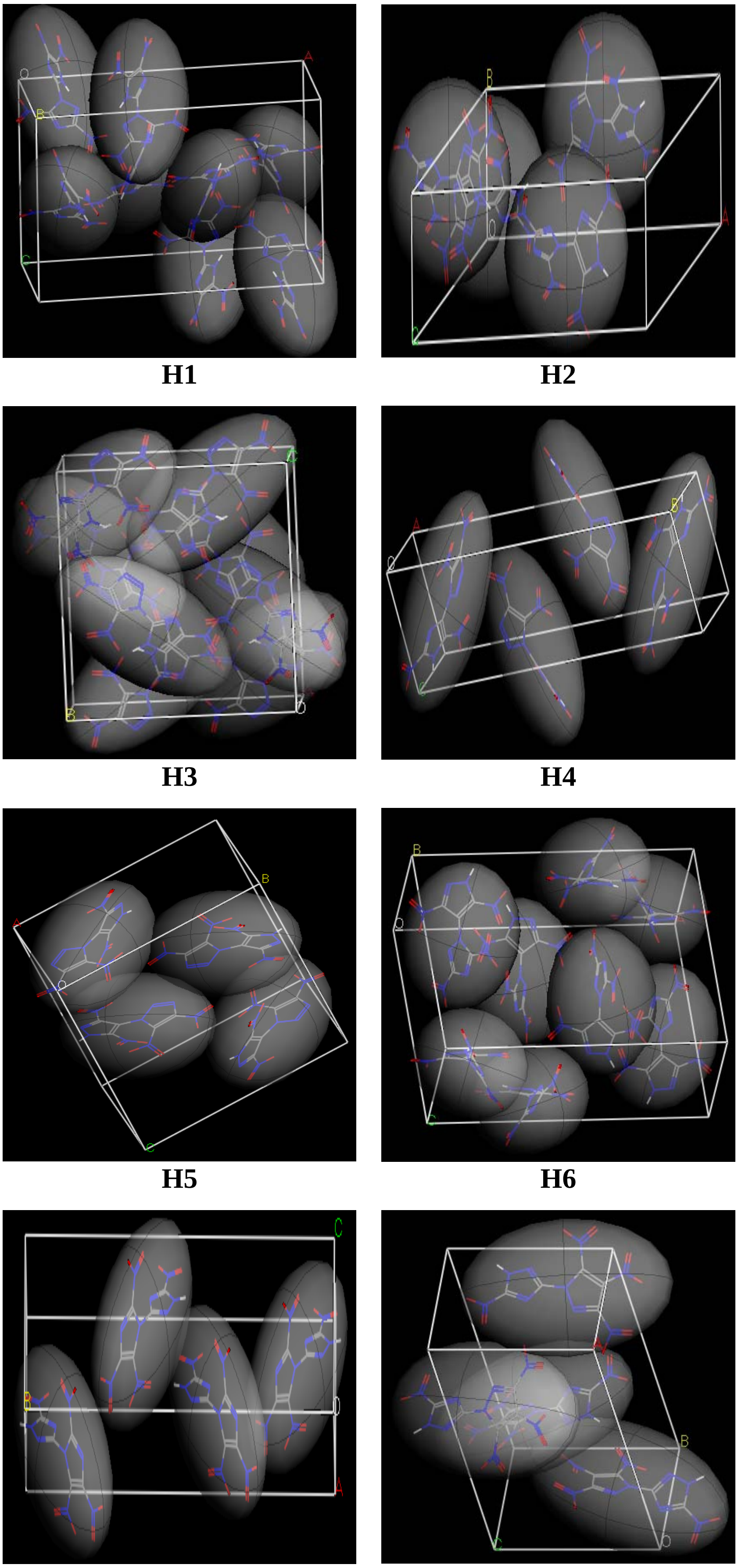

H1 H2 H3 H4 H5 H6 H7 H8

Fig. 3.4 Crystal structures of the designed compounds.

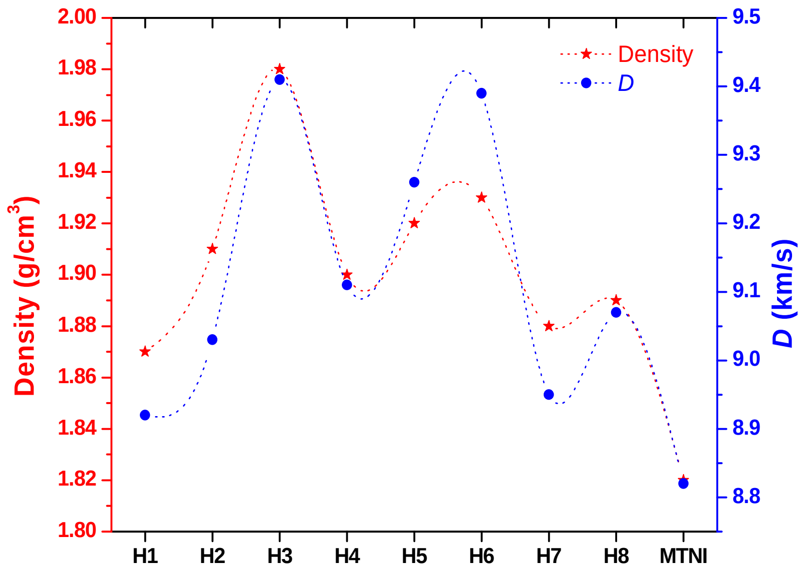

Fig. 3.5 Plot of density (g/cm^3) versus velocity of detonation (km/s).

3.1.4 Detonation characteristics

The detonation velocity (*D*) and detonation pressure (*P*) of the molecules have been computed by Kamlet-Jacobs empirical equations and summarized in Table 3.6. The calculated *D* and *P* values differ for energetic isomers as they posses different density and ΔH^0_f. Detonation performance is mainly dependent on crystal density (Fig. 3.5) and less on ΔH^0_f of the compound. Molecules **H3**, **H5**, and **H6** show higher performance in comparison to others due to their higher densities and ΔH^0_f. The calculated *D* and *P* for these compounds are higher than 9.25 km/s and 39.5 GPa, respectively. The substitution of 1,2,4-triazole with the 1,2,3-triazole enhances the performance in **H3** and **H4** as compared to **H1** and **H2**, respectively. Introduction of pyrazole in **H5** improves the performance of the compound than its imidazole isomer **H4** due to its higher density and ΔH^0_f. This shows that nitro groups and the five membered heterocycles that contain large amount of nitrogen could be responsible for the high performance of these compounds. All designed molecules show higher detonation performance than MTNI which may be due to the better oxygen balance, higher densities and ΔH^0_f.

3.1.5 Thermal stability

The present study explores the stability of the designed compounds by analyzing bond dissociation energy (BDE). BDE evaluate the strength of bonding that is fundamental to understand chemical process and provide useful information for understanding the stability of designed compounds. Recent reports revealed the relationship between BDE and stability; a higher value of the BDE brings stability in the respective compounds.[27,28] The calculated bond dissociation energies of the designed molecules are listed in Table 3.6. According to the criteria of HEMs, BDE should be higher than 80-120 kJ/mol.[29,30] Predicted BDE of MTNI molecule (250.34 kJ/mol) is found very close to earlier reported values.[8]

BDE is dependent on the electronic structure of the molecules and among the energetic azole isomers studied **H1**, **H2**, **H5**, and **H6** show BDE higher than 260 kJ/mol. In these compounds, nitro groups are far from each other due to the perpendicular arrangement of the azole rings which cause less repulsion between nitro groups. The nitro groups are attached to hetero aromatic ring and hence bond strength of C-NO_2 increases via π-electron delocalization. In case of **H3** and **H4**, where the attachment of 1,2,3-triazole on imidazole ring differs, exhibits BDE of about 252 kJ/mol. The repulsion between adjacent nitro groups is very high in these molecules. Similarly, **H7** and **H8** possess three nitro groups on imidazole and pyrazole rings, respectively and hence these compounds show lower BDE in the series. Overall study showed that designed molecules are having high BDE of about 250 kJ/mol and hence these molecules are expected to be stable. All designed molecules possess BDE higher than MTNI may be due to the azole rings and conjugation in molecular skeleton.

3.1.6 Sensitivity correlations

According to the criteria of high energy materials, compounds should be stable and insensitive enough for the practical use and safe handling. The relationship between the impact sensitivity and electronic structures of some nitro compounds can be established by the charge analysis of nitro group.[32] The higher negative charge the nitro group possesses, the lower the electron attraction ability and therefore the more stable the nitro compound. Computed $-Q_{NO_2}$ values of molecules are presented in Table 3.6. The higher $-Q_{NO_2}$, the larger is the impact insensitivity and hence $-Q_{NO_2}$ can be regarded as the criteria for estimating the impact sensitivities. Among the designed compounds **H2** and **H6** show $-Q_{NO_2}$ values higher than MTNI (0.170e). The nitro groups in these compounds are away from each other and minimize the repulsion and steric hindrance. **H8** shows lower value of the $-Q_{NO_2}$ due to the presence of three adjacent nitro groups on the pyrazole ring. $-Q_{NO_2}$ of the **H3** and **H4** are 0.158 and 0.162e, respectively. The adjacent nitro groups in **H3** increases the sensitivity of the molecule more than **H4**. The compounds **H1**, **H5** and **H7** show $-Q_{NO_2}$ values higher than 0.130e.

3.1.7 Conclusions

Electronic structures of the designed energetic azoles have been studied using the density functional theory at the B3LYP/6-31G* level. ΔH^0_f of azole isomers has been computed by designing appropriate isodesmic reactions and the detonation characteristics using Kamlet-Jacobs method. Results revealed that the azole isomers possess very high positive ΔH^0_f due to the presence of high nitrogen content five member azoles. Crystal density has been predicted using molecular packing calculations using the cvff force field and the predicted density is above 1.90 g/cm^3. Designed molecules have detonation velocity higher than 9.1 km/s and pressure above 37 GPa. Analysis of BDE reveals that energetic azoles are expected to be stable. Charge on the nitro group has been analyzed to correlate the impact sensitivity and it has been found that designed molecules are having better impact insensitivity than MTNI. Energetic properties of the designed molecules are compared with 1-methyl-2,4,5-trinitroimidazole and found that these molecules have higher energetic performance with better insensitivity. A structure-property relationship on these energetic azole isomers demonstrates that these molecules will be promising candidates for future HEMs.

3.2 Tetrazole Derivatives

Heterocyclic compounds like tetrazoles are of particular interest because nitrogen content of such compounds can be increased to over 70% by substitution with suitable functional groups.[33-36] Different tetrazole derivatives such as salts of 5,5'-azotetrazole,[37] bistetrazoles,[38] the perchlorate and nitrate of 1,5-diaminotetrazole,[39] salts of 1-methyl-5-nitriminotetrazolate,[40] alkali metal 5,5'-hydrazinebistetrazolate salts,[41] 5-nitroaminotetrazole salts,[42] and organic salts of nitrotetrazole[43] have been tested as potential materials for modifying the combustion rates of rocket propellants, as gas generators and explosive materials. In the present study, nitrogen-rich tetrazole derivatives were studied by using *ab initio* calculations based on hybrid density functional theory. Different molecules have been designed by attaching nitroazoles (imidazole, pyrazole and triazoles) to tertazole via C-C and C-N linkages. Systematic study on the energetic properties such as ΔH^0_f, density, detonation properties, thermal stability and sensitivity correlation has been carried out. Fig. 3.6 shows the molecular framework of the tetrazole derivatives.

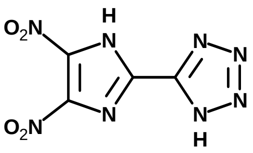

T1

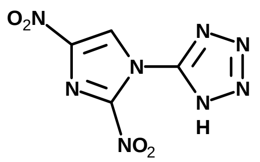

T2

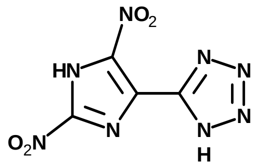

T3

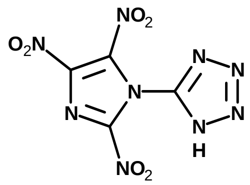

T4

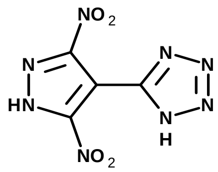

T5

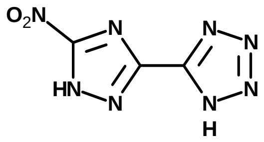

T6

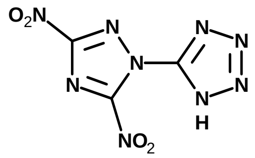

T7

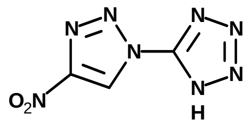

T8

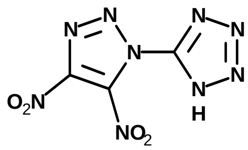

T9

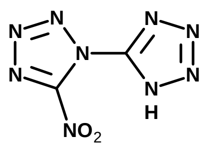

T10

Fig. 3.6 Molecular frameworks of the tetrazole derivatives.

Results and Discussion

Tetrazole has been introduced on the nitro azoles to improve the energetic performance along with the better stability and low sensitivity. A systematic structure-property relationship has been established by introducing nitro explosophore in the molecular skeleton possessing azole rings.

3.2.1 Molecular geometries

The tetrazole is substituted on the azole to improve nitrogen content and to study the effect on the energetic properties. All designed compounds contain nitro group as explosophore in their molecular skeleton. The tetrazole ring is connected with the azole rings through C-C or C-N bonds. The selected structural parameters of the designed molecules are listed in Table 3.8 to 3.12.

In the designed tetrazole derivatives, the bond lengths of C-NO_2 bond found to be higher than other C-C and C-N bonds in the molecular structure. The distance between N-H of the azole ring and nitro group is less than 2.8 Å, hence increases the chances for hydrogen bonding. When two nitro groups on the azole rings are adjacent (**T1**, **T4** & **T9**), oxygen atoms of other nitro group slightly modifies the molecular plane to reduce the steric hindrance and repulsive effect. The imidazole derivatives (**T1**, **T2**, **T3** and **T4**) reveals that introduction of three nitro groups on the imidazole increases the C-N and C-NO_2 bond lengths in **T4** due to the repulsion between adjacent nitro groups and their strong electron withdrawing effect in comparison with **T1**, **T2** and **T3**. **T1**, **T2** and **T3** have two nitro groups on the imidazole ring; however **T1** shows slight weaker C-NO_2 bond may be due to adjacent nitro groups.

The introduction of nitro groups in the molecular structure of 1,2,4-triazole derivatives (**T6** & **T7**) slightly increases the C-NO_2 bond lengths in **T7** (having two nitro groups on the triazole ring) than **T6** (having single nitro group on the triazole ring) and increases the torsional angle between 1,2,4-triazole and tetrazole rings. Similar trends are observed in 1,2,3-triazole derivatives (**T8** & **T9**). The torsional angle between the azole rings varies from 121 to 179^o. The close proximity of the nitro groups increases the distortion between azole rings linked via C-N bond to reduce the steric and repulsive effect of nitro groups.

Table 3.8: Selected structural parameters of **T1** and **T2** computed at the B3LYP/6-31G*.

	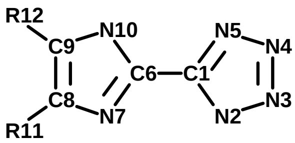		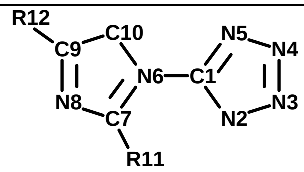	
	T1		**T2**	
Bond length (Å)	C1-N2	1.3475	C1-N2	1.3421
	N2-N3	1.3486	N2-N3	1.3495
	N3-N4	1.2958	N3-N4	1.2943
	N4-N5	1.3585	N4-N5	1.3561
	N5-C1	1.3220	N5-C1	1.3184
	C1-C6	1.4443	C1-N6	1.4102
	C6-N7	1.3287	N6-C7	1.3997
	N7-C8	1.3499	C7-N8	1.3040
	C8-C9	1.3873	N8-C9	1.3513
	C9-N10	1.3672	C9-C10	1.3734
	N10-C6	1.3581	C10-N6	1.3790
	C8-R11	1.4601	C7-R11	1.4516
	C9-R12	1.4367	C9-R12	1.4532
T.A. (^{o})	N7-C6-C1-N5	179.6	C7-N6-C1-N5	164.8
	N2-C1-C6-N10	179.4	N2-C1-N6-C10	167.5

R11, R12=NO_2; T.A. is the torsional angle.

Table 3.9: Selected structural parameters of **T3** and **T4** computed at the B3LYP/6-31G*.

	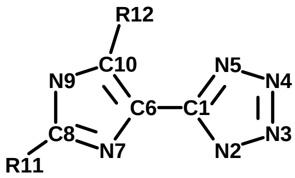		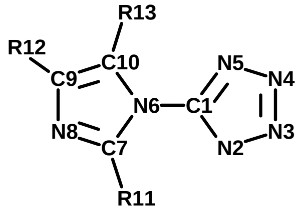	
	T3		**T4**	
Bond length (Å)	C1-N2	1.3439	C1-N2	1.3439
	N2-N3	1.3414	N2-N3	1.3455
	N3-N4	1.2994	N3-N4	1.2964
	N4-N5	1.3568	N4-N5	1.3578
	N5-C1	1.3235	N5-C1	1.3132
	C1-C6	1.4516	C1-N6	1.4131
	C6-N7	1.3721	N6-C7	1.3886
	N7-C8	1.3114	C7-N8	1.3013
	C8N-9	1.3490	N8-C9	1.3521
	N9-C10	1.3661	C9-C10	1.3777
	C10-C6	1.3969	C10-N6	1.3816
	C8-R11	1.4523	C7-R11	1.4550
	C10-R12	1.4393	C9-R12	1.4585
			C10-R13	1.4600
T.A. (°)	N7-C6-C1-N5	179.9	C7-N6-C1-N5	121.3
	N2-C1-C6-C10	179.9	N2-C1-N6-C10	132.5

R11, R12, R13=NO_2; T.A. is the torsional angle.

Table 3.10: Selected structural parameters of **T5** and **T6** computed at the B3LYP/6-31G*.

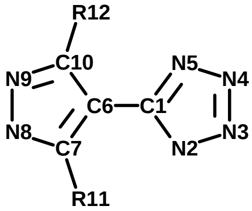

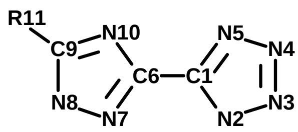

	T5		**T6**	
Bond length (Å)	C1-N2	1.3268	C1-N2	1.3519
	N2-N3	1.3516	N2-N3	1.3473
	N3-N4	1.3004	N3-N4	1.2961
	N4-N5	1.3407	N4-N5	1.3593
	N5-C1	1.3508	N5-C1	1.3211
	C1-C6	1.4562	C1-C6	1.4544
	C6-C7	1.3949	C6-N7	1.3407
	C7-N8	1.3558	N7-N8	1.3406
	N8-N9	1.3230	N8-C9	1.3497
	N9-C10	1.3308	C9-N10	1.3102
	C10-C6	1.4260	N10-C6	1.3616
	C7-R11	1.4496	C9-R11	1.4532
	C10-R12	1.4547		
T.A. (^{o})	C7-C6-C1-N5	152.9	N7-C6-C1-N5	179.9
	N2-C1-C6-C10	143.7	N2-C1-C6-N10	179.9

R11, R12=NO_2; T.A. is the torsional angle.

Table 3.11: Selected structural parameters of **T7** and **T8** computed at the B3LYP/6-31G*.

	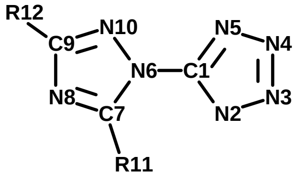		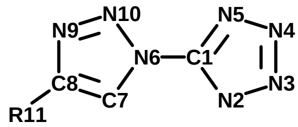	
	T7		**T8**	
Bond length (Å)	C1-N2	1.4216	C1-N2	1.3118
	N2-N3	1.3302	N2-N3	1.3658
	N3-N4	1.2928	N3-N4	1.2910
	N4-N5	1.3212	N4-N5	1.3556
	N5-C1	1.3866	N5-C1	1.3435
	C1-N6	1.4129	C1-N6	1.3906
	N6-C7	1.4327	N6-C7	1.3544
	C7-N8	1.3571	C7-C8	1.3751
	N8-C9	1.4172	C8-N9	1.3593
	C9N-10	1.3773	N9-N10	1.2901
	N10-N6	1.3394	N10-N6	1.3800
	C7-R11	1.5007	C8-R11	1.4470
	C9-R12	1.5063		
T.A. (^{o})	C7-N6-C1-N5	125.1	C7-N6-C1-N5	179.9
	N2-C1-N6-C10	132.4	N2-C1-N6-C10	179.9

R11, R12=NO_2; T.A. is the torsional angle.

Table 3.12: Selected structural parameters of **T9** and **T10** computed at the B3LYP/6-31G*.

	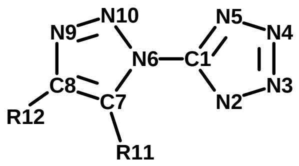		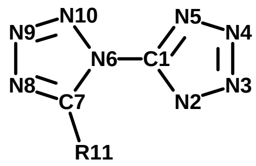	
	T9		**T10**	
Bond length (Å)	C1-N2	1.3479	C1-N2	1.3469
	N2-N3	1.3452	N2-N3	1.3459
	N3-N4	1.2973	N3-N4	1.2968
	N4-N5	1.3579	N4-N5	1.3578
	N5-C1	1.3142	N5-C1	1.3148
	C1-N6	1.4051	C1-N6	1.4050
	N6-C7	1.3651	N6-C7	1.3630
	C7-C8	1.3773	C7-N8	1.3060
	C8-N9	1.3515	N8-N9	1.3576
	N9-N10	1.2923	N9-N10	1.2889
	N10-N6	1.3760	N10-N6	1.3686
	C7-R11	1.4492	C7-R11	1.4542
	C8-R12	1.4542		
T.A. (°)	C7-N6-C1-N5	135.9	C7-N6-C1-N5	139.8
	N2-C1-N6-C10	137.4	N2-C1-N6-N10	142.8

R11, R12=NO_2; T.A. is the torsional angle.

3.2.2 Gas phase heat of formation

$\Delta H^0{}_f$ are well to evaluate the explosive performance and great importance due to involved in detonation performance of the energetic material. The total energies (E_0), zero point energies (ZPE) and thermal correction at the B3LYP/6-31G* level have been calculated for tetrazole derivatives. The calculated total energies and experimental gas phase $\Delta H^0{}_f$ of the reference compounds involved in isodesmic reactions are listed in Table 3.5. From Table 3.5, the $\Delta H^0{}_f$ of the different azoles shows high positive values clearly indicates their role in the total energy contribution. Table 3.13 summarizes the calculated ΔH^0_f of the tetrazole derivatives. All molecules show high positive ΔH^0_f may attribute to the presence of nitrogen rich azole rings, nitro substituents, and energetic C-N and N-N bonds of the corresponding molecules.

Table 3.13: Predicted energetic properties of the tetrazole derivatives.

Comp.	N. C. (%)	O. B. (%)	ΔH^0_f (kJ/mol)	Q (kJ/mol)	*D* (km/s)	*P* (GPa)	BDE (kJ/mol)
T1	49.5	-35.4	579.7	1219.4	8.53	32.27	256.4
T2	49.5	-35.4	641.8	1285.2	8.47	31.32	278.3
T3	49.5	-35.4	579.3	1219.0	8.33	30.15	272.8
T4	46.5	-14.8	714.5	1501.1	9.28	39.29	234.2
T5	49.5	-35.4	648.4	1292.1	8.52	31.76	280.4
T6	61.5	-43.9	664.2	1334.7	7.99	27.18	273.6
T7	55.5	-17.6	769.7	1435.8	8.83	33.94	261.6
T8	61.5	-43.9	776.9	1483.1	8.11	27.63	286.0
T9	55.5	-17.6	856.5	1527.2	8.99	35.41	255.6
T10	68.8	-21.9	1019.1	1705.4	9.06	34.87	262.6

The isodesmic reactions for the designed compounds are shown in Fig. 3.7. Compounds **T1**, **T2**, and **T3** are the isomers, differ in the structural arrangement and coupling between azole rings. **T2** shows higher ΔH^0_f than **T1**, and **T3** may be due to the strain introduced by C-N linkage between two azole rings. **T4** has ΔH^0_f (715 kJ/mol) higher than **T1**, **T2**, and **T3** due to the presence of three nitro groups on the imidazole ring in the molecular skeleton which results in steric hindrance and hence, repulsive energy. Generally, energy contribution from the pyrazole is higher than imidazole and hence **T5** shows better ΔH^0_f than **T1**, **T2**, and **T3**. Similarly, energy contribution from the 1,2,3-triazole is more than the 1,2,4-triazole therefore, **T8** and

T9 shows higher $\Delta H^0{}_f$ than **T6** and **T7**. All these compounds show nitrogen content over 50%. Due to the introduction of nitro groups **T7** and **T9** possess higher $\Delta H^0{}_f$ over **T6** and **T8**, respectively. **T6** and **T8** having single nitro group in the molecular framework but shows higher $\Delta H^0{}_f$ than the **T1**, **T2**, **T3**, and **T5** due to the better energy contribution from triazoles and high nitrogen content of these molecules. Among the designed tetrazole derivatives, **T10** shows the highest $\Delta H^0{}_f$ about 1019.08 kJ/mol, may be due to the presence of two tetrazole rings in the molecular framework which increases the $\Delta H^0{}_f$ remarkably. The nitrogen content of **T10** is 68.85% and found to be higher in the series; increase in nitrogen content improves the $\Delta H^0{}_f$. Though **T4**, **T7** and **T9** have low nitrogen content than their corresponding analogs but the $\Delta H^0{}_f$ is high because of the nitro groups.

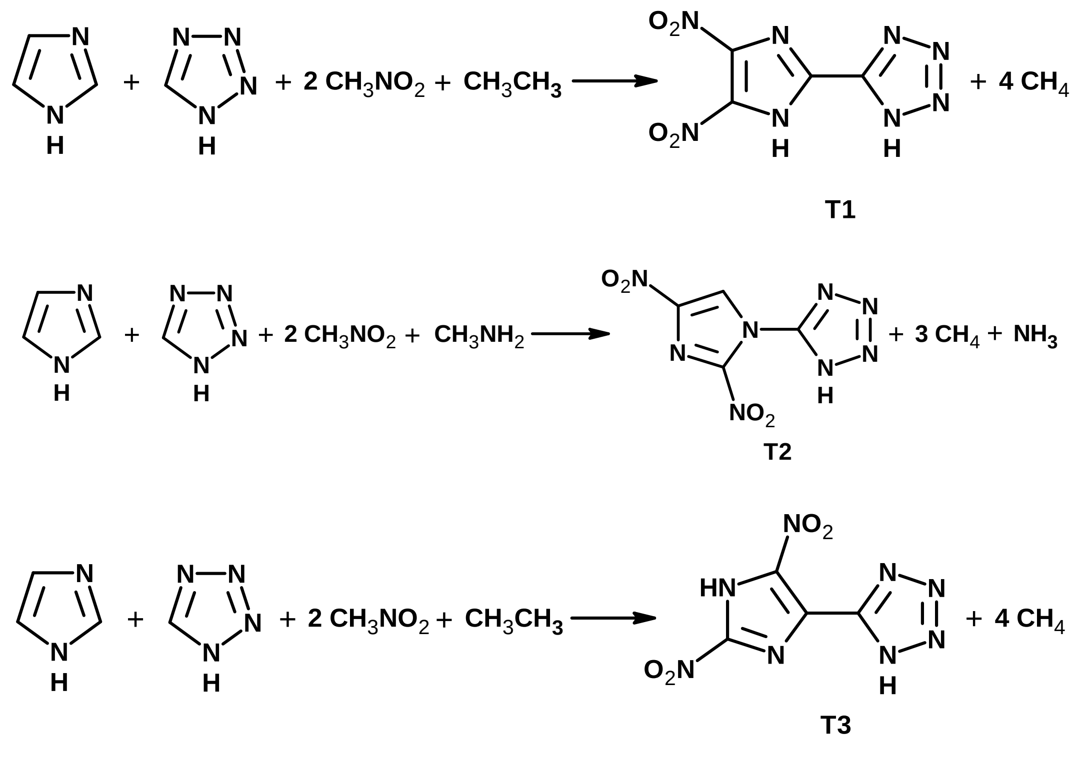

Fig. 3.7 Isodesmic reaction schemes for the tetrazole derivatives.

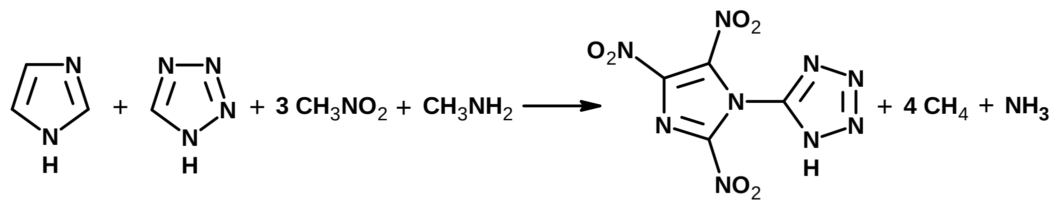

T4

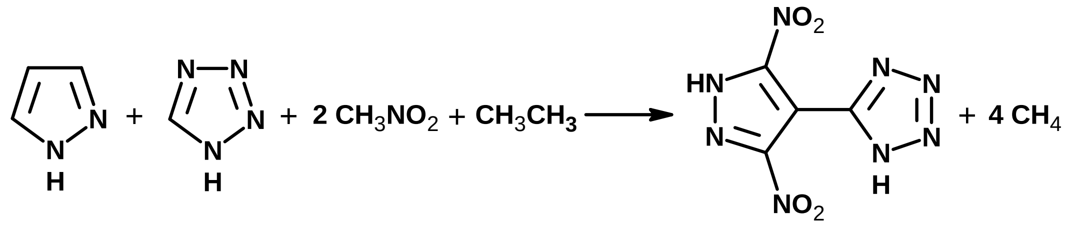

T5

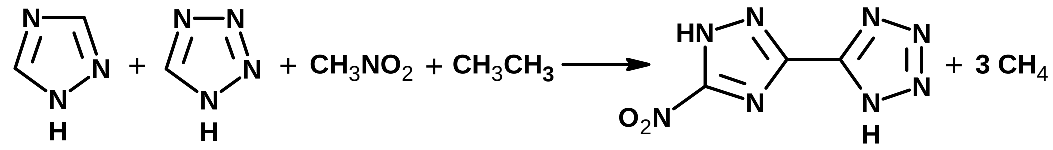

T6

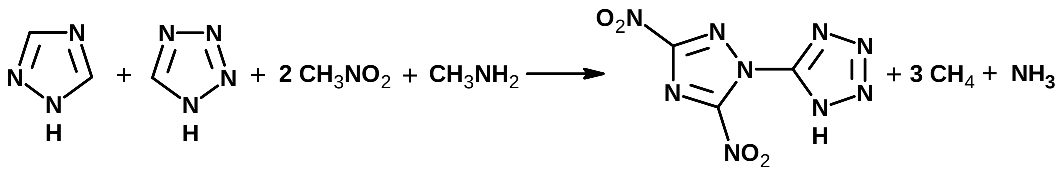

T7

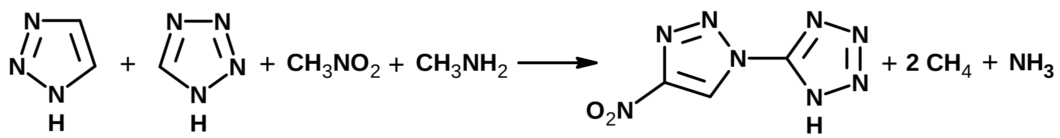

T8

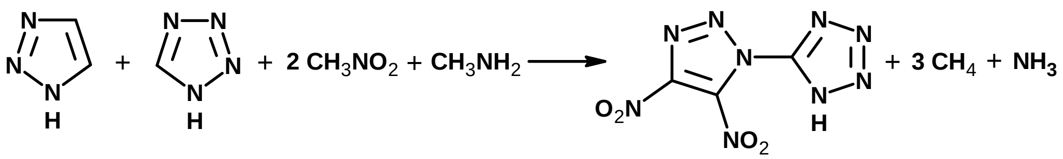

T9

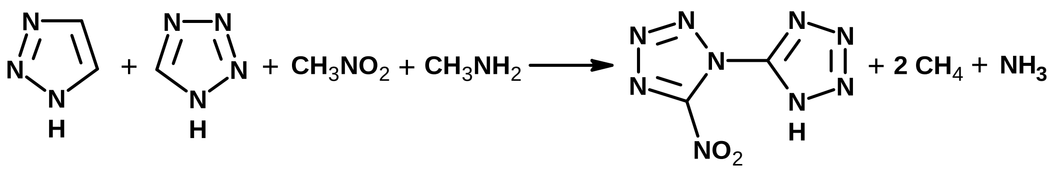

T10

Fig. 3.7 (Contd.)

3.2.3 Density

Density has major importance in designing the HEMs because detonation velocity (*D*) is proportional to density, while the Chapman-Jouguet detonation pressure (*P*) is proportional to the square of the initial density as suggested by Kamlet and Jacobs.[44,45] An increase in density is also desirable in terms of the amount of material who can be packed into volume limited warhead or propulsion configurations. Crystal structure densities have been predicted by the molecular packing calculations and found to be more reliable. The cvff force field has been used to predict the densities. Table 3.14 summarizes density and lattice parameters of the stable crystal polymorph based on minimum energy of tetrazole derivatives. Fig. 3.8 shows the relation between density and detonation velocity.

The densities for designed compounds have been found to be in the range of 1.68-1.89 g/cm^3. Increase in nitro group improves the density and it also increases the chances of hydrogen bonding between oxygen and acidic hydrogen on ring nitrogen.[8,11] Trinitroimidazole derivative (**T4**) possesses density higher than the dinitroimidazole derivatives (**T1**, **T2**, and **T3**). Similar phenomena observed in **T6**-**T7** and **T8**-**T9**. The replacement of the 1,2,4-triazole with the 1,2,3-triazole does not show significant change in the densities. The two azole rings in the molecular skeleton of **T1** and **T3** are bridged via C-C bond while in **T2** with the C-N linkage. **T1** shows higher density than **T2** and **T3** may be due to the adjacent arrangement of nitro groups on imidazole ring. The arrangement of nitro groups in the molecular skeleton allows other molecules to pack closely in the cell and increases the chances for inter and intra molecular hydrogen bonding. The presence of nitrogen rich azoles and nitro groups improves the density. Fig. 3.9 shows the stable crystal structures of the tetrazole derivatives.

Table 3.14: Density and lattice parameters of the tetrazole derivatives.

Compd.	Density (g/cm^3)	Space group	Lattice parameters					
			Length (Å)			Angle (^{o})		
			a	b	c	α	β	γ
T1	1.80	$P2_1/c$	19.96	7.72	17.49	90.0	161.8	90.0
T2	1.75	*Pbca*	10.17	16.83	10.14	90.0	90.0	90.0
T3	1.74	$P2_1/c$	13.25	6.51	17.86	90.0	145.6	90.0
T4	1.89	$P2_12_12_1$	10.35	10.42	8.86	90.0	90.0	90.0
T5	1.76	$P2_1$	9.86	6.21	7.07	90.0	84.5	90.0
T6	1.66	$P2_1/c$	5.14	13.47	10.85	90.0	75.7	90.0
T7	1.75	*Pbca*	9.62	14.51	12.43	90.0	90.0	90.0
T8	1.67	$P2_1/c$	7.80	8.39	13.28	90.0	58.6	90.0
T9	1.76	$P2_1/c$	9.56	10.95	15.22	90.0	147.0	90.0
T10	1.71	*Pbca*	23.23	8.58	7.19	90.0	90.0	90.0

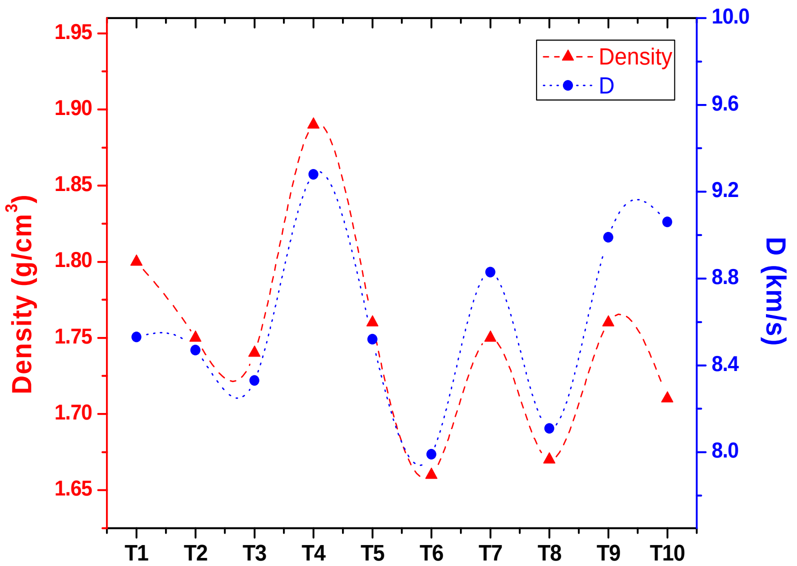

Fig. 3.8 Density (g/cm^3) and detonation velocity (km/s) profile of the tetrazole derivatives.

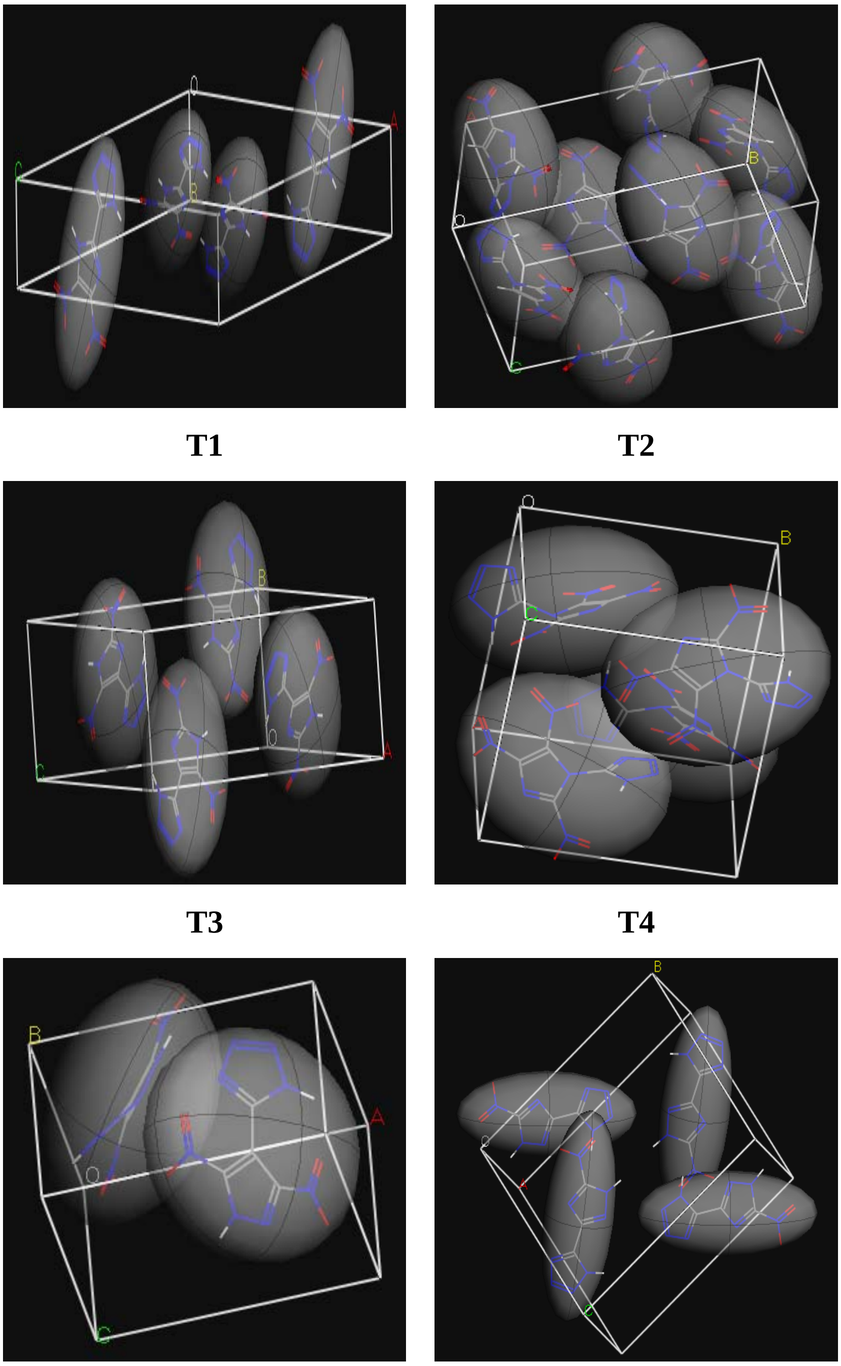

T1 T2

T3 T4

T5 T6

Fig. 3.9 Crystal structures of the tetrazole derivatives.

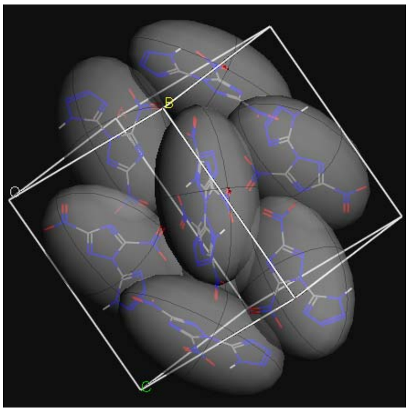

T7

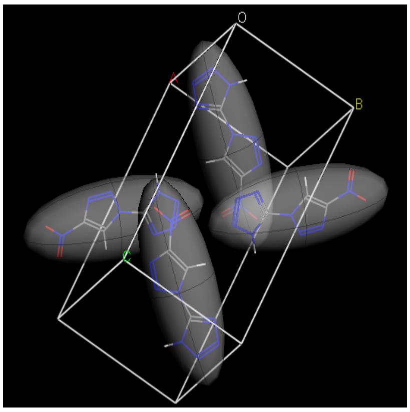

T8

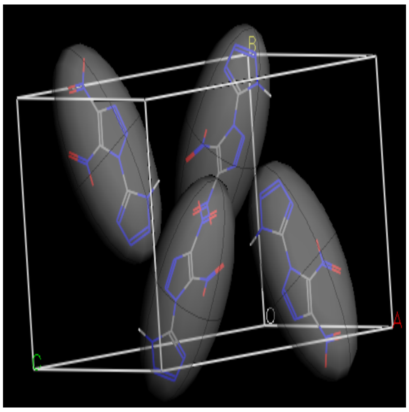

T9

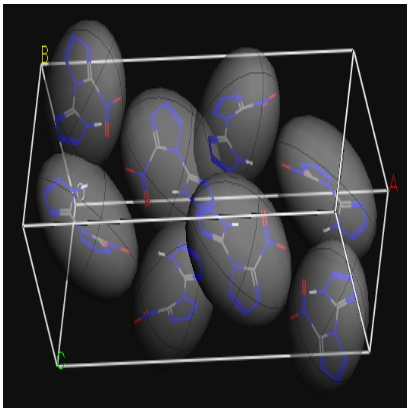

T10

Fig. 3.9 (Contd.)

3.2.4 Detonation characteristics

Among the criteria used in evaluating potential energetic system is detonation velocity (D) and pressure (P). The detonation velocity and pressure depend upon the energy release that accompanies the combustion and decomposition processes that are occurring.[46,47] D and P of the molecules have been computed by Kamlet-Jacobs empirical equations. Table 3.13 lists the calculated D and P values of the tetrazole derivatives. **T4** shows better detonation performance over the **T1**, **T2** and **T3** due to the higher ΔH^0_f, density and oxygen balance. **T4** shows D of 9.3 km/s and P over 39.3 GPa. Among the **T1**, **T2** and **T3**, **T1** shows better performance due to the higher density. The increase in nitro groups increase the density and ΔH^0_f hence, improves the detonation characteristics. Similar phenomena are observed in case of **T6-T7**, **T8-T9** derivatives. Replacement of 1,2,4-triazole with 1,2,3-triazole improves the density and $\Delta H^0{}_f$ and hence, detonation performance. **T9** shows better performance than **T7** and similar trends observed in **T6-T8**. The plot of density versus detonation velocity is shown in Fig. 3.8. Density shows more impact on the detonation properties as compared to $\Delta H^0{}_f$ and hence though **T5** has higher $\Delta H^0{}_f$ than **T1** shows less detonation performance. **T10** shows higher detonation performance due to high $\Delta H^0{}_f$ in the series and better density.

3.2.5 Thermal stability

Stability of the energetic compounds is essential for the practical interest of the explosive material. The thermal stability of energetic material determines its applicability for practical purpose. The present study explores the stability of the designed compounds on the basis of BDE. All the BDEs are calculated by employing the hybrid DFT using B3LYP method together with the 6-31G* basis set. The BDE for each possible trigger bond is often a key factor in investigating the pyrolysis mechanism for an energetic compound.[48] The strength of the weakest bond of explosive molecule plays an important role in the initiation event. The smaller the BDE, weaker the bond is. Different studies illustrate that C-NO_2 is the possible trigger bond in the nitro-aromatic compounds[49,50] and it can be ruptured easily during pyrolysis. All the predicted values of BDE are listed in Table 3.13.

The BDEs for the tetrazole derivatives found to be higher than 230 kJ/mol. These values satisfy the criteria of HEMs, and all designed compounds have good thermal stabilities. Relation between BDE of the C-NO_2 bond and charge on nitro groups is shown in Fig. 3.10. Generally, increase in nitro groups reduces the BDE for

C-NO_2.[49] The increase of nitro groups on the imidazole from two (**T1**, **T2**, and **T3**) to three (**T4**) reduces the BDE. Similar phenomena are observed in case of **T6-T7** and **T8-T9**. The pyrazole derivative (**T5**) is found to be more stable as compared to imidazole derivatives (**T1**, **T2** and **T3**). The arrangement of nitro groups on the pyrazole minimizes the steric hindrance and repulsive energy between nitro groups. All compounds are aromatic; show conjugation between two azole rings improves the π-electron delocalization and hence thermal stability.

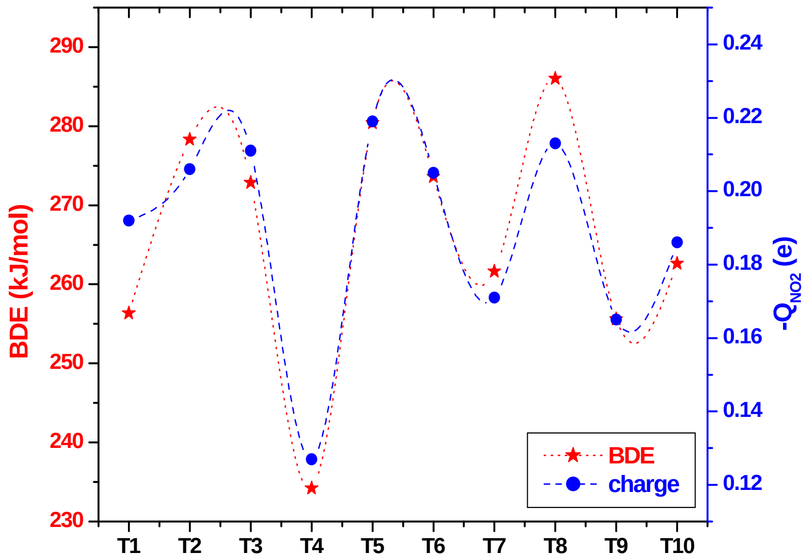

Fig. 3.10 Relationship between bond dissociation energy (kJ/mol) and net charge on nitro group (e).

3.2.6 Sensitivity correlations

Relationship between the impact sensitivity and electronic structures of some nitro compounds can be established by the charge analysis of nitro group.[51] In this work, the longest C-NO_2 bond is selected as the weakest bond. The charges on the corresponding atoms have been calculated by using natural bond orbital (NBO) analysis. Table 3.15 lists the computed $-Q_{NO_2}$ from NBO analysis and bond length of C-NO_2 weakest bond calculated at B3LYP/6-31G* level. The higher $-Q_{NO_2}$, the larger is the impact insensitivity and hence $-Q_{NO_2}$ can be regarded as the measure for estimating the impact sensitivities.

$-Q_{NO_2}$ calculated for the tetrazole derivatives ranges from 0.127 to 0.219 e. Increase in the number of nitro groups increases sensitivity. **T4** is found to be more sensitive as compared to other derivatives such as **T1**, **T2**, and **T3** due to three nitro groups. Introduction of more nitro groups on the ring increase the steric hindrance and repulsive energy between them and hence decreases the bond strength. Increase in sensitivity can be attributed to decrease in the strength of adjacent C-NO_2 bond. Similar trend observed in case of **T6-T7** and **T8-T9**. Over all sensitivity of the imidazole compounds (**T1**, **T2**, and **T3**) is higher as compared to pyrazole derivative (**T5**) due to the adjacent nitro groups responsible for the steric hindrance and strong repulsion. **T10** is having one in the molecular framework but found to be more sensitive than the other derivatives such as, **T1**, **T2**, **T3**, **T5**, **T6**, and **T8** due to the two tetrazole rings and nitramino group in the structure. Overall correlation reveals that designed compounds are insensitive.

Table 3.15: Computed $-Q_{NO_2}$ and C-NO_2 bond length of weakest bond.

Compd	T1	T2	T3	T4	T5	T6	T7	T8	T9	T10
$-Q_{NO_2}$ (e)	0.192	0.206	0.211	0.127	0.219	0.205	0.171	0.213	0.165	0.186
$R_{C\text{-}NO2}$ (Å)	1.460	1.453	1.452	1.459	1.455	1.453	1.469	1.447	1.449	1.454

3.2.7 Conclusions

The density functional theory at the B3LYP/6-31G* level is used to study electronic structures of the designed tetrazole derivatives in order to find them as potential HEMs. The important characteristics of energetic material such as ΔH^0_f, density, detonation performance, thermal stability, and impact sensitivity have been evaluated. The ΔH^0_f of the designed tetrazole derivatives shows the large positive values due to the presence of nitroazoles, energetic C-N and N-N bonds and tetrazole. ΔH^0_f has been improved by the number of nitro groups and their relative position. All compounds show the better densities and detonation performance. The increase in nitro groups improves the density and hence overall performance of the tetrazole derivatives. The unique mechanism of thermal pyrolysis has been depending on the nature of the C-NO_2 bond and skeleton of the structure. A structure-property relationship on tetrazole derivatives demonstrates that these molecules will be promising candidates for futuristic HEMs.

3.3 Azo Bridged Azole Derivatives

Heteroaromatic rings linked by an azo group have been extensively studied because the azo linkage improves the performance of the compound.[52] Aromatic azo compounds are directly obtainable from nitro compounds by reduction with different catalysts.[53-55] The compounds containing amino groups can be transformed to compounds containing azoic or azoxy group by intermolecular oxidation reactions using different oxidizing agents.[56-58]

Different synthetically reported azo-containing explosive such as, 5,5'-dinitro-3,3'-azo-1H-1,2,4-triazole (DNAT),[59] 4,4'-diamino-3,3'-azofurazan (DAAzF),[60] 3,3'-azobis(6-amino-s-tetrazine) (DAAT),[61] and tetrazole based energetic materials have proved to be unique.[33,35] These energetic materials combined with nitrogen-rich moiety increases the enthalpy of formation, which at the same time has a good thermal stability and low sensitivities. Hammerl et al.[62] reported the high nitrogen containing dehydrate, dihydrazinate and dihydrazinium salts of tetrazole compounds, which are stable at room temperature and almost insensitive to friction & impact. Recently, Klapotke et al.[38,41] reported the azo bridged bistetrazoles as insensitive energetic compounds. Chavez et al.[63] reported the synthesis and characterization of bis-(triaminoguanidinium)-3,3'-dinitro-5,5'-azo-1,2,4-triazolate (TAGDNAT), a novel high-nitrogen molecule, that derives its energy release from both high ΔH^0_f and intramolecular oxidation reactions.

Energetic azofurazan and azoxyfurazan compounds have found great application as an insensitive explosive,[64] as well as an energetic additive to modify the properties of rocket propellant and explosive formulations.[65] Huynh et al.[5] reported the synthesis and properties of novel hydrazo and azo bridged 1,3,5-triazines, which indicated that the hydrazo and azo linkages desensitize and enhance the melting point of the polyazido products. Zhang et al.[66] investigated the azoic and azoxy derivatives of 3,4-diaminofuran (DAF), 1,1-diamino-2,2-dinitroethylene (FOX-7), 1,3,5-triamino-2,4,6-trinitro-benzene (TATB), 2,6-diamino-3,5-dinitropyrazine(ANPZ) and 2,6-diamino-3,5-dinitropyrazine-1-oxide (LLM-105) computationally and reported the role of azo bridge in crystal density, ΔH^0_f, detonation performance and stability of the molecules. Recently, Zhang et al.[67] explored a systematic theoretical study of ΔH^0_f, electronic structure, energetic properties and thermal stability of the series of bridged difurazans with different linkages (-CH_2-CH_2-, -CH=CH-, -NH-NH-, -N=N-, -N(O)=N-) and substituents (-ONO_2, -NH_2, -NF_2, -N_3, -NO_2) by using DFT to investigate the role of different linkages and substituents in the design of efficient HEDMs.

In the present study, incorporation of azo linkage (-N=N-) is aimed to decrease sensitivity and increase energy content. Different azoles such as imidazole, pyrazole, triazoles, and isoxazole are coupled via -N=N- bridge. The $-NO_2$, $-NH_2$ and $-N_3$ groups are substituted on the azoles to study their effect on energetic properties. Density functional theory (DFT) has been used to predict the optimized structures, $\Delta H^0{}_f$ and detonation properties. Fig. 3.11 shows the molecular framework of the azo bridged azole derivatives.

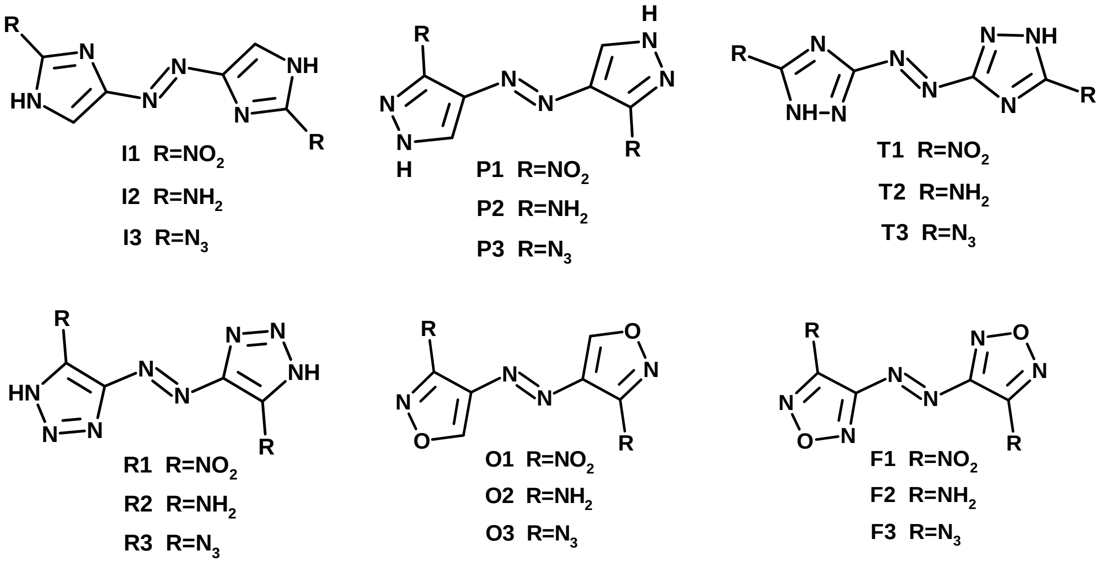

Fig. 3.11 Molecular frameworks of the designed azo bridged azole derivatives.

Results and discussion

Polynitrogen compounds are environmentally acceptable high energy materials. The present study discusses the predicted performance characteristics of azo bridged azole derivatives. A systematic structure-property relationship has been established by varying nitro, amino and azido substituents on the molecular skeleton possessing azole rings. The predicted energetic properties of the designed molecules have been compared with 3,3'-dinitro-4,4'-azofurazan (**F1**), 3,3'-diamino-4,4'-azofurazan (**F2**), and 3,3'-diazido-4,4'-azofurazan (**F3**) to evaluate the performance. These azofurazan derivatives show high explosive performance with better insensitivity.[64]

3.3.1 Molecular geometries

All designed compounds contain two explosophores ($-NO_2$, $-NH_2$, and $-N_3$) in their molecular skeleton. The azole rings with explosophores are bridged via azo bond (-N=N-) having bond length of 1.27 to 1.29 Å. The molecular backbone with trans geometry at azo bond is a planar structure and azo bond leads to the extended conjugation in the azole rings. A similar phenomenon is observed in hexanitrostilbene (HNS).[68,69] The azole maintains the trans geometry in the optimized structure on the azo bond to reduce the steric hindrance. The substituents are positioned in the plane of azole rings and hence shows extended resonance in the molecular skeleton due to their electron withdrawing/donating effect. In the designed compounds, the torsional angle in the molecular structure of the explosophore (C3-N4-C5-N8) and azo linkage (C3-N2-N1-C9) is found close to 180^o.

The selected structural parameters of the azo bridged azole derivatives are listed in Table 3.16 to 3.21. The bond lengths of C-NO_2 bonds (>1.43 Å) are found to be higher than its C-NH_2 (>1.36 Å) and C-N_3 (>1.37 Å) derivatives. Overall, the lengths of C-NO_2, C-NH_2 and C-N_3 linkages differ from isomer to isomer with the position of nitro groups and nature of azole rings. In all designed compounds, the order of increase in bond length of azo bond can be given as $NH_2>N_3>NO_2$. The replacement of imidazole (**I1**, **I2** & **I3**) with pyrazole (**P1**, **P2** & **P3**) in the designed compounds slightly increases the length of azo bond. Similarly, replacement of 1,2,4-triazole (**T1**, **T2** & **T3**) with 1,2,3-triazole (**R1**, **R2** & **R3**) in the designed compounds slightly increases the length of azo bond but reduces the C-N bond lengths in the molecular structure. In isoxazole (**O1**, **O2** & **O3**) and furazan (**F1**, **F2** & **F3**) derivatives, presence of additional nitrogen in the ring of furazan reduces the length of N=N, C-C and C-N bonds in the respective molecules.

Table 3.16: Selected structural parameters of **I1**, **I2** and **I3** optimized at the B3LYP/6-31G* level.

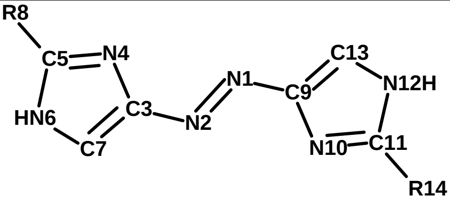

Bond length (Å)	**I1**	**I2**	**I3**
N1-N2	1.2653	1.2687	1.2672
N2-C3, N1-C9	1.3957	1.3914	1.3946
C3-N4, C9-N10	1.3695	1.3851	1.3828
N4-C5, N10-C11	1.3064	1.3115	1.3092
C5-N6, C11-N12	1.3686	1.3754	1.3703
N6-C7, N12-C13	1.3581	1.3698	1.3741
C7-C3, C13-C9	1.3986	1.3841	1.3859
C5-N8, C11-N14	1.4414	1.4154	1.3961

I1: R8, R14=NO_2; I2: R8, R14=NH_2 and I3: R8, R14=N_3

Table 3.17: Selected structural parameters of **P1**, **P2** and **P3** optimized at the B3LYP/6-31G* level.

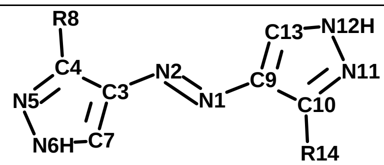

Bond length (Å)	**P1**	**P2**	**P3**
N1-N2	1.2663	1.2776	1.2712
N2-C3, N1-C9	1.3948	1.3799	1.3867
C3-C4, C9-C10	1.4238	1.4429	1.4441
C4-N5, C10-N11	1.3240	1.3306	1.3297
N5-N6, N11-N12	1.3442	1.3702	1.3552
N6-C7, N12-C13	1.3524	1.3432	1.3455
C7-C3, C13-C9	1.3920	1.3939	1.3917
C4-N8, C10-N14	1.4551	1.3759	1.4005

P1: R8, R14=NO_2; P2: R8, R14=NH_2 and P3: R8, R14=N_3

Table 3.18: Selected structural parameters of **T1**, **T2** and **T3** optimized at the B3LYP/6-31G* level.

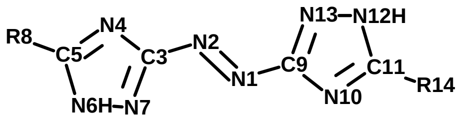

Bond length (Å)	**T1**	**T2**	**T3**
N1-N2	1.2589	1.2626	1.2617
N2-C3, N1-C9	1.3982	1.3978	1.3973
C3-N4, C9-N10	1.3673	1.3740	1.3726
N4-C5, N10-C11	1.3058	1.3159	1.3149
C5-N6, C11-N12	1.3544	1.3640	1.3584
N6-N7, N12-N13	1.3356	1.3592	1.3500
N7-C3, N13-C9	1.3423	1.3304	1.3378
C5-N8, C11-N14	1.4537	1.3823	1.3896

T1: R8, R14=NO_2; T2: R8, R14=NH_2 and T3: R8, R14=N_3

Table 3.19: Selected structural parameters of **R1**, **R2** and **R3** optimized at the B3LYP/6-31G* level.

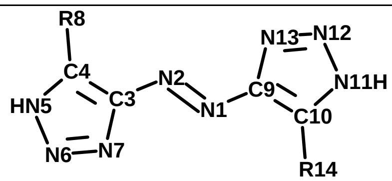

Bond length (Å)	**R1**	**R2**	**R3**
N1-N2	1.2638	1.2825	1.2705
N2-C3, N1-C9	1.3929	1.3759	1.3798
C3-C4, C9-C10	1.3916	1.4070	1.4102
C4-N5, C10-N11	1.3485	1.3503	1.3547
N5-N6, N11-N12	1.3449	1.3872	1.3607
N6-N7, N12-N13	1.3036	1.2892	1.2933
N7-C3, N13-C9	1.3692	1.3692	1.3703
C4-N8, C10-N14	1.4368	1.3622	1.3785

R1: R8, R14=NO_2; R2: R8, R14=NH_2 and R3: R8, R14=N_3

Table 3.20: Selected structural parameters of **O1**, **O2** and **O3** optimized at the B3LYP/6-31G* level.

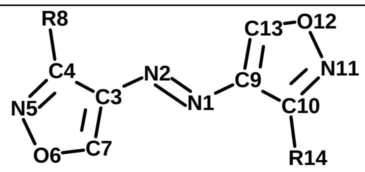

Bond length (Å)	**O1**	**O2**	**O3**
N1-N2	1.2650	1.2714	1.2687
N2-C3, N1-C9	1.3952	1.3855	1.3904
C3-C4, C9-C10	1.4290	1.4420	1.4351
C4-N5, C10-N11	1.3078	1.3175	1.3165
N5-O6, N11-O12	1.3909	1.4244	1.4083
O6-C7, O12-C13	1.3386	1.3297	1.3340
C7-C3, C13-C9	1.3735	1.3726	1.3729
C4-N8, C10-N14	1.4629	1.3715	1.3923

O1: R8, R14=NO_2; O2: R8, R14=NH_2 and O3: R8, R14=N_3

Table 3.21: Selected structural parameters of **F1**, **F2** and **F3** optimized at the B3LYP/6-31G* level.

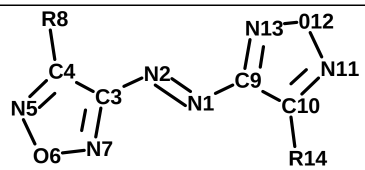

Bond length (Å)	**F1**	**F2**	**F3**
N1-N2	1.2542	1.2656	1.2622
N2-C3, N1-C9	1.4070	1.3894	1.3977
C3-C4, C9-C10	1.4272	1.4404	1.4354
C4-N5, C10-N11	1.3023	1.3139	1.3115
N5-O6, N11-O12	1.3634	1.4028	1.3871
O6-N7, O12-N13	1.3714	1.3481	1.3550
N7-C3, N13-C9	1.3131	1.3180	1.3165
C4-N8, C10-N14	1.4579	1.3616	1.3852

F1: R8, R14=NO_2; F2: R8, R14=NH_2 and F3: R8, R14=N_3

3.3.2 Gas phase heat of formation

The calculated and experimental gas phase $\Delta H^0{}_f$ of the reference compounds CH_4, CH_3NO_2, CH_3NH_2, CH_3N_3, CH_3NNCH_3, imidazole, pyrazole, 1,2,4-triazole, 1,2,3-triazole, isoxazole and furazan are listed in Table 3.5. $\Delta H^0{}_f$ of the different azoles have high positive values as shown in Table 3.5, which clearly indicate their role in the total energy contribution of the designed molecules. Constructed isodesmic reactions for the calculation of $\Delta H^0{}_f$ of designed compounds are shown in Fig. 3.12. Table 3.22 summarizes the calculated total energies and gas phase $\Delta H^0{}_f$ of the azo bridged azole derivatives. All designed molecules showing high positive $\Delta H^0{}_f$ may be attributed to the presence of nitrogen-rich azole rings, energetic nitro and azido substituents, and C-N and N-N bonds in the molecular skeleton of the corresponding molecules.

The calculated $\Delta H^0{}_f$ of the designed molecules have been compared with **F1**, **F2**, and **F3** to evaluate the performance. The predicted gas phase $\Delta H^0{}_f$ of **F1**, **F2**, and **F3** using isodesmic reaction approach are 753.43, 603.17, and 1261.36 kJ/mol, respectively. The predicted $\Delta H^0{}_f$ of **F1** and **F2** are comparable with the experimental values (**F1**=703.9; **F2**=536 kJ/mol).[70-72] **P1**, **P2** and **P3** show higher $\Delta H^0{}_f$ than **I1**, **I2** and **I3**, respectively due to the significant energy contribution from the pyrazole. Generally, energy contribution from the pyrazole and 1,2,3-triazole is higher than imidazole and 1,2,4-triazole, respectively. Similar phenomena is observed in case of 1,2,4-triazole (**T1**, **T2**, and **T3**) and 1,2,3-triazole (**R1**, **R2** and **R3**) molecules. The energy content of isoxazole is less and hence **O1**, **O2** and **O3** show less $\Delta H^0{}_f$ as compared to other derivatives. Polyazido compounds have high relative $\Delta H^0{}_f$ as one azido group adds about 87 kcal/mol of energy to a hydrocarbon compound.[73,74] All the azido molecules such as **I3**, **P3**, **T3**, **R3** and **O3** possess very high $\Delta H^0{}_f$ as compared to $-NO_2$ and $-NH_2$ derivatives. Substitution of azido group increases the nitrogen content, and these compounds possess very high $\Delta H^0{}_f$. All azido molecules exhibit $\Delta H^0{}_f$ higher than 980 kJ/mol. Overall study shows that **F1**, **F2**, and **F3** possess high positive $\Delta H^0{}_f$ than the designed molecules (except **R1**, **R2** and **R3**) due to the significant energy contribution from furazan ring over other five member heterocyclic rings.

Table 3.22: Calculated energetic characteristics of the azo bridged azole derivatives.

Compd.	N. C. (%)	O. B. (%)	E_0 (a.u.)	$\Delta H^0{}_f$ (kJ/mol)	Q (cal/g)	D (km/s)	P (GPa)
I1	44.44	-63.49	-969.52900	482.52	1125.96	7.34	22.54
I2	58.33	-133.33	-671.22516	469.91	584.95	5.96	14.23
I3	68.85	-91.80	-887.72288	1025.23	1004.25	6.57	17.11
P1	44.44	-63.49	-969.47457	628.09	1264.03	7.68	25.06
P2	58.33	-133.33	-671.19688	572.05	712.10	6.21	15.30
P3	68.85	-91.80	-887.67547	1164.96	1141.12	6.69	17.53
T1	55.12	-31.50	-1001.59344	669.91	1169.90	8.72	34.61
T2	72.16	-90.72	-703.31457	616.75	759.83	6.97	20.35
T3	79.67	-58.54	-919.80344	1182.67	1149.04	7.32	22.15
R1	55.12	-31.50	-1001.53648	840.19	1330.13	8.90	35.73
R2	72.16	-90.72	-703.27410	743.96	916.55	7.37	22.90
R3	79.67	-58.54	-919.74347	1361.09	1322.39	7.64	24.35
O1	33.07	-44.09	-1009.15479	476.15	1195.59	8.11	27.94
O2	43.30	-107.22	-710.89024	385.62	1070.87	6.48	16.86
O3	56.91	-71.54	-927.36777	981.29	1295.7	6.94	19.26
F1	43.75	-12.50	-1041.18054	753.43	1663.25	9.20	38.03
F2	57.13	-65.31	-742.93095	603.17	1374.00	7.51	23.62
F3	67.74	-38.71	-959.40008	1261.36	1428.66	7.33	20.56

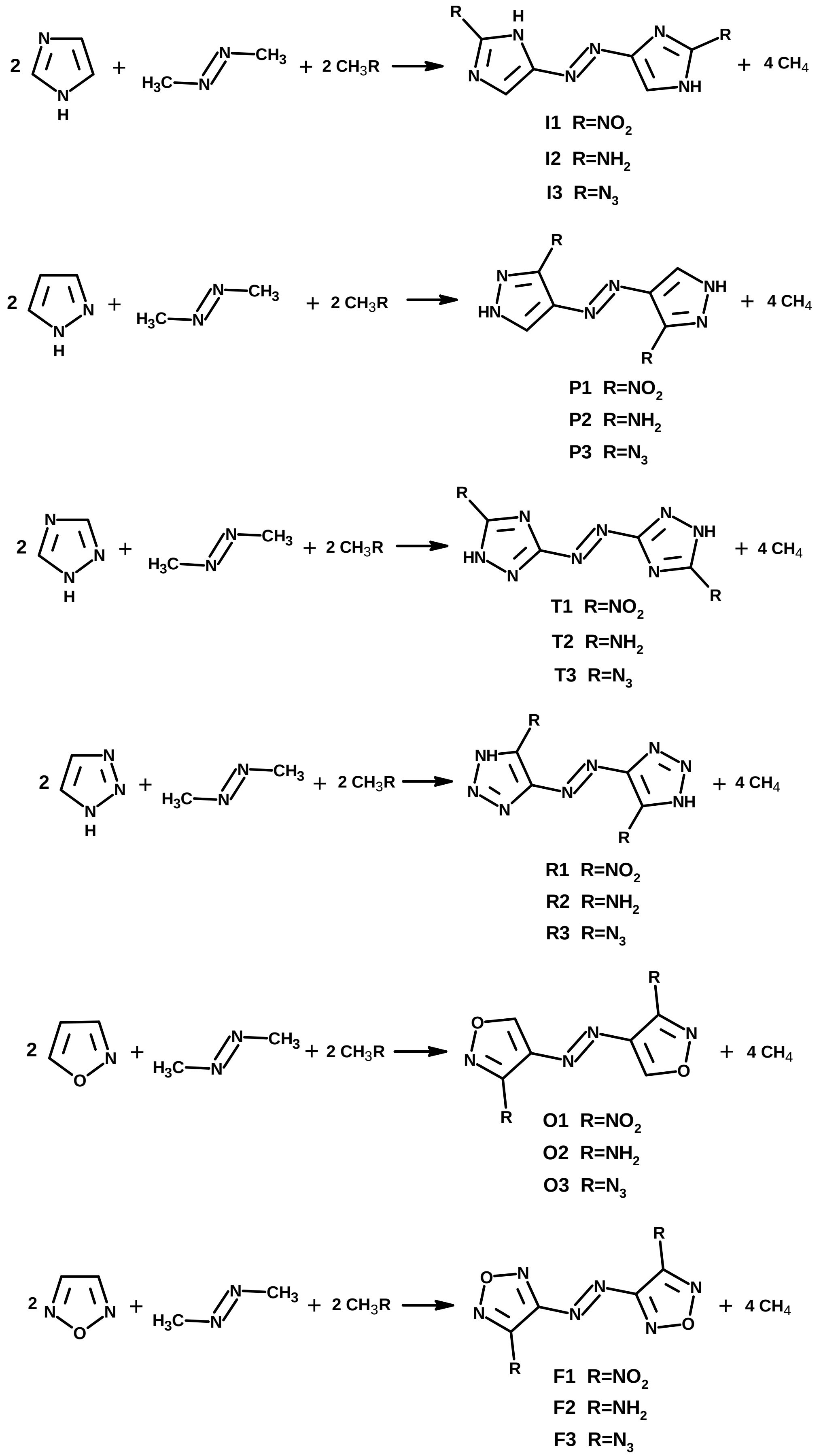

Fig. 3.12 Isodesmic reaction schemes for the azo bridged azole derivatives.

3.3.3 Density

The densities of the designed compounds have been predicted by using the polymorph calculation in Material studio. The predicted crystal densities and lattice parameters are summarized in Table 3.23. The substitution of nitro group has a significant role in increasing the density,[29,75] when compared with other substituent like amino and azido.

The increasing order of the density can be given as, NO_2>NH_2>N_3. However, the role of the amino group cannot be clearly defined since the packing pattern is highly dependent on the electronic structure of the molecule.[30,58] All the azole derivatives follow the same order. In general, introduction of the nitro group increases the chances for inter/intra molecular hydrogen bonding and the corresponding molecules are closely packed in the cell, thus improving the density. Predicted density of **F1** and **F2** molecules are 1.81 and 1.66 g/cm^3, respectively, found close to experimental values (**F1**=1.73; **F2**=1.70 g/cm^3).[76] The triazole derivatives (**T1-T3** and **R1-R3**) are found to be denser than imidazole (**I1-I3**), pyrazole (**P1-P3**) and isoxazole (**O1-O3**) derivatives. This shows that an increase in nitrogen content of the azole ring effectively improves the density. There is no significant change observed in the density by changing the molecular framework such as imidazole, pyrazole and isoxazole. The nitro, amino and azido derivatives show densities above 1.64, 1.51 and 1.48 g/cm^3, respectively. Fig. 3.13 shows the minimum energy crystal structures of designed compounds.

Table 3.23: The calculated densities and lattice parameters of the azo bridged azole derivatives.

Compd.	Density (g/cm^3)	Space group	Lattice parameters					
			Length (Å)			Angle (^{o})		
			a	b	c	α	β	γ
I1	1.64	$P2_1/c$	12.12	13.75	7.86	90.0	127.6	90.0
I2	1.53	*PBCA*	22.04	13.71	5.84	90.0	90.0	90.0
I3	1.51	$P2_1/c$	28.35	12.26	26.07	90.0	173.1	90.0
P1	1.68	*C2/c*	13.33	6.36	23.95	90.0	87.2	90.0
P2	1.51	P_1	8.84	8.36	8.02	65.3	120.9	116.4
P3	1.48	*Cc*	4.09	17.61	16.99	90.0	113.5	90.0
T1	1.88	$P2_1/c$	4.41	11.59	32.65	90.0	147.2	90.0
T2	1.64	P_1	4.74	10.92	9.38	98.6	104.6	115.7
T3	1.61	P_1	8.46	12.39	7.58	114.1	115.2	46.5
R1	1.85	$P2_12_12_1$	8.98	17.57	5.81	90.0	90.0	90.0
R2	1.66	P_1	8.83	8.96	14.77	47.9	80.7	106.4
R3	1.63	P_1	8.68	4.43	17.99	50.2	98.1	107.3
O1	1.68	$P2_1$	9.97	10.83	7.73	90.0	37.5	90.0
O2	1.54	$P2_1$	12.49	5.43	7.65	90.0	57.7	90.0
O3	1.53	$P2_1$	4.21	7.81	18.02	90.0	63.7	90.0
F1	1.81	P_1	4.95	23.35	6.17	81.8	98.7	138.9
F2	1.66	P_1	14.10	3.84	10.28	83.1	96.3	49.2
F3	1.43	*Cc*	10.20	8.89	13.09	90.0	76.7	90.0

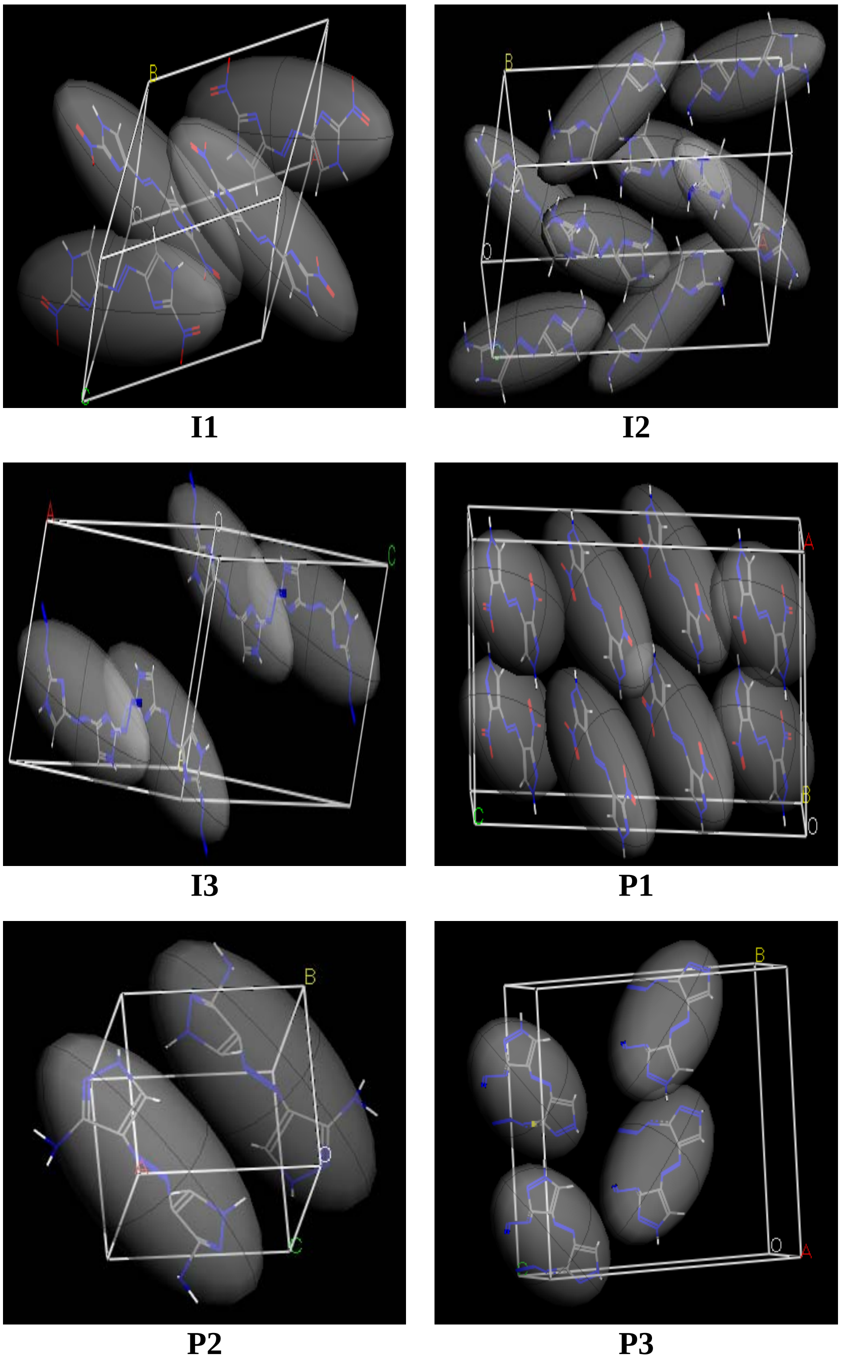

Fig. 3.13 Crystal structures of the designed compounds.

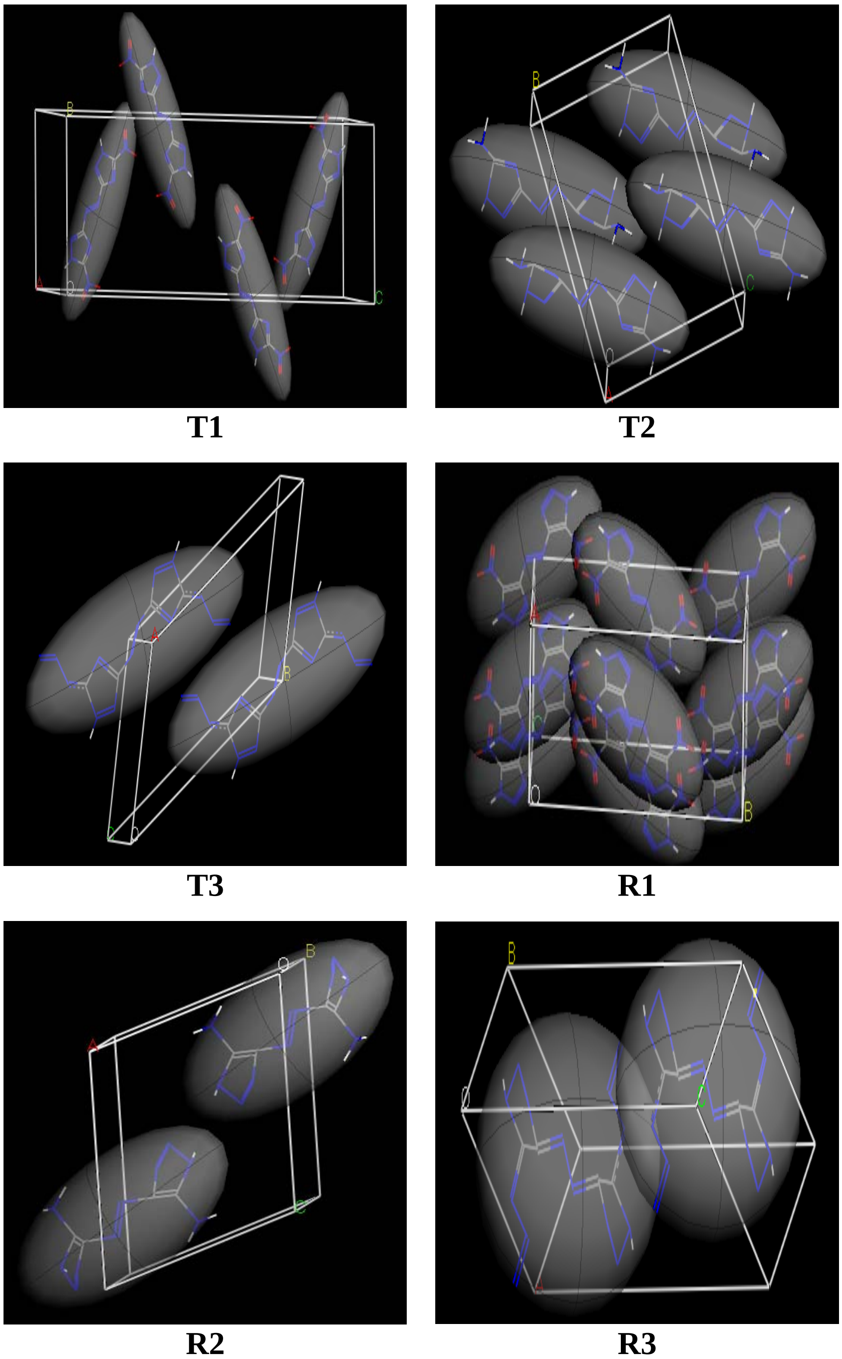

Fig. 3.13 (Contd.)

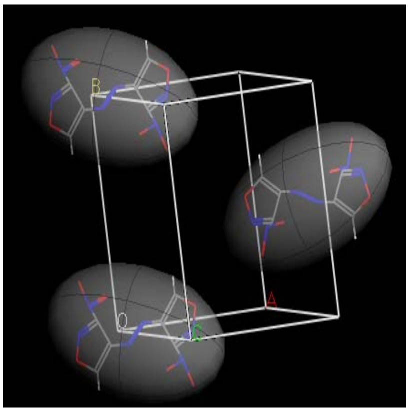

O1

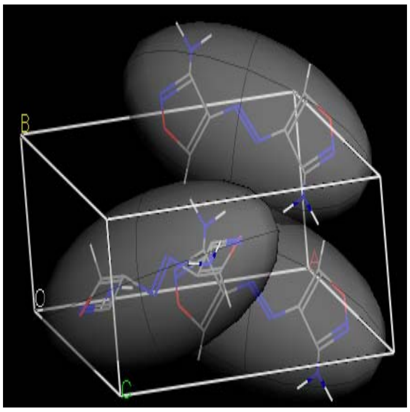

O2

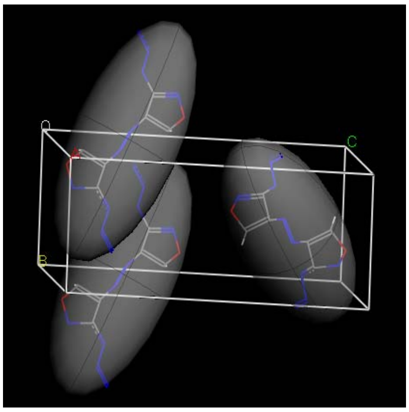

O3

Fig. 3.13 (Contd.)

3.3.4 Detonation characteristics

Detonation velocity and pressure of explosives have been highly dependent on density.[44] Table 3.22 presents the calculated detonation velocity and pressure for designed compounds. Performance of the nitro derivatives is superior to others, and it can be attributed to the high densities and oxygen balance which increases the concentration of detonation products like CO, CO_2, and H_2O. All nitro derivatives show detonation velocity of about 7.3 to 8.9 km/s and pressure of 21 to 36 GPa. The detonation performance is more dependent on density than ΔH^0_f. There is no significant change in the densities of amino and azido derivatives but the azido derivatives possess higher ΔH^0_f and hence, better detonation performance. Fig. 3.14 compares the velocity of detonation of designed compounds. The replacement of single nitrogen (in imidazole and pyrazole derivatives) with oxygen (in isoxazole derivatives) improves the detonation performance. Similar trend is observed in case of 1,2,4-triazole (**T1-T3**), 1,2,3-triazole (**R1-R3**) and furazan (**F1-F3**) derivatives. The increase in nitrogen content from imidazole/pyrazole to triazole derivatives significantly improves the detonation performance. The triazole (**T1-T3** and **R1-R3**) and isoxazole (**O1-O3**) derivatives are superior to imidazole (**I1-I3**) and pyrazole (**P1-P3**) derivatives due to the higher oxygen balance and densities. The relative order of increase in detonation performance can be given as NO_2>N_3>NH_2. All designed molecules show comparable detonation performance to **F1**, **F2** and **F3**.

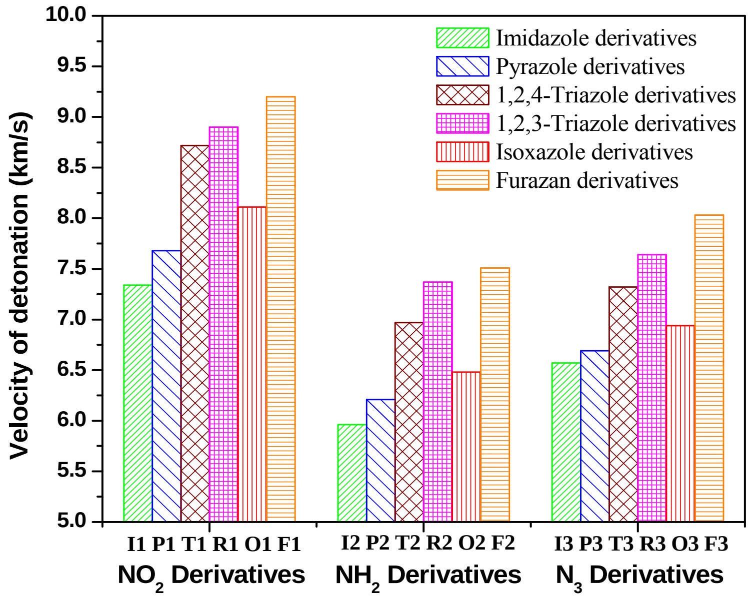

Fig. 3.14 Profile of velocity of detonation for the azo bridged azole derivatives.

3.3.5 Thermal stability

Aromaticity is expressed by a combination of properties in cyclic delocalized systems.[77] Nucleus independent chemical shift (NICS) is an important criterion to predict the stability of compounds with respect to aromaticity. Negative values of NICS indicate shielding presence of induced diatropic ring currents understood as aromaticity at the ring centre[78] and the more negative the NICS, the more aromatic the rings are. Table 3.24 summarizes the calculated NICS values at the ring centre of the azoles in the designed azole derivatives.

Table 3.24: Calculated band gap and NICS of the azo bridged azole derivatives.

Compd.	ΔE (eV)	NICS (ppm)	
		Left Ring	Right Ring
I1	3.8080	-12.18	-11.95
I2	3.9582	-11.45	-12.01
I3	3.6586	-11.77	-11.14
P1	3.8706	-13.38	-13.41
P2	3.9005	-11.86	-11.41
P3	3.6695	-12.31	-11.75
T1	4.1133	-11.52	-11.29
T2	4.1206	-9.94	-9.93
T3	3.8806	-10.47	-10.47
R1	3.5783	-10.52	-10.83
R2	3.5968	-10.83	-10.52
R3	3.2232	-10.69	-10.69
O1	4.0074	-11.30	-11.30
O2	4.0923	-9.52	-9.52
O3	3.7448	-9.93	-9.93
F1	3.7010	-10.43	-10.43
F2	4.1027	-9.29	-9.29
F3	3.3592	-10.30	-10.30

NICS at the left and right azole ring of the designed molecules (Fig. 3.11).

Heterocycles having $-NO_2$ groups increase the average NICS values. The presence of strong electron withdrawing $-NO_2$ and $-N_3$ groups, decreases the tendency of ring electrons to be localized, enhancing the diatropic ring current, which results in enhanced cyclic conjugation. The order of increasing NICS for the designed compounds is given as, NO_2>N_3>NH_2. Higher electron density in the ring may be due to the presence of more electronegative nitrogen. Among all designed molecules, NICS of the triazole and isoxazole rings are found to be lower than imidazole and pyrazole rings of the corresponding molecules. The replacement of the imidazole with pyrazole increases the ring current, and this can be clearly seen by comparing **I1-P1**, **I2-P2**, and **I3-P3**. This indicates that the pyrazoles are stable than the corresponding imidazole derivatives. All the molecules show NICS values above -9.8ppm.

3.3.6 Sensitivity correlations

The relative sensitivity of the material can be calculated by using band gap difference between highest occupied molecular orbital (HOMO) and lowest unoccupied molecular orbital (LUMO). Xiao et al.[79-81] research group suggested a principle of the easiest transition (PET) to predict the sensitivity of ionic metal azides. In principle, smaller the band gap (ΔE), easier the electron transition and larger the sensitivity will be. Table 3.24 lists the band gaps of the designed compounds obtained from B3LYP/6-31G* level calculations. Comparison of the band gaps of $-NO_2$, $-NH_2$ and $-N_3$ derivatives show that NH_2 molecules are more insensitive. The order of the increasing insensitivity is given as, $NH_2>NO_2>N_3$. Predicted band gaps of **F1**, **F2**, and **F3** are 3.7, 4.1 and 3.4 eV, respectively. The sensitivity of the azido derivatives may attribute to high nitrogen content, ΔH^0_f and energetic nature of the azide group. 1,2,4-triazole and isoxazole derivatives have band gap slightly higher than the other derivatives.

3.3.7 Conclusions

The energetic properties of the designed azole derivatives have been studied by using the density functional theory at the B3LYP/6-31G* level. Based on appropriate designed sets of isodesmic reactions, standard gas-phase ΔH^0_f are predicted. The azole derivatives possess high positive ΔH^0_f due to the major energy contribution from the five member azole rings, energetic nitro and azido groups. The nitro derivatives have higher densities as compared to amino and azido derivatives, which leads to better detonation performance. Thermal stability of the designed compounds has been evaluated by nucleus independent chemical shifts. The sensitivity correlation has been evaluated using the band gap analysis. Designed molecules have good thermal stability as evidenced from NICS index. The energetic properties of the designed molecules have been compared with 3,3'-dinitro-4,4'-azofurazan, 3,3'-diamino-4,4'-azofurazan, and 3,3'-diazido-4,4'-azofurazan. It has been found that these molecules have comparable energetic performance with better insensitivity and thermal stability. Overall performance of designed compounds is moderate and may find their applications in gas generators and smoke-free pyrotechnic fuels as they are rich in nitrogen content.

3.4 References

1. Miller, D. R.; Swenson, D. C.; Gillan, E. G. *J. Am. Chem. Soc.* **2004**, *126*, 5372.
2. Ye, C.; Gard, G. L.; Winter, R. W.; Syvret, R. G.; Twamley, B.; Shreeve, J. M. *Org. Lett.* **2007**, *9*, 3841.
3. Su, X.; Cheng, X.; Meng, C.; Yuan, X. *J. Hazard. Mater.* **2009**, *161*, 551.
4. Fried, L. E.; Manaa, M. R.; Pagoria, P. F.; Simpson, R. L. *Annu. Rev. Mater. Res.* **2001**, *31*, 291.
5. Huynh, M. H. V.; Hiskey, M. A.; Hartline, E. L.; Montoya, D. P.; Gilardi, R. *Angew. Chem. Int. Ed.* **2004**, *43*, 4924.
6. Pagoria, P. F.; Lee, G. S.; Mitchell, A. R.; Schmidt, R. D. *Thermochim. Acta* **2002**, *384*, 187.

7. Gutowski, K. E.; Rogers, R. D.; Dixon, D. A. *J. Phys. Chem. A* **2006**, *110*, 11890.

8. Su, X.; Cheng, X.; Ge, S. *J. Mol. Struct. (THEOCHEM)* **2009**, *895*, 44.

9. Hiskey, M. A.; Chavez, D. E.; Naud, D. L.; Son, S. F.; Berghout, H. L.; Bolme, C. A. *Proc. Int. Pyrotech. Semin.* **2000**, *27*, 3.

10. Singh, R. P.; Gao, H. X.; Meshri, D. T.; Shreeve, J. M. *Struct. Bond.* **2007**, *125*, 35.

11. Li, Y. F.; Fan, X. W.; Wang, Z. Y.; Ju, X. H. *J. Mol. Struct. (THEOCHEM)* **2009**, *896*, 96.

12. Cho, S. G.; Cho, J. R.; Goh, E. M.; Kim, J. K.; Damavarapu, R.; Surapaneni, R. *Propell. Explos. Pyrotech.* **2005**, *30*, 445.

13. Jadhav, H. S.; Talawar, M. B.; Sivabalan, R.; Dhavale, D. D.; Asthana, S. N.; Krishnamurthy, V. N. *J. Hazard. Mater.* **2007**, *143*, 192.

14. Williams, C. I.; Whitehead, M. A. *J. Mol. Struct. (THEOCHEM)* **1997**, *393*, 9.

15. Lide, D. R. *CRC Handbook of chemistry and physics*, CRC Press, 2003.

16. Wei, T.; Zhu, W. H.; Zhang, X. W.; Li, Y. F.; Xiao, H. M. *J. Phys. Chem. A* **2009**, *113*, 9404.

17. Aston, J. G.; Siller, C. W.; Messerly, G. H. *J. Am. Chem. Soc.* **1937**, *59*, 1743.

18. Knobel, Y. K.; Miroshnichenko, E. A.; Lebedev, Y. A. *Bull. Acad. Sci. USSR, Div. Chem. Sci.* **1971**, 425.

19. Chase, M. W. Jr. *J. Phys. Chem. Ref. Data* **1998**, *9*, 1.

20. Manion, J. A. *J. Phys. Chem. Ref. Data* **2002**, 123.

21. Cox, J. D.; Wagman, D. D.; Medvedev, V. A. *CODATA Key values for thermodynamics*, Hemisphere Publishing Corp, New York, 1984.

22. Zaheeruddin, M.; Lodhi, Z. H. *Phys. Chem.* (Peshawar Pak) **1991**, *10*, 111.

23. Jimenez, P.; Roux, M. V.; Turrion, C. *J. Chem. Thermodyn.* **1989**, *21*, 759.

24. Balepin, A. A.; Lebedev, V. P.; Miroshnichenko, E. A.; Koldobskii, G. I.; Ostovskii, V. A.; Larionov, B. P.; Gidaspov, B. V.; Lebedev, Yu. A. *Svoistva Veshchestv Str. Mol.* **1977**, 93.

25. Mondal, T.; Saritha, B.; Ghanta, S.; Roy, T. K.; Mahapatra, S.; Durga Prasad, M. *J. Mol. Struct. (THEOCHEM)* **2009**, *897*, 42.

26. Badgujar, D. M.; Talawar, M. B.; Asthana, S. N.; Mahulikar, P. P. *J. Hazard. Mater.* **2008**, *151*, 289.

27. Ju, X. H.; Li, Y. M.; Xiao, H. M. *J. Phys. Chem. A* **2005**, *109*, 934.

28. Rice, B. M.; Sahu, S.; Owens, F. J. *J. Mol. Struct. (THEOCHEM)* **2002**, *583*, 69.

29. Qiu, L.; Gong, X. D.; Zheng, J.; Xiao, H. M. *J. Hazard. Mater.* **2009**, *166*, 931.

30. Chung, G. S.; Schimidt, M. W.; Gordon, M. S. *J. Phys. Chem. A* **2000**, *104*, 5647.

31. Turker, L.; Atalar, T.; Gumus, S.; Camur, Y. *J. Hazard. Mater.* **2009**, *167*, 440.

32. Zhang, C.; Shu, Y.; Huang, Y.; Zhao, X.; Dong, H. *J. Phys. Chem. B* **2005**, *109*, 8978.

33. Klapotke, T. M.; Mayer, P.; Schulz, A.; Weigand, J. J. *J. Am. Chem. Soc.* **2005**, *127*, 2032.

34. Denffer, M. V.; Heeb, G.; Klapotke, T. M.; Kramer, G.; Spiess, G.; Welch, J. M. *Propell. Explos. Pyrotech.* **2005**, *30*, 191.

35. Klapotke, T. M.; Karaghiosoff, K.; Mayer, P.; Penger, A.; Welch, J. M. *Propell. Explos. Pyrotech.* **2006**, *31*, 188.

36. Lobbecke, S.; Pfeil, A.; Krause, H. H. *Propell. Explos. Pyrotech.* **1999**, *24*, 168.

37. Hammerl, A.; Holl, G.; Klapotke, T. M.; Mayer, P.; Noth, H.; Piotrowski, H.; Warchhold, M. *Eur. J. Inorg. Chem.* **2002**, *2002*, 834.

38. Klapotke, T. M.; Sabate, C. M. *Chem. Mater.* **2008**, *20*, 3629.

39. Galvez-Ruiz, J. C.; Holl, G.; Karaghiosoff, K.; Klapotke, T. M.; Lohnwitz, K.; Mayer, P.; Noth, H.; Polborn, K.; Rohbogner, C. J.; Suter, M.; Weigand, J. *J. Inorg. Chem.* **2005**, *44*, 4237.

40. Klapotke, T. M.; Stierstorfer, J.; Wallek, A. U. *Chem. Mater.* **2008**, *20*, 4519.

41. Ebespacher, M.; Klapotke, T. M.; Sabate, C. M. *New J. Chem.* **2009**, *33*, 517.

42. Xue, H.; Gao, H.; Twamley, B.; Shreeve, J. M. *Chem. Mater.* **2007**, *19*, 1731.

43. Xue, H.; Gao, Y.; Twamley, B.; Shreeve, J. M. *Inorg. Chem.* **2005**, *44*, 5068.

44. Mader, C. L. In: Markinas, P. L. (Ed) *Organic energetic compounds*, Nova science publishers, Commack, NY, 1996.

45. Strehlow, R. A. *Combustion fundamentals*, McGraw-Hill, New York, 1985.

46. Kamlet, M. J.; Jacobs, S. J. *J. Chem. Phys.* **1968**, *48*, 23.

47. Kamlet, M. J.; Ablard, J. E. *J. Chem. Phys.* **1968**, *48*, 36.

48. Xu, X. J.; Xiao, H. M.; Ju, X. H.; Gong, X. D.; Zhu, W. H. *J. Phys. Chem. A* **2006**, *110*, 5929.

49. Fan, X. W.; Ju, X. H.; Xiao, H. M. *J. Hazard. Mater.* **2008**, *156*, 342.

50. Murray, J. S.; Concha, M. C.; Politzer, P. *Mol. Phys.* **2009**, *107*, 89.

51. Zhang, C. Y. *J. Phys. Chem. A* **2006**, *110*, 14029.

52. Li, S. H.; Shi, H. G.; Sun, C. H.; Li, X. T.; Pang, S. P.; Yu, Y. Z.; Zhao, X. Q. *J. Chem. Crystallogr.* **2009**, *39*, 13.

53. Shine, H. J.; Chamness, J. T. *J. Org. Chem.* **1963**, *28*, 1232.

54. Alper, H.; Paik, H. N. *J. Organomet. Chem.* **1979**, *172*, 463.

55. Wada, S.; Urano, M.; Suzuki. H. *J. Org. Chem.* **2002**, *67*, 8254.

56. Goldstein, S. L.; McNelis, E. *J. Org. Chem.* **1973**, *38*, 183.

57. Firouzabadi, H.; Mohajer, D.; Moghadam, M. E. *Bull. Chem. Soc. Jpn.* **1988**, *61*, 2185.

58. Patel, S.; Mishra, B. K. *Tetrahedron Lett.* **2004**, *45*, 1371.

59. Naud, D. L.; Hiskey, M. A.; Harry, H. H. *J. Energ. Mater.* **2003**, *21*, 57.

60. Chavez, D. E.; Hill, L.; Hiskey, M. A.; Kinkead, S. *J. Energ. Mater.* **2000**, *18*, 219.

61. Chavez, D. E.; Hiskey, M. A.; Gilardi, R. D. *Angew. Chem. Int. Ed.* **2000**, *39*, 1791.

62. Hammerl, A.; Klapotke, T. M.; Noth, H.; Warchhold, M.; Holl, G.; Kaiser, M. *Inorg. Chem.* **2001**, *40*, 3570.

63. Chavez, D. E.; Tappan, B. C.; Mason, B. A.; Parrish, D. *Propell. Explos. Pyrotech.* **2009**, *34*, 475.

64. Sheremetev, A. B.; Kulagina, V. O.; Aleksandrova, N. S.; Dmitriev, D. E.; Strelenko, Y. A.; Lebedev, V. P.; Matyushin, Y. N. *Propell. Explos. Pyrotech.* **1998**, *23*, 142.

65. Hong, W. L.; Tian, D. Y.; Liu, J. H.; Wang, F. *J. Solid Rocket Tech.* **2001**, *29*, 41.

66. Zhang, C. Y.; Shu, Y. J.; Zhao, X. D.; Dong, H. S.; Wang, X. F. *J. Mol. Struct. (THEOCHEM)* **2005**, *728*, 129.

67. Zhang, X. W.; Zhu, W. H.; Xiao, H. M. *J. Phys. Chem. A* **2010**, *114*, 603.

68. Shipp, K. G. *J. Org. Chem.* **1964**, *29*, 2620.

69. Sikder, A. K.; Sikder, N. *J. Hazard. Mater.* **2004**, *112*, 1.

70. Royce, W. B.; Brill, T. B. *Propell. Explos. Pyrotech.* **2000**, *25*, 247.

71. Royce, W. B.; Thomas, B. B. *Propell. Explos. Pyrotech.* **2000**, *25*, 241.

72. Shaposhnikov, S. D.; Korobov, N. V.; Sergievskii, A. V.; Pirogov, S. V.; Melnikova, S. F.; Tselinskii, I. V. *Russ. J. Org. Chem.* **2002**, *38*, 1351.

73. Ye, C.; Gao, H.; Boatz, J. A.; Drake, G. W.; Twamley, B.; Shreeve, J. M. *Angew. Chem. Int. Ed.* **2006**, *45*, 7262.

74. Petrie, M. A.; Sheehy, J. A.; Boatz, J. A.; Rasul, G.; Prakash, G. K. S.; Olah, G. A.; Christe, K. O. *J. Am. Chem. Soc.* **1997**, *119*, 8802.

75. Qiu, L.; Xiao, H. M.; Gong, X. D.; Ju, X. H.; Zhu, W. H. *J. Phys. Chem. A* **2006**, *110*, 3797.

76. Li, J.; Huang, Y.; Dong, H. *Propell. Explos. Pyrotech.* **2004**, *29*, 231.

77. Schleyer, P. v. R. *Chem. Rev.* **2001**, *101*, 1115.

78. Schleyer, P. v. R.; Manoharan, M.; Wang, Z. X.; Kiran, B.; Jiao, H. J.; Puchta, R.; Hommes, N. J. R. V. *Org. Lett.* **2001**, *3*, 2465.

79. Xiao, H. M.; Li, Y. F. *Banding and electronic structures of metal azides*, Science Press, Beijing, 1996.

80. Xu, X. J.; Zhu, W. H.; Xiao, H. M. *J. Phys. Chem. B* **2007**, *111*, 2090.

81. Wang, G. X.; Shi, C. H.; Gong, X. D.; Xiao, H. M. *J. Hazard. Mater.* **2009**, *169*, 813.

Chapter IV

Energetic Azines as Nitrogen-rich Molecular Framework

High material performance has been the prime importance in the development and study of new energetic materials for various applications. Traditional explosives, nitrate esters, nitroarenes, nitramines, must contain sufficient NO_2 groups to self-oxidize the carbon and hydrogen atoms of the molecule. In designing new energetic materials, one area of emphasis has been on increasing the nitrogen content (N. C.) at the expense of carbon/hydrogen content. As a potential class of energetic materials, nitrogen-rich compounds offer high thermal stability, heats of formation, density, and oxygen balance than their carbocyclic analogues.[1-3] Over the past few years, s-tetrazines, s-triazines and s-heptazines (Fig. 4.1) have played a key role in the synthesis of high performance energetic materials.[4-8] This novel high-nitrogen energetic compounds possess high positive heat of formation ($\Delta H^0{}_f$) and high thermal stability that result in numerous applications, such as effective precursors of carbon nanospheres and carbon nitride nanomaterials, solid fuels in micropropulsion systems, gas generators and smoke-free pyrotechnic fuels.[9-14]

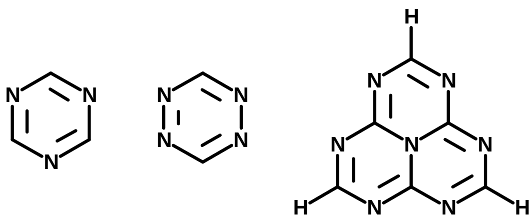

Fig. 4.1 Molecular frameworks of s-triazine, s-tetrazine and s-heptazine.

4.1 Heptazine Derivatives

In recent years, 1,3,5-triazine (s-triazine) based carbon nitride (CNx) materials have been investigated by various researchers.[11,15-17] The s-heptazine structure was first postulated by Pauling and Sturdivant[18] as a component of the polymer melon [-$C_6H_7(NH_2)$-NH-]$_n$. s-Heptazine is symmetrical heterocyclic azadienes, composed of three fused s-triazine rings. Such s-triazine monocyclic systems have been subjected to theoretical and experimental studies. Recently, Zheng et al.[19] studied the electronic structure of 1,3,4,6,7,9,9b-heptaazaphenalenes by density functional theory (DFT). Studies on the geometry of heptaazaphenalene derivatives revealed that they have a highly symmetrical structure with a planar and rigid hetero ring. Further, they confirmed the existence of considerable conjugation over the parent ring, which is an advantage in terms of the stability of these compounds. Kroke et al.[20] reported the synthesis and detailed structural characterization of functionalized 1,3,4,6,7,9,9b-heptaazaphenalene derivatives and 2,5,8-trichloro-1,3,4,6,7,9,9b-heptaazaphenalene. Similar to their s-triazine counterparts, s-heptazine-based precursors are thermally robust candidates as promising precursors to nitrogen-rich, sp^2-bonded carbon nitride materials. Energetic groups like nitro and azido, and nitrogen-rich heterocycles (imidazloes, triazoles, etc.) proved to enhance the energetic behavior of the explosive. Hence, the molecular structures with diverse substituents, viz. azido, amino, nitro, and nitrogen-rich heterocycles at various positions in the basic s-heptazine ring have been considered. The structures of the designed compounds are shown in Fig. 4.2.

Results and discussion

Recently, Gillan et al.[12] demonstrated a synthetic route for heptazine and 2,5,8-triazido-s-heptazine. They also indicated that these compounds can act as potential energetic materials. Strout et al.[21,22] studied the nitrogen-rich molecules by theoretical calculations to predict their energetic properties as high energy materials. This study focuses on an electronic structure of designed molecules and its effect on energetic characteristics using density functional techniques.

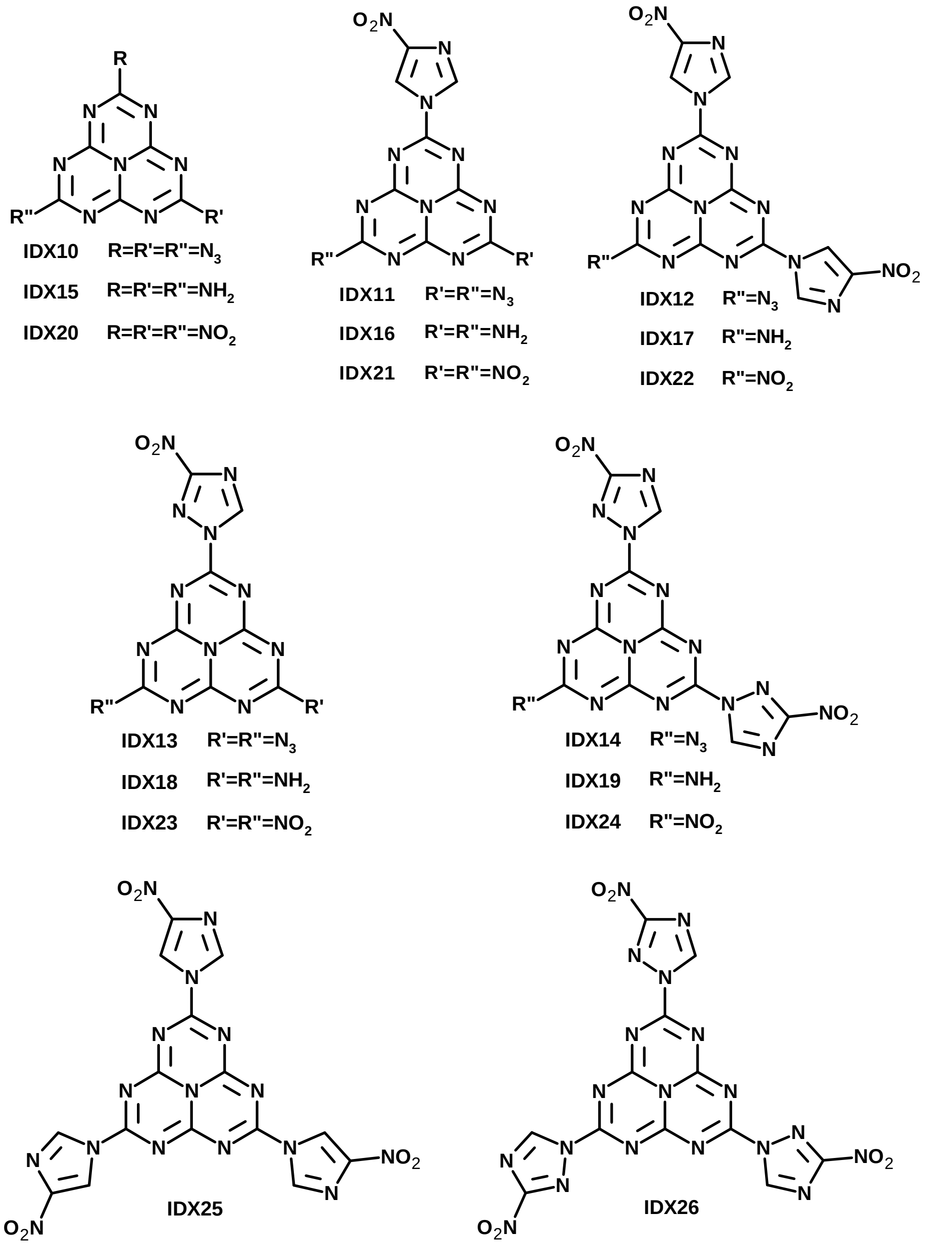

Fig. 4.2 Designed heptazine derivatives.

4.1.1 Molecular geometries

All designed compounds contain cyclic planar, conjugated nitrogen-rich backbone. Nitrogen at the centre of the ring possesses sp^3 hybridization. The three different explosophores (NO_2, NH_2, and N_3), nitroimidazole and nitrotriazole rings are arranged symmetrically on the molecular skeleton. The explosophores are far apart from each other (> 8 Å); hence reduce the chances for the steric repulsion. All the explosophores positioned in the plane of azole rings (torsional angle ≈ 180^o) and hence shows resonance in the molecular skeleton due to their electron withdrawing/donating effect. The selected structural parameters of the designed molecules are listed in Table 4.1 to 4.6.

Comparison of **IDX10**, **IDX15** and **IDX20** reveals that introduction of -NH_2 group slightly increases the C-N bond lengths (N1-C2, N1-C6, N1-C10) at the centre of ring, while strengthens C=N bonds due to its electron donating effect. The optimized geometries of heptazine derivatives reveal that -NO_2, -N_3, -NH_2, nitroimidazole and nitrotriazole substituents are in the plane of heptazine backbone (torsional angle ≈ 180^o). The replacement of single -NO_2, -N_3 and -NH_2 substituents on the heptazine by nitroimidazole (**IDX11**, **IDX16** & **IDX21**) and nitrotriazole (**IDX13**, **IDX18** & **IDX23**) increases the C-N bond lengths in the molecular structure but reduces the C-N_3, C-NO_2 and C-NH_2 bond lengths. Similar trend is observed with the replacement of two -NO_2, -N_3 and -NH_2 substituents on the heptazine by nitroimidazole (**IDX12**, **IDX17** & **IDX22**) and nitrotriazole (**IDX14**, **IDX19** & **IDX24**). The symmetric arrangement of nitroimidazole (**IDX25**) and nitrotriazole (**IDX26**) strengthens the C-N and C=N bonds of the heptazine backbone. The nitroimidazole and nitrotriazole in **IDX25** and **IDX26** molecules lies in the plane of heptazine ring. The bond lengths of C-NO_2 bond (> 1.41 Å) found to be higher than other C-C and C-N bonds in the molecular structure.

Table 4.1: Selected structural parameters of **H**, **IDX10**, **IDX15** and **IDX20**.

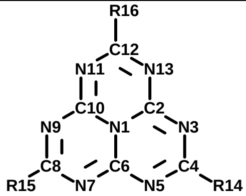

	Parameter	**H**	**IDX10**	**IDX15**	**IDX20**
Bond length (Å)	N1-C2, N1-C6, N1-C10	1.4082	1.4093	1.4125	1.4096
	C2-N3, C6-N7, C10-N11, C2-N13, C10-N9, C6-N5	1.3358	1.3285	1.3278	1.3334
	N3-C4, N5-C4, N7-C8, C8-N9, N11-C12, C12-N13	1.3329	1.3356	1.3463	1.3193
	C4-N14, C8-N15, C12-N16	-	1.3915	1.3485	1.4996

H: R14, R15, R16=H; IDX10: R14, R15, R16=N_3; IDX15: R14, R15, R16=NH_2; IDX20: R14, R15, R16=NO_2

Table 4.2: Selected structural parameters of **IDX11**, **IDX16** and **IDX21**.

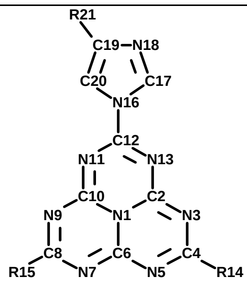

	Parameter	**IDX11**	**IDX16**	**IDX21**
Bond length (Å)	N1-C6,	1.4101	1.4159	1.4098
	N1-C2, N1-C10	1.4068	1.4091	1.4210
	C2-N3, C10-N9	1.3264	1.3175	1.3402
	N3-C4, C8-N9	1.3443	1.3542	1.3147
	N5-C4, N7-C8	1.3345	1.3443	1.3232
	C6-N7, C6-N5	1.3284	1.3268	1.3323
	C10-N11, C2-N13	1.3327	1.3408	1.3178
	N11-C12, C12-N13	1.3334	1.3274	1.3447
	C4-N14, C8-N15	1.3881	1.3428	1.4922
	C12-N16	1.3981	1.4068	1.3809
	C19-N21	1.4470	1.4448	1.4279

IDX11: R14, R15=N_3; IDX16: R14, R15=NH_2; IDX21: R14, R15=NO_2

Table 4.3: Selected structural parameters of **IDX12**, **IDX17** and **IDX22**.

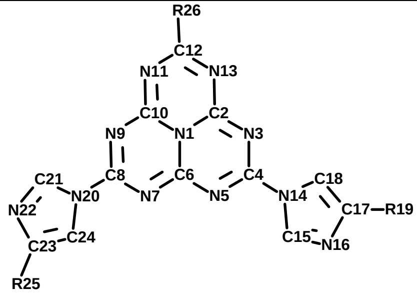

	Parameter	**IDX12**	**IDX17**	**IDX22**
Bond length (Å)	N1-C2, N1-C10	1.4112	1.4119	1.4089
	N1-C6	1.4067	1.4056	1.4089
	C2-N3, C10-N9	1.3335	1.3385	1.3246
	N3-C4, C8-N9	1.3308	1.3275	1.3370
	N5-C4, N7-C8	1.3356	1.3354	1.3336
	C6-N5, C6-N7	1.3290	1.3302	1.3296
	C4-N14, C8-N20	1.3941	1.3983	1.3885
	C10-N11, C2-N13,	1.3243	1.3176	1.3369
	N11-C12, C12-N13	1.3375	1.3517	1.3188
	C12-N26	1.3845	1.3381	1.4877
	C17-N19, C23-N25	1.4481	1.4471	1.4494

IDX12: R26=N_3; IDX17: R26=NH_2; IDX22: R26=NO_2

Table 4.4: Selected structural parameters of **IDX13**, **IDX18** and **IDX23**.

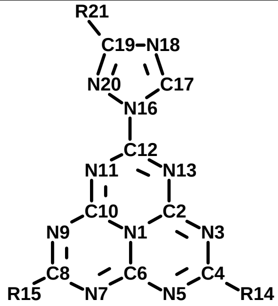

	Parameter	**IDX13**	**IDX18**	**IDX23**
Bond length (Å)	N1-C6,	1.4106	1.4161	1.4099
	N1-C2, N1-C10	1.4076	1.4105	1.4105
	C2-N3, C10-N9	1.3242	1.3159	1.3359
	N3-C4, C8-N9	1.3452	1.3545	1.3179
	N5-C4, N7-C8	1.3349	1.3445	1.3206
	C6-N7, C6-N5	1.3279	1.3265	1.3325
	C10-N11, C2-N13	1.3359	1.3431	1.3278
	N11-C12, C12-N13	1.3233	1.3187	1.3269
	C4-N14, C8-N15	1.3864	1.3422	1.4927
	C12-N16	1.4105	1.4190	1.3988
	C19-N21	1.4662	1.4643	1.4685

IDX13: R14, R15=N_3; IDX18: R14, R15=NH_2; IDX23: R14, R15=NO_2

Table 4.5: Selected structural parameters of **IDX14**, **IDX19** and **IDX24**.

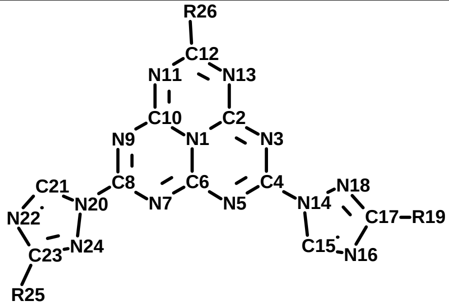

	Parameter	**IDX14**	**IDX19**	**IDX24**
Bond length (Å)	N1-C2, N1-C10	1.4086	1.4130	1.4096
	N1-C6	1.4049	1.4038	1.4068
	C2-N3, C10-N9	1.3365	1.3422	1.3284
	N3-C4, C8-N9	1.3218	1.3175	1.3267
	N5-C4, N7-C8	1.3358	1.3375	1.3351
	C6-N5, C6-N7	1.3305	1.3300	1.3295
	C4-N14, C8-N20	1.4069	1.4108	1.4012
	C10-N11, C2-N13,	1.3232	1.3153	1.3349
	N11-C12, C12-N13	1.3451	1.3525	1.3192
	C12-N26	1.3820	1.3365	1.4919
	C17-N19, C23-N25	1.4671	1.4662	1.4682

IDX14: R26=N_3; IDX19: R26=NH_2; IDX24: R26=NO_2

Table 4.6: Selected structural parameters of **IDX25** and **IDX26**.

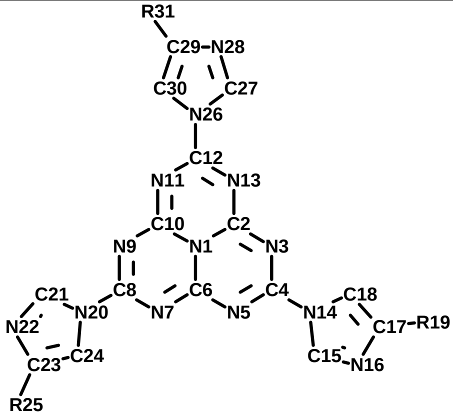

	Parameter	IDX25	IDX26
Bond length (Å)	N1-C2, N1-C6, N1-C10	1.4081	1.4078
	C2-N3, C6-N7, C10-N11, C2-N13, C10-N9, C6-N5	1.3298	1.3319
	N3-C4, N5-C4, N7-C8, C8-N9, N11-C12, C12-N13	1.3339	1.3252
	C4-N14, C8-N15, C12-N16	1.3911	1.4032
	C17-N19, C23-N25, C29-N31	1.4490	1.4679

IDX25 & IDX26: R19, R25, R31=NO_2

4.1.2 Gas phase heat of formation

Heat of formation (ΔH^0_f) is one of the most important thermochemical properties of energetic materials because it is related directly with detonation parameters. The zero point energies and thermal correction for model compounds have been calculated at the B3LYP/6-31G* level. ΔH^0_f of model compounds has been predicted by appropriate design of isodesmic reactions.[23] The isodesmic reaction, in which a number of electron pairs and chemical bond types are conserved in the reaction,[24] allows reducing of errors inherent in the approximate treatment of the electron correlation in the solutions to quantum mechanic equations. Recently, isodesmic reaction approach has been used for determination of ΔH^0_f within few kcal/mol of deviations from experimental value.[25] The calculated and experimental gas phase ΔH^0_f of the reference compounds s-triazine, imidazole, 1,2,4-triazole, CH_4, NH_3, CH_3N_3, CH_3NO_2, CH_3NH_2 are listed in Table. 4.7. ΔH^0_f of the designed compounds which have been predicted by isodesmic approach are summarized in Table 4.8. All the predicted molecules show that high positive ΔH^0_f may be due to the high nitrogen content, conjugation, planarity, stability of structure based on s-triazine and a large number of inherently energetic N-N and C-N bonds.

Table 4.7: Total energy (E_0) at the B3LYP/6-31G* level and experimental ΔH^0_f for the reference compounds.

Compd.	E_0 (au)	ΔH^0_f (kJ/mol)
CH_4	-40.46935	-74.6
NH_3	-56.50961	-45.9
CH_3NH_2	-95.78444	-22.5
CH_3NO_2	-244.95385	-74.7
CH_3N_3	-204.03725	238.4
Imidazole	-226.13859	129.5
Pyrazole	-226.12249	179.4
1,2,4-Triazole	-242.18478	192.7
1,2,3-Triazole	-242.15867	271.7
Tetrazole	-258.24639	326.0
s-Tetrazine	-296.26445	487.2
s-Triazine	-280.29414	225.8

Fig. 4.3 shows the isodesmic reaction schemes for the designed molecules and calculated ΔH^0_f of the parent s-heptazine (H) by a similar reaction is about 812 kJ/mol. Comparison of **IDX10**, **IDX20** with the parent heptazine ring clearly indicates that introduction of explosophores like azido, nitro etc., increases the ΔH^0_f of the parent system. This proves that azido and nitro explosophores are the main origin of the energy center in the designed molecules. The role of the azido group in ΔH^0_f is

more profound than that of the nitro group, as also found by Li et al.[26] This may be attributed to the higher nitrogen content of **IDX10**; however, introduction of a nitro group enhances the oxygen balance and hence the overall performance. Introduction of an amino group (**IDX15**) brings down the ΔH^0_f, as supported by Li et al.[26,27] Imidazole and triazole are natural frameworks for energetic materials as they have inherently high nitrogen content.[28] Adding these functionalities to the ring structure typically alters the ΔH^0_f, making it more positive, which is a desired characteristic for most energetic materials.[3] A systematic substitution of nitro, azido and amino groups by nitroimidazole and nitrotriazole was attempted. Substitution by imidazole or 1,2,4-triazole with a nitro group shows a remarkable increase in ΔH^0_f; various s-heptazine derivatives are compared in Figs. 4.4 & 4.5, indicating that addition of nitrogen-rich heterocycle increases the ΔH^0_f. Replacement of the azido group in **IDX10** by nitroimidazole (in **IDX11** and **IDX12**) and nitrotriazole (in **IDX13** and **IDX14**) increases the ΔH^0_f significantly, which indicates that corresponding rings contribute significantly to the total ΔH^0_f of the molecules. The energy contribution to the overall gas phase ΔH^0_f of imidazole (129.5 kJ/mol) is lower than triazole ring (192.7 kJ/mol). This can be clearly seen in **IDX11** and **IDX13**; in which ΔH^0_f is increased by 78 kJ/mol and in **IDX12** and **IDX14** ΔH^0_f is increased by 159 kJ/mol. A similar trend is observed in the case of amino (**IDX16** to **IDX18** by 79 kJ/mol; **IDX17** to **IDX19** by 157 kJ/mol and nitro derivatives (**IDX21** to **IDX23** by 158 kJ/mol; **IDX22** to **IDX24** by 166 kJ/mol). Overall, tri-substituted **IDX25** and **IDX26** is calculated to have high gas phase ΔH^0_f viz., 1658.26 and 1898.24 kJ/mol, respectively. Comparison of **IDX11**, **IDX16** and **IDX21**, in which one of the functional groups (azido, amino and nitro) is replaced by a nitroimidazole group shows the following order of ΔH^0_f **IDX11**>**IDX21**>**IDX16**. Similarly, in the case of the nitro triazole substitution, the order is **IDX13**>**IDX23**>**IDX18**, which indicates that azido and nitro derivatives exhibit higher $\Delta H^0{}_f$ than amino derivatives. In the case of diheterocyclic-substituted compounds, a similar order is found, viz., **IDX12**>**IDX22**>**IDX17** and **IDX14**>**IDX24**>**IDX19**. Overall, nitro heterocycle substitution increases the $\Delta H^0{}_f$, and energy contribution from the triazole ring is higher than that from the imidazole ring.

Table 4.8: Calculated energetic properties of designed heptazine derivatives.

Compd.	N.C. (%)	E_0 (au)	$\Delta H^0{}_f$ (kJ/mol)	Q (cal/g)	*D* (km/s)	*P* (GPa)
H	56.65	-613.58273	811.99	1121.79	6.68	18.90
IDX10	75.67	-1104.36584	1187.29	958.68	7.10	22.35
IDX11	61.20	-1370.23891	1340.16	1105.23	7.50	25.44
IDX12	51.37	-1636.11027	1497.39	1207.11	7.56	25.60
IDX13	64.84	-1386.26805	1418.59	1110.55	7.81	27.84
IDX14	57.53	-1668.16769	1656.55	1216.82	8.05	29.43
IDX15	64.20	-779.67234	761.69	835.08	7.46	25.48
IDX16	53.49	-1153.78194	1026.61	1149.52	7.39	24.52
IDX17	47.80	-1527.88398	1334.84	1265.43	7.50	25.31
IDX18	57.77	-1169.81110	1105.02	1205.36	7.64	26.37
IDX19	54.36	-1559.94246	1491.25	1273.87	7.94	28.45
IDX20	45.46	-1227.01346	891.82	1206.67	9.25	40.10
IDX21	44.92	-1451.91241	1225.85	1291.08	8.49	32.74
IDX22	44.54	-1676.99293	1397.95	1262.21	7.93	28.17
IDX23	48.53	-1468.03149	1383.55	1346.31	8.95	36.90
IDX24	50.68	-1709.04827	1563.17	1274.85	8.49	32.48
IDX25	44.26	-1901.98024	1658.26	1282.53	7.54	25.15
IDX26	52.26	-1950.06592	1898.24	1295.20	8.12	29.41

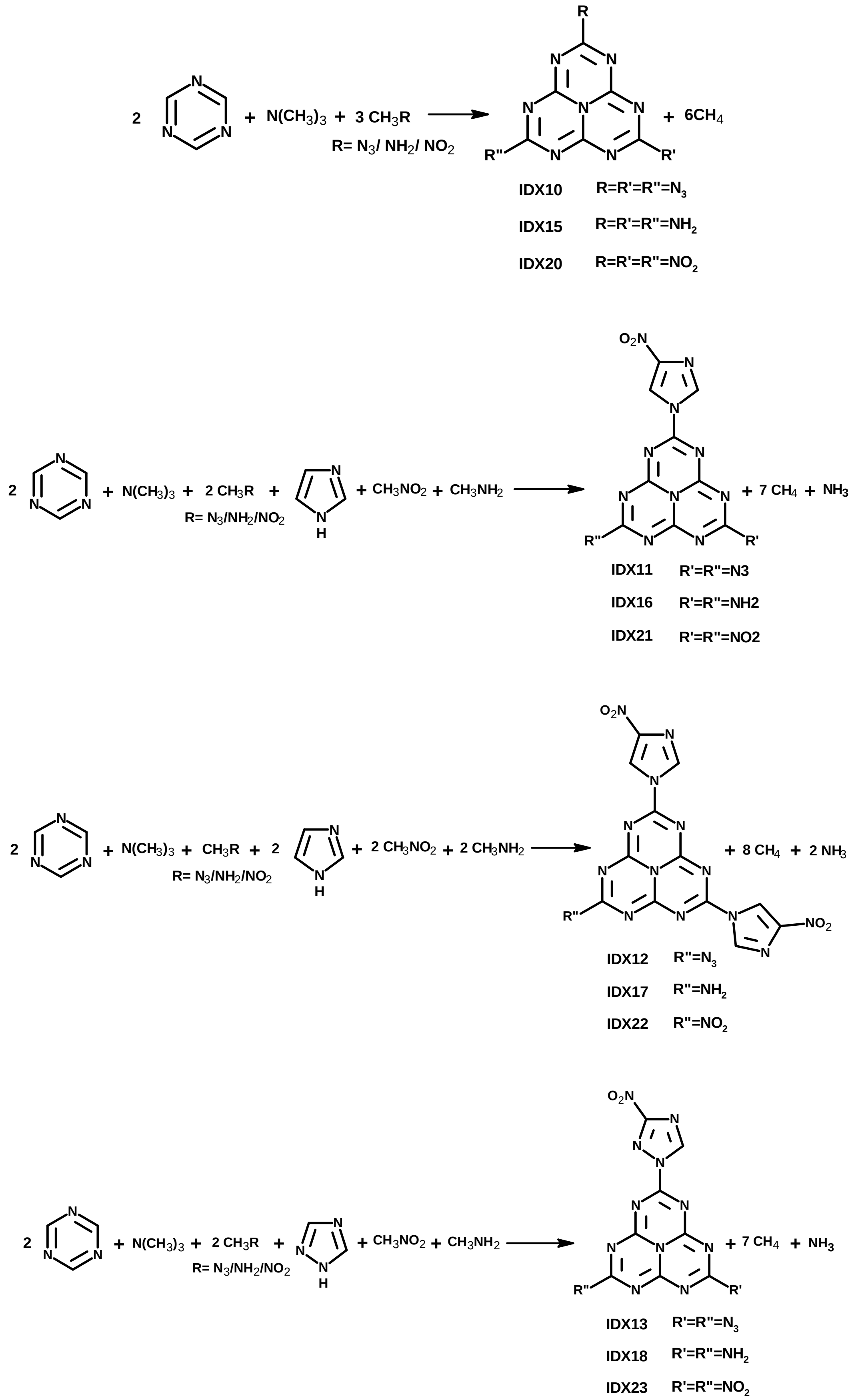

Fig. 4.3 Isodesmic reaction schemes for heptazine derivatives.

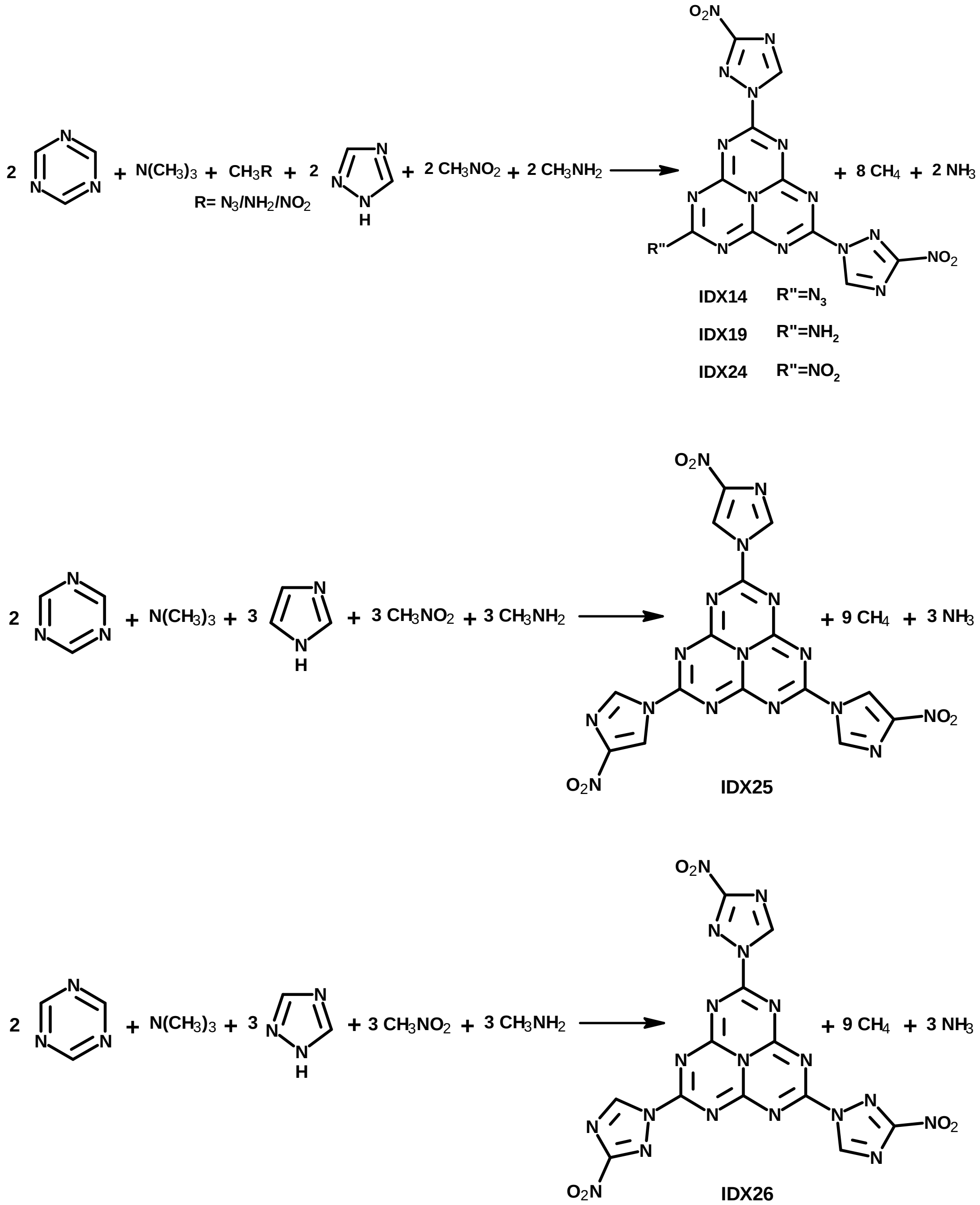

Fig. 4.3 (Contd.)

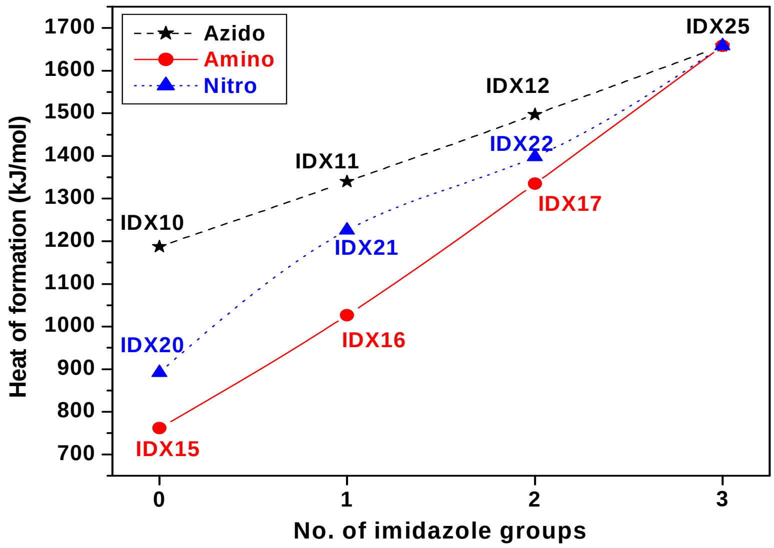

Fig. 4.4 Plot of number of imidazole groups versus heat of formation (kJ/mol).

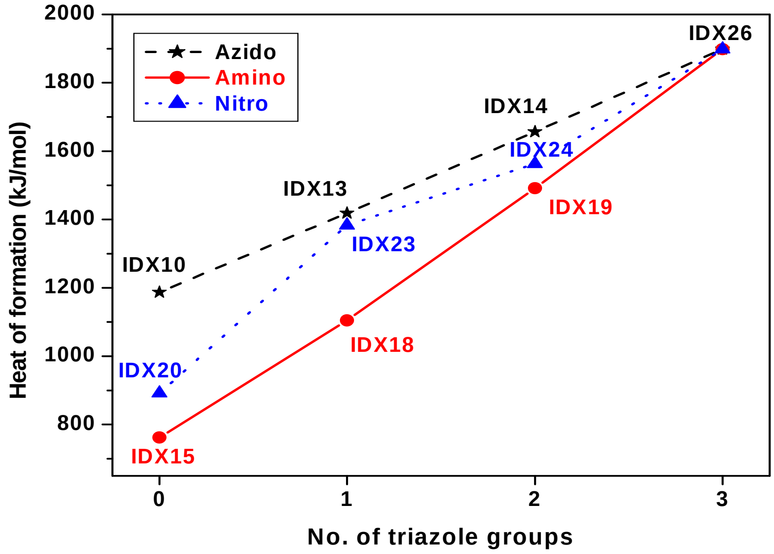

Fig. 4.5 Plot of number of triazole groups versus heat of formation (kJ/mol).

4.1.3 Density

Density is a condensed phase property and its prediction involves challenges as it is associated with different intermolecular interactions affecting crystal pattern and cell volume. In general, possible ways of improving the density are (1) increasing the concentration of nitro groups, which increases the opportunity for hydrogen bonding; (2) making larger compounds; and (3) replacing single bonds with double bonds.[29-32] As bond length decreases, molecular volume is expected to decrease.[33] In the present study, these design principles were used while designing the model compounds and the calculated densities from packing calculations are shown in Table 4.9.

Table 4.9: Calculated cell parameters and densities of the heptazine derivatives.

Compd.	Density (g/cm^3)	Space group	Lattice parameters					
			Length (Å)			Angle (°)		
			a	b	c	α	β	γ
H	1.67	*P1*	14.8	6.8	8.1	106.5	128.0	116.4
IDX10	1.80	*P21/c*	3.4	23.4	17.1	90.0	165.6	90.0
IDX11	1.86	*P1*	10.4	7.6	10.2	77.5	57.0	90.0
IDX12	1.83	*P21/c*	19.9	18.7	21.8	90.0	168.6	90.0
IDX13	1.89	*PBCA*	7.1	21.4	17.1	90.0	90.0	90.0
IDX14	1.87	*PNA21*	18.0	12.3	7.0	90.0	90.0	90.0
IDX15	1.90	*P21/c*	9.8	3.7	25.2	90.0	59.4	90.0
IDX16	1.84	*C2/c*	69.4	4.3	52.2	90.0	171.5	90.0
IDX17	1.83	*P1*	12.2	15.8	4.9	123.0	78.6	85.2
IDX18	1.86	*P21/c*	8.9	33.0	33.7	90.0	173.5	90.0
IDX19	1.85	*P1*	11.5	11.8	11.5	138.5	46.7	116.1
IDX20	1.98	*Cc*	3.4	31.5	10.7	90.0	61.0	90.0
IDX21	1.87	*P1*	18.1	7.9	13.3	54.1	145.7	140.9
IDX22	1.83	*P21/c*	4.1	16.4	25.7	90.0	68.8	90.0
IDX23	1.92	*P21/c*	15.7	9.7	8.6	90.0	99.7	90.0
IDX24	1.89	*PBCA*	7.6	22.4	18.2	90.0	90.0	90.0
IDX25	1.79	*P21*	4.2	12.7	21.6	90.0	126.3	90.0
IDX26	1.82	*PBCA*	35.6	7.4	14.2	90.0	90.0	90.0

Introduction of one imidazole and triazole ring increases the density of heptazine viz., 1.80 g/cm^3 increases the density to 1.86 (**IDX11**) and 1.89 g/cm^3 (**IDX13**), respectively. However, further introduction of additional heterocyclic ring in **IDX12** and **IDX14** decreases the density to 1.83 and 1.87 g/cm^3, respectively, as compared to **IDX11** and **IDX13**. This may be attributed to the increase in molecular volume and the orientation of the ring in space. The density of triaminoheptazine (**IDX15**) is 1.90 g/cm^3 and results reveal that replacement of the amino group with nitroimidazoles/nitrotriazoles decreases the density. The amino group lies in the same plane of the molecule to maximize lone pair delocalization with the heterocyclic π-electron system, and further helps in increasing hydrogen bonding with nitro groups of the hetero ring. The symmetrical trinitroheptazine (**IDX20**) possesses a very high density of 1.98 g/cm^3, which may be due to the high content of oxygen and nitrogen. Nitro derivatives of heptazine follow a similar trend of amino and azido derivatives when introducing the heterocyclic ring. In the case of **IDX25** and **IDX26**, the molecular volume is very high due to the presence of three nitro substituted heterocyclic rings, and hence the overall density is less. The overall density of the designed molecules varies from 1.8 to 2 g/cm^3. Fig. 4.6 shows the predicted crystal structures of the heptazine derivatives.

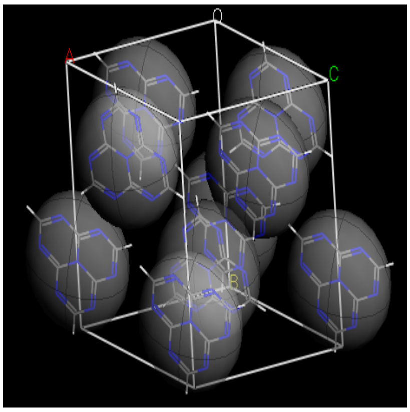

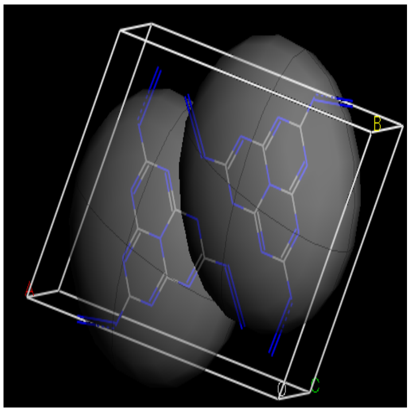

H **IDX10**

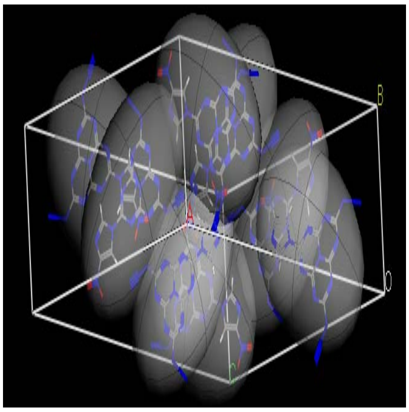

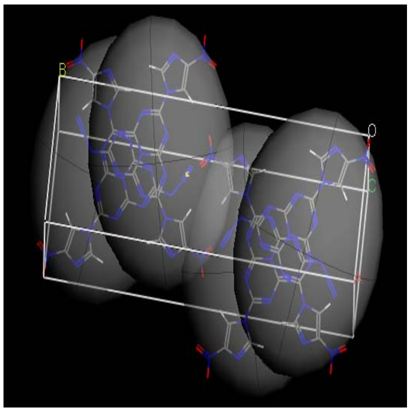

IDX11 **IDX12**

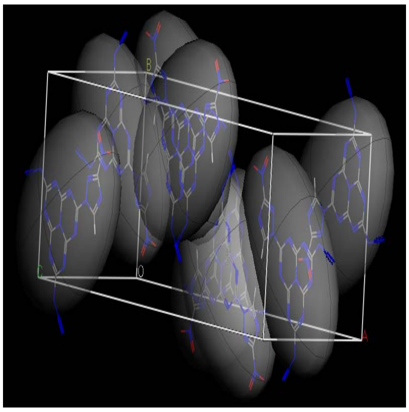

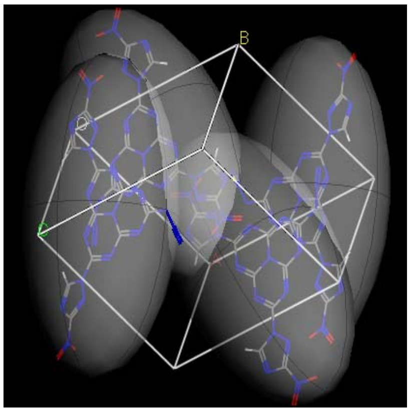

IDX13 **IDX14**

Fig. 4.6 Predicted crystal structures of the heptazine derivatives.

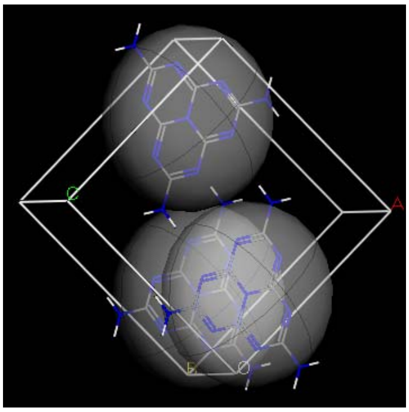

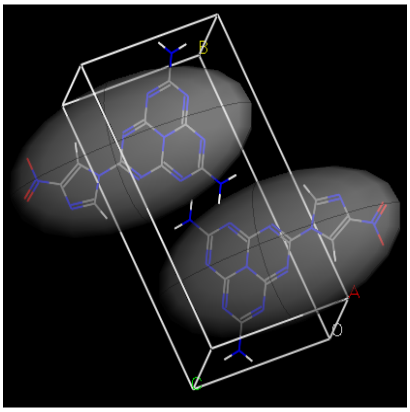

IDX15 **IDX16**

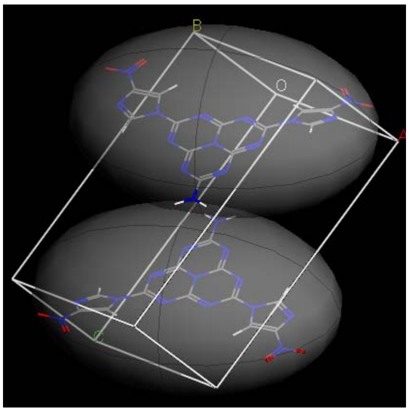

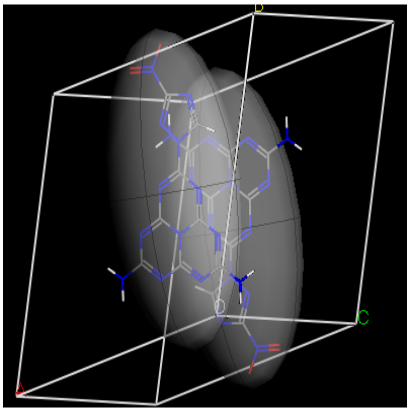

IDX17 **IDX18**

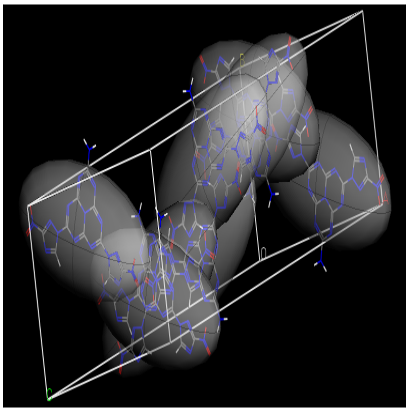

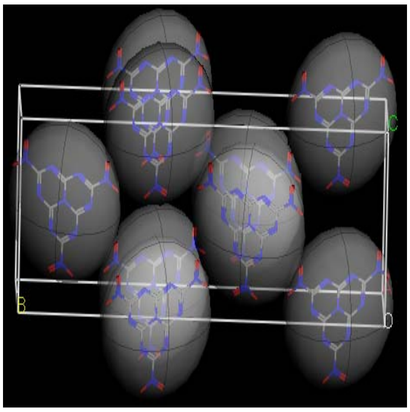

IDX19 **IDX20**

Fig. 4.6 (Contd.)

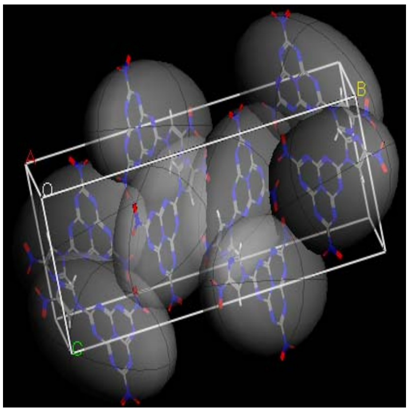

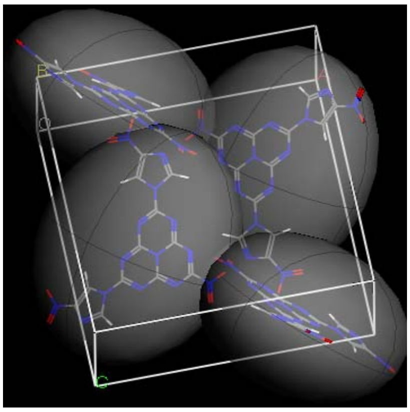

IDX21 IDX22

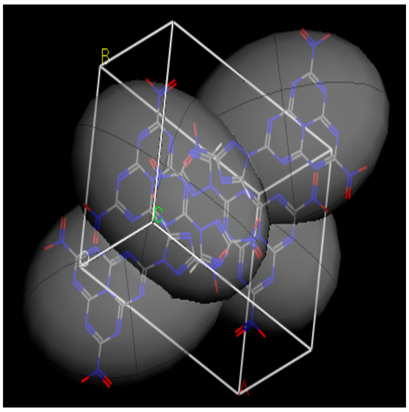

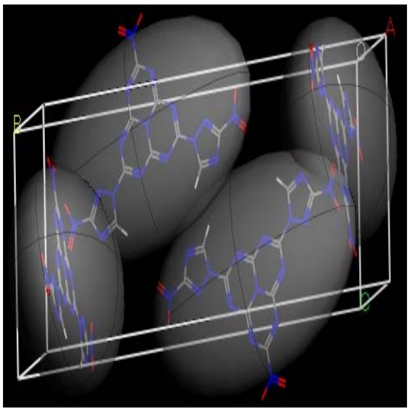

IDX23 IDX24

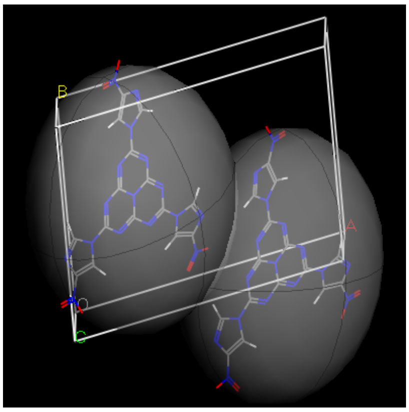

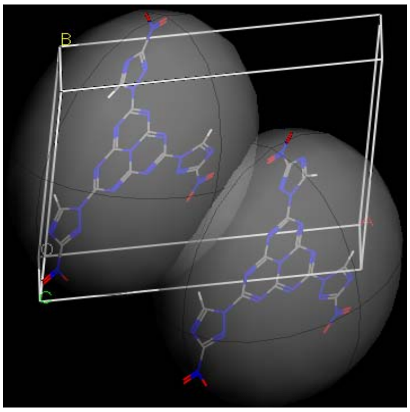

IDX25 IDX26

Fig. 4.6 (Contd.)

4.1.4 Detonation characteristics

Table 4.8 represents detonation velocity (*D*) and pressure (*P*) for the predicted molecules computed by Kamlet-Jacobs empirical equations. Overall computed detonation velocity ranges from about 7.1 to 9.3 km/s and oxygen balance is negative in all cases. Fig. 4.7a-c show the dependence on density of the detonation velocity and clearly indicates that nitrotriazole-substituted derivatives show overall high detonation velocity. Cho et al.[34] also reported that the performance of an explosive is highly sensitive to its crystalline density, but somewhat less sensitive to its ΔH^0_f. Comparison of azido derivative reveals the order of detonation performance as **IDX14**>**IDX13**>**IDX12**>**IDX11**>**IDX10**. Replacement of azido groups with nitroimidazole and nitrotriazole groups enhances the detonation performance of the molecules due to higher densities and greater mole of gaseous detonation products per gram of explosive (N).

In the case of amino derivatives, **IDX16** exhibits a lower performance than its parent molecule **IDX15** even after an energetic nitroimidazole group is introduced. Performance reduction can be attributed to the decrease in density. Comparison of amino derivatives reveals that these compounds (**IDX17**, **IDX18** and **IDX19**) have low density as compared to **IDX15**. However, ΔH^0_f of these compounds is very high. The order of the detonation performance for the amino series derivatives can be given as **IDX16**<**IDX15**<**IDX17**<**IDX18**<**IDX19**. In general, these derivatives exhibit about 7.6 km/s detonation velocity, and 25.5 GPa detonation pressure. The number of moles of gaseous detonation products per gram of explosive (N) is less due to the low oxygen balance in these amino derivatives.

Nitro derivatives of heptazine (**IDX20**, **IDX21**, **IDX22**, **IDX23**, and **IDX24**) show higher performance than azido and amino derivatives due to better oxygen balance, density and ΔH^0_f of these molecules. Molecules **IDX21** and **IDX22** possess lower densities than the parent **IDX20**, which results in poorer performance than **IDX20**. **IDX23** and **IDX24** show comparable performance to **IDX20**. Detonation performance increases as the moles of gaseous detonation products per gram of explosive increases. Among the nitro derivatives, **IDX20** possess a high detonation velocity of 9.25 km/s, while other derivatives exhibit a detonation velocity of about 8 km/s and detonation pressure of 35 GPa. Their order of their detonation performance can be given as **IDX22<IDX24<IDX21<IDX23<IDX20**. The designed molecules **IDX25** and **IDX26** have higher $\Delta H^0{}_f$ but poor densities. Further, **IDX25** has low moles of gaseous detonation products per gram of explosive as compared to **IDX26**, which results in **IDX26** being superior to **IDX25**.

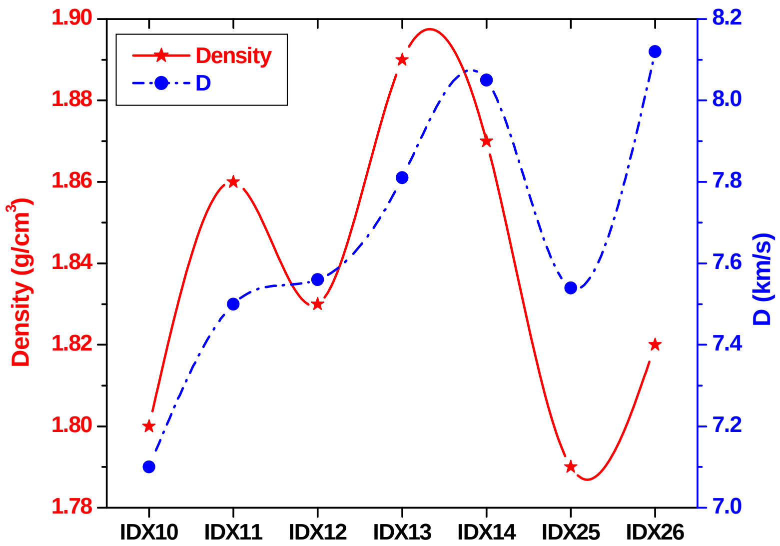

(a)

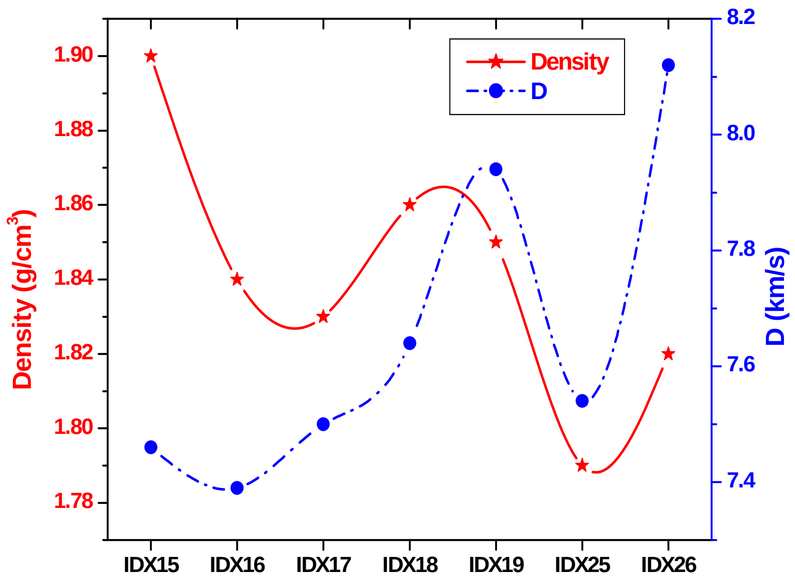

(b)

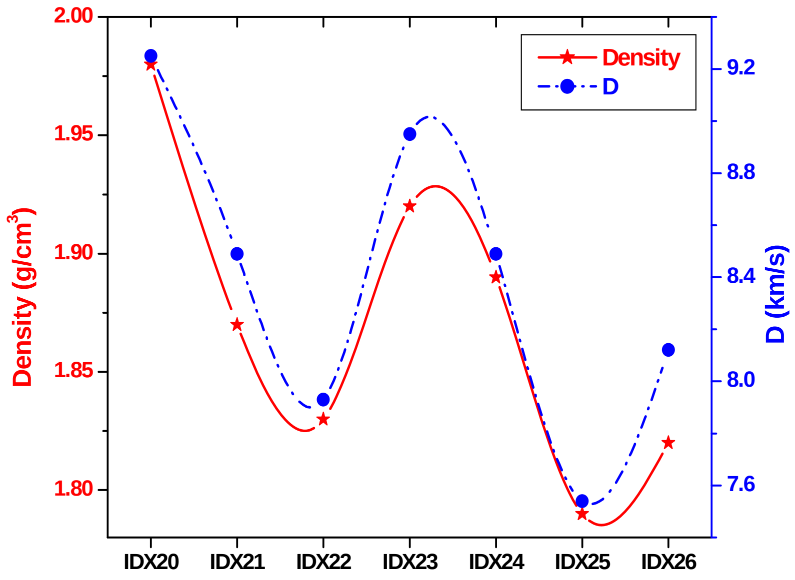

(c)

Fig. 4.7 Density and detonation velocity (D) profiles of (a) azide derivatives, (b) amino derivatives, and (c) nitro derivatives of heptazine.

4.1.5 Thermal stability

NICS is expressed by a combination of properties in cyclic delocalized systems and can be discussed in terms of energetic, structural and magnetic criteria. Negative values of NICS indicate the shielding presence of induced diatropic ring currents that are understood as aromaticity at specific points;[35] more negative the NICS, more aromatic the rings. Further, cyclic electron delocalization results in enhanced stability, bond length equalization, and special magnetic as well as chemical and physical properties.[36,37] NICS values of the individual rings of s-heptazine have been represented as NICS (1), NICS (2) and NICS (3) in Fig. 4.8. The predicted NICS values are listed in Table 4.10.

The NICS value for the parent s-heptazine ring is found to be 4.84 ppm, while for the designed molecules the values are calculated to be less than those of the parent molecule. This indicates that substitution brings stability in the compounds due to the electronic effects of substituents (azido, amino, nitro, nitroimidazole and nitrotriazole groups). The diatropic current of the ring increases due to substituted groups and the electrons are expected to be located mainly on the nitrogen atoms due to their high electronegativity compared to the carbon atom. Comparison of **H**, **IDX10**, **IDX15** and **IDX20** reveals that the profound electron donating effect of the amino group increases the ring current strongly, which leads to lower values of NICS. Further, the symmetric arrangement of the azido (**IDX10**), amino (**IDX15**) and nitro (**IDX20**) groups increases stability through delocalization of π-electrons, thus enhancing cyclic conjugation; accordingly, their order of stability is **IDX15**>**IDX10**>**IDX20**>**H**. Substitution of the nitro imidazole group on **IDX11**, **IDX16**, and **IDX21** shows an increase in NICS (2) at the corresponding ring of the heptazine, which may be due to its own contribution towards aromaticity; the same trend has been found in the case of triazole compounds. In tri-heterocycle-substituted molecules, **IDX25** shows better stabilization than **IDX26**, this can be attributed to the better contribution of the imidazole ring compared to triazole.

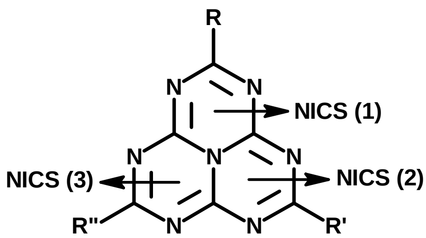

Fig. 4.8 NICS values calculated at the ring centers of heptazine derivatives.

Table 4.10: Calculated NICS and band gap of the heptazine derivatives.

Compd.	NICS(1) ppm	NICS(2) ppm	NICS(3) ppm	ΔE (hartree)
H	4.84	4.83	4.85	0.1434
IDX10	1.45	1.46	1.45	0.1504
IDX11	1.48	2.18	1.42	0.1462
IDX12	1.48	2.17	2.18	0.1410
IDX13	1.62	2.22	1.65	0.1480
IDX14	1.68	2.41	2.39	0.1468
IDX15	0.09	0.80	0.79	0.1824
IDX16	-0.02	0.17	-0.01	0.1605
IDX17	1.45	1.79	1.79	0.1499
IDX18	1.15	1. 48	1.20	0.1540
IDX19	1.61	1.97	1.97	0.1511
IDX20	2.75	2.72	2.73	0.1414
IDX21	-1.85	2.35	-1.74	0.1362
IDX22	1.44	2.57	2.57	0.1353
IDX23	2.07	3.41	2.18	0.1444
IDX24	1.59	2.96	2.96	0.1433
IDX25	2.23	2.34	2.23	0.1347
IDX26	2.49	2.69	2.58	0.1429

4.1.6 Sensitivity correlations

The band gap between the HOMO and LUMO has been suggested to be a measure of the sensitivity of the material.[38] In principle, the band gap (ΔE) between HOMO and LUMO is used as a criterion to predict the sensitivity of the material; smaller the ΔE, easier the electron transition and larger the sensitivity. The band gap of designed heptazine derivatives obtained using B3LYP/6-31G* method is compiled in Table 4.10. It is well known that the introduction of an amino group into polynitrobenzenes can increase stability under stimuli of impact and shock.[39,40] From the ΔE values of the heptazine derivatives, it can be seen that molecule **IDX15** possess a high band gap of 0.18 hartree, which indicates that **IDX15** will be relatively more insensitive than the designed molecules. Comparison of **IDX10**, **IDX15** and **IDX20** reveals that trinitro derivatives are more sensitive than azido and amino derivatives. Replacement of the amino group with other heterocycles increase the sensitivity as seen in **IDX16**, **IDX17**, **IDX18**, **IDX19**, **IDX25** and **IDX26**. A similar trend is observed in azido and nitro derivatives. Comparison of **IDX25** and **IDX26** indicates that nitro triazole has better insensitivity characteristics than nitro imidazole. Nitro derivatives of heptazine possess better energetic performance characteristics than others. However, NICS analysis and insensitivity correlations revealed that amino derivatives are better candidates considering insensitivity and stability.

4.1.7 Conclusions

Molecular structures with diverse energetic substituents at varying positions in the basic heptazine ring have been designed for HEM applications. DFT methods were used to predict gas phase heats of formation using an isodesmic approach, while crystal density was determined by packing calculations. Among the designed molecules, nitro derivatives of heptazine exhibited the best performance characteristics, while amino derivatives are better in terms of insensitivity and stability. Although the designed molecules are not superior to reported HEMs, these molecules may find potential applications in gas generators and smoke-free pyrotechnic fuels as they are rich in nitrogen content. In addition, the study finds its usefulness in realizing structure-property correlations.

4.2 Tetrazine Derivatives

s-Tetrazine chemistry has been known for more than one century[41,42] and their photo-physical, electrochemical, fluorescence spectroscopy, coordination, and explosive properties have been briefly recognized.[43-48] s-Tetrazine is an azo compound with an high nitrogen content (68.27%), making it of interest for the theoretical and synthesis of highly energetic materials. s-Tetrazines have demonstrated powerful synthetic utility through their ability to participate in inverse electron demand Diels-Alder reactions[49,50] providing access to a wide range of heterocycles based high energy materials. In contrast to traditional energetic materials, tetrazines are nitrogen-rich materials having large number of N-N and C-N bonds and therefore possess large positive enthalpy of formation (487.2 kJ/mol).[51] In the present study, different five member heterocycles such as imidazole, pyrazole, 1,2,4-triazole, 1,2,3-triazole, and tetrazole have been substituted on the s-tetrazine at C3 and C6 position to study the characteristic changes in the ΔH^0_f. Different substituents such as $-NO_2$, $-NH_2$ and $-N_3$ have attached to the azoles to understand the role of substituents and nitrogen-rich molecular skeleton. The designed s-tetrazine derivatives have been shown in Fig. 4.9.

Results and discussion

The present study investigates the important energetic properties including ΔH^0_f, densities, detonation performance, stability and sensitivity by employing density functional theory methods. A systematic structure-property relationship has been established by varying different substituents on the tetrazine backbone.

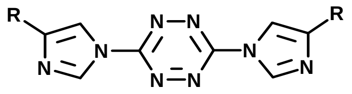

TI1 R=NO_2
TI2 R=NH_2
TI3 R=N_3

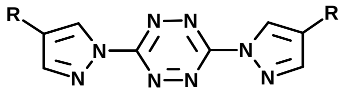

TP1 R=NO_2
TP2 R=NH_2
TP3 R=N_3

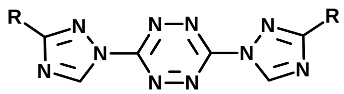

TT1 R=NO_2
TT2 R=NH_2
TT3 R=N_3

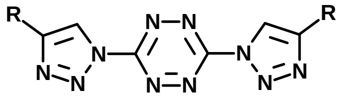

TS1 R=NO_2
TS2 R=NH_2
TS3 R=N_3

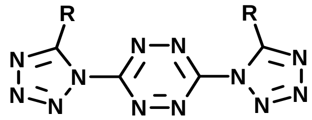

TR1 R=NO_2
TR2 R=NH_2
TR3 R=N_3

Fig. 4.9 Molecular framework of the s-tetrazine derivatives.

4.2.1 Molecular geometries

All designed compounds contain tetrazine as nitrogen-rich backbone to which substituted azole attached at C3 and C6 position. The three different explosophores (NO_2, NH_2, and N_3) substituted on the azole rings at C4 position and linked to the tetrazine via C-N bond. The explosophores are far apart from each other; hence reduce the chances for the steric hindrance and repulsion between them. All the explosophores positioned in the plane of azole rings and hence shows resonance in the molecular skeleton due to their electron donating/withdrawing effect. The distance between the explosophores is found above 10 Å. The selected structural parameters of the designed molecules are listed in Table 4.11 to 4.15. The bond lengths of C-NO_2 bond found to be higher than other C-NH_2 and C-N_3 bonds in the molecular structure. In the imidazole, pyrazole and triazole derivatives, azole rings are in the plane of tetrazine shows torsional angle 178 to 180^o. In case of tetrazole derivatives (**TR1**, **TR2** and **TR3**), torsional angle deviates from 126 to 178^o. The deviation is may be due to the steric hindrance and repulsion between explosophores on the molecular skeleton. The replacement of nitro and azido explosophore with amino strengthens the C-N bond between the tetrazine and azole, due to its electron donating effect. The replacement of imidazole (**TI1-TI3**) with pyrazole (**TP1-TP3**) reduces the N-N and C-N bond lengths of tetrazine, while increases the C-N bond length (C6-N7 & C3-N12) between azole rings and tetrazine. Similarly, the replacement of 1,2,4-triazole (**TT1-TT3**) with 1,2,3-triazole (**TS1-TS3**) is not showing great effect on N-N and C-N bond lengths of ring but increase the C-N distances between the tetrazine and triazole. The lengths of trigger C-NO_2 linkages differ from isomer to isomer with the azole rings.

Table 4.11: The selected structural parameters of the imidazole derivatives (TI1, TI2 and TI3).

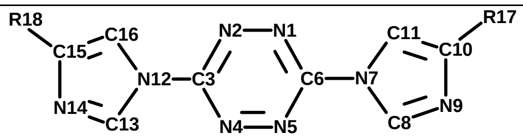

	Parameter	TI1	TI2	TI3
Bond length (Å)	N1-N2,N4-N5	1.3142	1.3196	1.3174
	C3-N2,C3-N4,N1-C6,C6-N5	1.3415	1.3423	1.3416
	C3-N12,C6-N7	1.3931	1.3831	1.3872
	N7-C8,N12-C13	1.3972	1.3823	1.3864
	C8-N9,C13-N14	1.3019	1.3056	1.3047
	N9-C10,N14-C15	1.3712	1.3884	1.3850
	C10-C11,C15-C16	1.3669	1.3726	1.3694
	C11-N7,C16-N12	1.3851	1.4027	1.3959
	C10-N16,C15-N18	1.4487	1.3874	1.3958
T.A. (°)	N2-C3-N12-C13,N1-C6-N7-C8	180.0	180.0	180.0
	N16-C10-N9-C8,N18-C15-N14-C13	180.0	177.0	180.0

TI1: R17, R18=NO_2; TI2: R17, R18=NH_2; TI3: R17, R18=N_3, T.A. is torsional angle.

Table 4.12: The selected structural parameters of the pyrazole derivatives (TP1, TP2 and TP3).

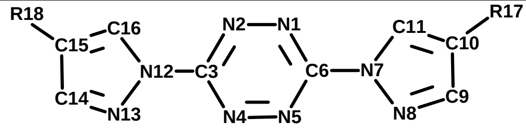

	Parameter	TP1	TP2	TP3
Bond length (Å)	N1-N2,N4-N5	1.3129	1.3164	1.3152
	C3-N2,C3-N4,N1-C6,C6-N5	1.3403	1.3422	1.3407
	C3-N12,C6-N7	1.3994	1.3891	1.3928
	N7-C8,N12-C13	1.3599	1.3599	1.3648
	N8-C9,N13-C14	1.3211	1.3211	1.3187
	C9-C10,C14-C15	1.4207	1.4304	1.4259
	C10-C11,C15-C16	1.3757	1.3757	1.3751
	C11-N7,C16-N12	1.3857	1.3857	1.3785
	C10-N17,C15-N18	1.4356	1.3967	1.4026
T.A. (°)	N2-C3-N12-N13,N1-C6-N7-N8	180.0	180.0	180.0
	N17-C10-C9-N8,N18-C15-C14-N13	180.0	176.5	180.0

TP1: R17, R18=NO_2; TP2: R17, R18=NH_2; TP3: R17, R18=N_3, T.A. is torsional angle.

Table 4.13: The selected structural parameters of the 1,2,4-triazole derivatives (TT1, TT2 and TT3).

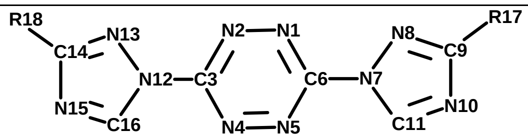

	Parameter	**TT1**	**TT2**	**TT3**
Bond length (Å)	N1-N2,N4-N5	1.3152	1.3173	1.3165
	C3-N2,C3-N4,N1-C6,C6-N5	1.3405	1.3431	1.3419
	C3-N12,C6-N7	1.4015	1.3889	1.3931
	N7-N8,N12-N13	1.3588	1.3794	1.3708
	N8-C9,N13-C14	1.3150	1.3239	1.3237
	C9-N10,C14-N15	1.3604	1.3823	1.3727
	N10-C11,N15-C16	1.3089	1.3081	1.3078
	C11-N7,C16-N12	1.3784	1.3699	1.3734
	C9-N17,C14-N18	1.4674	1.3700	1.3900
T.A. (°)	N2-C3-N12-C16,N1-C6-N7-C11	180.0	180.0	180.0
	N17-C9-N10-C11,N8,N18-C14-N15-C16	180.0	177.3	180.0

TT1: R17, R18=NO_2; TT2: R17, R18=NH_2; TT3: R17, R18=N_3, T.A. is torsional angle.

Table 4.14: The selected structural parameters of the 1,2,3-triazole derivatives (TS1, TS2 and TS3).

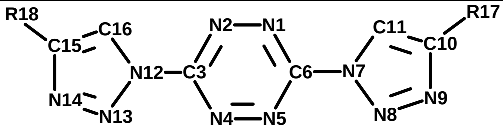

	Parameter	TS1	TS2	TS3
Bond length (Å)	N1-N2,N4-N5	1.3155	1.3187	1.3180
	C3-N2,C3-N4,N1-C6,C6-N5	1.3379	1.3392	1.3382
	C3-N12,C6-N7	1.4030	1.3933	1.3972
	N7-N8,N12-N13	1.3898	1.3662	1.3727
	N8-N9,N13-N14	1.2852	1.2933	1.2909
	N9-C10,N14-C15	1.3640	1.3786	1.3759
	C10-C11,C15-C16	1.3691	1.3742	1.3721
	C11-N7,C16-N12	1.3613	1.3787	1.3719
	C10-N17,C15-N18	1.4471	1.3839	1.3915
T.A. (°)	N2-C3-N12-N13,N1-C6-N7-N8	180.0	180.0	180.0
	N17-C10-N9-N8,N18-C15-N14-N13	180.0	177.0	180.0

TS1: R17, R18=NO_2; TS2: R17, R18=NH_2; TS3: R17, R18=N_3, T.A. is torsional angle.

Table 4.15: The selected structural parameters of the tetrazole derivatives (TR1, TR2 and TR3).

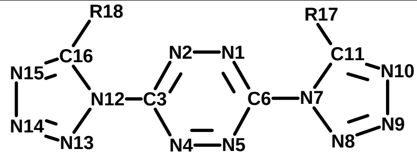

	Parameter	TR1	TR2	TR3
Bond length (Å)	N1-N2,N4-N5	1.3128	1.3219	1.3179
	C3-N2,C3-N4,N1-C6,C6-N5	1.3358	1.3397	1.3374
	C3-N12,C6-N7	1.4127	1.3861	1.4004
	N7-N8,N12-N13	1.3661	1.4044	1.3852
	N8-N9,N13-N14	1.2884	1.2727	1.2787
	N9-N10,N14-N15	1.3628	1.3656	1.3653
	N10-C11,N15-C16	1.3041	1.3208	1.3163
	C11-N7,C16-N12	1.3578	1.3774	1.3665
	C11-N17,C16-N18	1.4589	1.3508	1.4004
T.A. (°)	N2-C3-N12-N13,N1-C6-N7-N8	126.4	172.4	149.5
	N17-C11-N10-N9,N18-C16-N15-N14	175.0	177.8	178.2

TR1: R17, R18=NO_2; TR2: R17, R18=NH_2; TR3: R17, R18=N_3, T.A. is torsional angle.

4.2.2 Gas phase heat of formation

The zero point energies and thermal correction for tetrazine derivatives have been calculated at the B3LYP/6-31G* level. $\Delta H^0{}_f$ of tetrazine derivatives have been predicted using B3LYP method in combination with the 6-31G* basis set through appropriate design of isodesmic reactions. The calculated and experimental gas phase $\Delta H^0{}_f$ of the reference compounds are listed in Table 4.7. $\Delta H^0{}_f$ of the designed compounds predicted from isodesmic reactions have been summarized in Table 4.16. Fig. 4.10 shows the isodesmic reactions used for the calculation of $\Delta H^0{}_f$ of tetrazine derivatives. All the designed compounds show the high positive $\Delta H^0{}_f$ and it may be attributed to the large number of energetic N-N and C-N bonds of the molecular framework.

Table 4.16: Calculated explosive properties for s-tetrazine derivatives.

Compd.	E_0 (au)	N. C. (%)	O. B. (%)	ΔH^0_f (kJ/mol)	Q (cal/g)	D (km/s)	P (GPa)
TI1	-1155.17659	46.1	-73.7	797.98	1181.38	7.25	22.18
TI2	-856.87968	57.4	-131.2	791.64	775.44	6.46	17.45
TI3	-1073.37277	66.2	-97.3	1346.81	1087.48	6.42	16.13
TP1	-1155.13330	46.1	-73.7	926.27	1282.24	7.70	25.98
TP2	-856.83659	57.4	-131.2	915.77	897.03	6.81	19.70
TP3	-1073.31971	66.2	-97.3	1501.41	1212.32	6.77	18.44
TT1	-1187.23721	54.9	-47.1	1052.39	1269.84	7.78	25.36
TT2	-888.97283	68.3	-97.5	916.34	890.29	6.79	18.91
TT3	-1105.45059	75.2	-69.8	1511.46	1212.24	6.99	19.72
TS1	-1187.19095	54.9	-47.1	1149.29	1345.52	8.22	29.38
TS2	-888.90155	68.3	-97.5	1124.43	1092.46	7.14	20.94
TS3	-1105.39065	75.2	-69.8	1689.79	1355.27	7.16	20.59
TR1	-1219.23120	63.6	-20.8	1613.26	1594.96	9.09	36.01
TR2	-920.99718	79.0	-64.5	1442.51	1390.19	8.19	28.72
TR3	-1137.45878	84.0	-42.7	2080.07	1657.16	7.84	25.13

Among the designed compounds the azido derivatives such as **TI3**, **TP3**, **TT3**, **TS3**, and **TR3** show very high positive ΔH^0_f (>1300 kJ/mol). Azido group is more energetic than the nitro and amino substituents and significantly enhances ΔH^0_f of the designed compounds.[51] The contribution of substituents in the total ΔH^0_f can be given as N_3>NO_2>NH_2. Among the different azoles, the energy contribution from tetrazole is very high (326 kJ/mol) and hence **TR1**, **TR2**, and **TR3** shows higher ΔH^0_f as compared to other derivatives. ΔH^0_f of the pyrazole is higher than the imidazole, hence **TP1**, **TP2** and **TP3** shows higher ΔH^0_f than **TI1**, **TI2**, and **TI3**, respectively. Similarly, energy contribution of the 1,2,3-triazole is higher than the 1,2,4-triazole and hence, **TT1**, **TT2** and **TT3** shows lower ΔH^0_f than **TS1**, **TS2** and **TS3**, respectively. The introduction of different azole rings on tetrazine improves the nitrogen content and ΔH^0_f. Fig. 4.11 compares the heat of formation of tetrazine derivatives. Substitution of azido group increases the nitrogen content and these compounds possess high ΔH^0_f. Though amino compounds have higher nitrogen content than nitro compounds but the nitro compounds increases the energy and improves the oxygen balance of the compound and hence, nitro derivatives show higher ΔH^0_f.

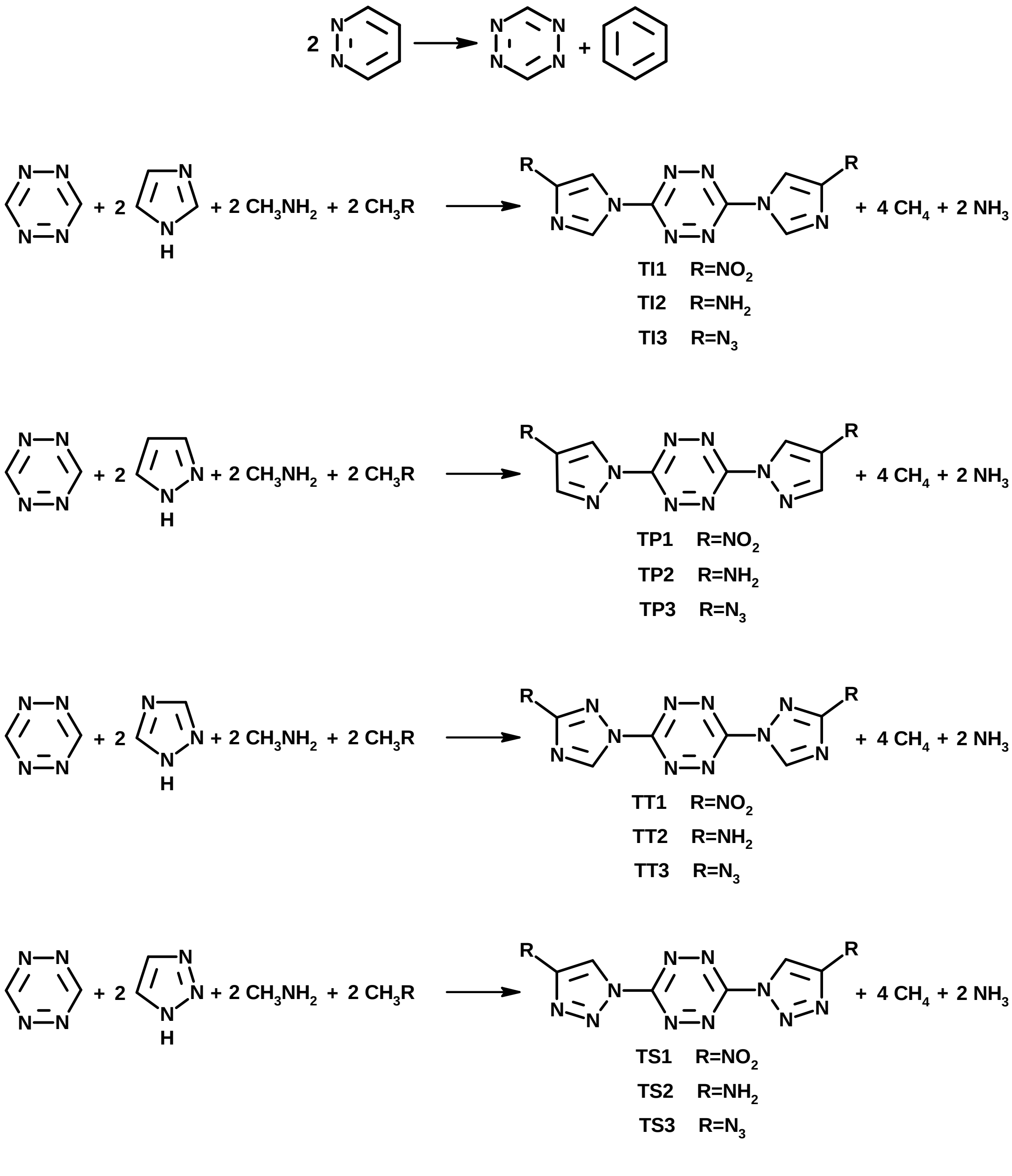

Fig. 4.10 Isodesmic reaction schemes for the tetrazine derivatives.

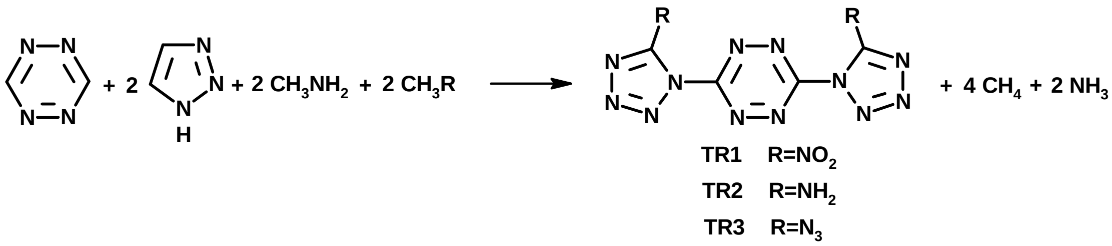

Fig. 4.10 (Contd.)

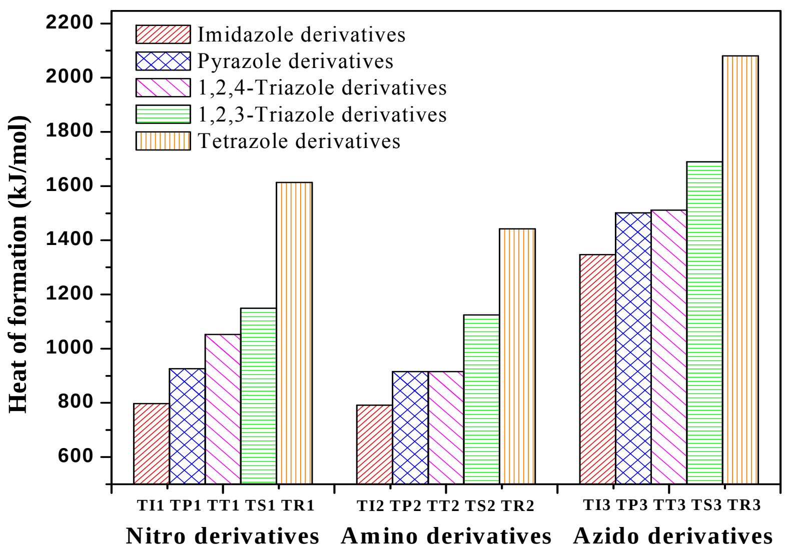

Fig. 4.11 Heat of formation (kJ/mol) profile of the tetrazine derivatives.

4.2.3 Density

Crystal packing calculations have been used for the prediction of densities of the designed compounds. The calculated densities and lattice parameters are listed in Table 4.17. The results reveal that substitution of nitro group play important role in increasing the density as compared to other substituents like amino and azido. However, the role of the amino group cannot be clearly defined since the packing pattern is highly dependent on the electronic structure of the molecule. The pyrazole derivatives (**TP1**, **TP2** & **TP3**) show slightly higher densities as compared to imidazole derivatives (**TI1**, **TI2** & **TI3**). The tetrazole compounds viz., **TR1**, **TR2**, and **TR3** are denser in the designed tetrazine derivatives and their densities are 1.75, 1.70, and 1.58 g/cm^3, respectively. The nitro derivative of 1,2,3-triazole (**TS1**) shows higher density than corresponding 1,2,4-triazole derivative (**TT1**). Comparison of **TT2** and **TS2** shows that there is no significant change in density by changing the molecular skeleton. A similar phenomenon is observed in case of **TT3** and **TS3**. The representative crystal structures of the tetrazine derivatives are shown in Fig. 4.12.

Table 4.17: Calculated crystal densities and lattice parameters of the s-tetrazine derivatives.

Compd.	Density (g/cm^3)	Space group	Lattice parameters					
			Length (Å)			Angle (°)		
			a	b	c	α	β	γ
TI1	1.66	*P2$_1$/c*	18.5	12.8	13.6	90.0	157.2	90.0
TI2	1.64	*C2/c*	19.4	9.7	18.5	90.0	145.1	90.0
TI3	1.48	*P1*	11.9	10.1	8.6	101.1	124.0	112.7
TP1	1.74	*P2$_1$/c*	10.8	4.7	22.9	90.0	101.3	90.0
TP2	1.68	*Cc*	17.1	10.1	8.7	90.0	138.5	90.0
TP3	1.54	*P2$_1$/c*	22.2	10.6	11.9	90.0	152.6	90.0
TT1	1.64	*PNA2$_1$*	17.9	12.2	5.7	90.0	90.0	90.0
TT2	1.59	*P2$_1$/c*	7.9	19.8	7.5	90.0	118.9	90.0
TT3	1.55	*P2$_1$*	16.6	10.2	3.7	90.0	81.1	90.0
TS1	1.74	*P2$_1$/c*	15.6	17.0	17.6	90.0	165.5	90.0
TS2	1.59	*P1*	7.3	15.7	5.2	82.5	99.7	118.0
TS3	1.54	*P2$_1$/c*	8.5	18.6	9.3	90.0	118.3	90.0
TR1	1.75	*P2$_1$*	8.4	12.5	7.3	90.0	130.3	90.0
TR2	1.70	*C2/c*	27.4	4.0	21.8	90.0	124.6	90.0
TR3	1.58	*P2$_1$/c*	33.9	13.3	30.7	90.0	174.6	90.0

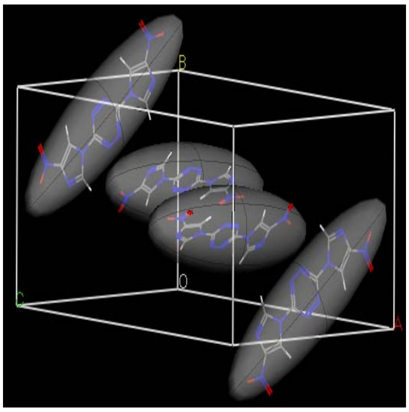

TI1

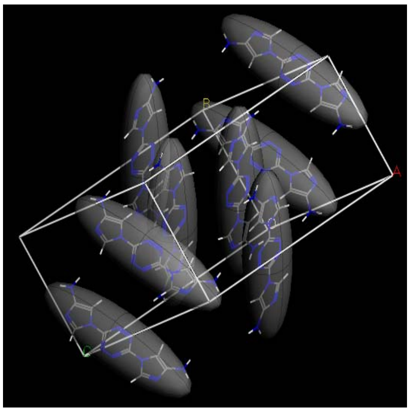

TI2

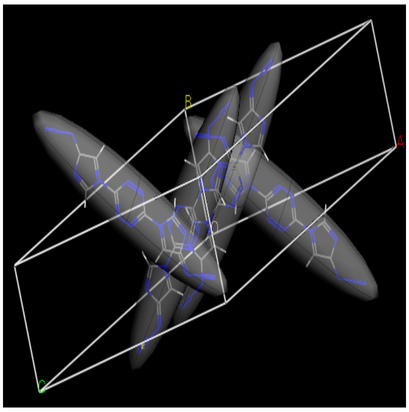

TI3

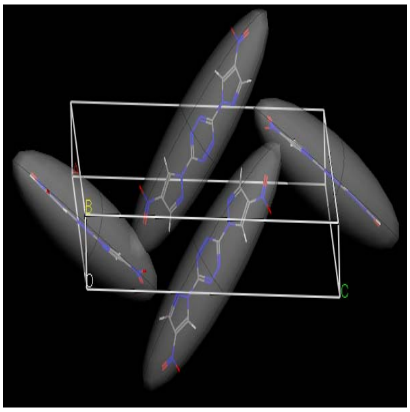

TP1

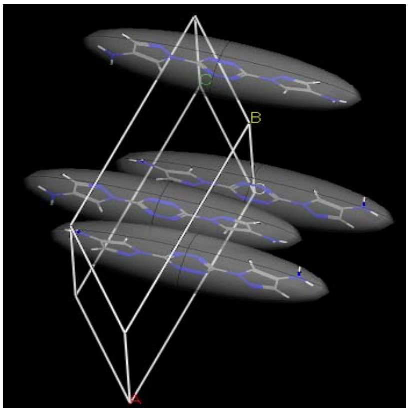

TP2

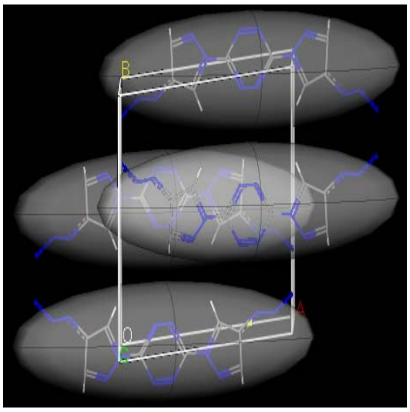

TP3

Fig. 4.12 Crystal structures of the tetrazine derivatives.

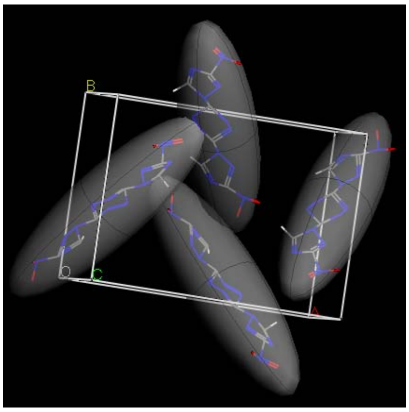

TT1

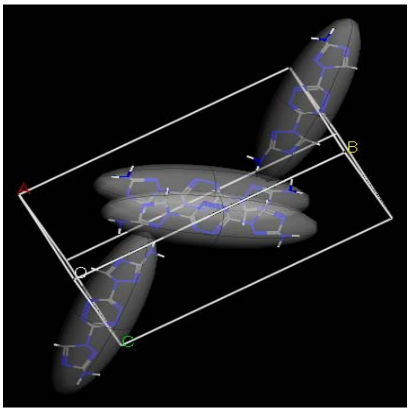

TT2

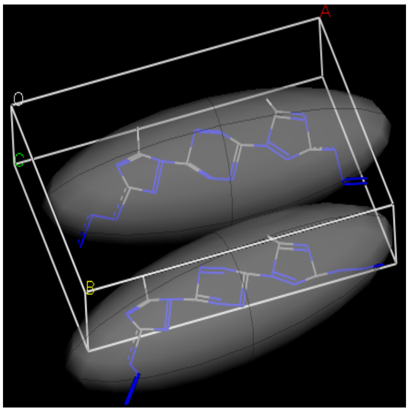

TT3

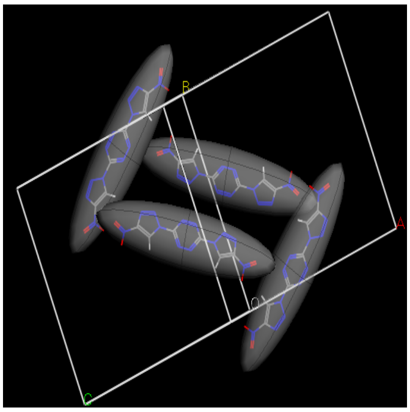

TS1

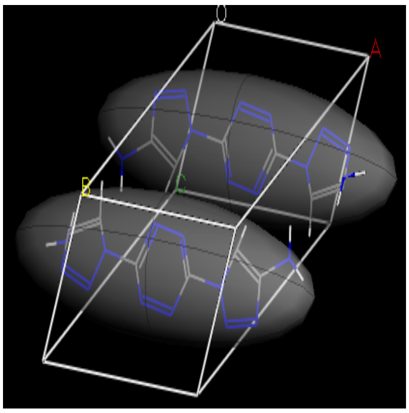

TS2

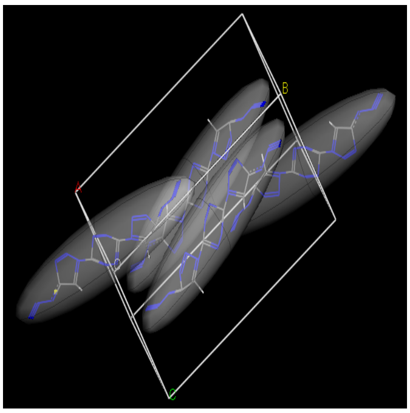

TS3

Fig. 4.12 (Contd.)

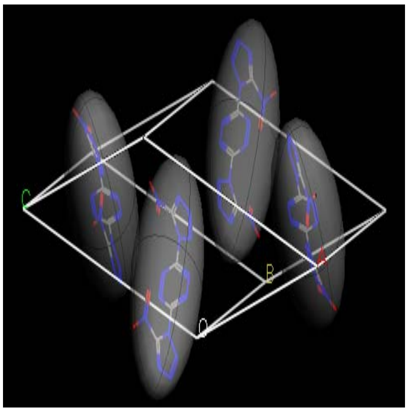

TR1

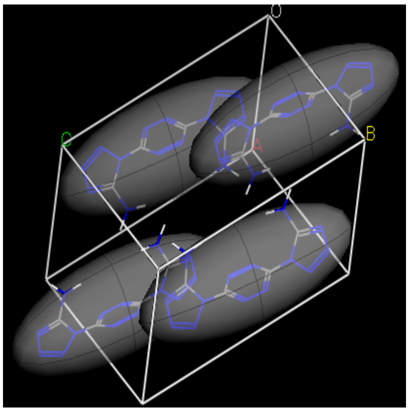

TR2

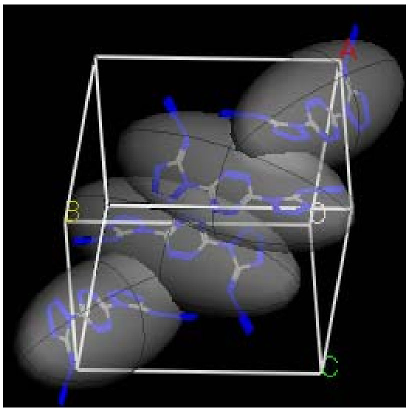

TR3

Fig. 4.12 (Contd.)

4.2.4 Detonation characteristics

Computed values of velocity of detonation (*D*) and detonation pressure (*P*) are summarized in Table 4.16. The results reveal that though azido derivatives have high ΔH^0_f but due to the low densities overall performance is less. The detonation performance is more dependent on density rather than ΔH^0_f. Fig. 4.13 compares the calculated detonation velocities of the tetrazine derivatives. The performance of nitro derivatives is better due to the higher densities and oxygen balance which increase the concentration of detonation products like CO, CO_2, and H_2O. The nitro derivatives (**TI1**, **TP1**, **TT1**, **TS1**, and **TR1**) show *D* about 7.5 to 9.09 km/s and *P* of 25.8 to 36 GPa. The tetrazole derivatives (**TR1**, **TR2** and **TR3**) show better performance in the series due to the better densities, oxygen balance and high nitrogen content. The ΔH^0_f

and densities of pyrazole derivatives is higher than that of imidazole derivatives, therefore **TP1**, **TP2**, and **TP3** shows better performance over corresponding **TI1**, **TI2**, and **TI3**, respectively. Similar phenomena observed in case of 1,2,3-triazole and 1,2,4-triazole derivatives.

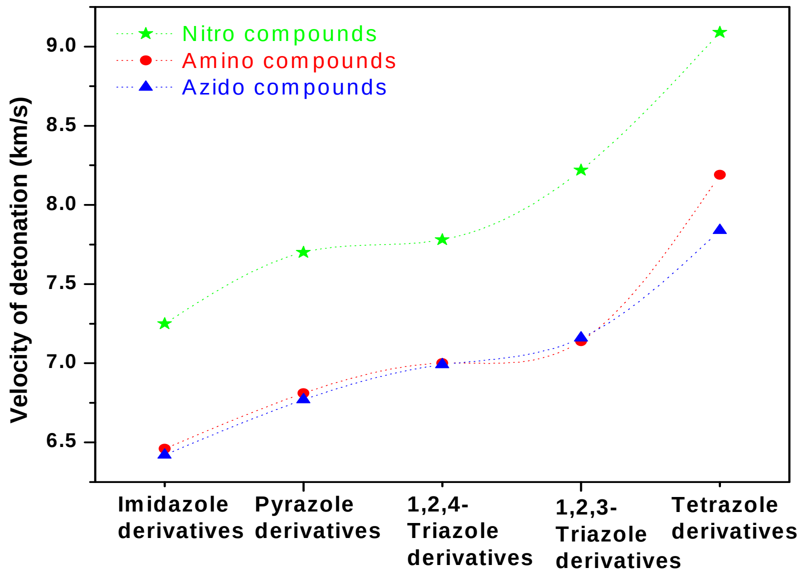

Fig. 4.13 The profile of velocity of detonation (km/s) of the tetrazine derivatives.

4.2.5 Thermal stability

Aromaticity is expressed by a combination of properties in cyclic delocalized systems.[52] The nucleus independent chemical shift (NICS) has been important criteria to predict the stability of compounds with respect to the aromaticity. Negative values of NICS indicate shielding presence of induced diatropic ring currents understood as aromaticity at ring centre.[53] NICS values of the individual of s-tetrazine rings have been represented as NICS (1) while, for the substituted rings (imidazole, pyrazole, triazoles, and tetrazole) have been represented as NICS (2) (Fig. 4.14). The NICS (1) and NICS (2) values are represented in the Table 4.18.

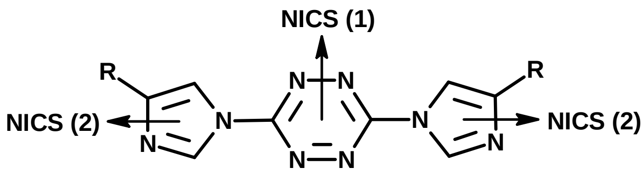

Fig. 4.14 NICS values calculated at the ring centers of tetrazine derivatives.

Table 4.18: Calculated NICS at 1Å above the ring centre and band gap of the s-tetrazine derivatives.

Compd.	NICS (1) (ppm)	NICS (2) (ppm)	ΔE (hartree)
TI1	-7.96	-8.37	0.0829
TI2	-6.25	-7.14	0.1257
TI3	-6.94	-7.63	0.0894
TP1	-8.27	-9.05	0.1037
TP2	-7.16	-8.55	0.1327
TP3	-7.52	-8.93	0.1116
TT1	-8.56	-9.71	0.1053
TT2	-7.39	-7.92	0.1337
TT3	-7.83	-8.66	0.1135
TS1	-8.48	-10.39	0.1009
TS2	-7.42	-9.59	0.1322
TS3	-8.46	-10.39	0.1071
TR1	-14.24	-11.41	0.1166
TR2	-8.53	-9.41	0.1382
TR3	-13.14	-10.23	0.1314

All designed compounds show higher negative values of NICS due to the aromaticity and better stability due to delocalization of π-electrons in the ring. Rings having -NO_2 groups increases the average NICS values. The presence of strongly electron withdrawing -NO_2 and -N_3 groups, which decrease the tendency of electrons to be localized, enhances the diatropic ring current, thus enhancing cyclic conjugation.

The order of increasing NICS for the tetrazine derivatives is given as, NO_2>N_3>NH_2. The tetrazole substituted tetrazines (**TR1**, **TR2**, and **TR3**) shows high negative values for the NICS may be due to the symmetry, nitrogen content of the rings and effect of tetrazole. Nitrogen is more electronegative than carbon and may be responsible for the higher electron density in the ring. All the compounds show NICS values in the range of -6.5 to -14 ppm. This NICS values show that all compounds are stable and possess high diatropic ring current. The stability is due to the linear, symmetric, conjugated, and heterocyclic skeleton of the s-tetrazine derivatives.

4.2.6 Sensitivity correlation

The band gap (ΔE) between the HOMO and LUMO has been correlated with the sensitivity of material.[54] The band gap of predicted tetrazine derivatives obtained using B3LYP/6-31G* method is listed in Table 4.18. In general, smaller is the ΔE, easier the electron transition and larger the sensitivity. Introduction of an amino group into aromatic skeleton is well known strategy to increase stability and insensitivity under stimuli of impact and shock due to its electron donating nature.[55,56] From the ΔE values of the tetrazine derivatives, it can be seen that amino derivatives (**TI2**, **TP2**, **TT2**, **TS2**, and **TR2**) are insensitive than nitro derivatives (**TI1**, **TP1**, **TT1**, **TS1**, and **TR1**) and azido (**TI3**, **TP3**, **TT3**, **TS3**, and **TR3**) derivatives. The order of sensitivity in the tetrazine derivatives can be given as NO_2>N_3>NH_2. Among the designed molecules, imidazole derivatives (**TI1**, **TI2** and **TI3**) reveal lower band gap and more sensitive. However, tetrazole derivatives (**TR1**, **TR2** and **TR3**) shows higher band gap in the series. The replacement of 1,2,4-triazole in **TT1**, **TT2** and **TT3** with 1,2,3-triazole in **TS1**, **TS2** and **TS3** slightly reduces the band gap. Overall insensitivity correlations revealed that amino derivatives are better candidates in terms of insensitivity.

4.2.7 Conclusions

In summary, by using first-principles calculations at the DFT level, the energetic properties of the s-tetrazine derivatives have been studied. Based on designed sets of isodesmic reactions, standard gas-phase heats of formation are predicted. The results reveals that the high-nitrogen compounds, with their high-energy content, are a very promising set of potential energetic materials. Among the designed compounds, azido derivatives show very high positive ΔH^0_f (>1300 kJ/mol). The introduction of nitro group increases the density (1.66 g/cm^3) and hence overall detonation performance of the molecule than the amino and azido derivatives. NICS study showed that diatropic currents exist in the heterocyclic rings. These values show that all the designed compounds have good thermal stabilities.

4.3 Triazine Derivatives

s-Triazine[57,58] is six-member heterocycle consisting of 52% nitrogen. s-Triazine is an intriguing heterocycle for energetic materials and exhibits a high degree of thermal stability.[59] Triazine rings have been studied for use in a number of applications such as herbicides, chemicals, synthesis, dyes and polymers.[60-63] Energetic materials based on triazine show the desirable properties of high nitrogen contents and astonishing kinetic and thermal stabilities due to aromaticity. The density functional theory is used to predict the geometries, heats of formation and other energetic properties. The designed triazine derivatives are shown in Fig. 4.15.

Results and discussion

The present study brings out the structure-property relationships of triazine derivatives by comparing their characteristics like gas phase ΔH^0_f, density (ρ_o), detonation performance (*D* and *P*), stability and the insensitivity. Different substituents such as -NO_2, -NH_2 and -N_3 have attached to the triazine ring via C-N linkage of azoles to understand the role of substituents and nitrogen-rich molecular skeleton. These substituents are the essential functional groups usually contained in propellants and explosives.

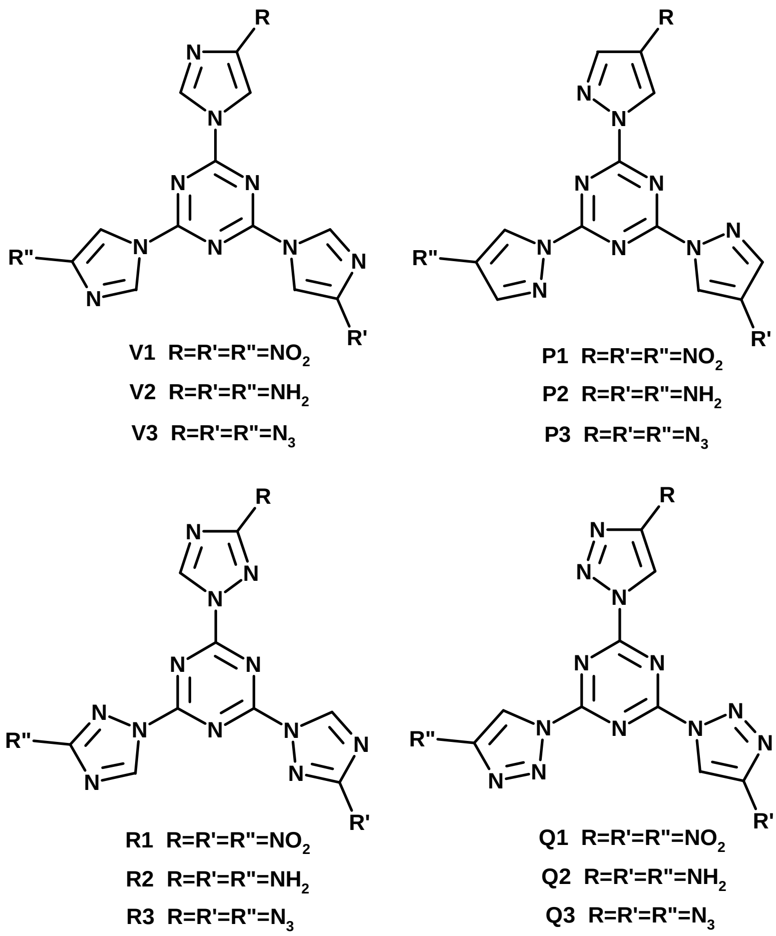

Fig. 4.15 Molecular structures of the designed s-triazine derivatives.

4.3.1 Molecular geometries

All designed compounds contain triazine as nitrogen-rich backbone to which three substituted azole attached at C2, C4 and C6 position. The three different explosophores (NO_2, NH_2, and N_3) substituted on the azole rings at C4 position and linked to the tetrazine via C-N bond. The explosophores are far apart from each other; hence reduce the chances for the steric hindrance and repulsion between them. All the explosophores positioned in the plane of azole rings and hence shows extended resonance in the molecular skeleton due to their electron withdrawing/donating effect. The distance between the explosophores found above 7 Å. The selected structural parameters of the designed molecules are listed in Table 4.19 to 4.22.

The bond lengths of C-NO_2 (> 1.46 Å) bond found to be higher than other C-NH_2 (> 1.39 Å) and C-N_3 (> 1.40 Å) bonds in the molecular structure. In the imidazole, pyrazole and triazole derivatives, azole rings are in the plane of triazine shows torsional angle 178 to 180^o. The replacement of nitro and azido explosophore with amino strengthens the C-N bond between the triazine and azole, due to its electron donating effect. The lengths of C-NO_2 linkages differ from isomer to isomer with the azole rings. The replacement of imidazole (**V1**-**V3**) with pyrazole (**P1**-**P3**) reduces the C-N bond lengths of triazine backbone in the pyrazole derivatives, while increases the C-N bond lengths between triazine and azoles. Similarly, replacement of 1,2,4-triazole (**R1**-**R3**) with 1,2,3-triazole (**Q1**-**Q3**) slightly reduces the C-N bond lengths in 1,2,3-triazole derivatives. However, C-N bond lengths between triazoles and triazine are found to be higher in 1,2,3-triazole derivatives than 1,2,4-triazole derivatives. The electron donating effect of amino group strengthens the C-N and N-N bonds of azoles and the C-N distance between triazine and azoles.

Table 4.19: The selected structural parameters of the imidazole derivatives (**V1**, **V2** and **V3**).

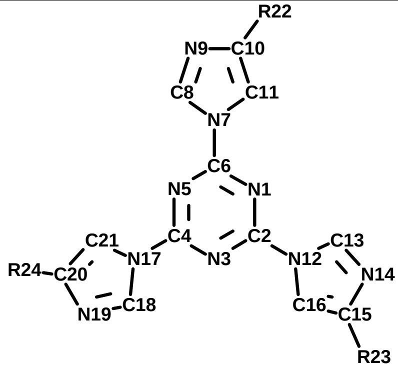

	Parameter	**V1**	**V2**	**V3**
Bond length (Å)	N1-C2,C2-N3,N3-C4,C4-N5,N5-C6,C6-N1	1.3345	1.3365	1.3355
	C2-N12,C4-N17,C6-N7	1.3932	1.3848	1.3883
	N7-C8,N12-C13,N17-C18	1.3982	1.3829	1.3967
	C8-N9,C13-N14,C18-N19	1.3002	1.3040	1.3029
	N9-C10,N14-C15,N19-C20	1.3735	1.3910	1.3877
	C10-C11,C15-C16,C20-C21	1.3648	1.3702	1.3675
	C11-N7,C16-N12,C21-N17	1.3868	1.4038	1.3874
	C10-N22,C15-N23,C20-N24	1.4493	1.3886	1.3957
T.A. (°)	C2-N1-C6-N7,C6-N1-C2-N12,C2-N3-C4-N17	180.0	180.0	180.0
	C18-N19-C20-N24,N22-C10-N9-C8, N23-C15-N14-C13	180.0	177.8	180.0

V1: R22, R23, R24=NO_2; V2: R22, R23, R24=NH_2; V3: R22, R23, R24=N_3, T.A. is torsional angle.

Table 4.20: The selected structural parameters of the pyrazole derivatives (**P1**, **P2** and **P3**).

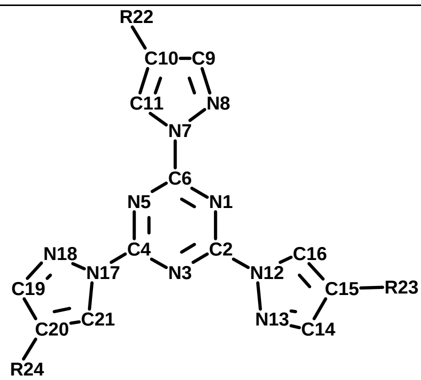

	Parameter	**P1**	**P2**	**P3**
Bond length (Å)	N1-C2,C2-N3,N3-C4,C4-N5,N5-C6,C6-N1	1.3265	1.3290	1.3280
	C2-N12,C4-N17,C6-N7	1.3992	1.3904	1.3934
	N7-N8,N12-N13,N17-N18	1.3751	1.3613	1.3659
	N8-C9,N13-C14,N18-C19	1.3154	1.3191	1.3167
	C9-C10,C14-C15,C19-C20	1.4235	1.4326	1.4285
	C10-C11,C15-C16,C20-C21	1.3709	1.3732	1.3749
	C11-N7,C16-N12,C21-N17	1.3691	1.3872	1.3804
	C10-N22,C15-N23,C20-N24	1.4361	1.3990	1.4033
T.A. (°)	C2-N1-C6-N7,C6-N1-C2-N12,C2-N3-C4-N17	180.0	180.0	180.0
	N22-C10-C11-N7,N23-C15-C14-N13, C24-C20-C19-N18	180.0	176.5	180.0

P1: R22, R23, R24=NO_2; P2: R22, R23, R24=NH_2; P3: R22, R23, R24=N_3, T.A. is torsional angle.

Table 4.21: The selected structural parameters of the 1,2,4-triazole derivatives (**R1**, **R2** and **R3**).

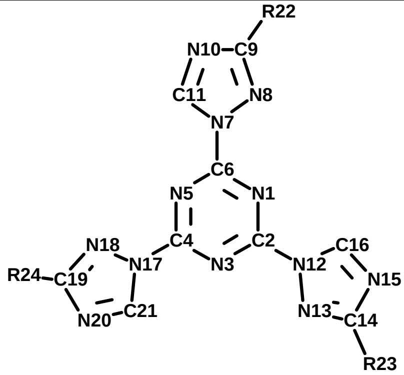

	Parameter	R1	R2	R3
Bond length (Å)	N1-C2,C2-N3,N3-C4,C4-N5,N5-C6,C6-N1	1.3277	1.3324	1.3301
	C2-N12,C4-N17,C6-N7	1.3989	1.3887	1.3918
	N7-N8,N12-N13,N17-N18	1.3604	1.3791	1.3712
	N8-C9,N13-C14,N18-C19	1.3126	1.3213	1.3214
	C9-N10,C14-N15,C19-N20	1.3638	1.3856	1.3761
	N10-C11,N15-C16,N20-C21	1.3067	1.3062	1.3056
	C11-N7,C16-N12,C21-N17	1.3822	1.3727	1.3768
	C9-N22,C14-N23,C19-N24	1.4684	1.3712	1.3900
T.A. (°)	C2-N1-C6-N7,C6-N1-C2-N12,C2-N3-C4-N17	180.0	180.0	180.0
	N7-N8-C9-N22,N12-N13-C14-N23, N17-N18-C19-N24	180.0	177.3	180.0

R1: R22, R23, R24=NO_2; R2: R22, R23, R24=NH_2; R3: R22, R23, R24=N_3, T.A. is torsional angle.

Table 4.22: The selected structural parameters of the 1,2,3-triazole derivatives (**Q1**, **Q2** and **Q3**).

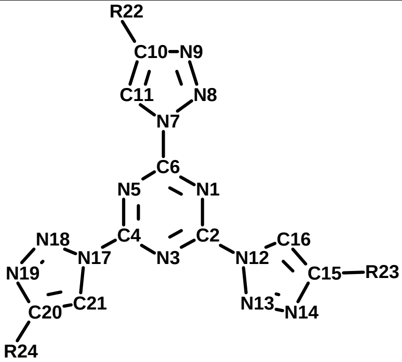

	Parameter	Q1	Q2	Q3
Bond length (Å)	N1-C2,C2-N3,N3-C4,C4-N5,N5-C6,C6-N1	1.3267	1.3285	1.3279
	C2-N12,C4-N17,C6-N7	1.4004	1.3935	1.3967
	N7-N8,N12-N13,N17-N18	1.3923	1.3679	1.3745
	N8-N9,N13-N14,N18-N19	1.2826	1.2909	1.2883
	N9-C10,N14-C15,N19-C20	1.3676	1.3819	1.3796
	C10-C11,C15-C16,C20-C21	1.3668	1.3716	1.3698
	C11-N7,C16-N12,C21-N17	1.3637	1.3804	1.3738
	C10-N22,C15-N23,C20-N24	1.4475	1.3848	1.3916
T.A. (°)	C2-N1-C6-N7,C6-N1-C2-N12,C2-N3-C4-N17	180.0	180.0	180.0
	N8-N9-C10-N22,N13-N14-C15-N23, N18-N19-C20-N24	180.0	177.9	180.0

Q1: R22, R23, R24=NO_2; Q2: R22, R23, R24=NH_2; Q3: R22, R23, R24=N_3, T.A. is torsional angle.

4.3.2 Gas phase heat of formation

In the present study, the $\Delta H^0{}_f$ have been calculated for triazine derivatives using DFT-B3LYP method with 6-31G* basis sets via designed isodesmic reactions (Fig. 4.16). The calculated and experimental gas phase $\Delta H^0{}_f$ of the reference compounds are listed in Table 4.7. Substituted groups that are attached to azole rings include $-NO_2$, $-NH_2$ and $-N_3$. The different five member heterocycles such as imidazole, pyrazole, 1,2,4-triazole and 1,2,3-triazole have been substituted on the s-triazine to study the changes in the $\Delta H^0{}_f$ systematically. Table 4.23 lists the calculated energetic properties of the triazine derivatives. Among the designed compounds, the azido derivatives (**V3**, **P3**, **R3** and **Q3**) exhibit very high positive ΔH^0_f. The contribution of substituents in the total ΔH^0_f can be given as N_3>NO_2>NH_2.

Table 4.23: Calculated energetic properties of the designed s-triazine derivatives.

Compd.	E_0 (au)	N. C. (%)	O. B. (%)	ΔH^0_f (kJ/mol)	Q (cal/g)	*D* (km/s)	*P* (GPa)
V1	-1568.68086	40.58	-81.16	640.92	980.22	6.60	17.82
V2	-1121.23483	51.85	-148.15	635.82	469.03	5.16	10.32
V3	-1445.97517	62.69	-107.46	1466.64	871.98	5.97	13.95
P1	-1568.61407	40.58	-81.16	840.50	1095.44	7.19	22.33
P2	-1121.18034	51.85	-148.15	802.29	591.83	5.47	11.59
P3	-1445.89641	62.69	-107.46	1696.35	1008.55	6.21	15.20
R1	-1616.77209	50.36	-51.80	956.82	1041.37	7.36	22.70
R2	-1169.37588	64.22	-110.09	819.30	598.83	5.91	13.99
R3	-1494.09293	72.59	-77.04	1710.94	1009.69	6.62	17.76
Q1	-1616.70175	50.36	-51.80	1173.23	1165.41	7.51	23.43
Q2	-1169.26753	64.22	-110.09	1135.23	829.75	6.22	15.00
Q3	-1494.00211	72.59	-77.04	1980.81	1168.95	6.65	17.43

The ΔH^0_f of the pyrazole (179.4 kJ/mol) is higher than the imidazole (129.5 kJ/mol), hence **P1**, **P2** and **P3** shows higher ΔH^0_f than **V1**, **V2**, and **V3**. Similarly, energy contribution of the 1,2,3-tetrazole (271.7 kJ/mol) is higher than the 1,2,4-triazole (192.7 kJ/mol) and hence **Q1**, **Q2** and **Q3** shows higher ΔH^0_f than **R1**, **R2** and **R3**. The introduction of different azoles on s-triazine improves the nitrogen content and ΔH^0_f. Increase in nitrogen content enhances the ΔH^0_f. Substitution of azido group increases the nitrogen content and these compounds possess very high ΔH^0_f. Though amino derivatives have higher nitrogen content but the nitro derivatives increases the energy and improves the oxygen balance of the compounds and hence, nitro derivatives possess higher ΔH^0_f than amino derivatives. Fig. 4.17 compares the heat of formation of triazine derivatives. s-Triazine compounds form a unique class of energetic materials whose energy is derived from their very high ΔH^0_f directly attributable to the large number of inherently energetic N-N and C-N bonds rather than from overall heats of combustion.

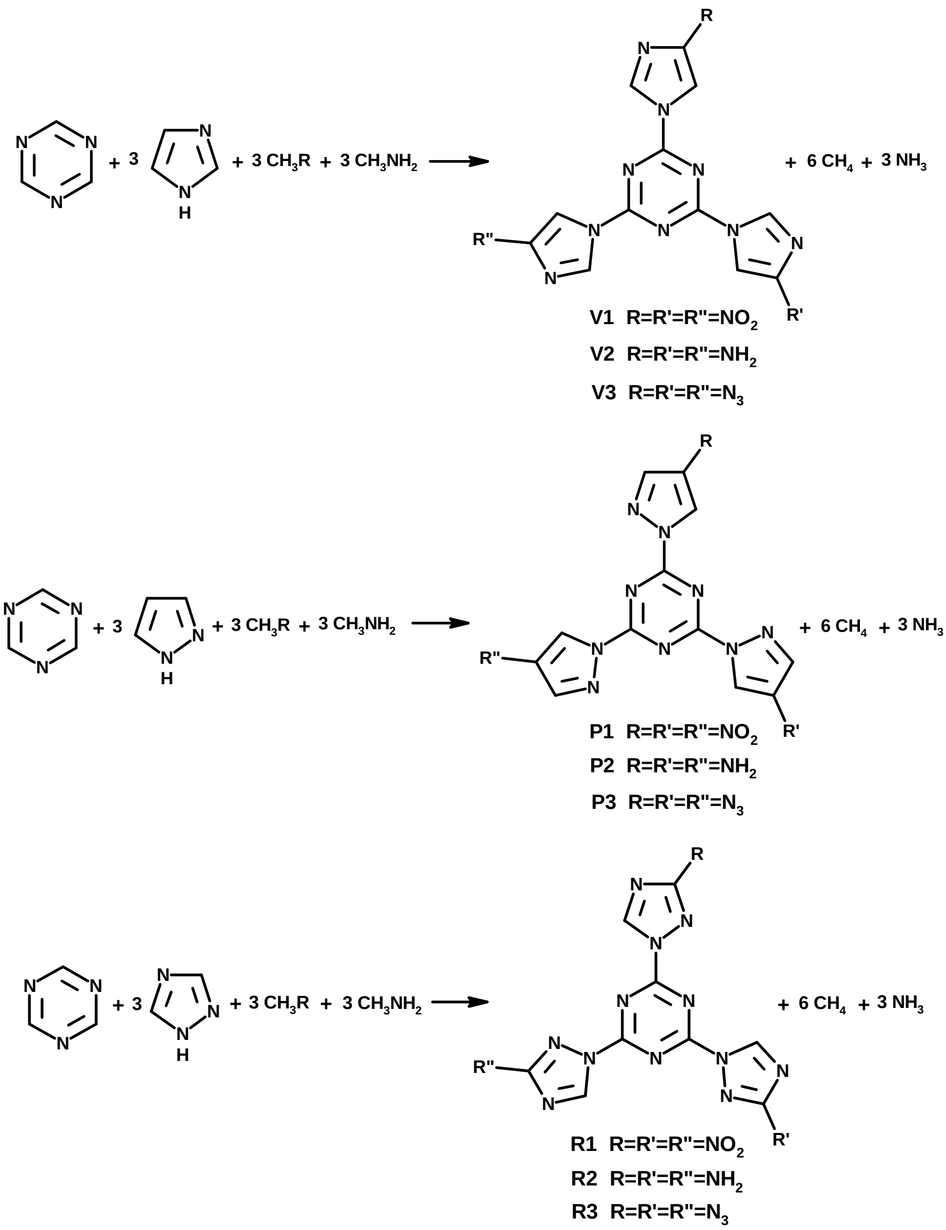

Fig. 4.16 Isodesmic reactions scheme for the triazine derivatives.

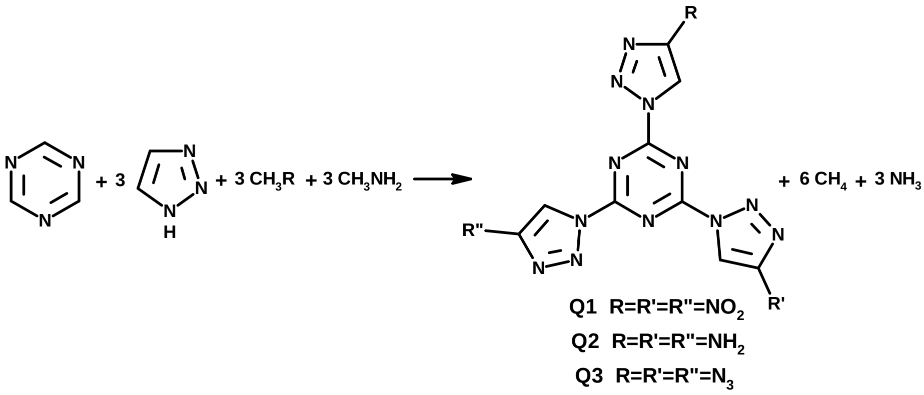

Fig. 4.16 (Contd.)

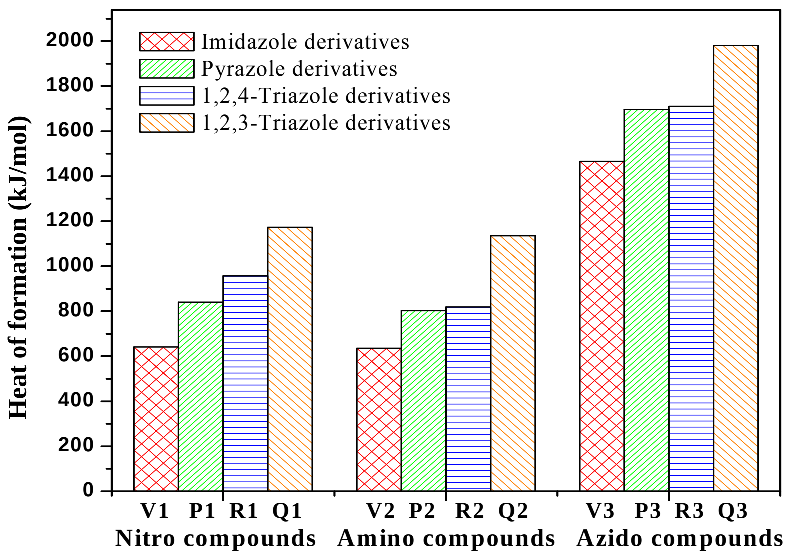

Fig. 4.17 Heat of formation (kJ/mol) profile of the triazine derivatives.

4.3.3 Density

Density is one of the most important factors that determine the performance of an explosive, since the detonation pressure (*P*) is dependent on the square of the density and the detonation velocity (*D*) is proportional to the density according to an empirical equation proposed by Kamlet and Jacobs.[64] The densities of the designed compounds have been predicted by using the crystal packing calculations in Material studio. The calculated densities and lattice parameters of the s-triazine derivatives are listed in Table 4.24. The substitution of -NO_2 group play important role in increasing the density as compared to other substituents like -NH_2 and -N_3. The increasing order of the density can be given as, NO_2>NH_2>N_3. All the triazine derivatives follow the same order. The nitro substituted derivatives like **V1**, **P1**, **R1** and **Q1** possess higher densities and their densities are 1.58, 1.72, 1.64 and 1.62 g/cm^3, respectively. The nitro derivative of pyrazole (**P1**) exhibit higher density than corresponding nitro imidazole derivative (**V1**), while amino and azido derivatives reveals comparable densities. The 1,2,4-triazole derivatives (**R1**, **R2** and **R3**) are found to be denser than corresponding 1,2,3-triazole derivatives (**Q1**, **Q2** and **Q3**). Crystal structures of the s-triazine derivatives are shown in Fig. 4.18.

Table 4.24: The calculated densities and lattice parameters of the triazine derivatives.

Compd.	Density (g/cm^3)	Space group	Lattice parameters					
			Length (Å)			Angle (°)		
			a	b	c	α	β	γ
V1	1.58	*P1*	11.5	8.5	13.4	89.8	128.6	113.9
V2	1.46	*C2*	34.2	4.3	18.2	90.0	145.1	90.0
V3	1.48	*P1*	13.3	1.5	19.5	77.7	69.3	66.4
P1	1.72	$P2_1/c$	4.4	34.3	11.8	90.0	116.2	90.0
P2	1.46	$P2_12_12_1$	17.3	22.1	3.9	90.0	90.0	90.0
P3	1.49	*P1*	25.7	3.9	21.9	66.9	145.4	130.8
R1	1.64	*Pbca*	17.2	18.4	10.8	90.0	90.0	90.0
R2	1.53	$P2_1/c$	19.1	19.7	20.3	90.0	169.0	90.0
R3	1.56	*P1*	12.7	8.1	11.4	74.2	57.2	61.9
Q1	1.62	*P1*	12.1	7.9	12.9	116.6	106.8	112.4
Q2	1.46	*P1*	15.8	5.7	9.5	99.9	100.4	111.5
Q3	1.49	*P1*	6.2	13.9	13.6	54.5	105.6	100.8

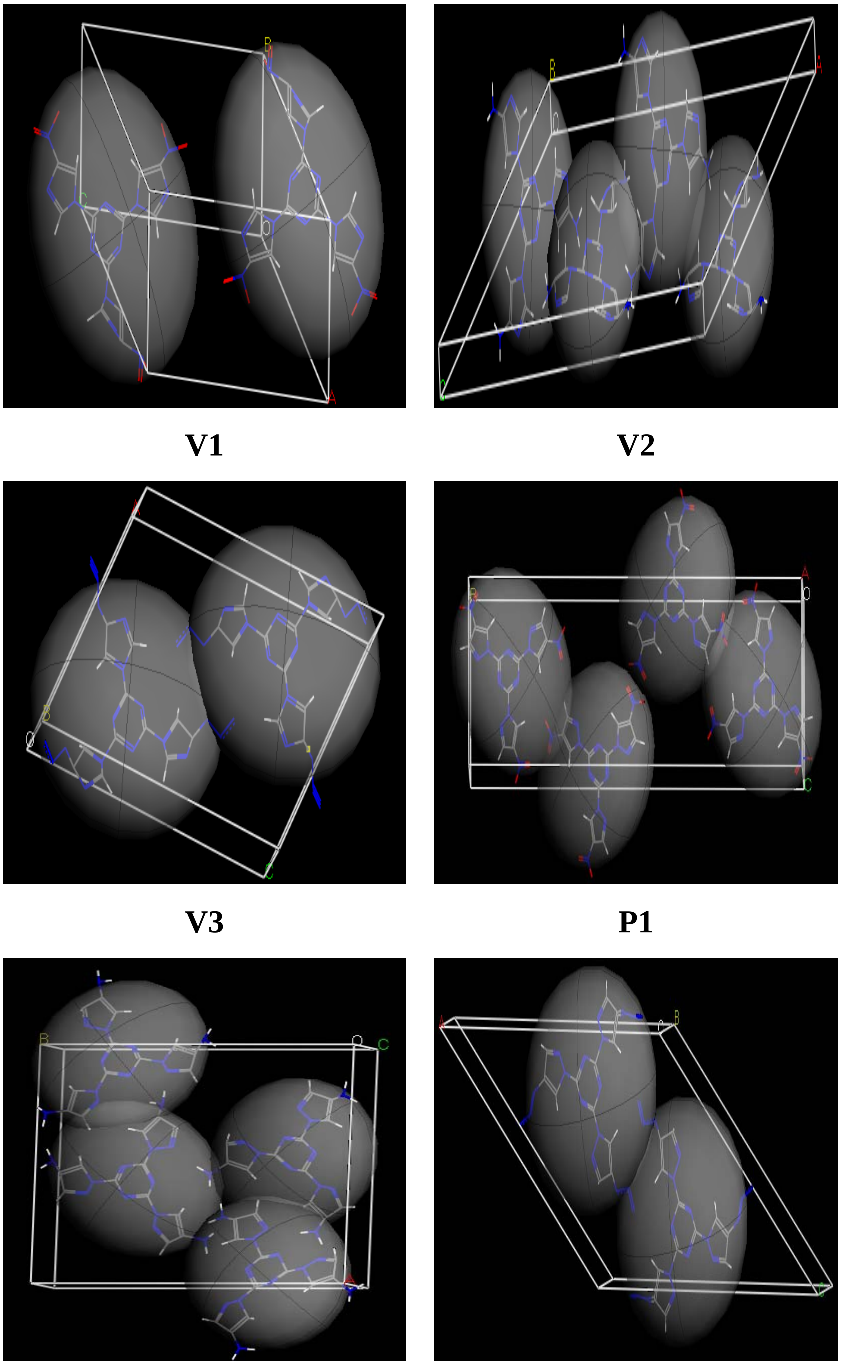

Fig. 4.18 Crystal structures of the triazine derivatives.

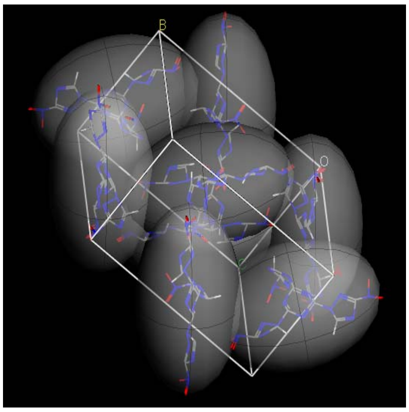

R1

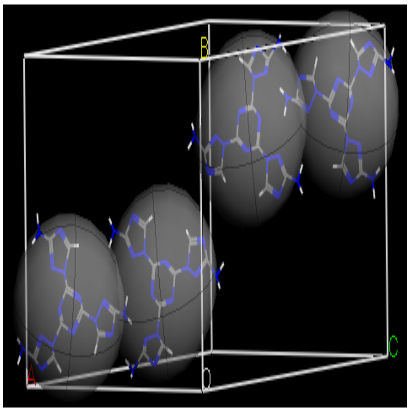

R2

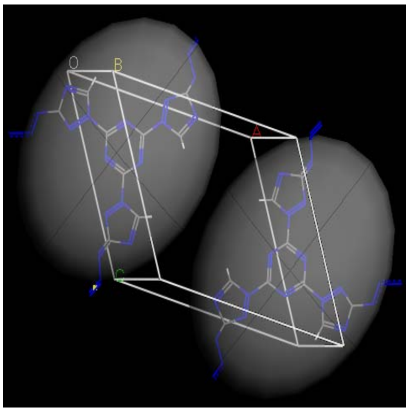

R3

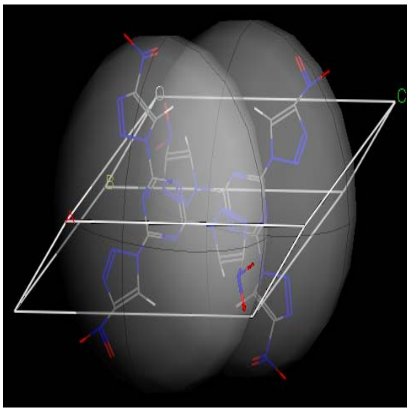

Q1

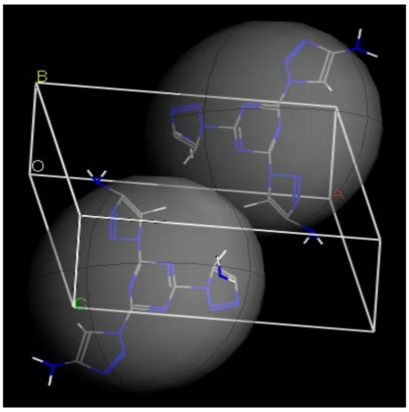

Q2

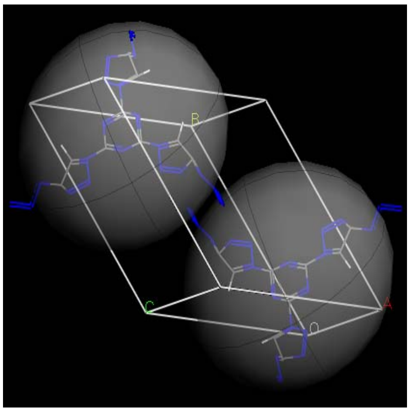

Q3

Fig. 4.18 (Contd.)

4.3.4 Detonation characteristics

Computed values of velocity of detonation (D) and detonation pressure (P) are summarized in Table 4.23. The results reveal that though azido derivatives have high ΔH^0_f but due to the low densities overall performance is less. The performance of nitro derivatives is better due to the high densities and oxygen balance which increase the concentration of detonation products like CO, CO_2, and H_2O. The nitro derivatives **V1**, **P1**, **R1** and **Q1** show *D* about 6.6 to 7.5 km/s and *P* of 17.8 to 23.4 GPa. The triazole derivatives show better performance in the series due to the higher ΔH^0_f and densities. The order of the performance can be given as, NO_2>N_3>NH_2. The poor performance of the amino compounds (**V2**, **P2**, **R2** and **Q2**) is attributed to lower densities and ΔH^0_f. Fig. 4.19 compares the detonation velocities of the triazine derivatives.

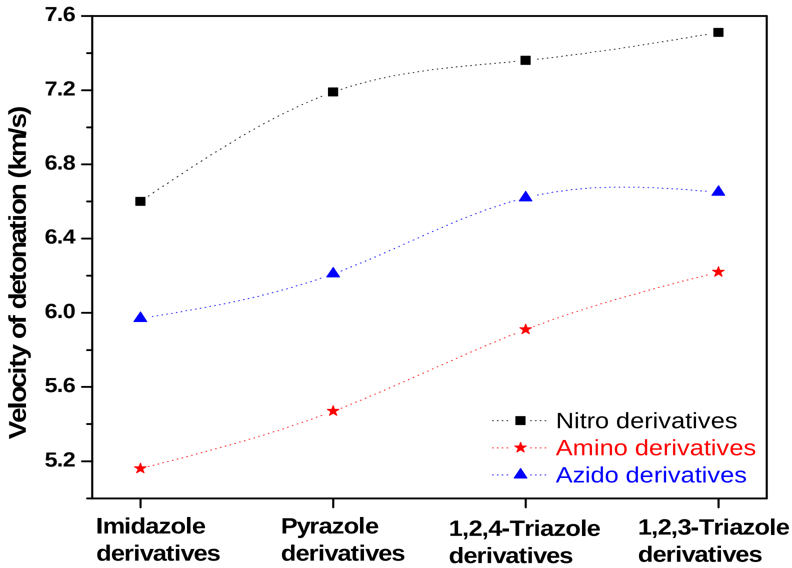

Fig. 4.19 The profile of velocity of detonation (km/s) of the triazine derivatives.

4.3.5 Thermal stability

Nucleus independent chemical shift (NICS) 1Å above the ring centre has been evaluated for the stability on the basis of aromaticity. The NICS has been important criteria to predict the stability of compounds with respect to the aromaticity. Negative values of NICS indicate shielding presence of induced diatropic ring currents understood as aromaticity at ring centre.[53] The NICS 1Å above the ring centre for the imidazole, pyrazole, 1,2,4-triazole, 1,2,3-triazole and s-triazine are -11.5, -12.4, -12.4, -13.6 and -10.2 ppm, respectively. NICS values for the individual rings of the triazine derivatives have been presented as NICS (A), NICS (B), NICS (C) and NICS (D) (Fig. 4.20). NICS (A) represent NICS for the s-triazine while NICS (B), NICS (C) and NICS (D) for the substituted azoles. The computed values are summarized in the Table 4.25. All designed compounds show higher negative values of NICS due to the aromaticity and better stability due to delocalization of π-electrons in the ring. Rings having $-NO_2$ groups increases the average NICS values. The presence of strongly electron withdrawing $-NO_2$ and $-N_3$ groups, which decrease the tendency of electrons to be localized, enhances the diatropic ring current, thus enhancing cyclic conjugation.

The order of increasing NICS for the triazine derivatives is given as, $NO_2 > N_3 > NH_2$. The 1,2,3-triazole substituted triazines (**Q1**, **Q2** and **Q3**) shows high negative values for the NICS may be due to the azole rings. Nitrogen is more electronegative than carbon and may be responsible for the higher electron density in the ring. Due to the substituted azole rings on the s-triazine decreases the electron density to the ring centre. In all the derivatives triazine ring show NICS above -5 ppm. All substituted azole rings show NICS values above -7.7 ppm. This NICS values show that all compounds are stable and possess high diatropic ring current. The stability is due to the linear, symmetric, conjugated, and heterocyclic skeleton of the s-triazine derivatives.

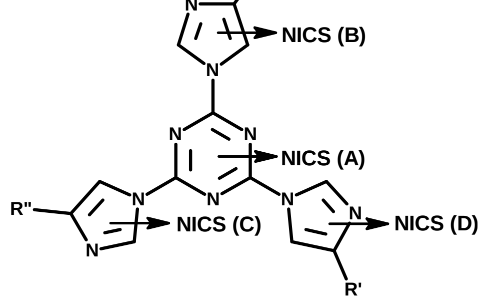

Fig. 4.20 NICS values calculated at the ring centers of s-triazine derivatives.

Table 4.25: NICS at 1Å above the ring centre of designed s-triazine derivatives.

Compd.	NICS (A) (ppm)	NICS (B) (ppm)	NICS (C) (ppm)	NICS (D) (ppm)	ΔE (hartree)
V1	-5.66	-8.65	-8.66	-8.64	0.1339
V2	-4.58	-7.71	-7.72	-7.72	0.1645
V3	-5.02	-8.11	-8.11	-8.09	0.1367
P1	-6.08	-9.50	-9.32	-9.39	0.1516
P2	-5.11	-9.19	-9.22	-9.16	0.1804
P3	-5.46	-9.45	-9.43	-9.43	0.1532
R1	-6.32	-9.86	-9.95	-10.06	0.1531
R2	-5.26	-8.24	-8.28	-8.35	0.1654
R3	-5.64	-8.98	-9.01	-9.09	0.1547
Q1	-6.47	-11.17	-10.94	-10.44	0.1363
Q2	-5.71	-10.57	-11.37	-11.20	0.1685
Q3	-5.75	-10.46	-10.34	-10.24	0.1395

NICS (A), NICS (B), NICS (C) and NICS (D) represent NICS 1Å above the ring centre of the corresponding ring as shown in Fig. 4.20.

4.3.6 Sensitivity correlations

The band gap of predicted triazine derivatives is summarized in Table 4.25. Xiao et al. research group suggested a principle of easiest transition (PET) to predict the sensitivity of ionic metal azides.[65] The principle states that, smaller band gap (ΔE) between the highest occupied molecular orbital (HOMO) and lowest unoccupied molecular orbital (LUMO), easier the electron transition and larger the sensitivity will be. Many experimental results have been illustrated by the principle.[54,66-69] Comparison of **V1**, **V2** and **V3** reveals that nitro derivatives are more sensitive than amino and azido derivatives. The order of sensitivity can be given as NO_2>N_3>NH_2. A similar trend is observed in all the triazine derivatives. Amino derivatives (**V1**, **P1**, **R1** and **Q1**) found to be more insensitive due to its electron donating effect, which strengthens the bonds in the structure. Replacement of imidazole (**V1**, **V2** and **V3**) with the pyrazole (**P1**, **P2** and **P3**) slightly increases the band gap, similar phenomena is observed in case of 1,2,3-triazole and 1,2,4-triazole derivatives. Analysis of the band gap of triazine derivatives shows that amino derivatives are more insensitive candidates and restricts the easy electron transition.

4.3.7 Conclusions

In the present study, the energetic properties of the designed s-triazine derivatives have been studied by using the density functional theory. Based on appropriate designed sets of isodesmic reactions, standard gas-phase $\Delta H^0{}_f$ are predicted. All the triazine derivatives show $\Delta H^0{}_f$ higher than 630 kJ/mol. The nitro derivatives show highest densities as compared to amino and azido derivatives hence, the better detonation performance. The nitro derivatives possess density above 1.58 g/cm^3, detonation velocity and pressure over 6.6 km/s and 17.8 GPa, respectively. Thermal stability of the designed compounds has been evaluated by using nucleus independent chemical shifts. Overall performance of triazine derivatives is moderate and may find their applications in solid fuels in micropropulsion systems, carbon nitride nanomaterials and smoke-free pyrotechnic fuels as they are rich in nitrogen content.

4.4 References

1. Agrawal, J. P. *Prog. Energy Combust. Sci.* **1998**, *24*, 1.
2. Hiskey, M. A.; Chavez, D. E.; Naud, D. L.; Son, S. F.; Berghout, H. L.; Bolme, C. A. *Proc. Int. Pyrotech. Semin.* **2000**, *27*, 3.
3. Gutowski, K. E.; Rogers, R. D.; Dixon, D. A. *J. Phys. Chem. A* **2006**, *110*, 11890.
4. Zhou, H. W.; Wong, N. B.; Tian, A.; Li, W. K. *J. Mol. Graph. Model.* **2007**, *28*, 788.

5. Gao, H. X.; Wang, R.; Twamley, B.; Hiskey, M. A.; Shreeve, J. M. *Chem. Commun.* **2006**, 4007.
6. Chavez, D. E.; Hiskey, M. A.; Gilardi, R. D. *Angew. Chem.* **2000**, *112*, 1861.
7. Coburn, M. D.; Hiskey, M. A.; Lee, K. Y.; Ott, D. G.; Stinecipher, M. M. *J. Heterocycl. Chem.* **1993**, *30*, 1593.
8. Licht, H. H.; Ritter, H. *J. Energ. Mater*. **1994**, *12*, 223.
9. Huynh, M. H. V.; Hiskey, M. A.; Archuleta, J. G.; Roemer, E. L.; Gilardi, R. D. *Angew. Chem. Int. Ed.* **2004**, *43*, 5658.
10. Huynh, M. H. V.; Hiskey, M. A.; Archuleta, J. G.; Roemer, E. L. *Angew. Chem. Int. Ed.* **2005**, *44*, 737.
11. Gillan, E. G. *Chem. Mater*. **2000**, *12*, 3906.
12. Miller, D. R.; Swenson, D. C.; Gillan, E. G. *J. Am. Chem. Soc.* **2004**, *126*, 5372.
13. Chavez, D. E.; Hiskey, M. A.; Naud, D. L. *J. Pyrotech.* **1999**, *10*, 17.
14. Xue, H.; Gao, Y.; Twamley, B.; Shreeve, J. M. *Chem. Mater.* **2005**, *17*, 191.
15. Khabashesku, V. N.; Zimmerman, J. L.; Margrave, J. L. *Chem. Mater.* **2000**, *12*, 3264.
16. Wang, J.; Miller, D. R.; Gillan, E. G. *Carbon* **2003**, *41*, 2031.
17. Ye, C.; Gard, G. L.; Winter, R. W.; Syvret, R. G.; Twamley, B.; Shreeve, J. M. *Org. Lett*. **2007**, *9*, 3841.
18. Pauling, L.; Sturdivant, J. H. *Proc. Natl. Acad. Sci. USA* **1937**, *23*, 615.
19. Zheng, W.; Wong, N.; Wang, W.; Zhou, G.; Tian, A. *J. Phys. Chem. A* **2004**, *108*, 97.
20. Kroke, E.; Schwarz, M.; Bordon, E. H.; Kroll, P.; Noll, B.; Norman, A. D. *New J. Chem.* **2002**, *26*, 508.
21. Strout, D. L. *J. Phys. Chem. A* **2005**, *109*, 1478.

22. Strout, D. L. *J. Chem. Theor. Comput.* **2005**, *1*, 561.

23. Hehre, W. J.; Ditchfield, R.; Radom, L.; Pople, J. A. *J. Am. Chem. Soc.* **1970**, *92*, 4796.

24. Hehre, W. J.; Radom, L.; Pople, J. A. *Ab initio molecular orbital theory*, Wiley, New York, 1986.

25. Li, X. H.; Zhang, R. Z.; Yang, X. D.; Zhang, H. *J. Mol. Struct. (THEOCHEM)* **2007**, *815*, 151.

26. Li, Y. F.; Fan, X. W.; Wang, Z. Y.; Ju, X. H. *J. Mol. Struct. (THEOCHEM)* **2009**, *896*, 96.

27. Li, J.; Huang, Y.; Dong, H. *Propell. Explos. Pyrotech.* **2004**, *29*, 231.

28. Bulusu, S.; Damavarapu, R.; Autera, J. R.; Behrens, R.; Minier, L. M. Jr.; Villanueva, J.; Jayasuriya, K.; Axenord, T. *J. Phys. Chem.* **1995**, *99*, 5009.

29. Sikder, A. K.; Sikder, N. *J. Hazard. Mater.* **2004**, *112*, 1.

30. Cho, S. G.; Goh, E. M.; Cho, J. R.; Kim, J. K. *Propell. Explos. Pyrotech.* **2006**, *31*, 33.

31. Licht, H. H.; Ritter, H. *Propell. Explos. Pyrotech.* **1997**, *22*, 333.

32. Politzer, P.; Martinez, J.; Murray, J. S.; Concha, M. C.; Toro-Labbe, A. *Mol. Phys.* **2009**, *107*, 2095.

33. Mondal, T.; Saritha, B.; Ghanta, S.; Roy, T. K.; Mahapatra, S.; Durga Prasad, M. *J. Mol. Struct. (THEOCHEM)* **2009**, *897*, 42.

34. Cho, S. G.; Goh, E. M.; Kim, J. K. *Bull. Korean Chem. Soc.* **2001**, *22*, 775.

35. Turker, L.; Atalar, T.; Gumus, S.; Camur, Y. *J. Hazard. Mater.* **2009**, *167*, 440.

36. Minkin, V. I.; Glukhovtsev, M. N.; Simkin, B. Y. *Aromaticity and antiaromaticity*, Wiley, New York, 1994.

37. Garratt, P. J. *Aromaticity*, Wiley, New York, 1986.

38. Xu, X. J.; Zhu, W. H.; Xiao, H. M. *J. Phys. Chem. B* **2007**, *111*, 2090.

39. Kamlet, M. J.; Adolph, H. G. *Propell. Explos. Pyrotech.* **1979**, *4*, 30.

40. Bliss, D. E.; Christian, S. L.; Wilson, W. S. *J. Energ. Mater.* **1991**, *9*, 319.

41. Katritzky, A. R. *Handbook of heterocyclic chemistry*, Pergamon Press, 1986.

42. Saracoglu, N. *Tetrahedron* **2007**, *63*, 4199.

43. Spanget-Larsen, J.; Thulstrup, E. W.; Waluk, *J. Chem. Phys.* **2000**, *254*, 135.

44. Gleiter, R.; Schehlmann, V.; Spanget-Larsen, J.; Fischer, H.; Neugebauer, F. A. *J. Org. Chem.* **1988**, *53*, 5756.

45. Qing, Z.; Audebert, P.; Clavier, G.; Miomandre, F.; Tang, J.; Vu, T. T.; Renault, R. M. *J. Electroanalytical. Chem.* **2009**, *632*, 39.

46. Kaim, W. *Coord. Chem. Rev.* **2002**, *230*, 126.

47. Chavez, D. E.; Gilardi, R. D.; Hiskey, M. A. *Angew. Chem. Int. Ed.* **2000**, *39*, 1791.

48. Huynh, M. H. V.; Hiskey, M. A.; Chavez, D. E.; Naud, D. L.; Gilardi, R. D. *J. Am. Chem. Soc.* **2005**, *127*, 12537.

49. Boger, D. L.; Weinreb, S. M. *Hetero Diels–Alder methodology in organic synthesis*, Academic Press, New York, 1987.

50. Hamasaki, A.; Ducray, R.; Boger, D. L. *J. Org. Chem.* **2006**, *71*, 185.

51. Wei, T.; Zhu, W. H.; Zhang, X. W.; Li, Y. F.; Xiao, H. M. *J. Phys. Chem. A* **2009**, *113*, 9404.

52. Schleyer, P. v. R. *Chem. Rev.* **2001**, *101*, 1115.

53. Schleyer, P. v. R.; Maerker, C.; Dransfeld, A.; Jiao, H. J.; Hommes, N. J. R. V. *J. Am. Chem. Soc.* **1996**, *118*, 6317.

54. Xu, X. J.; Zhu, W. H.; Xiao, H. M. *J. Phys. Chem. B* **2007**, *111*, 2090.

55. Kamlet, M. J.; Adolph, H. G. *Propell. Explos. Pyrotech.***1979**, *4*, 30.

56. Bliss, D. E.; Christian, S. L.; Wilson, W. S. *J. Energ. Mater.* **1991**, *9*, 319.

57. Gilchrist, T. L. *Heterocyclic chemistry*, Pitman publishing, London, 1985.

58. Smolin, E. M.; Rapoport, L. *Chemistry of heterocyclic compounds: s-Triazines and derivatives*, Wiley interscience publishers, 2008.

59. Carpel, P.; Walker, *The ring index*, American Chemical Society, Washington DC, New York, 1960.

60. Sanderson, J. T.; Seinen, W.; Giesy, J. P.; Berg, M. *Toxicol. Sci.* **2000**, *54*, 121.

61. Farland, J. M.; LeBaron, H. M.; Burnside, O. *The triazine herbicides*, Elsevier, 2008.

62. Klenke, B.; Barrett, M. P.; Brun, R.; Gilbert, I. H. *J. Antimicrob. Chemother*. **2003**, *52*, 290.

63. Trepanier, D. L.; Shriver, K. L.; Eble, J. N. *J. Med. Chem.* **1969**, *12*, 257.

64. Kamlet, M. J.; Jacobs, S. J. *J. Chem. Phys.* **1968**, *48*, 23.

65. Xiao, H. M.; Li, Y. F. *Sci. China Ser. B* **1995**, *38*, 538.

66. Xiao, H. M.; Li, Y. F.; Qian, J. J. *Acta Phys. Chim. Sin.* **1994**, *10*, 235.

67. Xiao, H. M.; Li, Y. F. *Banding and electronic structures of metal azides*, Science Press, Beijing, 1996.

68. Xu, X. J.; Zhu, W. H.; Xiao, H. M. *J. Phys. Chem. B* **2007**, *111*, 2090.

69. Wang, G. X.; Shi, C. H.; Gong, X. D.; Xiao, H. M. *J. Hazard. Mater.* **2009**, *169*, 813.

Chapter V

General Summary

Energetic materials are the molecules or formulations whose enthalpy of formation is as high as possible, and which are capable of releasing on demand, in a controlled fashion and without oxygen, the chemical energy stored in the molecular building blocks forming the substance. The explosives can be classified as thermally stable, high performance, melt-castable and insensitive high explosives from their stability point of view. A numerous progress in this field reveals that higher performance has always been a prime requirement. In addition to high performance, safety, reliability, stability and sensitivity plays a vital role in their selection for the end-use. The over all aim of the high energy materials researchers is to develop the more powerful energetic material formulations in comparison to currently known benchmark materials/compositions.

Computational chemistry is an emerging field of materials science and it is widely explored to study the chemistry of energetic materials. Recent days, many computational approaches have been developed to screen the molecules for energetic materials applications. The particular importance in designing new explosives is the ability to predict performance of compounds before the laborious and expensive task of synthesizing them. The significant key properties of energetic materials are heat of formation ($\Delta H^0{}_f$), density, detonation performance, thermal stability and sensitivity. Heat of formation is a measure of energy content of an energetic material that can decompose, ignite and explode by heat or impact, have been calculated using isodesmic approach. Density is one of the most important physical properties of energetic materials that are used to initially assess potential performance in a weapon. An increase in density is also desirable in terms of the amount of material that can be packed into volume-limited warhead or propulsion configurations. Density is predicted by the crystal structure packing calculations as it is superior to the group additive approaches. The explosive performance characteristics viz., detonation velocity (*D*) and pressure (*P*) are evaluated by Kamlet-Jacobs empirical relations from their theoretical densities and calculated heat of formation. Stability of the energetic compounds is of prime importance for the practical interest and safe handling of the explosive material. Approaches such as bond dissociation energy of the trigger bond and nucleus independent chemical shift are used to predict the thermal stability of the designed molecules. The analysis of charge on the nitro group and the energy difference between highest occupied molecular orbital (HOMO) and lowest unoccupied molecular orbital (LUMO) have been correlated with the impact sensitivity.

The present study has explored the molecular design of strained systems and nitrogen-rich energetic azoles & azines in search of high performance and insensitive energetic materials. In search of high performance explosives, molecular structure containing fused and strained ring systems occupies a prominent role as they possess high density and energy. On the other hand, heterocycles that contain large amount of nitrogen are relatively dense, possess high heat of formation are explored as gas generators and smoke-free pyrotechnic fuels with moderate detonation characteristics. Hence, this study has covered design and structure-performance relationship studies on strained and nitrogen-rich energetic azoles & azines by quantum/molecular mechanical calculations.

The strained hexaazaisowurtzitane and bicyclo[1.1.1]pentane based caged energetic compounds are designed and structure-performance relationships among them are discussed in Chapter II. Energetic materials of the strained-ring and cage families constitute a promising class of high explosives as they have high strain energies locked in the structure. Among this family, the 2,4,6,8,10,12-hexanitro-

2,4,6,8,10,12-hexaazaisowurtzitane (CL-20) is superior in performance (D~9.58 km/s and P~46.6 GPa), but highly sensitive to impact and friction. Hence, the molecular structure of CL-20 is tailored to obtain improved insensitivity characteristics. The amino and triazole group are introduced in the CL-20 cage, which are the simplest means to enhance thermal stability and also alters the $\Delta H^0{}_f$, making them more positive. The results reveal that introduction of a nitrotriazole group increases the energy content significantly and improves the detonation performance. The computational study identified **IDX1**, **IDX4**, and **IDX7** as potential replacements for CL-20 in various energetic formulations. These molecules show $\Delta H^0{}_f$ and density above 750 kJ/mol and 1.85 g/cm^3, respectively. Further, charge analysis of nitro group revealed that these molecules show better impact sensitivity than the CL-20.

Bicyclo[1.1.1]pentane is a highly strained hydrocarbon system due to close proximity of non-bonded bridge head carbons. The nitro groups are introduced into bicyclo[1.1.1]pentane cage to improve the oxygen balance, $\Delta H^0{}_f$ and density, hence the detonation performance. Among the designed compounds, **S3**, **S4**, and **S5** show high detonation performance (*D* higher than 8.7 km/s and *P* over 33 GPa) with better thermal stability and insensitivity.

Chapter III evaluates the azole based energetic materials. Five member heterocycles such as imidazole, pyrazole, triazole, tetrazole, etc., are the natural framework for energetic materials due to their high nitrogen content. Generally, smaller amounts of hydrogen and carbon in azole contribute to a better oxygen balance. Additionally, these heterocycles are relatively dense; possess higher $\Delta H^0{}_f$ with enhanced thermal stability more than normally found with their carbocyclic analogues.

The energetic azoles with bi & tri nitrogen heterocycles with varying nitro groups are designed. Energetic azoles are rich in nitrogen, with nitrogen content of about 40% and oxygen balance is -12.7%. The $\Delta H^0{}_f$ for predicted compounds (**H1-H8**) show high positive values in the range of 420 to 660 kJ/mol. The density for designed molecules is above 1.85 g/cm^3. Energetic azoles have detonation velocity higher than 9.1 km/s and pressure above 37 GPa. A structure-property relationship on these energetic azoles demonstrated that these molecules will be promising candidates for high performance applications.

Nitrogen-rich tetrazole derivatives have been designed by attaching nitroazoles (imidazole, pyrazole and triazoles) to tertazole via C-C and C-N linkages. Tetrazole has been introduced on the nitro azoles to improve the energetic performance along with the better stability and low sensitivity. Among the designed compounds **T4**, **T9** and **T10** shows detonation velocity above 9 km/s and pressure over 35 GPa.

The different azoles such as imidazole, pyrazole, triazoles, and isoxazole are coupled via -N=N- bridge. The incorporation of azo linkage (-N=N-) is aimed to decrease sensitivity and increase energy content. The $-NO_2$, $-NH_2$ and $-N_3$ groups are substituted on the azoles to evaluate their effect on energetic properties. Azole derivatives possess high positive $\Delta H^0{}_f$ due to the major energy contribution from the five member azole rings, energetic nitro and azido groups. The nitro derivatives (**I1**, **P1**, **T1**, **R1** and **O1**) have higher densities as compared to amino and azido derivatives, which exhibited better detonation performance.

Chapter IV details energetic characteristics and structure-performance relationships of s-heptazine, s-tetrazine and s-triazine based materials. These heterocycles have played a key role in the synthesis of high performance energetic materials due to their high nitrogen content, positive ΔH^0_f and higher thermal stability. s-Heptazine is symmetrical heterocyclic azadienes, composed of three fused s-triazine rings. A systematic substitution of nitro, azido, amino, nitroimidazole and nitrotriazole groups is attempted in order to design a novel high energy material with optimal performance characteristics. The results reveals that substitution by imidazole or 1,2,4-triazole with a nitro group shows a remarkable increase in ΔH^0_f. Among the heptazine derivatives, the azido molecules (**IDX10-IDX14**) shows significantly high heat of formation (> 1150 kJ/mol) than the nitro (> 850 kJ/mol) and amino (> 750 kJ/mol) derivatives. All the designed compounds show densities above 1.80 g/cm^3. Nitro derivatives of heptazines (**IDX20-IDX24**) show higher performance than azido and amino derivatives due to better oxygen balance, density and ΔH^0_f of these molecules. Their detonation velocity and pressure found over 8 km/s and 27 GPa, respectively.

s-Tetrazine is an azo compound with a high nitrogen content (68.27%), making it of interest for the theoretical and synthesis of high energetic materials. In the designed compounds, different five membered heterocycles such as imidazole, pyrazole, 1,2,4-triazole, 1,2,3-triazole, and tetrazole have been substituted on the s-tetrazine at C3 and C6 position to evaluate the characteristic changes in the ΔH^0_f. Different substituents such as $-NO_2$, $-NH_2$ and $-N_3$ have attached to the azoles to understand the role of substituents and nitrogen-rich molecular skeleton. The azido molecules (**TI3**, **TP3**, **TT3**, **TS3** and **TR3**) show very high positive ΔH^0_f (>1300 kJ/mol). Substitution of nitro group play important role in increasing the density as compared to other substituent like amino and azido.

s-Triazine is an intriguing heterocycle for energetic materials and exhibits a high degree of thermal stability. Similar to tetrazine derivatives, the nitro, amino and azido explosophores are attached to azoles and bridged to the triazine via C-N linkage. Among the designed triazine derivatives, the azido molecules (**V3**, **P3**, **R3** and **Q3**) exhibit very high positive ΔH^0_f (> 1450 kJ/mol). The nitro substituted derivatives like **V1**, **P1**, **R1** and **Q1** possess higher densities (> 1.60 g/cm^3). The detonation velocity and pressure of nitro derivatives found above 6 km/s and 18 GPa, respectively.

The calculations presented herein showed that these predictive methodologies are valuable computational tools to be used in the rapid assessment and screening of energetic materials. Overall study revealed that few of the strained hexaazaisowurtzitane and bicyclo[1.1.1]pentane based cage energetic compounds show high performance with better insensitivity characteristics. Energetic azoles illustrate high performance, while azo bridged azole derivatives show poor performance. Further, s-heptazine, s-tetrazine and s-triazine derivatives have moderate performance characteristics, while these derivatives are better in terms of insensitivity and stability. Hence, these molecules may find potential applications in gas generators, smoke-free pyrotechnic fuels, effective precursors of carbon nanospheres and carbon nitride nanomaterials, solid fuels in micropropulsion systems, etc., as they are rich in nitrogen content.

Further improvement can be done in this direction by designing nitrogen-rich energetic materials and their *N*-oxides. The role of different groups (such as $-NHNH_2$, $-NHNO_2$, -CN, $-NF_2$, $-ONO_2$, -NO, etc.) on the energetic properties can be evaluated. Computational approaches for the prediction of condensed phase heat of formation can be developed as most of the energetic materials are solid at ambient temperature. Further, intra and inter molecular interactions existing in the crystal structure can be studied to understand the sensitivity behavior of energetic materials.

List of Publications

1. **V. D. Ghule,** P. M. Jadhav, R. S. Patil, S. Radhakrishnan and T. Soman, Quantum-chemical studies on hexaazaisowurtzitanes. ***J. Phys. Chem. A*** 114, 2010, 498-503.
2. **V. D. Ghule**, S. Radhakrishnan, P. M. Jadhav, R. S. Patil and S. P. Tewari, Electronic structure calculations and structure-property relationships on aromatic nitro compounds. ***Adv. Sci. Lett.*** 4, 2010, 136-141.
3. **V. D. Ghule**, S. Radhakrishnan, P. M. Jadhav and T. Soman, Molecular dynamics simulations on polythiophenes for chemical sensing applications. ***Molecular Simulation*** 36, 2010, 63-68.
4. R. S. Patil, S. Radhakrishnan, P. M. Jadhav, **V. D. Ghule** and T. Soman, Quantum-chemical studies on TATB processes. ***J. Energ. Mater.*** 28, 2010, 98-113.
5. **V. D. Ghule**, S. Radhakrishnan, P. M. Jadhav and S. P. Tewari, Theoretical studies on polynitrobicyclo[1.1.1]pentanes in search of novel high energy density materials. ***Chemical Papers***, 65, 2011, 380-388.
6. **V. D. Ghule,** S. Radhakrishnan, P. M. Jadhav and S. P. Tewari, Theoretical studies on nitrogen-rich energetic azoles. ***J. Mol. Model.*** 17, 2011, 1507-1515.
7. **V. D. Ghule**, S. Radhakrishnan and P. M. Jadhav, Computational studies on tetrazole derivatives as potential high energy materials. ***Struct. Chem.*** 22, 2011, 775-782.
8. **V. D. Ghule**, P. M. Jadhav, S. Radhakrishnan and R. K. Pandey, Computational design and structure-property relationship studies on heptazines. ***J. Mol. Model.*** 2011, DOI: 10.1007/s00894-011-0959-x.

9. **V. D. Ghule**, S. Radhakrishnan, P. M. Jadhav and S. P. Tewari, Quantum chemical studies on energetic azo bridged azoles. ***J. Energ. Mater.*** 2011 (In Press).
10. **V. D. Ghule**, S. Radhakrishnan, P. M. Jadhav and S. P. Tewari, Quantum-chemical investigation of substituted s-tetrazine derivatives as high energy materials (Communicated).
11. **V. D. Ghule**, S. Radhakrishnan, P. M. Jadhav and S. P. Tewari, Computational study on substituted s-triazine derivatives (Communicated).